To the Graduate Council:

I am submitting herewith a dissertation written by Hiromoto Kuroda entitled "An Experimental Study of Temperature Separation in Swirling Flow." I have examined the final copy of this dissertation for form and content and recommend that it be accepted in partial fulfillment of the requirements for the degree of Doctor of Philosophy, with a major in Engineering Science.

M. Kurosaka, Major Professor

We have read this dissertation and recommend its acceptance:

Accepted for the Council:

Vice Chancellor
Graduate Studies and Research

AN EXPERIMENTAL STUDY OF TEMPERATURE SEPARATION IN SWIRLING FLOW

A Dissertation

Presented for the

Doctor of Philosophy

Degree

The University of Tennessee, Knoxville

Hiromoto Kuroda

December 1983

ACKNOWLEDGMENTS

The author's deepest thanks are extended to Dr. Mitsuru Kurosaka, chairman of his dissertation committee and faculty advisor, for invaluable guidance, support and encouragement throughout the study of this investigation.

Special thanks are also extended to Drs. John E. Caruthers, John B. Steinhoff, James M. Wu, and Robert L. Young for their many constructive criticisms and suggestions and the knowledge they tried to impart to the author as members of his examination committee.

The author expresses his gratitude to Mr. J. R. Goodman and Mr. R. D. Fizer, who helped in conducting the experiments in this study, and Mr. L. Lester, who gave him the convenience to modify the test rig.

Acknowledgments are also in order for many of his colleagues for simply being available whenever they could be helpful.

The author wishes to extend sincere thanks to Mrs. Becky Eldridge for her excellent typing of the manuscript of this dissertation.

This study was supported by the Air Force Office of Scientific Research, under contract no. F49620-78-C-0045.

The author would like to thank his wife, Yasuko, for her moral support and for taking care of their two sons, Akihiro and Nobuhiro.

The Defense Academy of Japan gave him an opportunity to study at The University of Tennessee Space Institute.

ABSTRACT

The objective of the present investigation is to substantiate the mechanism of acoustic streaming; this was carried out by conducting detailed internal surveys of a Ranque-Hilsch swirling flow test rig at the condition when the vortex whistle was attenuated or excited. This control of the vortex whistle was accomplished by two methods.

In the first method where the vortex whistle was attenuated by placing a restriction at the exhaust, a Rankine vortex was observed to form, accompanied by an almost uniform total temperature distribution in the radial direction except for a dip near the vortex core; when the vortex whistle emerged by the removal of the restriction, a forced vortex was formed, accompanied by an almost linear distribution of total temperature in the radial direction. This establishes that the total temperature separation is indeed caused by acoustic streaming induced by the vortex whistle, which serves to deform a base Rankine vortex into a forced vortex.

In the second method where the vortex whistle was suppressed by the installation of an acoustic suppressor, at the time of sound suppression the total temperature at the centerline leapt upwards while the total temperature at the periphery took a sudden plunge. In spite of this, a result to be expected, the forced vortex formed before the sound suppression did not revert to a Rankine vortex. The cause of this unexpected result was traced to a contaminating effect of back flow entraining ambient air. Besides, the role of tuning mechanism of acoustic suppressor was identified to be that of suppressing the

second harmonic of the vortex whistle rather than the previously-held fundamental frequency.

In addition, another phenomenon of intense heating caused by a pure tone sound, generically different from the vortex whistle was found; this may be related to Hartmann-Sprenger resonance tube effect.

TABLE OF CONTENTS

CHAPTER PAGE

LIST OF FIGURES

LIST OF SYMBOLS

a	Speed of sound
c_p	Specific heat at constant pressure
D	Diameter of main pipe ($D = 2r_o$)
d	Diameter of exit opening area
f, f^*	Frequency of pure tone (f_{11}, f_{21}, f^*_{11}, f^*_{02})
G	Mass flow
l	Acoustic cavity length
M	Mach number
m	Wave number in the tangential direction
p^*, p	Total and static pressure of fluid
Q	Energy flux
q	Magnitude of velocity vector
R	Specific gas constant
Re	Reynolds number
r	Radial coordinate
S	Entropy
T^*, T	Total and static temperature of fluid
t	Time
u, v, w	Radial, tangential and axial velocity of fluid

Greek Letters

α	Flow angle in the main pipe
γ	Specific heat ratio
θ	Angular coordinate

Greek Letters (Continued)

λ	Ratio of wall and interface radii between forced and free vortex
ρ^*, ρ	Density of fluid
μ	Viscosity of fluid
Ω	Angular velocity of forced vortex
ω	Angular velocity

Superscript

*	Total or stagnation value (except frequency)

Subscripts

c	Console
in	Inlet
o	Main pipe wall
t	Tuned condition
max	Maximum

CHAPTER I

INTRODUCTION

The effect of sound waves upon the flow is now being recognized to be closely related to the total temperature separation [1, 2, 3];[1] this phenomenon, where the sounds modify the steady base flow, is caused by the mechanism known as acoustic streaming [4]. Although the study of the steady flow upon the sound waves has been a subject of numerous investigations, the converse problem--the effect of unsteady waves on the time-averaged flow field--does not appear to have drawn as much attention as it warrants. Lord Rayleigh [5] first analyzed the problem of acoustic streaming using the Kundt's tubes; hence acoustic streaming is not, by itself, a newly-found phenomenon. Since then, these problems have sporadically evoked the interest of physicists [6-13]. Yet, this interaction of the unsteady disturbance on the mean flow has remained, in the main, a subject of only scientific interest; its practical implications do not appear to have received equally deserved recognition.

There do exist, however, the important acoustic streaming phenomena which bear direct relation to the engineering applications.

As an example, this causes the intense heating in the resonance tube or Hartmann-Sprenger tube [14, 15], a cylindrical tube open at its upstream end, closed at the downstream end, and immersed in a jet flow. Merkli and Thomann [16] succeeded in tracing the phenomenon of

[1]Numbers in brackets refer to similarly-numbered references in the Bibliography.

Hartmann-Sprenger tube to acoustic streaming by using the nonlinear acoustic theory. According to them, acoustic streaming induced by resonant oscillations of a gas-filled pipe can produce extreme heating of its closed end, which corresponds to a node of the resonant wave; the compensating cooling takes place in the middle of the pipe, which corresponds to a loop.

As the second example, extremely low recovery temperature measured in the near-wake region of a thermally insulated cylinder [17] or other body [18] in high subsonic flow is attributed to streaming induced by von Kármán vortex streets [19]. If the cylinder is not thermally insulated but its surface temperature is maintained to be constant by heating elements, the higher heat transfer rate is found in the separated flow region of the cylinder [20, 21]. This phenomenon involves obvious implications related to such technological applications as gas turbine cooling.

The next example, the Ranque-Hilsch or vortex tube effect due to the acoustic streaming, is the subject of the present investigation.

The tube's name came from the first two investigators [22, 23]. In the Ranque-Hilsch tube, compressed air is injected tangentially near one end of the tube. The swirling air thus created separates spontaneously into hot and cold streams. Many studies, both analytical and experimental, have been conducted on the behavior of the vortex tube. But, unfortunately, almost all investigators have deduced fallaciously that the total temperature separation is due to the turbulent shearing work done by Reynolds stresses (For the critical review and history of the past investigations, see [1], [2] and [24].).

Now it has long been recognized that a high-intensity whistle sound--the so-called vortex whistle--emanates from contained vortex flow in general and from the Ranque-Hilsch tube in particular. Although so far it has been regarded as a mere, annoying by-product of such swirling flows and nothing more, according to Kurosaka [1, 2], who analyzed acoustic streaming for a swirling gas within a cylindrical duct, acoustic streaming induced by the "vortex whistle" produces the Ranque-Hilsch effect; the reason why the total temperature becomes separated in the radial direction was explained as the result of transformation of a Rankine vortex, presumed to be formed in the absence of the vortex whistle, to a forced vortex caused by acoustic streaming induced by the vortex whistle (Figure 1).

The first experimental confirmation of the theory is described in detail by Chu [24]. An acoustic chamber, specially designed and tuned to the frequency of the vortex whistle, was installed on a uni-flow type Ranque-Hilsch tube. When one of the frequencies of the vortex whistle, which increases as the flow is increased, hit the tuned frequency, the sound level suddenly tumbled. At that time, the centerline temperature immediately shot up. Almost all of his measurements were restricted to that of the centerline temperature; no detailed internal flow survey such as radial profiles were conducted because of the small size of the vortex tube used in his experiments.

The objective of the present study is to obtain the internal flow measurements of an upscale Ranque-Hilsch swirling flow test rig in order to examine, in detail, how the acoustic streaming affects the flow pattern and energy separation.

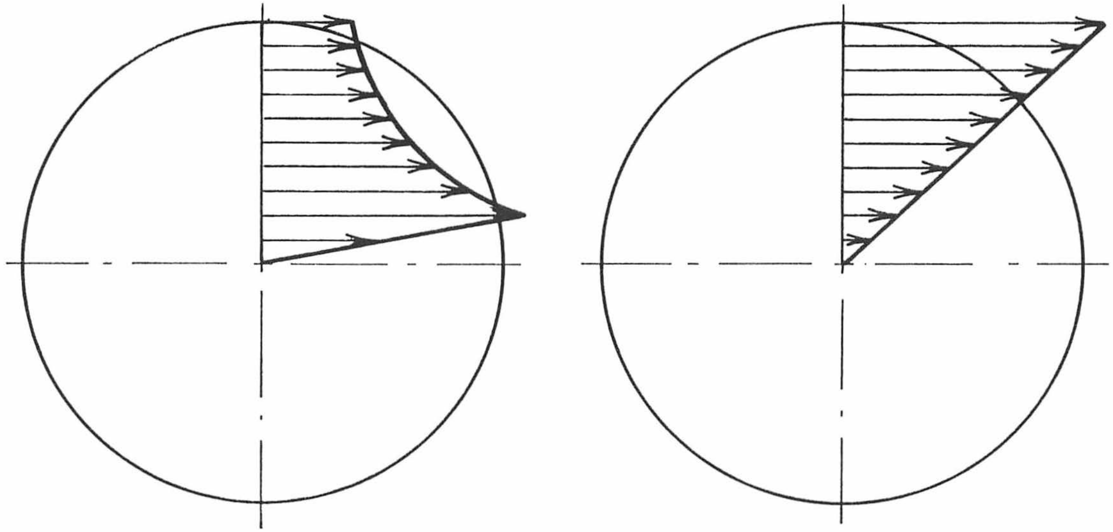

(a) Rankine vortex in the absence of acoustic streaming

(b) Forced vortex with acoustic streaming

Figure 1. Deformation of swirl by acoustic streaming.

CHAPTER II

EXPERIMENTAL SET-UP

The most common arrangement of a Ranque-Hilsch tube or vortex tube is the combination of a swirl generator and two solid pipes [26-31]. The feature of the vortex tube is that incoming air, upon leaving the swirl generator, becomes separated into two outlet flows; one flows through the main pipe with hotter temperature than that of the inlet; the other with colder temperature exhausts from the so-called "cold end orifice." For the present experiment, the cold end orifice was completely closed. Even by closing the cold end pipe, the total temperature in this "uni-flow" arrangement, shown in Figure 2, is shown to remain separated in the radial direction; and because of its simpler flow pattern, our investigations here, as well as the preceding ones, focused upon this uni-flow type.

The compressed air from a surge tank enters a manifold through an inlet pipe. Within the manifold, a swirl generator is located. The swirl generator, with three inches inner diameter, has four tangentially drilled nozzles of 1/4 inch diameter, all equally spaced around circumference. The air leaving swirl generator nozzles is therefore imparted a swirling motion. One end of the manifold is closed by a cold end plug. The swirling air, therefore, escapes only in one direction through the main pipe.

As already stated, the size of the test rig used to obtain the results of Refs. [1], [3], [24], and [25] was too small to allow the detailed radial survey of flow field; the diameter of its main pipe

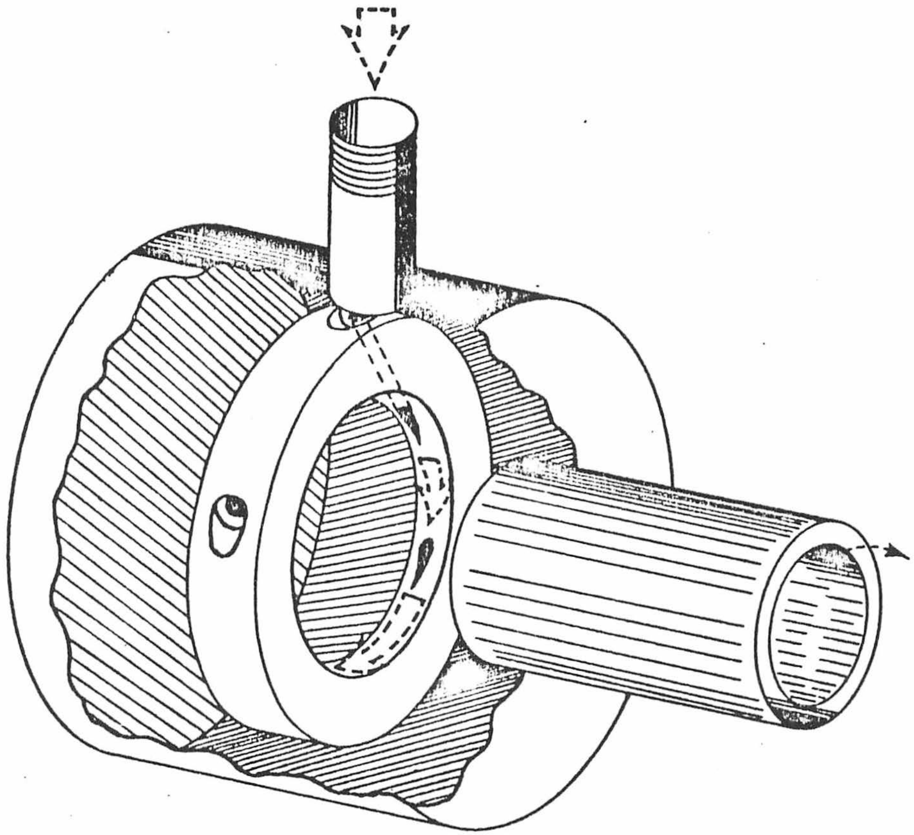

Figure 2. Layout of uni-flow vortex tube.

was only 11/16 inch. Therefore, an upscaled version of the test rig has been constructed; its diameter is now enlarged to two inches. It is sufficiently large to allow the insertion of probes without causing major disturbance of flow. The test rig is placed in the reverberation chamber of the Acoustics Laboratory of The University of Tennessee Space Institute.

Both a solid and porous pipe were manufactured and used as the main pipe in the following ways:

1. the solid main pipe,
2. the porous main pipe with the acoustic chamber,
3. the porous main pipe with the acoustic chamber, fitted with smaller exit-area plate, and
4. the solid main pipe fitted with smaller exit-area plate.

A. Solid Main Pipe

This standard pipe serves as the baseline configuration; as shown in Figure 3 together with the swirl generator, the diameter of the pipe is 2 inches, its length 5.25 inches.

B. Porous Main Pipe

The aforementioned solid main pipe can be replaced with a porous main pipe, shown in Figures 4 and 5, where a number of 0.046 inch diameter holes are drilled. An acoustic chamber, made of Teflon, fits on this porous main pipe. The chamber has the acoustic cavities, 0.177 inch in diameter, and cavity arrangement consists of 22 axial rows and 30 circumferential columns. To each cavity, a tuning rod is inserted.

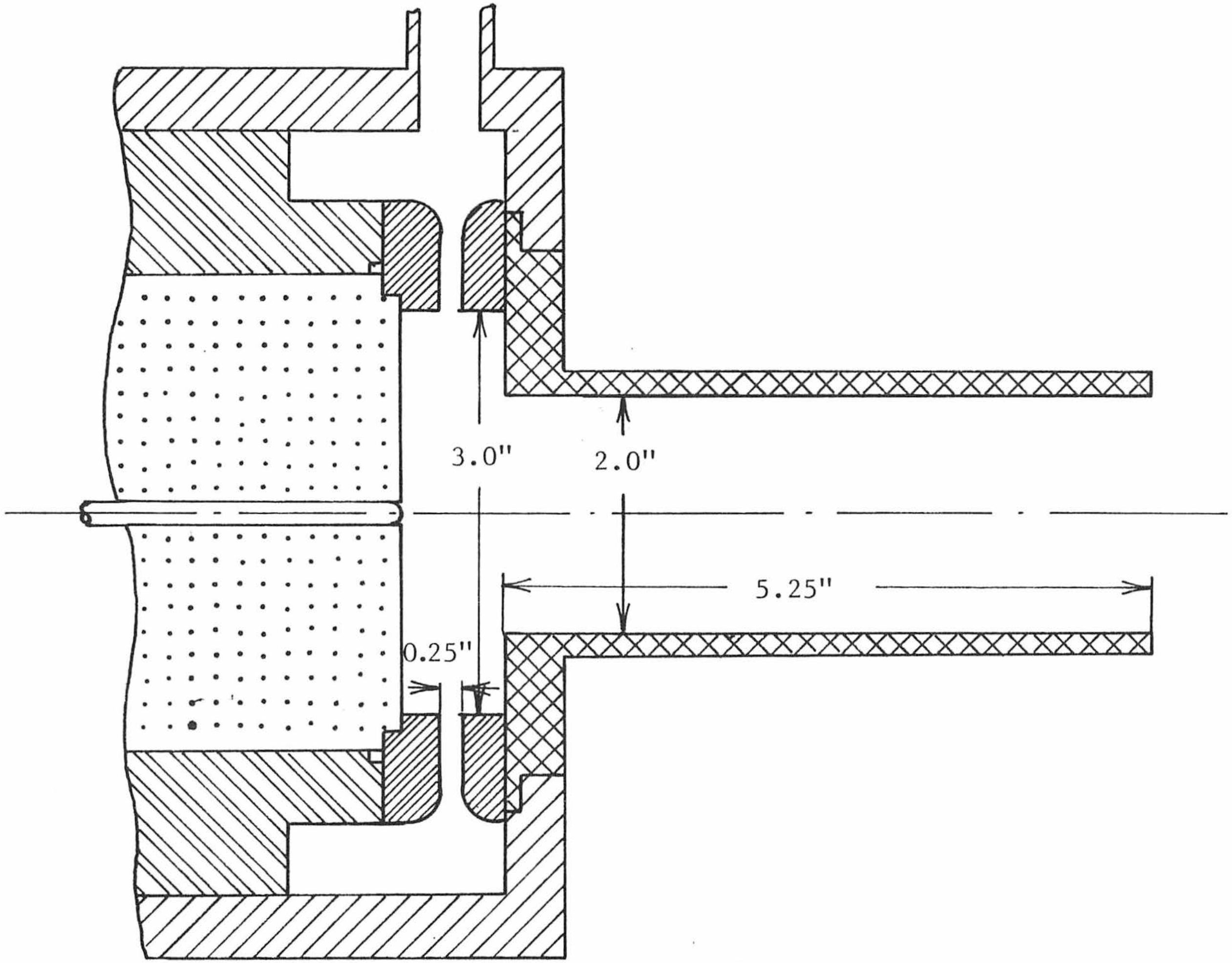

Figure 3. Swirl generator with solid main pipe.

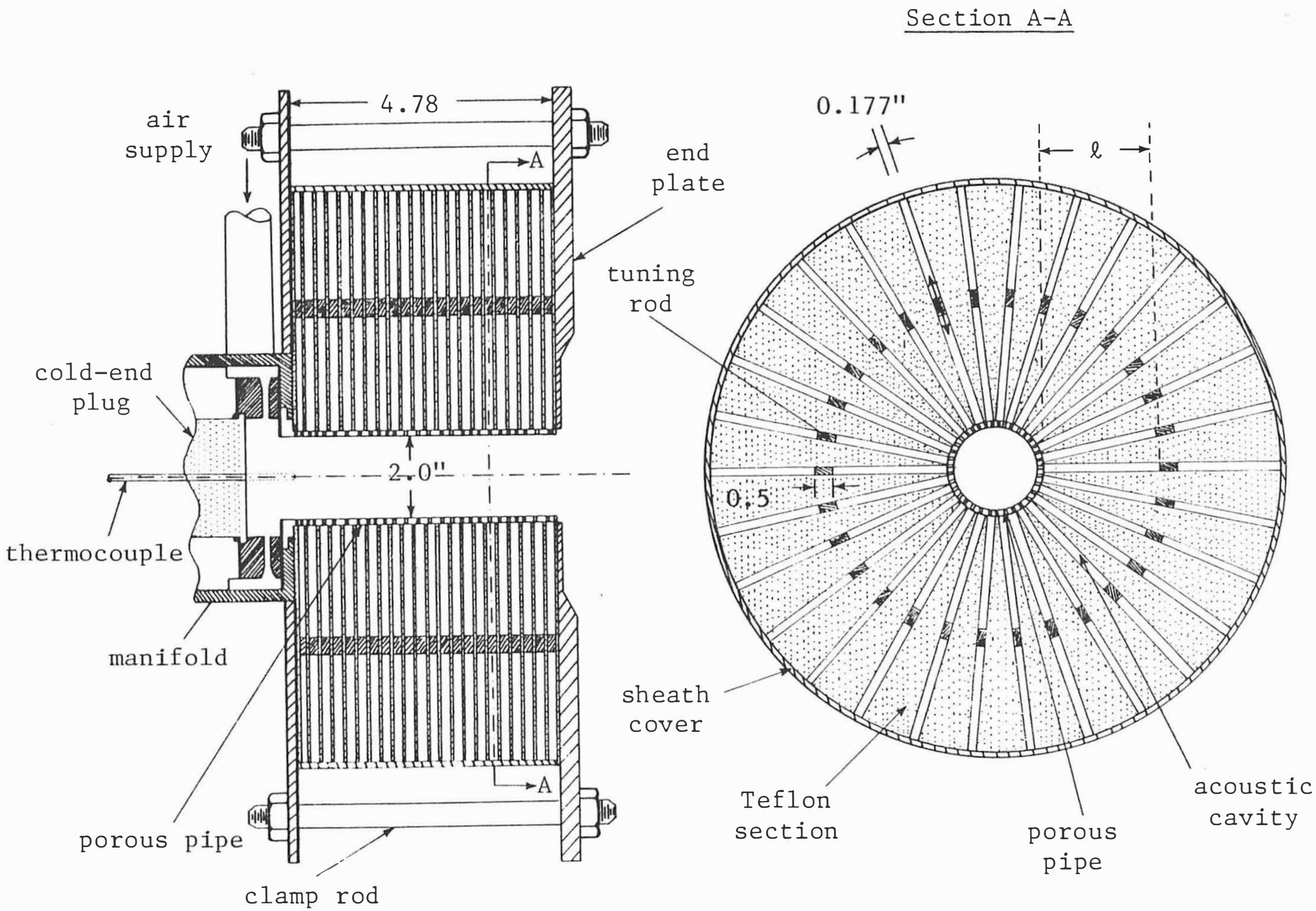

Figure 4. Layout of porous main pipe test rig.

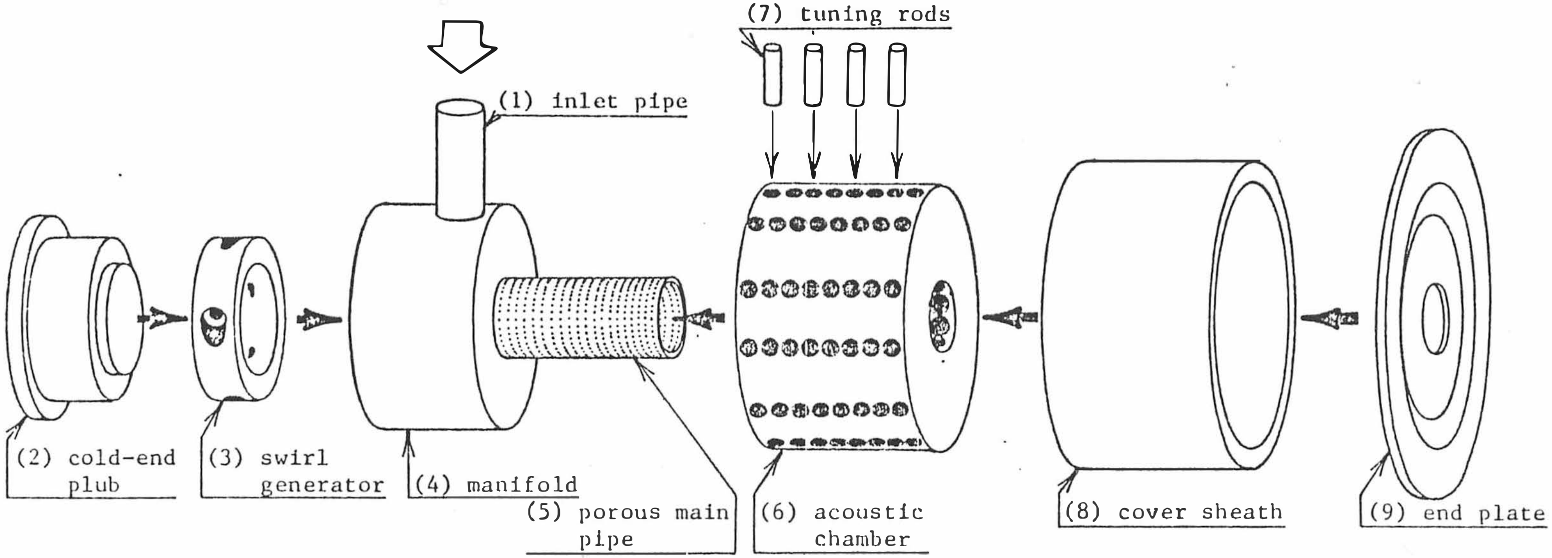

Figure 5. Exploded view of test rig.

By varying the cavity length, ℓ of Figure 4, the vortex whistle can be attenuated at any desired tuned frequency, f_t. In order to reduce leakage through the acoustic cavities, the acoustic chamber is covered by a Teflon sheath. The entire assembly is clamped by an end plate. During the experiment, it was always ascertained that the air does not leak from the test rig.

C. Shape of End Plate

During this experiment, it was found that the shape of the end plate, (9) of Figure 5, plays an important role in the generation or the suppression of the vortex whistle; this, in turn, affects the Ranque-Hilsch effect. Two different kinds of the end plates were made for this experiment. The purpose of the first kind is to block partially the exit area of the main pipe; they have openings near the centerline of the main pipe, but its diameter is smaller than that of the main pipe. The following diameters of openings were used: 0.3, 0.4, 0.5, 0.6, 0.8, 1.0, 1.25 and 1.5 inches. The thickness of these plates is 1/16 inch. These plates can be installed either to the solid or porous main pipe.

The second kind, shown in Figure 6, has an opening with a diameter nominally equal to that of the main pipe; they were only installed with the porous main pipe. These shapes were found to be intimately related to the effect of the sound suppression and subsequent change in the flow field. The effect of these end plates will be discussed later.

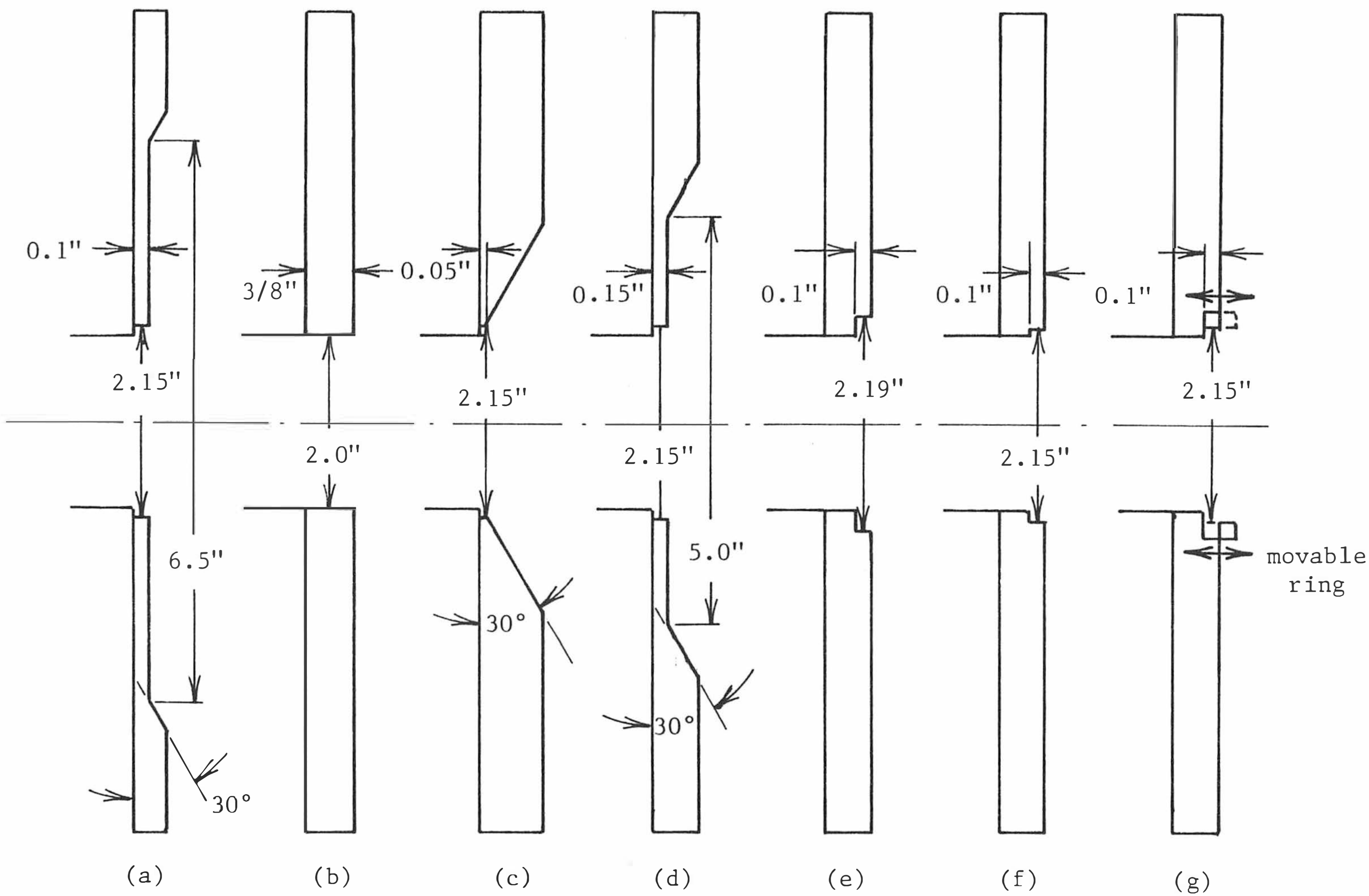

Figure 6. Shapes of end plates.

Henceforth, the following symbols, shown in Figure 7, will be used to designate the various combination of the main pipe(s), acoustic chamber and end plate(s).

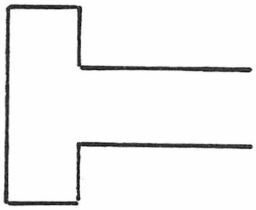

(1) solid main pipe

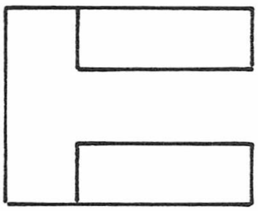

(2) porous main pipe with
acoustic chamber

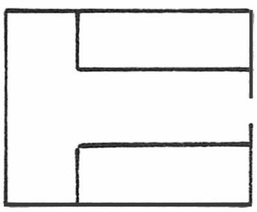

(3) porous main pipe, with
acoustic chamber, fitted
with smaller exit-area
plate

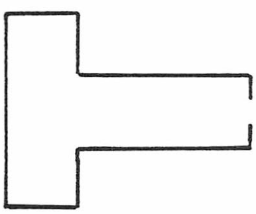

(4) solid main pipe fitted
with smaller exit-area
plate

Figure 7. Abbreviated figures showing various types of test rig.

CHAPTER III

INSTRUMENTATION AND DATA REDUCTION

The measurements inside of the main pipe were carried out with the pressure and temperature probes. The total and static pressures, the total temperature and the flow angle were measured as the time-averaged, mean values. The sound frequency and the sound pressure level were measured with the microphone.

A. Pressure Measurement

In general, the measurements of internal flow are difficult because of the disturbance of flow caused by the insertion of probes. Furthermore, the measurements in swirling flow are more difficult than other internal flows. This is because the presence of strong radial pressure gradients in the swirling flow poses a difficulty in reducing the error in data obtained from multi-probe holes; they are, strictly speaking, located at different radii.

The velocity component in radial direction of the vortex tube can be assumed to be very small, as compared with the axial or tangential velocity components [28-33]; thus, it is necessary only to measure the axial and tangential velocity components.

The important factor in the probe selection is its size. Obviously, the velocities measured by a probe will differ from those in absence of the probe, and the difference increases with increasing probe size.

To assure the greatest possible accuracy in this experiment, the probes were made as small as possible, but with enough strength and reasonable response times. Thus, the size of the probes were chosen to be 1/16 inch in its outer diameter. Initially the probe shapes, shown in Figure 8, were chosen from Ref. [32]; (a) a transverse-cylinder probe, (b) a wedge-type combination probe, and (c) a three-tube combination probe. These three-hole pressure probes were intended to be used for measuring the magnitude of velocity vector and its direction.

The reading of the center-hole pressure gives the total pressure once the pressure difference between the other two adjacent holes is adjusted to zero by rotating the probe, while these readings of the adjacent holes provide the static pressure.

These pressure probes were calibrated in the calibration rig of a free round jet; the calibration curve is shown in Figure 9. Even when the calibration curves are prepared in such a free jet, near the wall surface the transverse-cylinder probe and the wedge-type combination probe deviate from the free jet characteristics because of the presence of a horseshoe vortex on the wall. To avoid the effect of the horseshoe vortex, the three-tube combination probe, a rake-type, was mainly used to measure the pressure. At the time of calibration, this was compared with standard-sized rake-type probe to measure the pressure near the wall of the calibration rig; it was confirmed that in the three-tube combination probe the effect of horseshoe vortex can be virtually eliminated.

To measure the pressure at given axial station, first either the tuning rod of the desired cavity or the cover plug at that

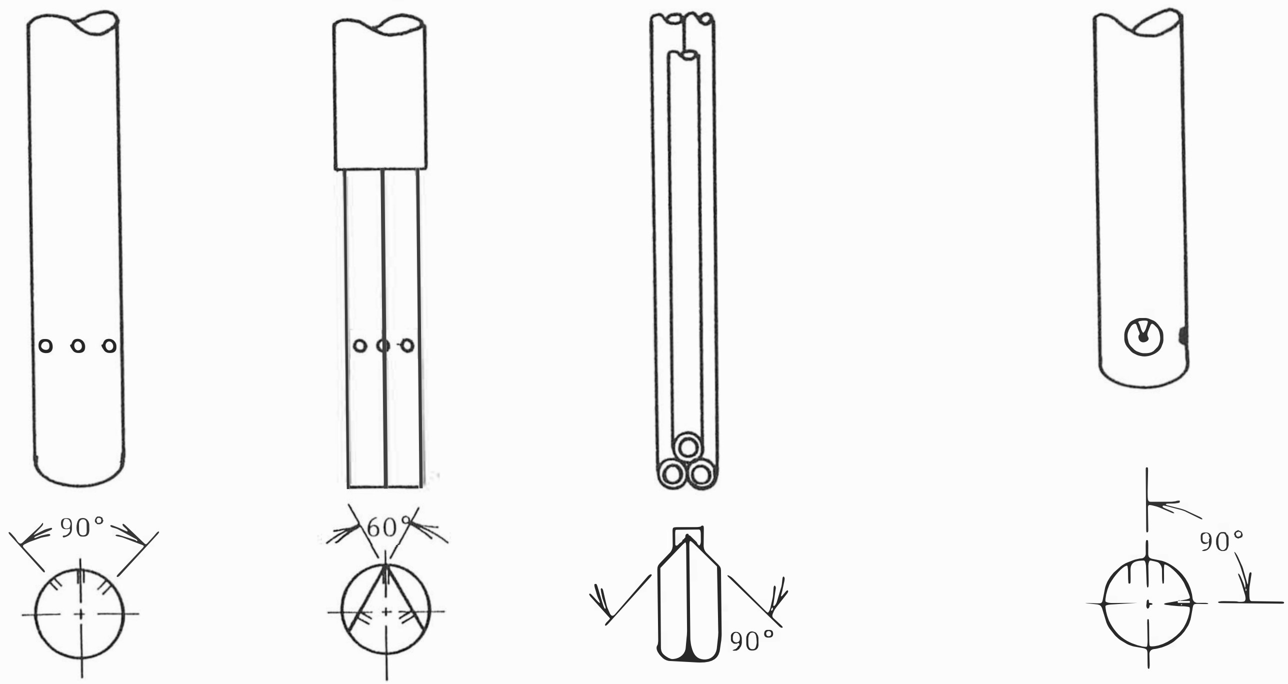

(a) transverse-cylinder probe

(b) wedge-type combination probe

(c) three-tube combination probe

(d) total temperature probe

Figure 8. Pressure and temperature probes.

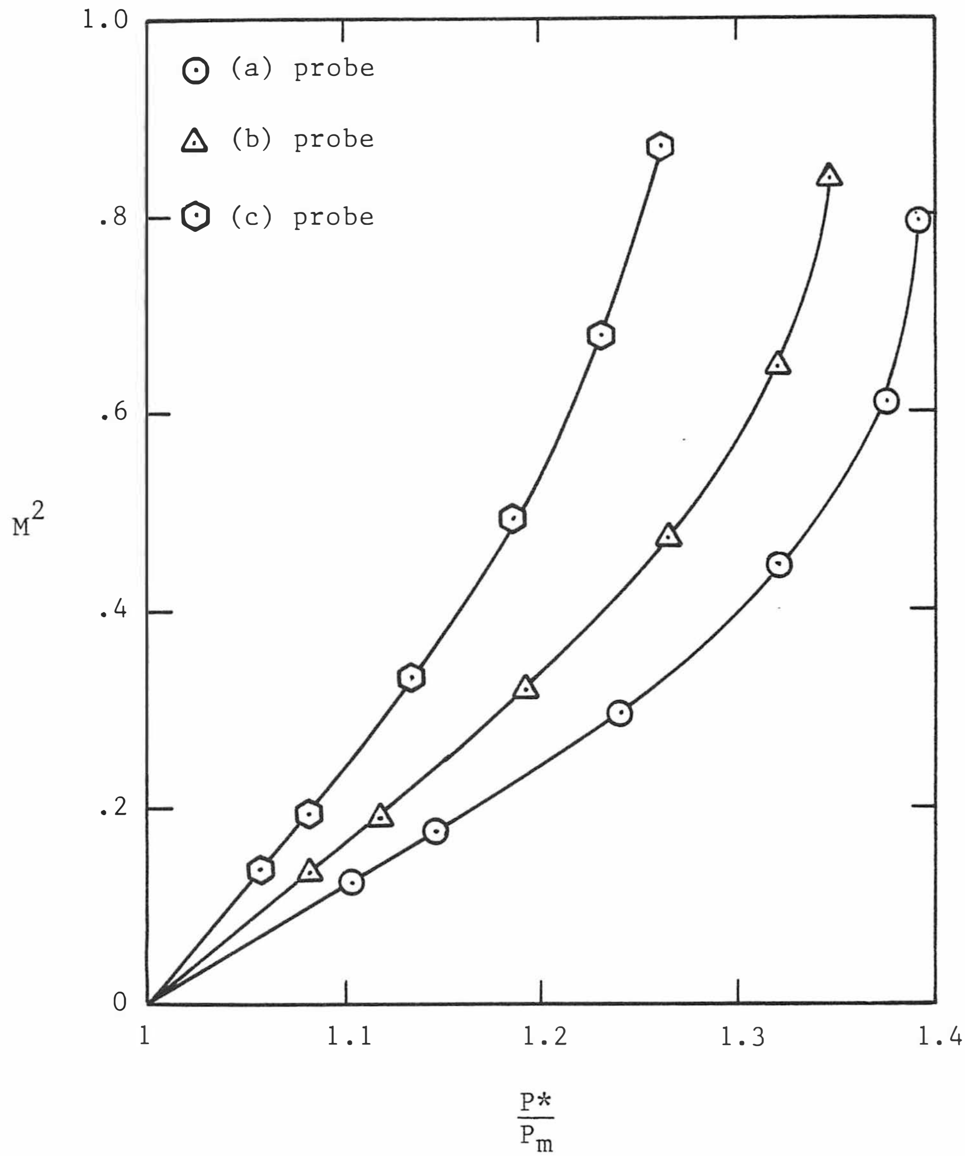

Figure 9. Calibration curve of pressure probes.

position on the main pipe was removed. The pressure probe was radially inserted into the main pipe. At the same time, the probe was mounted on the traversing unit attached to the test rig.

B. Temperature Measurement

The temperature probe, as shown in Figure 8(d), was designed to give a high recovery factor. To reduce the heat conduction from the Chromel-Alumel thermocouple, the thermocouple wires were insulated from the outer stainless steel tube; its outer diameter was the same as that of the pressure probe (1/16 inch). The temperature probe was also calibrated, and the reading of the temperature was interpreted directly as a total temperature. This probe was used for determining the radial total temperature distribution in the main pipe by interchanging with a pressure probe mounted on the traversing unit.

For the centerline temperature measurement, the Chromel-Alumel thermocouple with a stainless steel sheath pipe, the outer diameter of which was 1/8 inch, was inserted through the cold end plug. Upon calibration, this thermocouple did not exactly measure the total temperature because of the low recovery factor. Fortunately, at the main pipe centerline, the velocity is so small that the total temperature is almost equal to the static temperature. One can, therefore, assume safely that the measurement with this thermocouple gives, for all practical purposes, the total temperature at the centerline of the main pipe. This axial insertion also gives less disturbance in the flow of the main pipe.

C. Sound Measurement

The sound measurement was completely the same as that of Refs. [3] and [24]. A condenser microphone was nominally located at a distance of three feet away from the main pipe axis; in certain cases, the microphone was placed within the pipe, flush with the pipe wall.

D. Data Reduction

Figure 10 shows the cylindrical coordinate system; v and w are tangential and axial velocity components, respectively, and these nomenclatures are to be used throughout the present thesis. Henceforth, these velocities and other flow quantities denote time-averaged, mean values.

Once the total and static pressure, p^*, p, the total temperature, T^*, and the flow direction, α, are measured, the tangential and axial velocity components, v, w, and the static temperature, T, can be calculated by the relationship of an isentropic flow assumption. The equations are

$$T^* = T\left(1 + \frac{\gamma-1}{2} M^2\right) \tag{1}$$

$$p^* = p\left(1 + \frac{\gamma-1}{2} M^2\right)^{\gamma/(\gamma-1)} \tag{2}$$

$$a = \sqrt{\gamma RT} \tag{3}$$

$$p = \rho RT, \quad p^* = \rho^* RT^* \tag{4}$$

$$q = Ma, \quad v = q \sin\alpha, \quad w = q \cos\alpha. \tag{5}$$

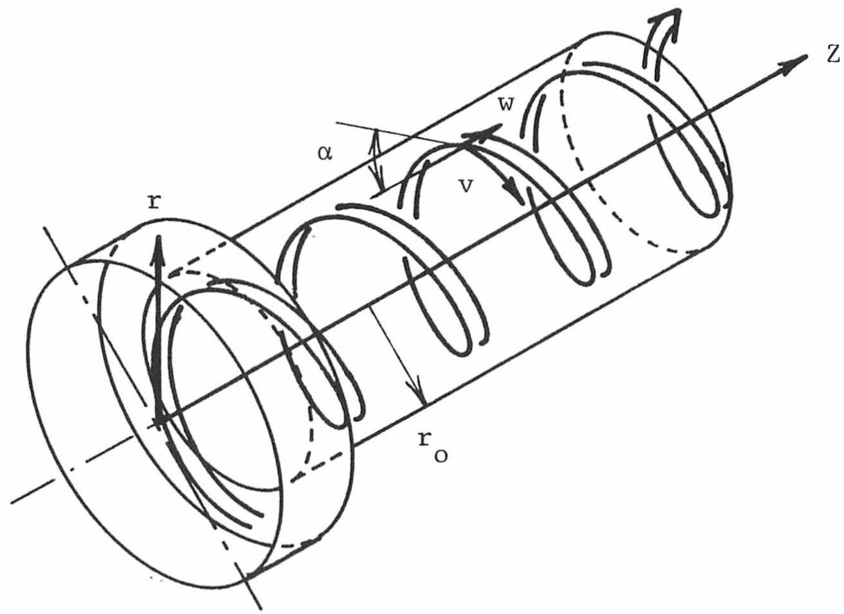

Figure 10. Definition of coordinates.

The magnitude of the velocity vector and the static temperature can be obtained as

$$q = \left[\frac{2\gamma}{\gamma-1} RT^* \left\{ 1 - \left(\frac{p}{p^*}\right)^{(\gamma-1)/\gamma} \right\} \right]^{1/2} \tag{6}$$

$$T = T^* \left(\frac{p}{p^*}\right)^{(\gamma-1)/\gamma} \tag{7}$$

In this experiment, the air was used as an operating fluid so that

$$\gamma = 1.4, \quad R = 1716 \text{ lbf ft/slug } {}^\circ\text{R} \tag{8}$$

The mass flow, G, and the energy flux, Q, through the main pipe can be calculated by integrating the flux from centerline to the periphery of the main pipe:

$$G = 2\pi \int_0^{r_o} \rho r w \, dr \tag{9}$$

$$Q = 2\pi C_p \int_0^{r_o} \rho r w T^* \, dr \tag{10}$$

$$\text{where} \quad \rho = \frac{p^*}{RT^*} \left(\frac{p}{p^*}\right)^{1/\gamma} \tag{11}$$

This mass flow was always checked against the one through the ASME orifice installed in the upstream of the test rig. The latter was the 1-D and 1/2-D tap orifice [33], with 0.772 inch and 3.0 inches in orifice and pipe diameters, respectively. The mass flow is given by

$$G_{in} = 0.5419\,K \left(1 - 0.294 \frac{p_1 - p_2}{p_1}\right) \sqrt{\frac{p_1 (p_1 - p_2)}{T_1^*}} \tag{12}$$

where p_1, $T_1{}^*$ are the values at the 1-D upstream tap, p_2, the pressure at 1/2-D downstream tap. K is the flow coefficient, a function of the Reynolds number based on pipe D', $Re_{D'}$, that is,

$$Re_{D'} = \frac{4}{\pi} \frac{G_{in}}{D'\mu} . \tag{13}$$

In equation (13) the Sutherland formula for viscosity [34],

$$\mu = 7.287 \times 10^{-7} \frac{T^{3/2}}{T+199} \quad \text{lbm/ft sec} \tag{14}$$

was used to determine the viscosity.

The flow coefficient is given as [33]

$$K = 0.59320 + 0.86614/\sqrt{Re_{D'}} \tag{15}$$

However, the value of K is found to deviate from this in our test rig; our calibration shows that K is given, more adequately, by

$$K = 0.57411 + 6.24412/\sqrt{Re_{D'}} - 279.135/Re_{D'} \tag{16}$$

Since the radial velocity is negligibly small, the following radial equilibrium between the radial pressure gradient and centrifugal force holds in the inviscid region, the one outside of the wall boundary layer and outside of the centerline:

$$\frac{\partial p}{\partial r} = \frac{\rho v^2}{r} . \tag{17}$$

From this equation, the tangential velocity can also be calculated by

$$v = \sqrt{\frac{r}{\rho} \cdot \frac{\partial p}{\partial r}} \tag{18}$$

On the other hand, using equations (1) through (5), equation (18) becomes

$$\frac{\partial p}{\partial r} = \frac{1}{r} \left\{ \left(\frac{p^*}{p}\right)^{(\gamma-1)/\gamma} - 1 \right\} \frac{2\gamma}{\gamma-1} \, p \sin^2 \alpha . \tag{19}$$

At a fixed axial distance, this equation can be regarded as an ordinary differential equation for the unknown p, once p* and α are known as functions of r. This equation can easily be solved by using the fourth order Runge-Kutta method, with initial condition given at an appropriate value of r.

Finally, the entropy is related to the temperature and pressure of the fluid by

$$S - S_{in} = c_p \ln \frac{T}{T_{in}} - R \ln \frac{p}{p_{in}} \tag{20}$$

By using equations (1) and (2), equation (20) may be rewritten as

$$S - S_{in} = R \left(\frac{\gamma}{\gamma-1} \ln \frac{T^*}{T_{in}} - \ln \frac{p^*}{p_{in}} \right) \tag{21}$$

CHAPTER IV

EXPERIMENTAL RESULTS AND DISCUSSION

A. Vortex Whistle in the Solid Main Pipe

To compare the measured frequency of the vortex whistle with the one calculated from the analysis, an experiment was initially conducted to measure the velocities and frequencies in the solid main pipe. Previously in Chu [24], such frequency-tangential velocity relationship was compared favorably with the analysis, but the tangential velocity was not directly measured; instead it was estimated by an indirect means. Here the size of the upscaled version enabled us to measure the tangential velocity directly.

Figures 11 and 12 show the examples of the velocity distributions and frequency spectra. We discuss these in detail shortly, but before making comparison with the analysis, it suffices here to note the presence of pure tones in the frequency spectra of Figures 11 and 12.

Details of the mathematical analysis of the unsteady swirling flow in a pipe is given by Kurosaka [1]. As a part of this analysis, the frequency-swirl relationship of an unflow type Ranque-Hilsch tube is determined, from the inviscid flow model, as

$$\omega = \pm \left(|m| - 1 + \lambda^{-2|m|} \right) \Omega \qquad (22)$$

where ω is the lowest eigenvalue of the tangential wave with wave number, m, λ, the ratio of the wall radius, r_o, and the interface between

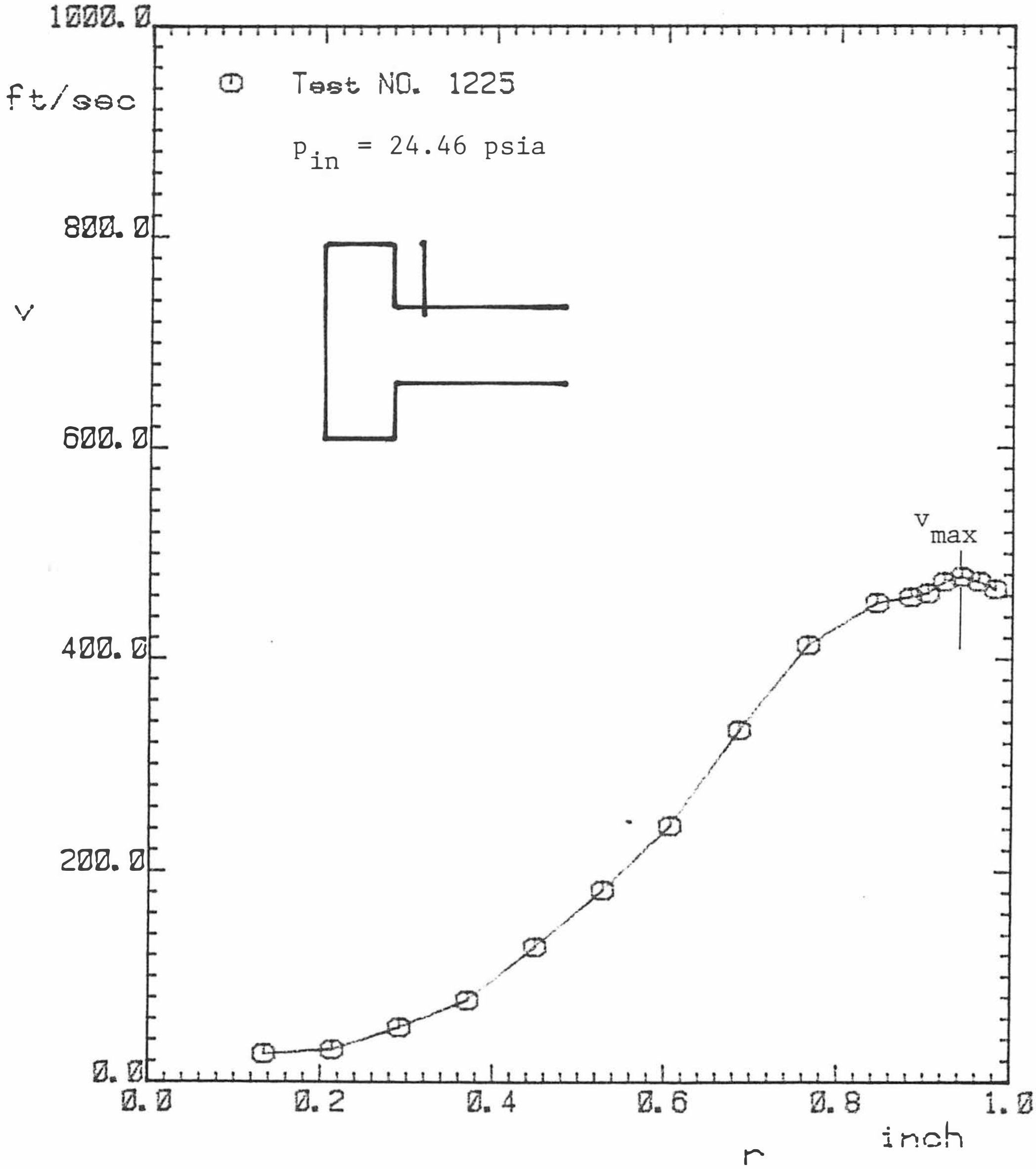

Figure 11. Velocity distribution and frequency spectrum for solid main pipe (low pressure)

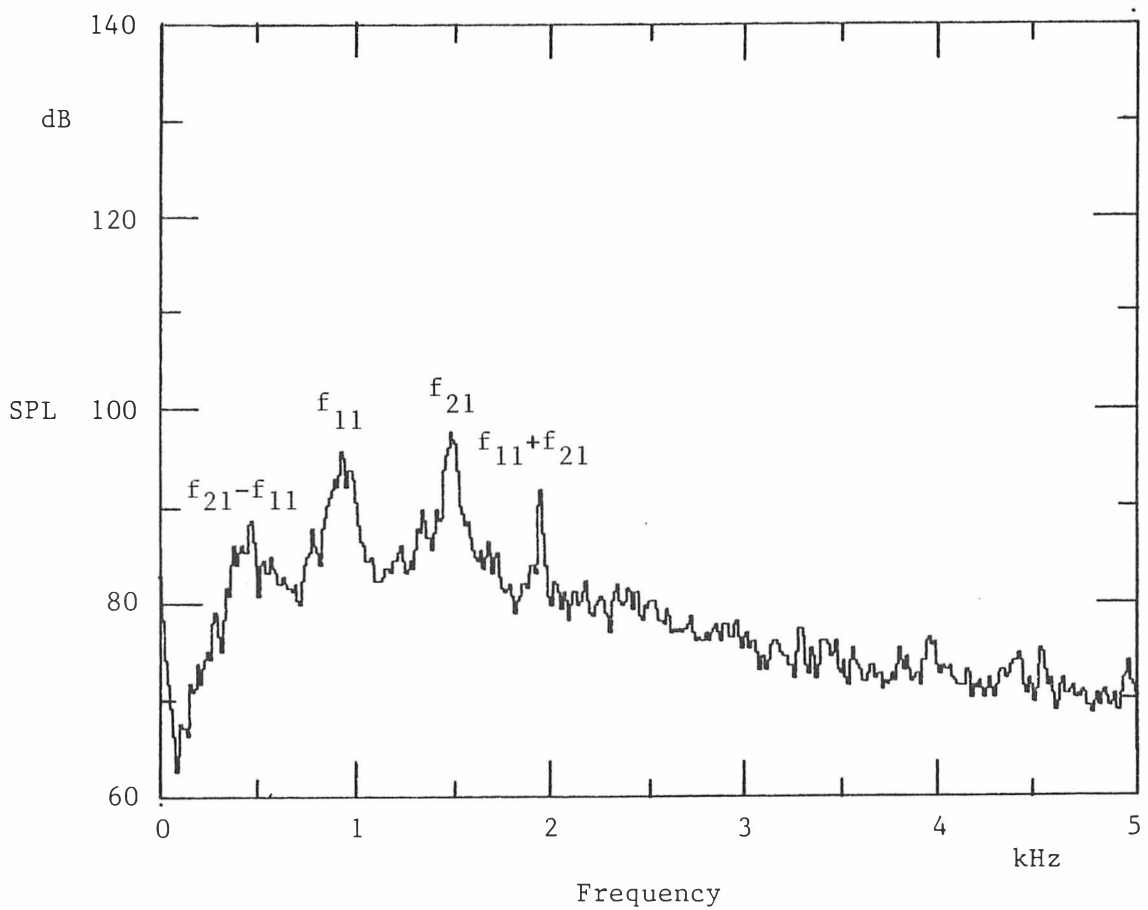

Figure 11. (Continued)

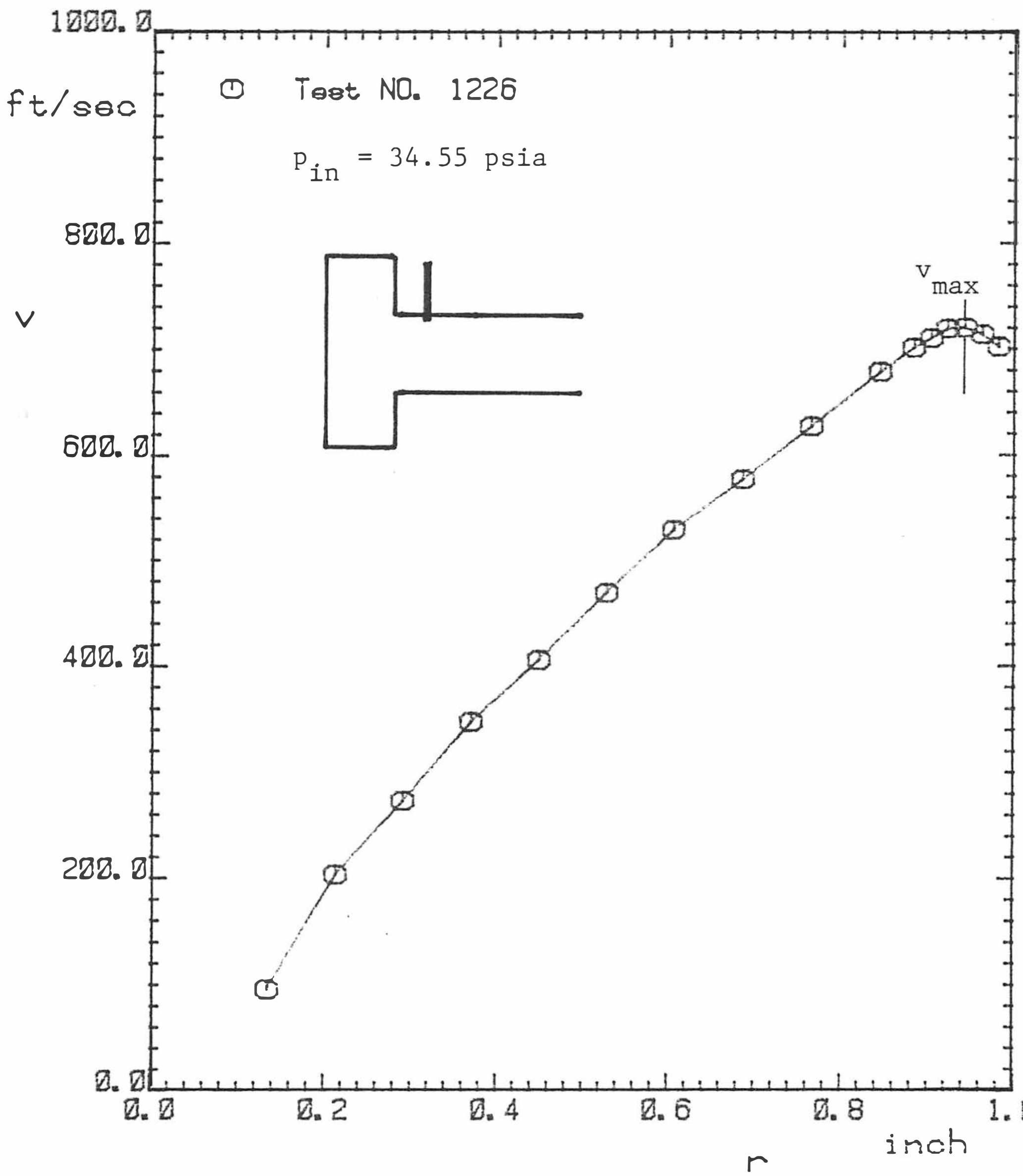

Figure 12. Velocity distribution and frequency spectrum for solid main pipe (high pressure)

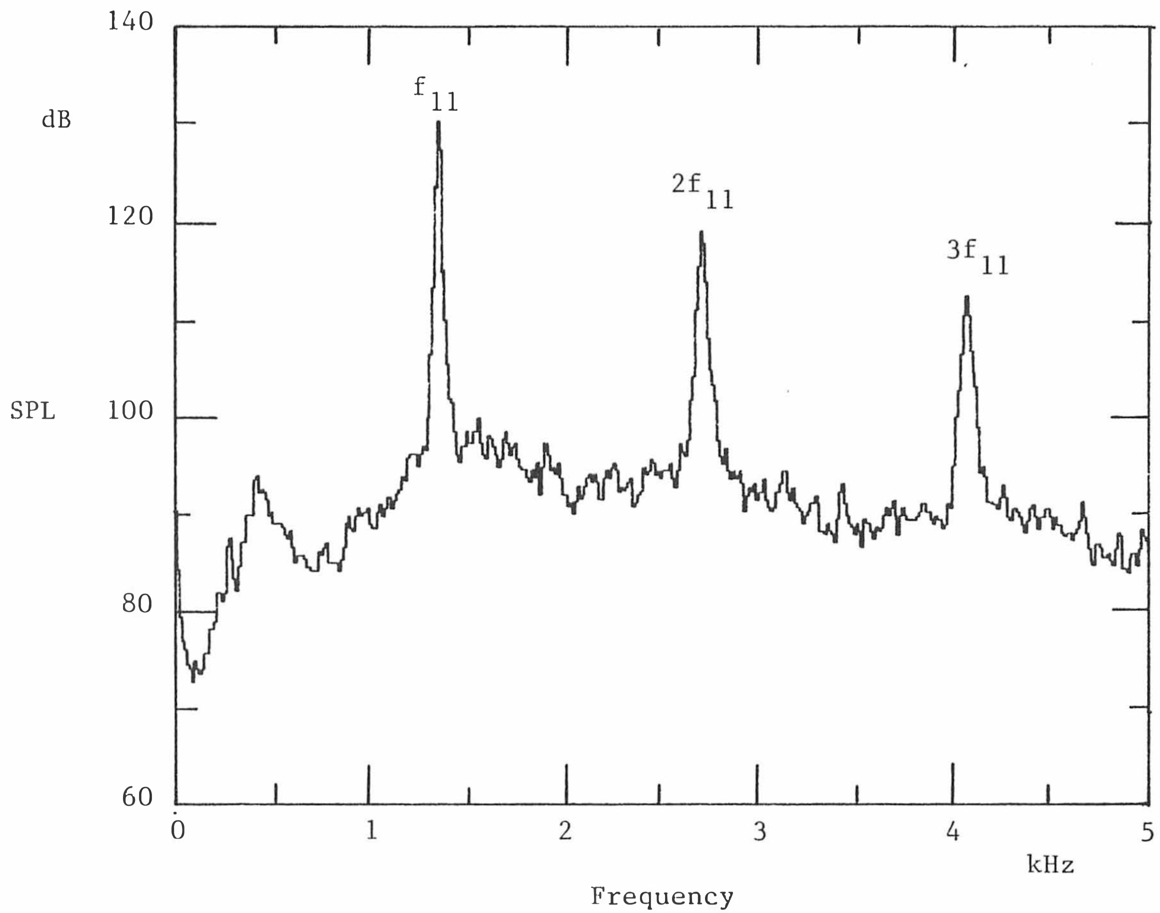

Figure 12. (Continued)

a forced and free vortex, r_i, and Ω, angular velocity of the forced vortex.

The above tangential wave number, m, of the pure tone, where the unsteady disturbances are of the type $e^{i(m\theta - \omega t)}$, is determined from a Lissajous figure. This is obtained by placing two microphones at the same axial and radial positions near the main pipe, but varying relative position in the circumferential direction. These two microphone signals can individually filter only the fundamental frequencies/higher harmonics through two identical filters.

Figure 13(a) shows the example of the Lissajous figure for 90° microphone arrangement using the filters corresponding to the fundamental frequency. From this circle-like figure, the tangential wave number of the pure tone corresponding to the first peak of Figures 11 and 12, denoted as f_{11}, is found, by the reason described in Appendix A, to be the first tangential wave mode, $|m| = 1$. When the first microphone filters f_{11} and the second filters the second peak of Figure 12, the Lissajous figure takes the form of Figure 13(b), and from this the frequency of the second peak is found to be exactly twice that of the first peak, again by the reason stated in Appendix A.

At the low inlet pressure, as Figure 11 shows, the next peak is denoted as f_{21}. The wave number, m , corresponding to this is found to be equal to two, again as shown in the appendix, but the frequency of f_{21} is not equal to twice of f_{11} but only 60% higher. Therefore, this is not the second harmonics, and we will return to this in IV-E. When the peak corresponding to f_{21} becomes as dominant as that of f_{11},

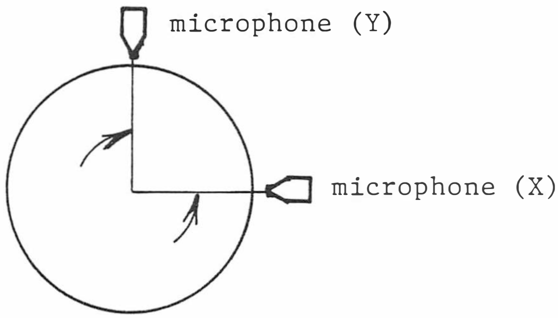

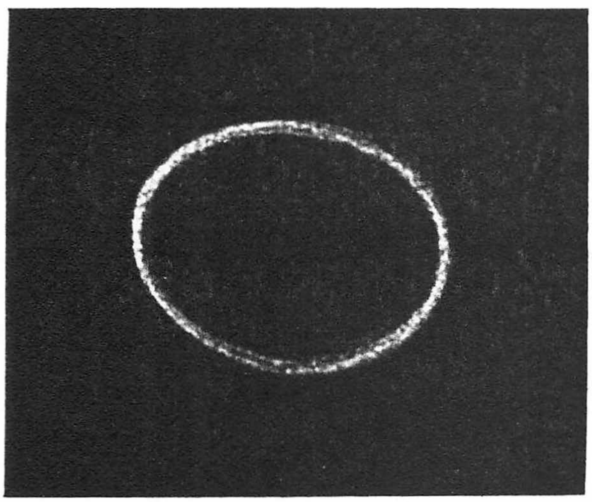

(a)

(X) and (Y) filter only the first peak, f_{11}, of Figure 12.

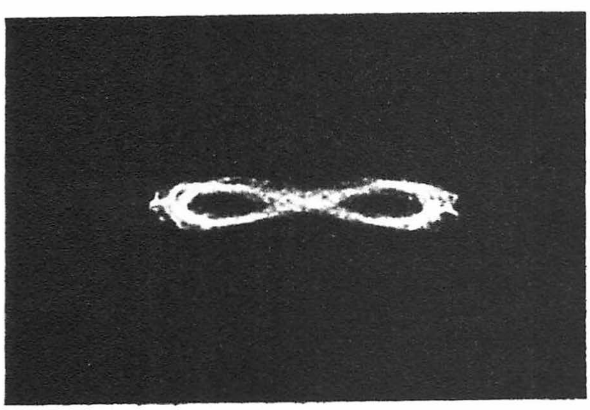

(b)

(X) filters the first peak, f_{11};

(Y) the second peak of Figure 12.

Figure 13. Example of Lissajous figure.

these two frequencies create combination tones: $n_1 f_{11} \pm n_2 f_{21}$ (where n_1 and n_2 are positive integer).

The velocity distribution, shown in Figures 11 and 12, was measured at the axial position located as practically as possible to close the manifold. This position was at Z = 2 inches, which corresponds to the fourth acoustic cavity of the porous main pipe. Note that the tangential velocity distribution is more or less like a forced vortex; it is more so at the higher pressure of Figure 12 than that of the lower pressure of Figure 11.

Figure 14 shows the relationship between the maximum value of the radial distribution of the tangential velocity, v_{max}, and the fundamental frequency of the first tangential wave mode, f_{11}; the radial locations of v_{max} are shown in Figures 11 and 12. The solid line of Figure 14 shows the theoretical calculation from Ref. [1], which is given by

$$\text{for } |m| = 1, \qquad f_{11} = \frac{v_o}{2\pi r_o} \tag{23}$$

where v_o is the tangential velocity at the outer edge of the boundary layer on the wall. The experiment appears to show a good agreement with theory [1].

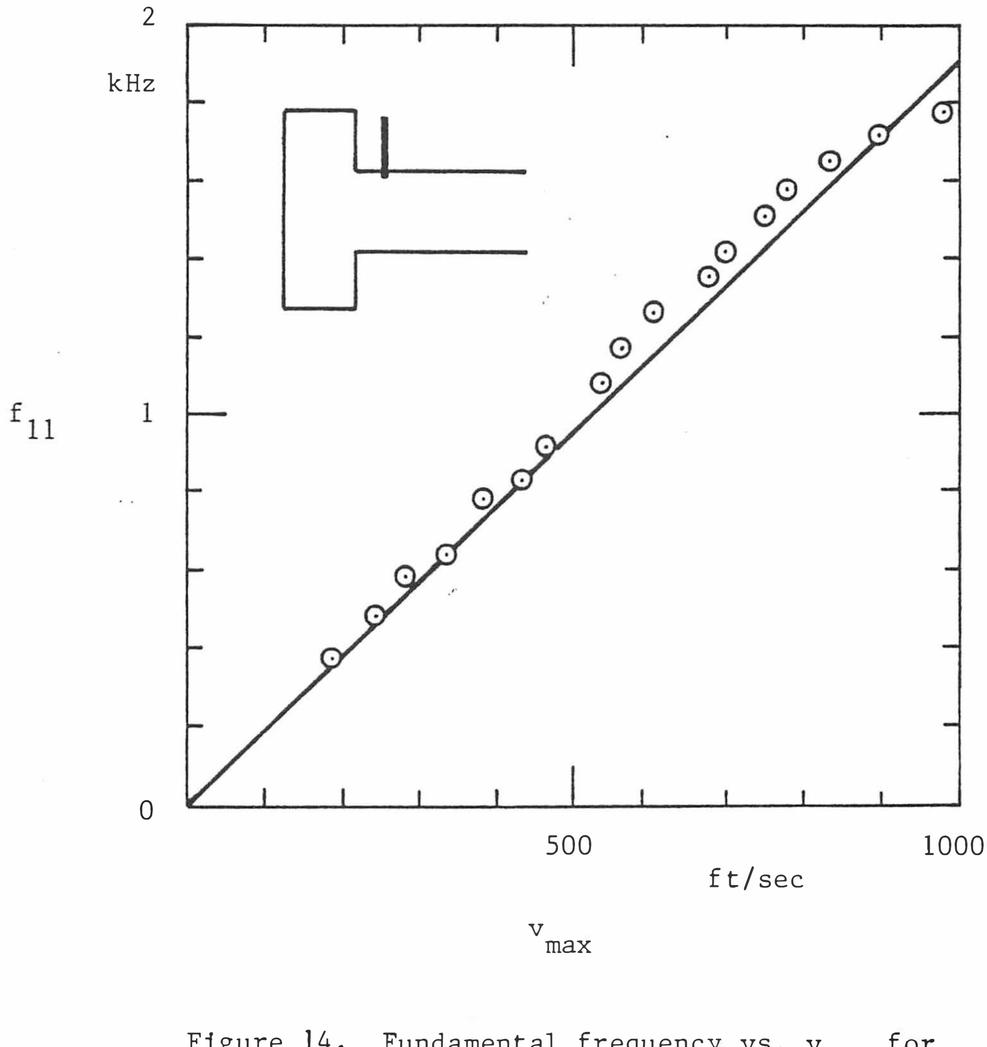

Figure 14. Fundamental frequency vs. v_{max} for solid main pipe.

B. Change from a Forced Vortex to a Rankine Vortex

It was found that the vortex whistle disappears when the opening at the end of the main pipe is partially closed. At the same time, the flow is found to change from a forced vortex to a Rankine vortex.

Figure 15 shows the total and static pressure, tangential velocity, total temperature, entropy and frequency spectrum when the end of the main pipe is fully open. The tangential velocity, Figure 15(b), is, as mentioned, like a forced vortex, except the region near the boundary layer. Figure 15(d) shows that the total temperature near the pipe centerline becomes cold, while the one near the pipe periphery exceeds its inlet temperature. This is precisely the figure showing the radial separation of total temperature or the Ranque-Hilsch effect. The centerline temperature, shown in this figure, was measured by the centerline thermocouple with radial survey probe withdrawn.

From the point of the thermal energy balance, it is expected that the total temperature defect relative to its upcoming value must be accompanied by the excess total temperature. Now it may not appear possible that a relatively narrow area near the periphery, corresponding to the excess temperature, can balance with a seemingly wider area near the centerline corresponding to the temperature defect. The balance is, however, achieved by the two reasons: (1) the larger radius near the periphery serves to enlarge the annular area, and (2) the axial velocity near the centerline has a reverse flow, as seen

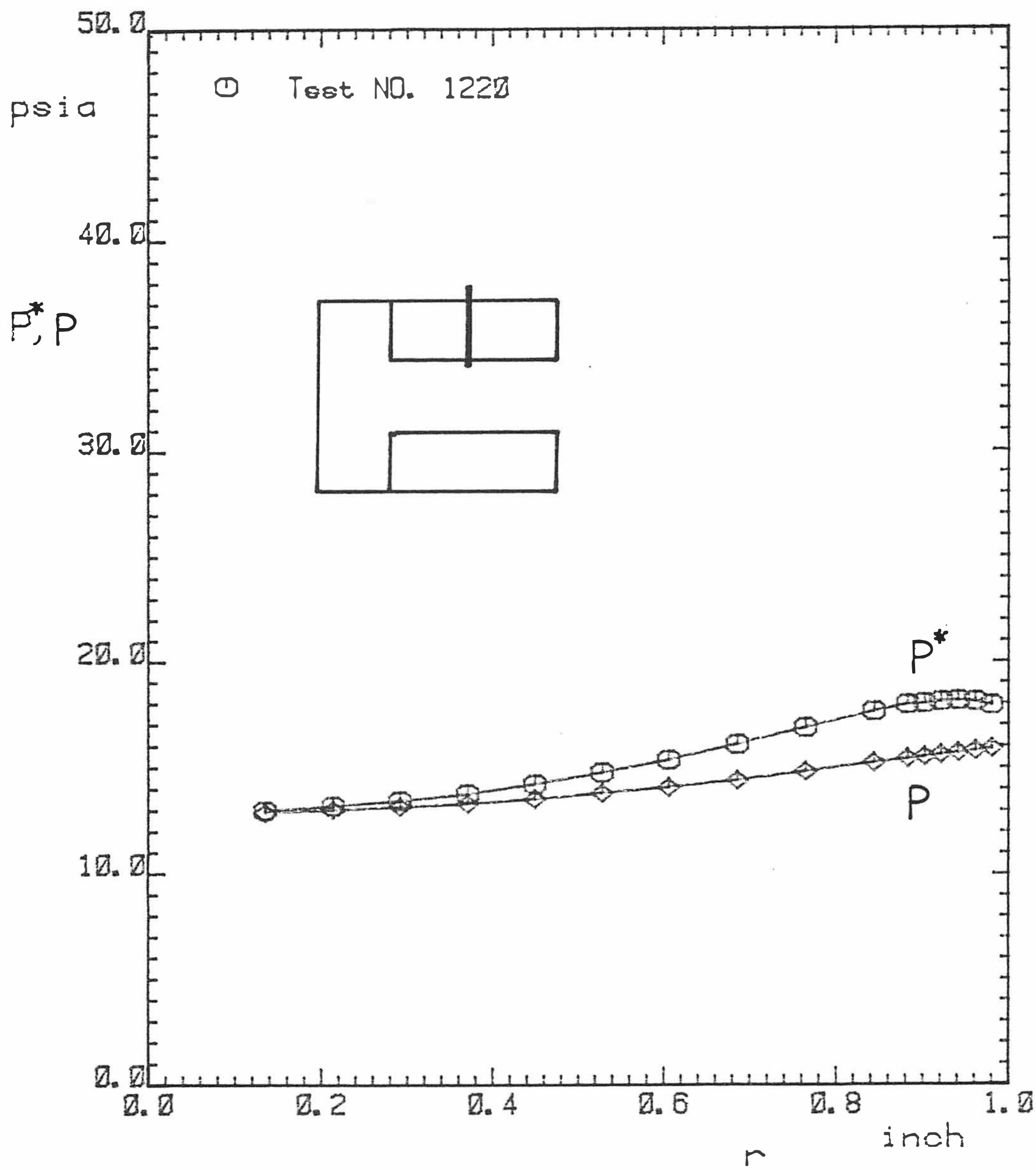

(a) total and static pressure

Figure 15. Data for fully opened exit area.

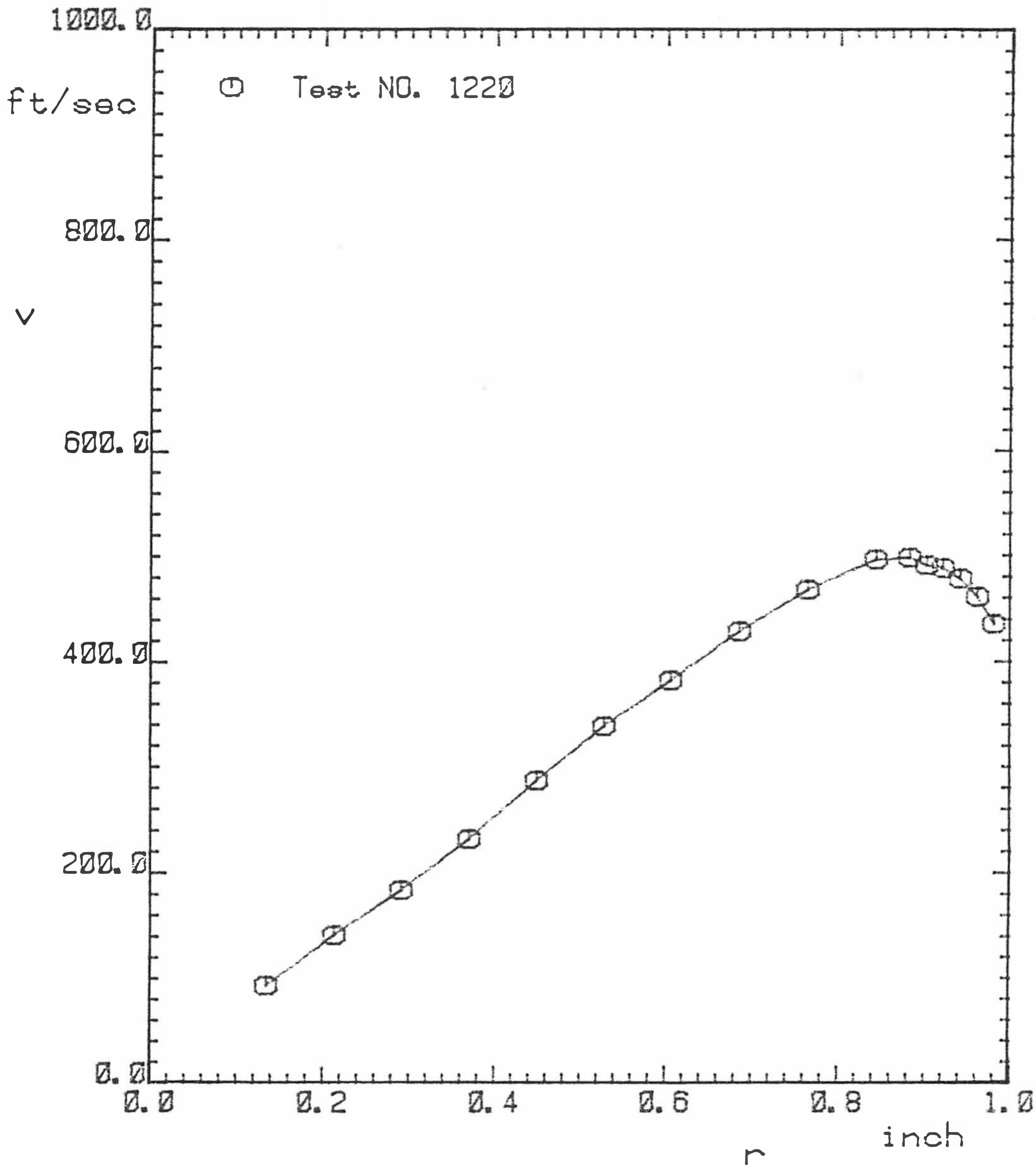

(b) tangential velocity

Figure 15. (Continued)

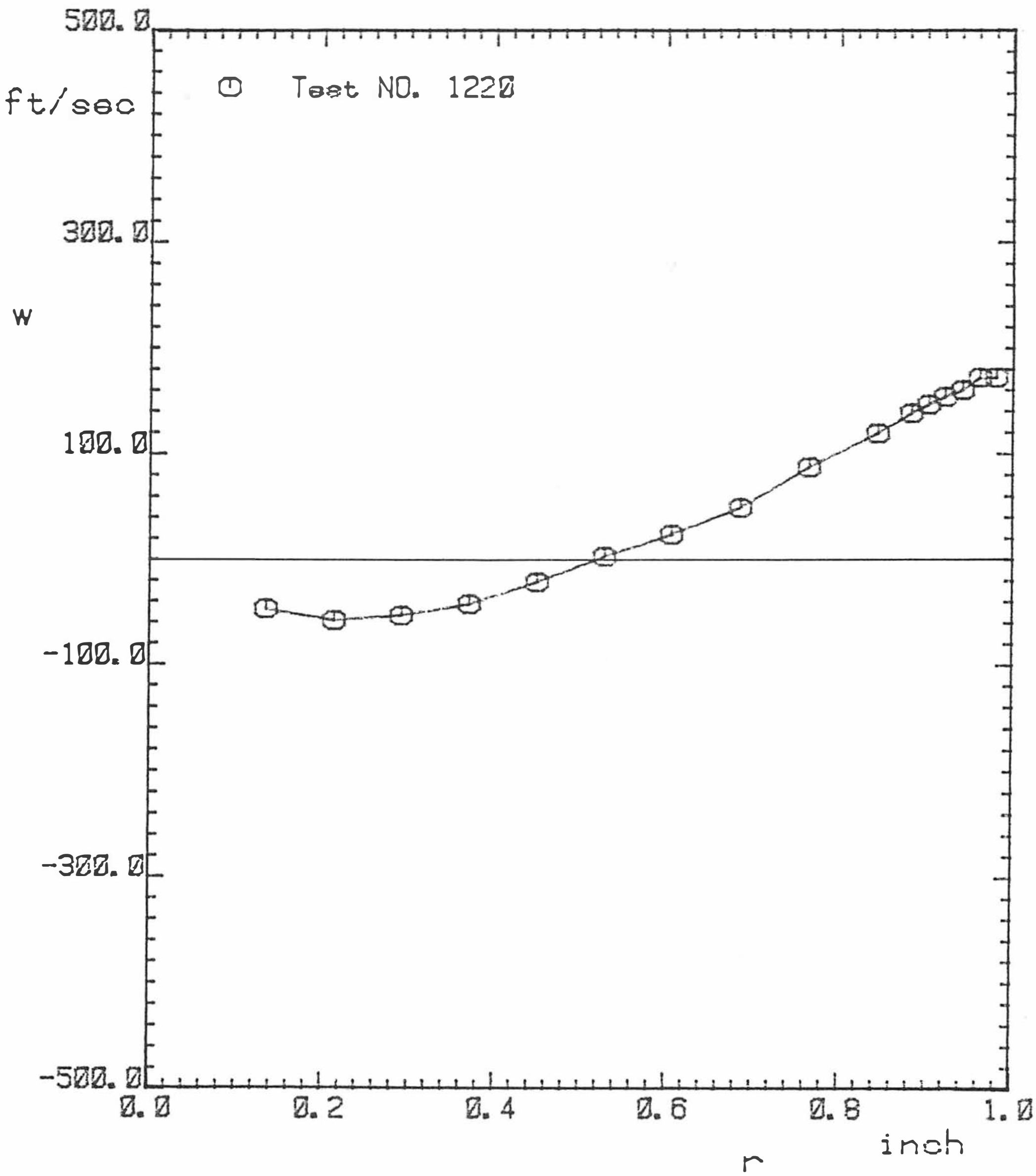

(c) axial velocity

Figure 15. (Continued)

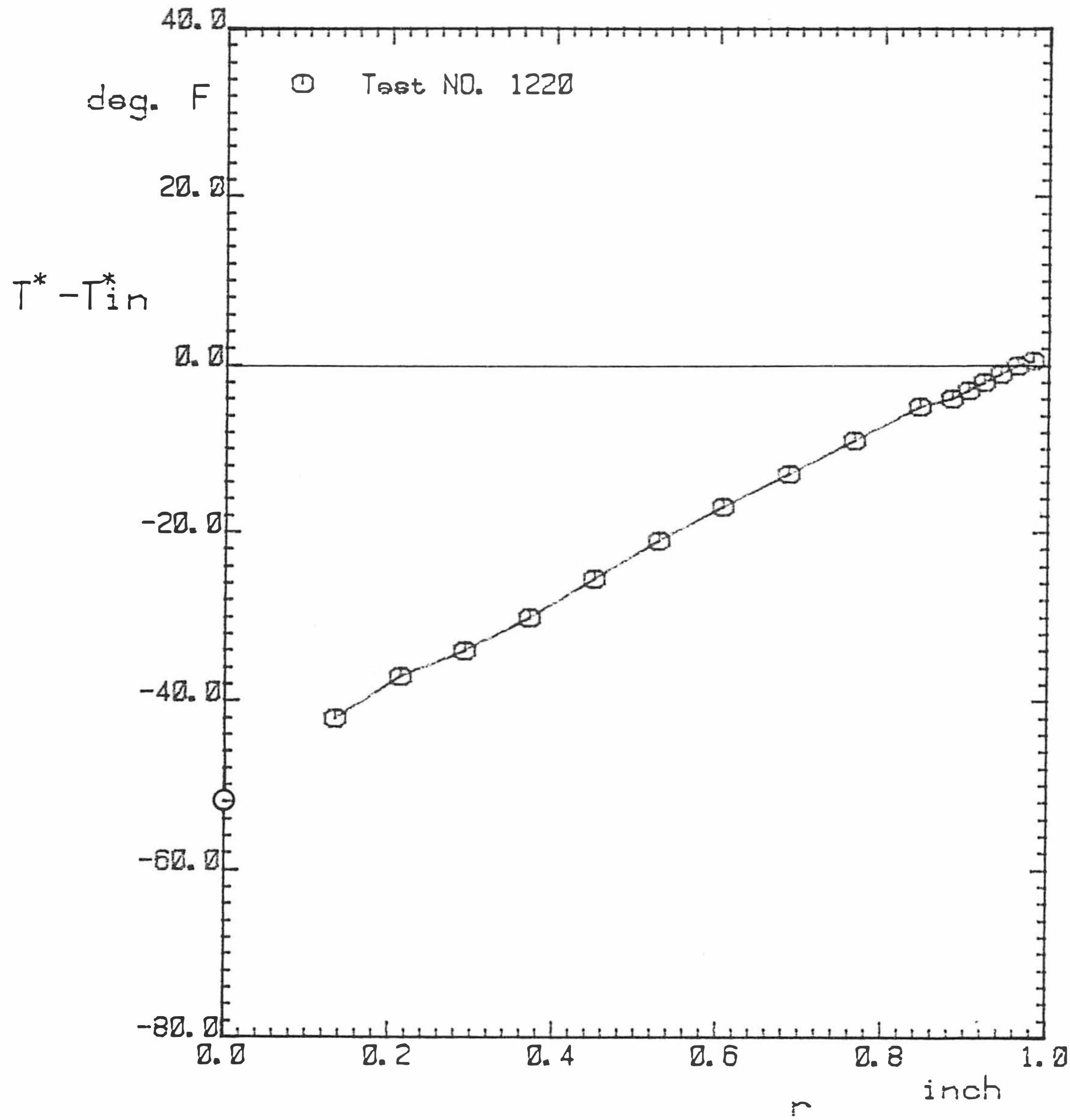

(d) total temperature

Figure 15. (Continued)

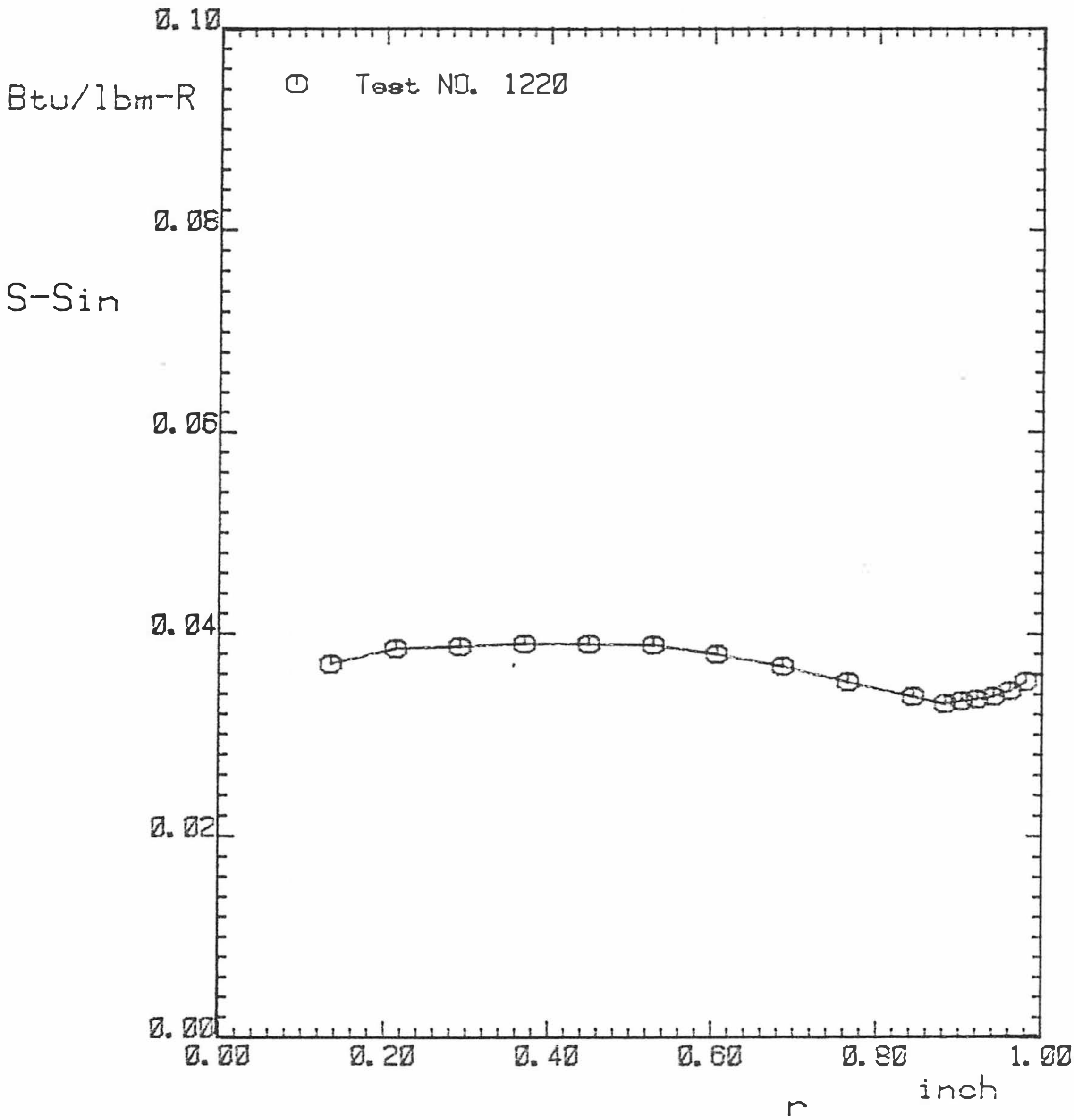

(e) entropy

Figure 15. (Continued)

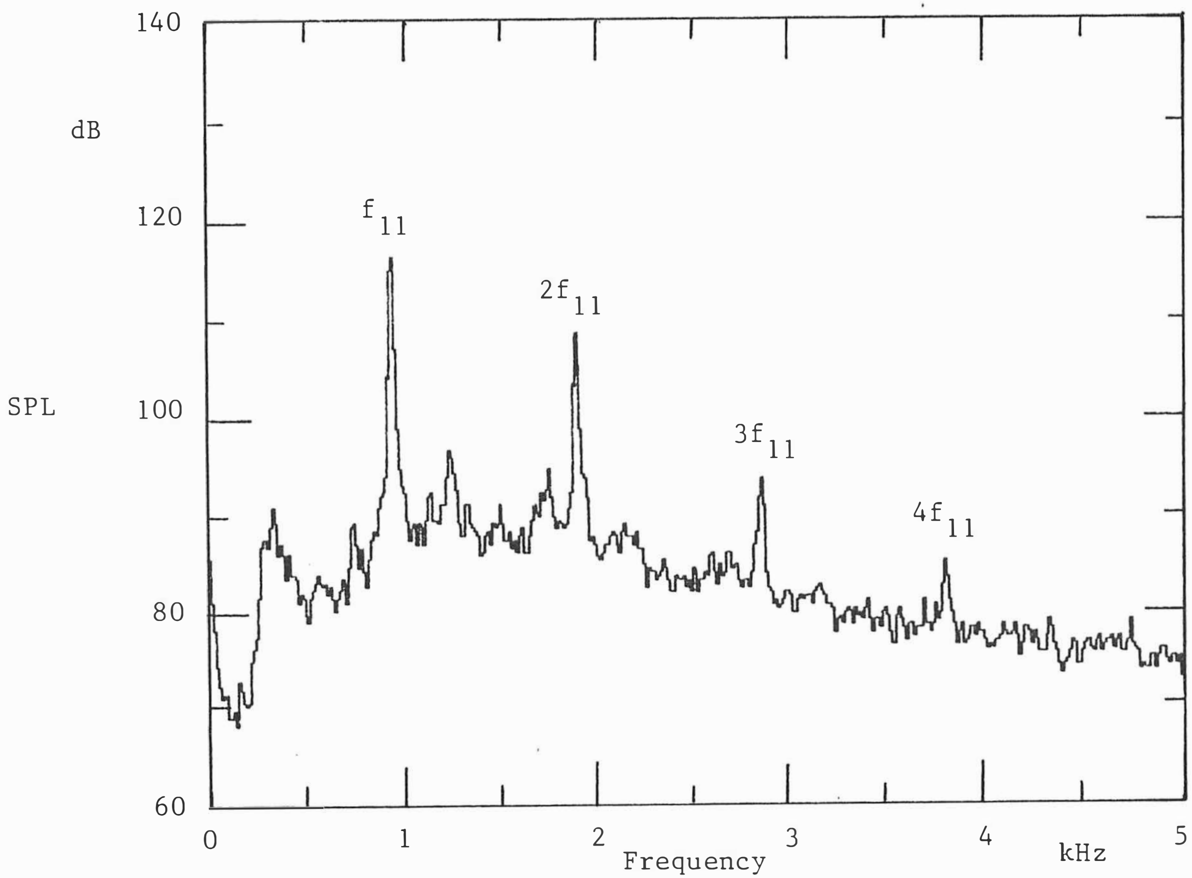

(f) frequency spectrum

Figure 15. (Continued)

from Figure 15(c); this back flow will be discussed later in detail. The reverse flow near the centerline serves to reduce the mass flow carrying the lower thermal energy. Also, Figure 15(e) shows that the entropy outside of the boundary layer is more or less uniform in the radial direction; this reconfirms that the flow external to the boundary layer can indeed be approximated as the inviscid region. The aforementioned presence of pure tones or vortex whistle, with the fundamental frequency and its higher harmonics, is also easily recognizable in Figure 15(f).

Figure 16 shows the radial survey for the exit plate with an opening of 0.4 inch in diameter; corresponding to this reduced exit area, the tangential velocity of Figure 16(b) is observed to change to a Rankine vortex. The total temperature (Figure 16(d)) becomes almost constant except in a core region near the pipe centerline; the frequency spectrum of Figure 16(f) has no distinctive peaks corresponding to the vortex whistle. This does support our view that acoustic streaming induced by the vortex whistle introduces the total temperature separation. The increase of entropy near the centerline, shown in Figure 16(e), is what is to be expected from the presence of high shear corresponding to the large tangential velocity near the core.

The process of a transition from the fully open tube to the above 0.4 inch opening is shown in Figures 17, 18 and 19; they correspond to 1.5, 1.25 and 1.0 inch of exit diameter, respectively. At d = 1.5 inches, the forced vortex no longer fills up the entire tube. The tangential velocity near the periphery becomes flattened, and the region of a forced vortex becomes reduced. As comparison

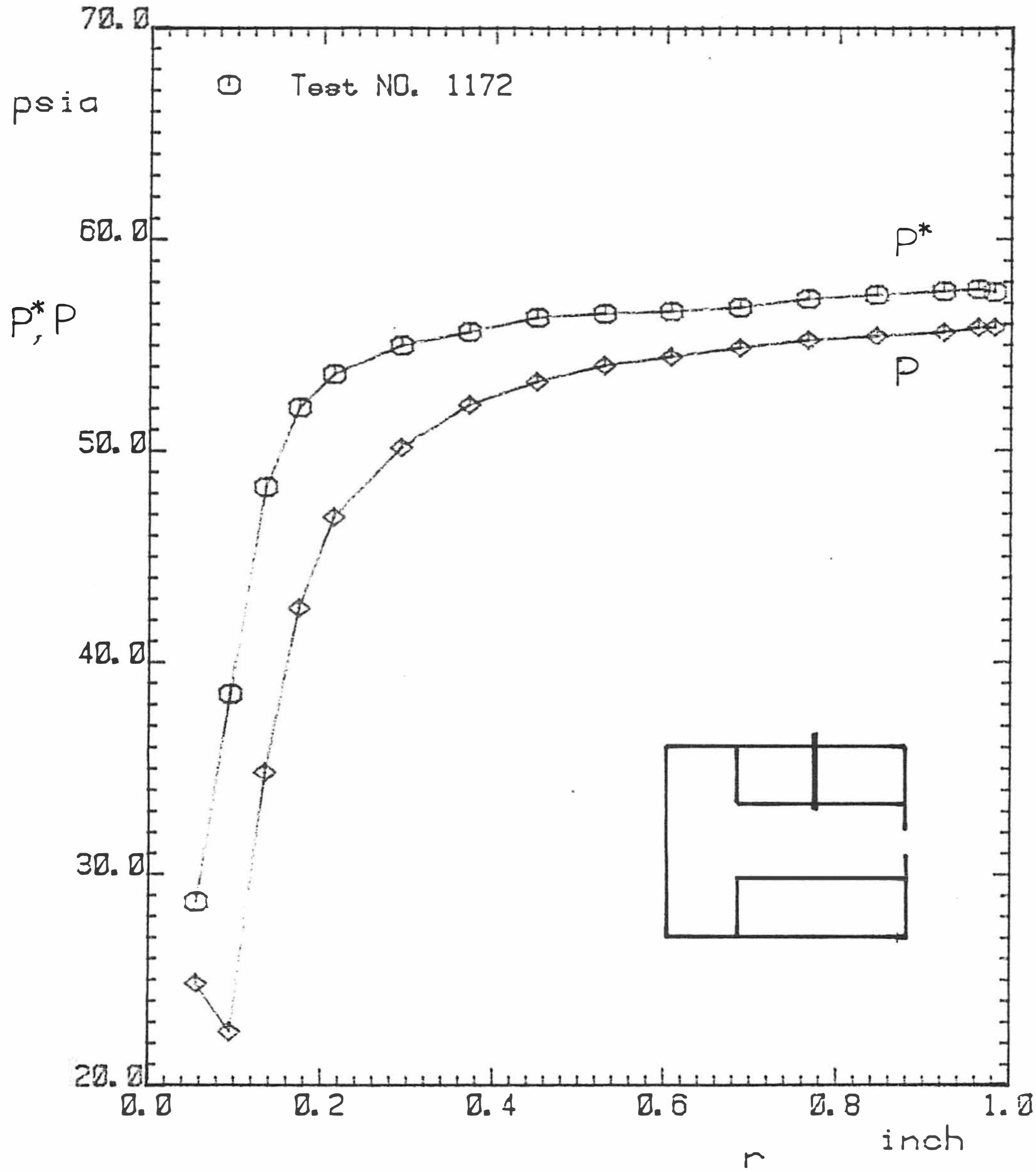

(a) total and static pressures

Figure 16. Data for 0.4 inch exit opening diameter.

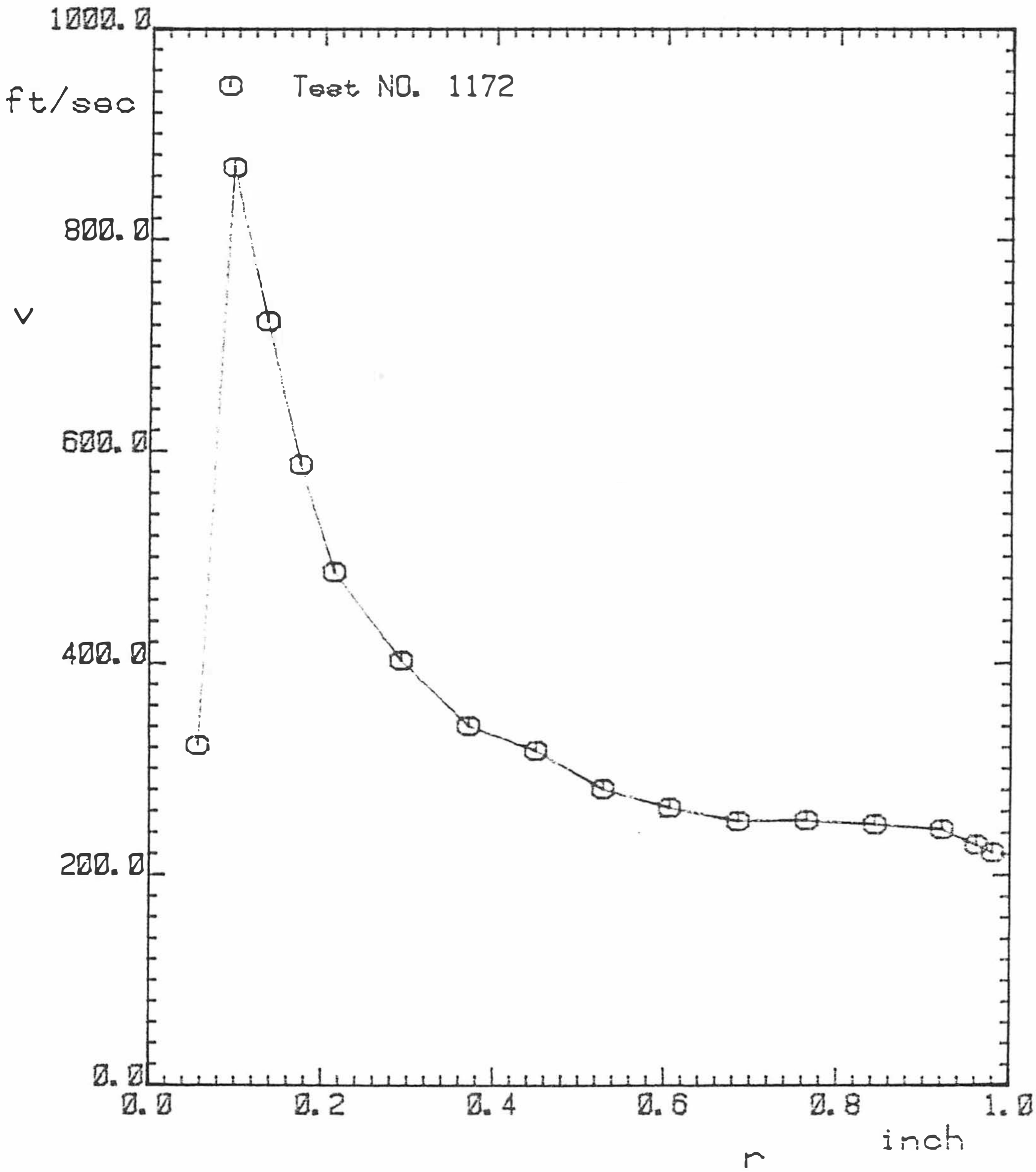

(b) tangential velocity

Figure 16. (Continued)

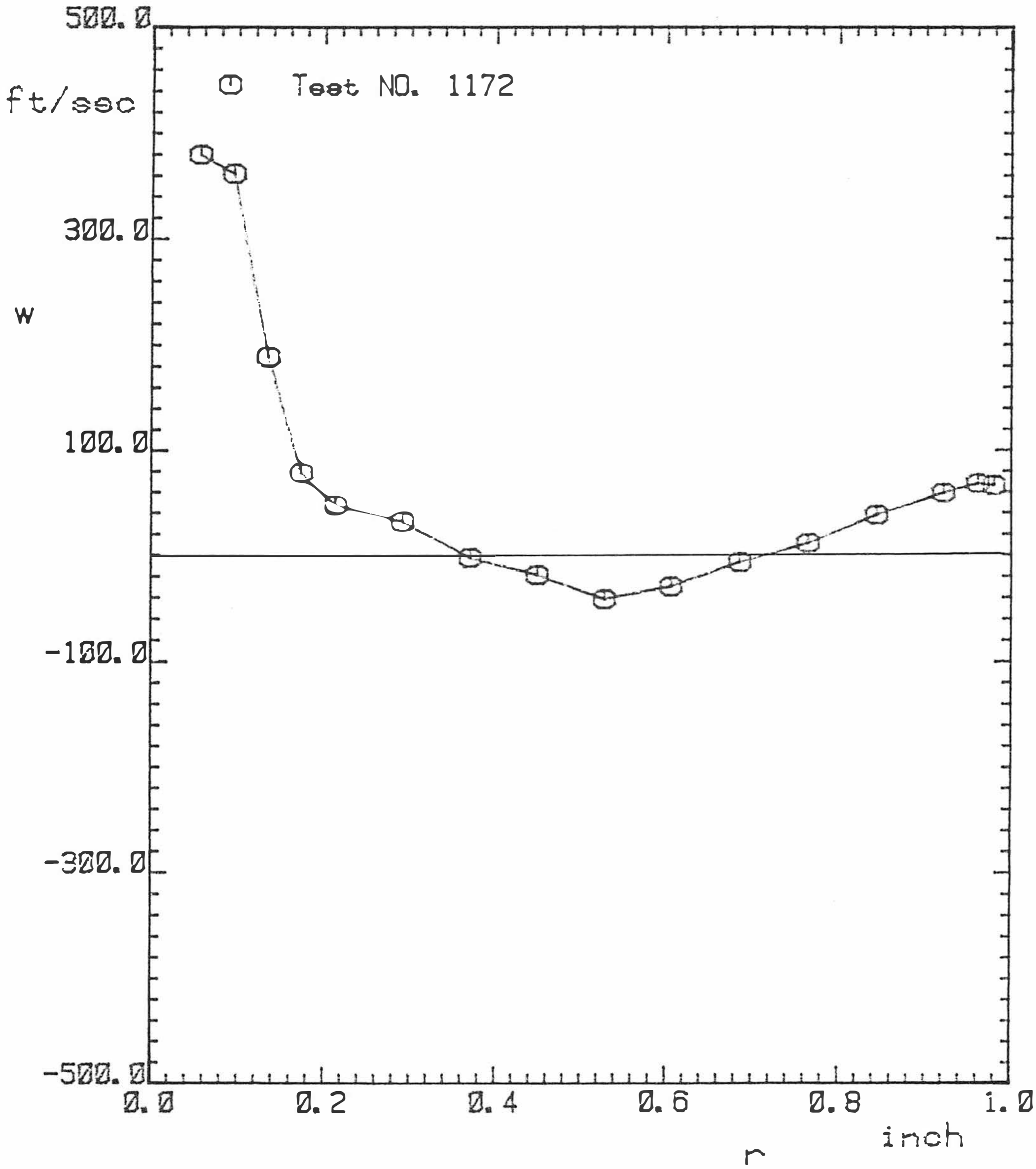

(c) axial velocity

Figure 16. (Continued)

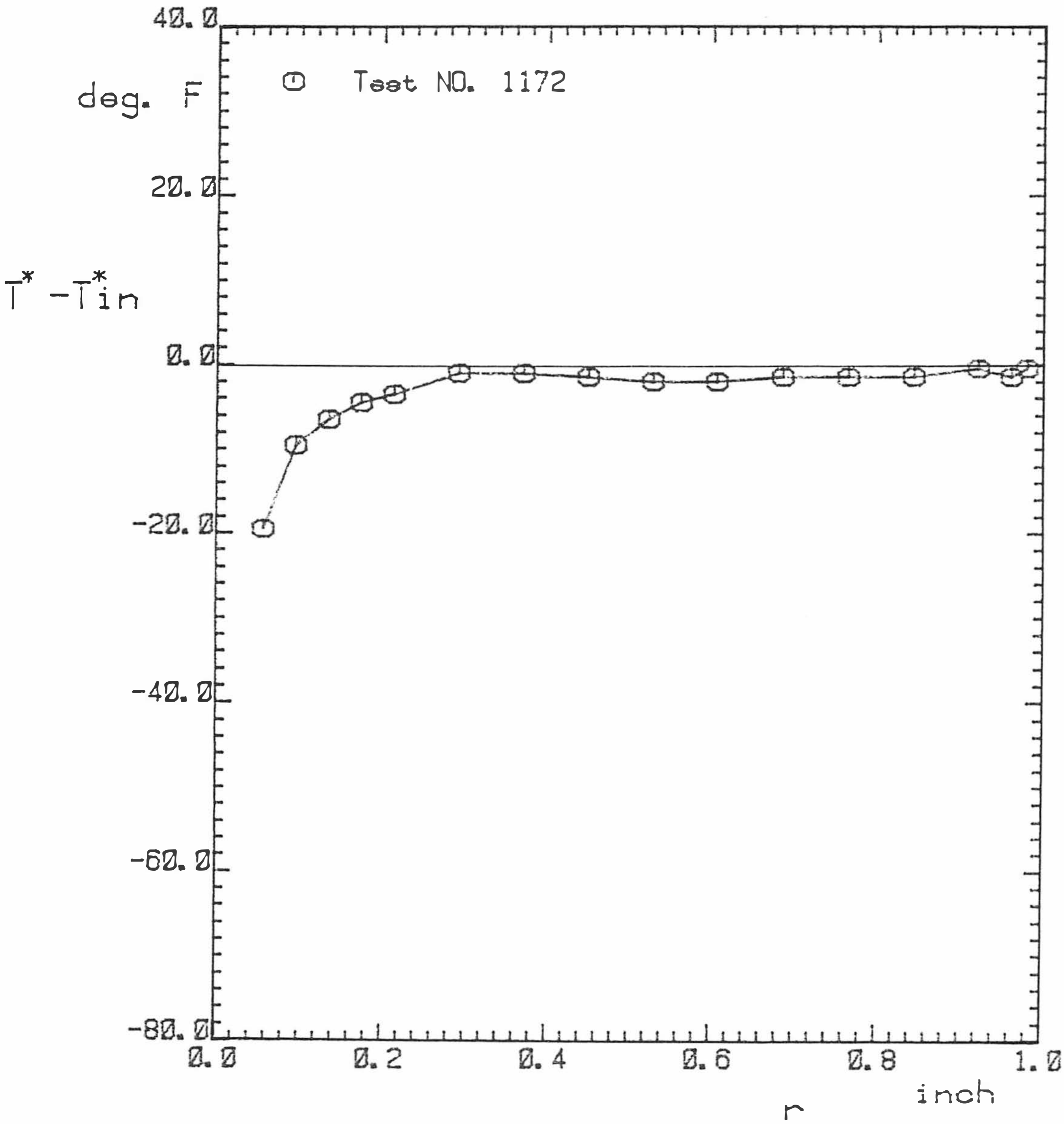

(d) total temperature

Figure 16. (Continued)

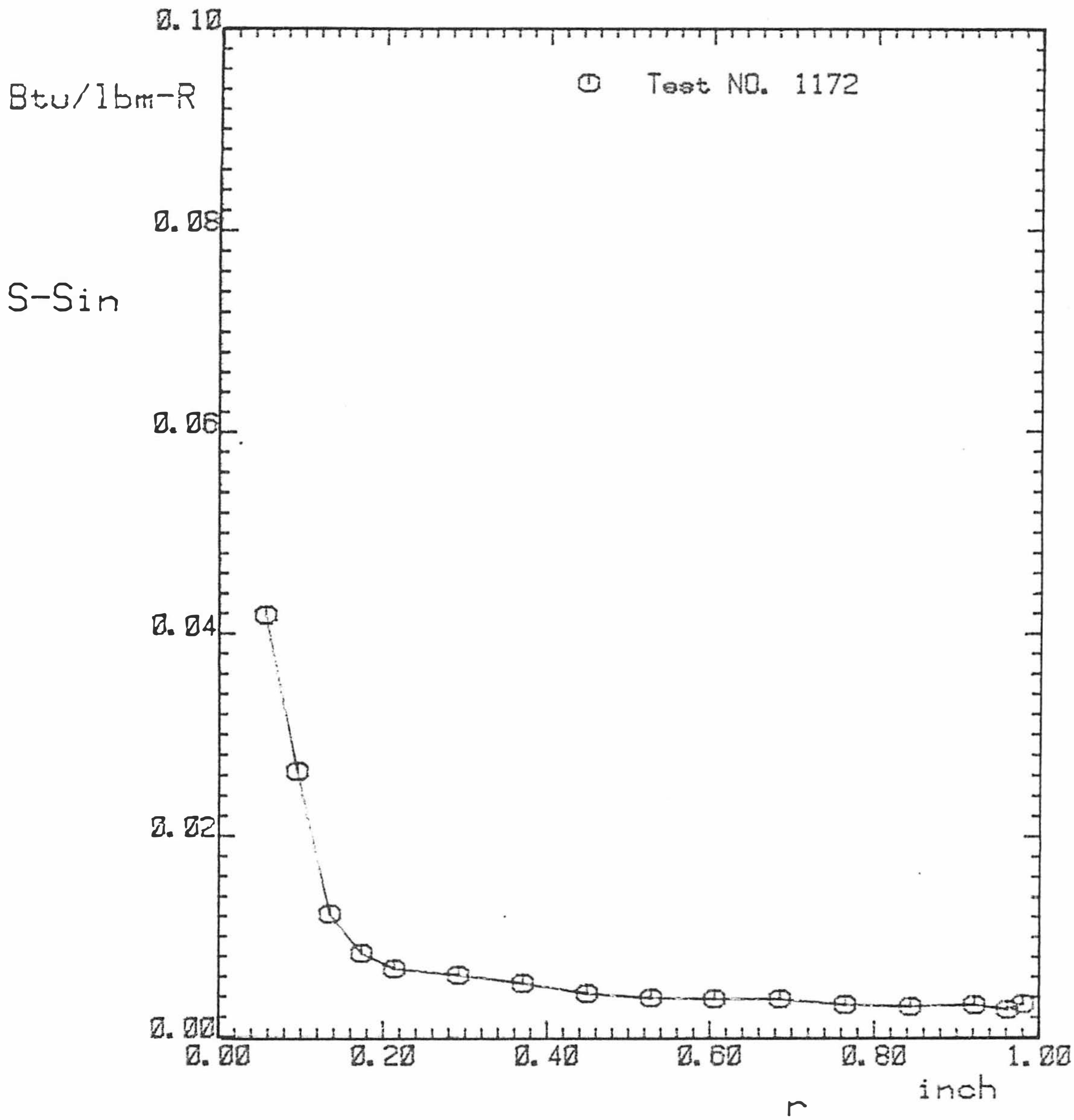

(e) entropy

Figure 16. (Continued)

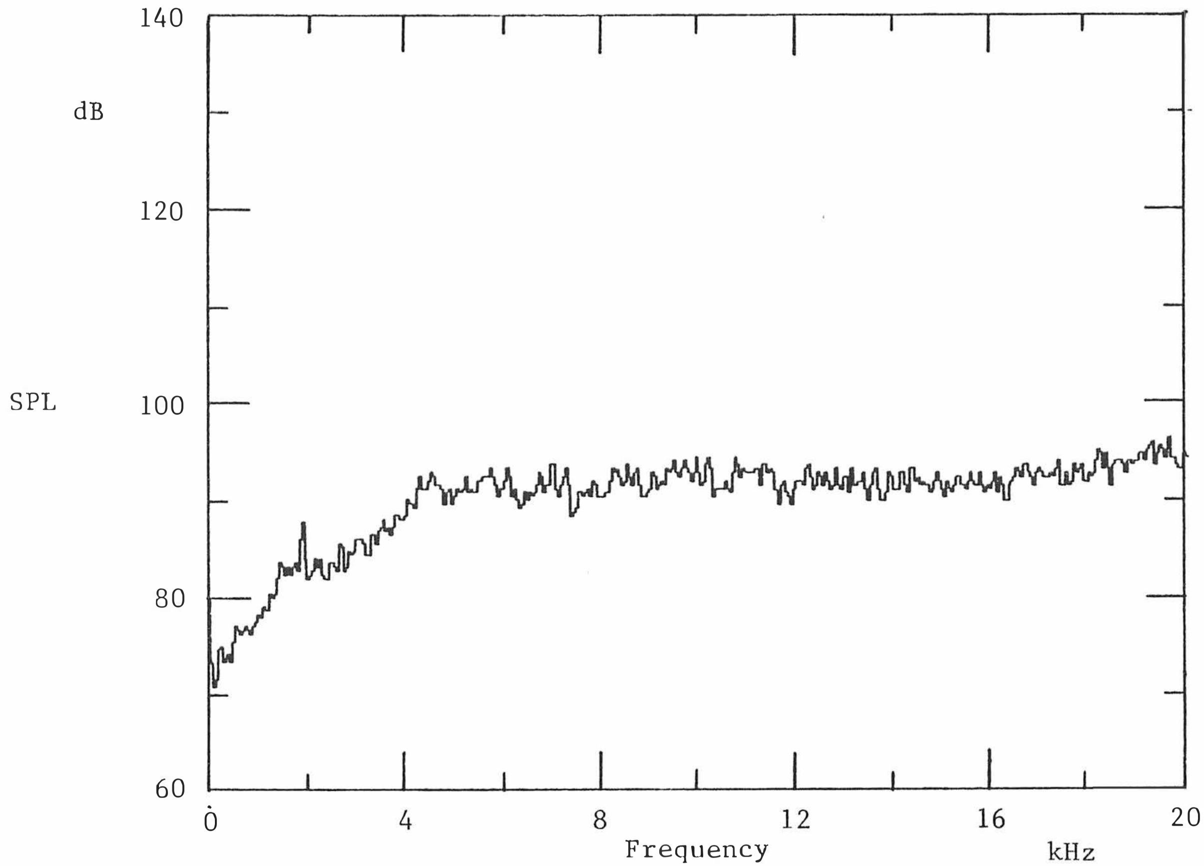

(f) frequency spectrum

Figure 16. (Continued)

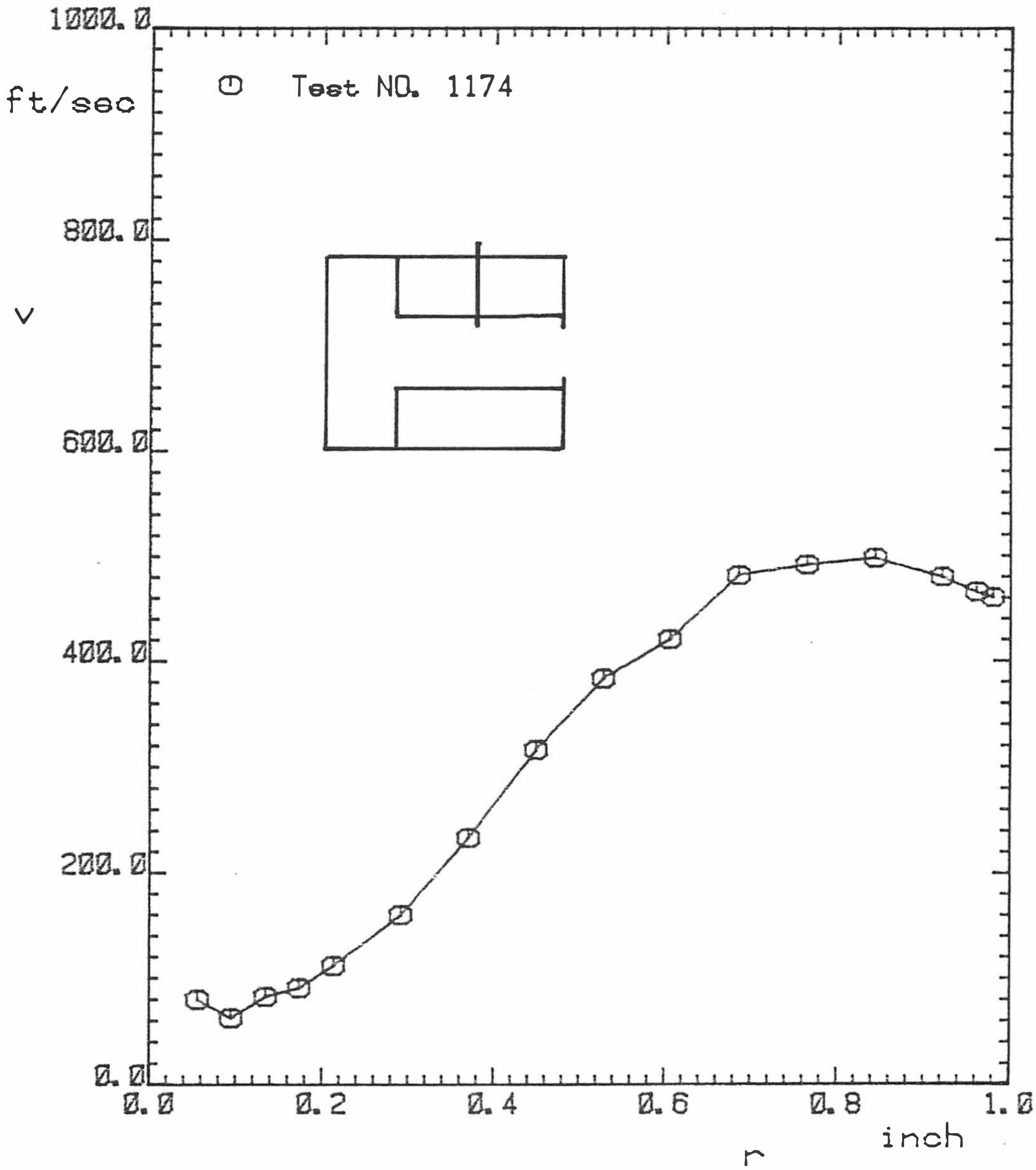

(a) tangential velocity

Figure 17. Data for 1.5 inches exit opening diameter.

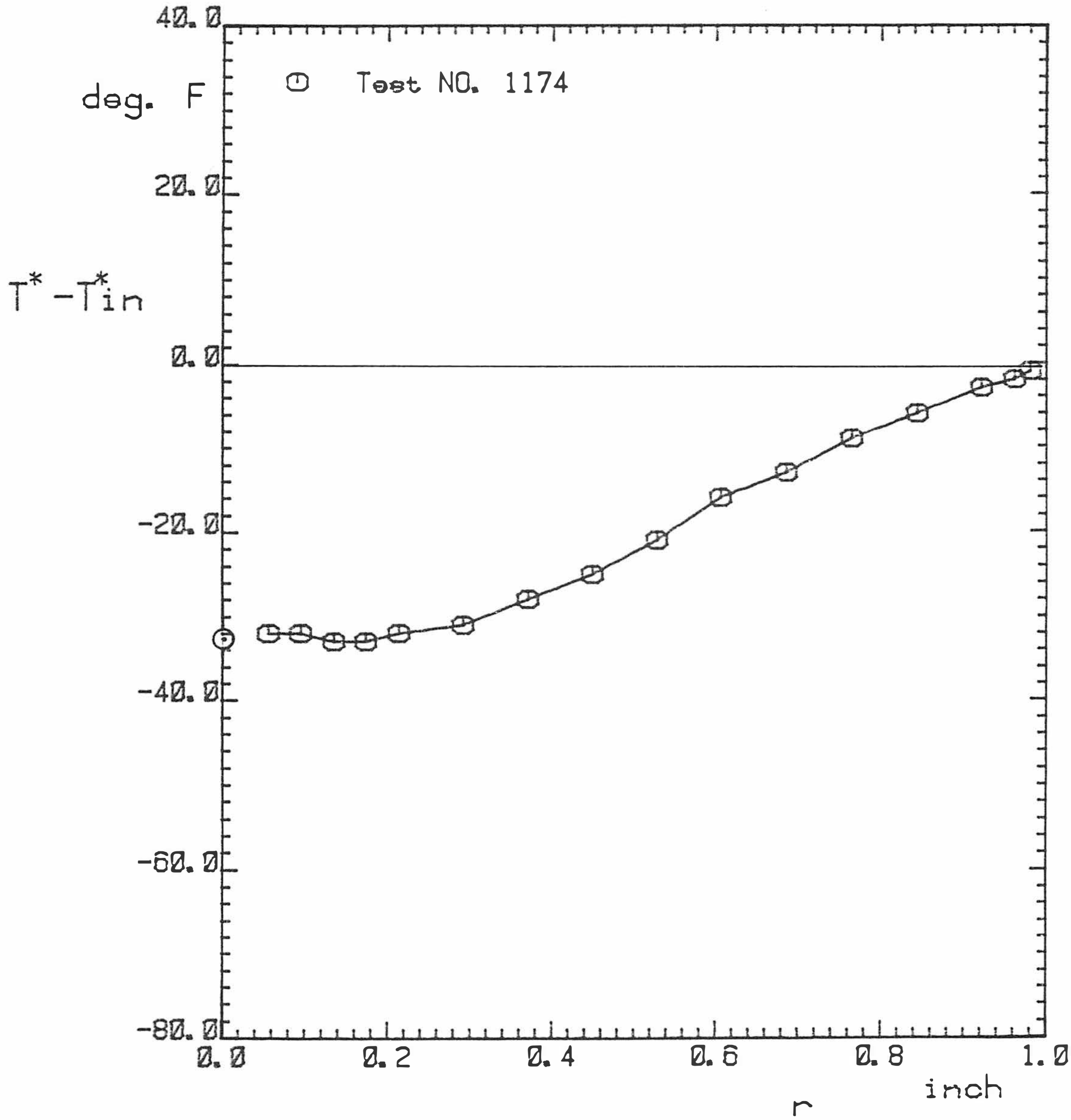

(b) total temperature

Figure 17. (Continued)

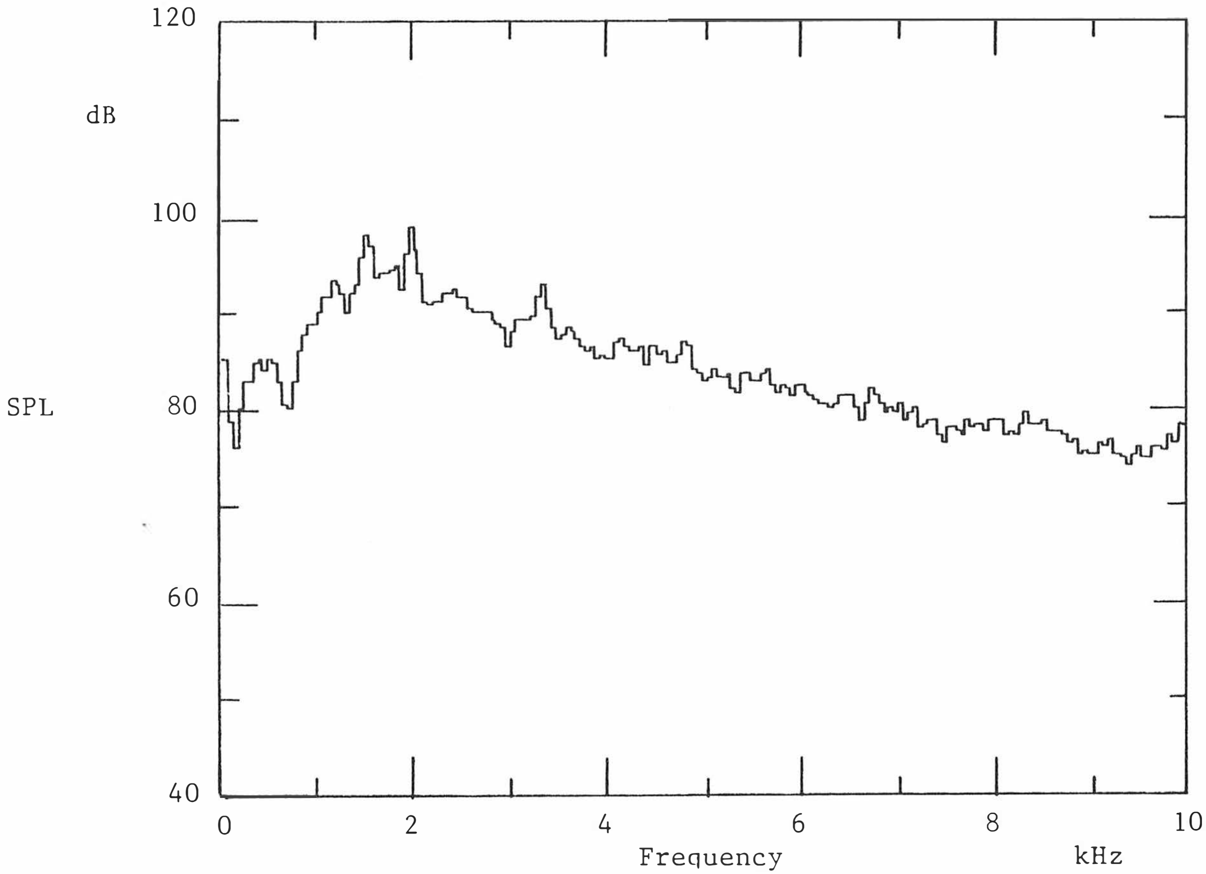

(c) frequency spectrum

Figure 17. (Continued)

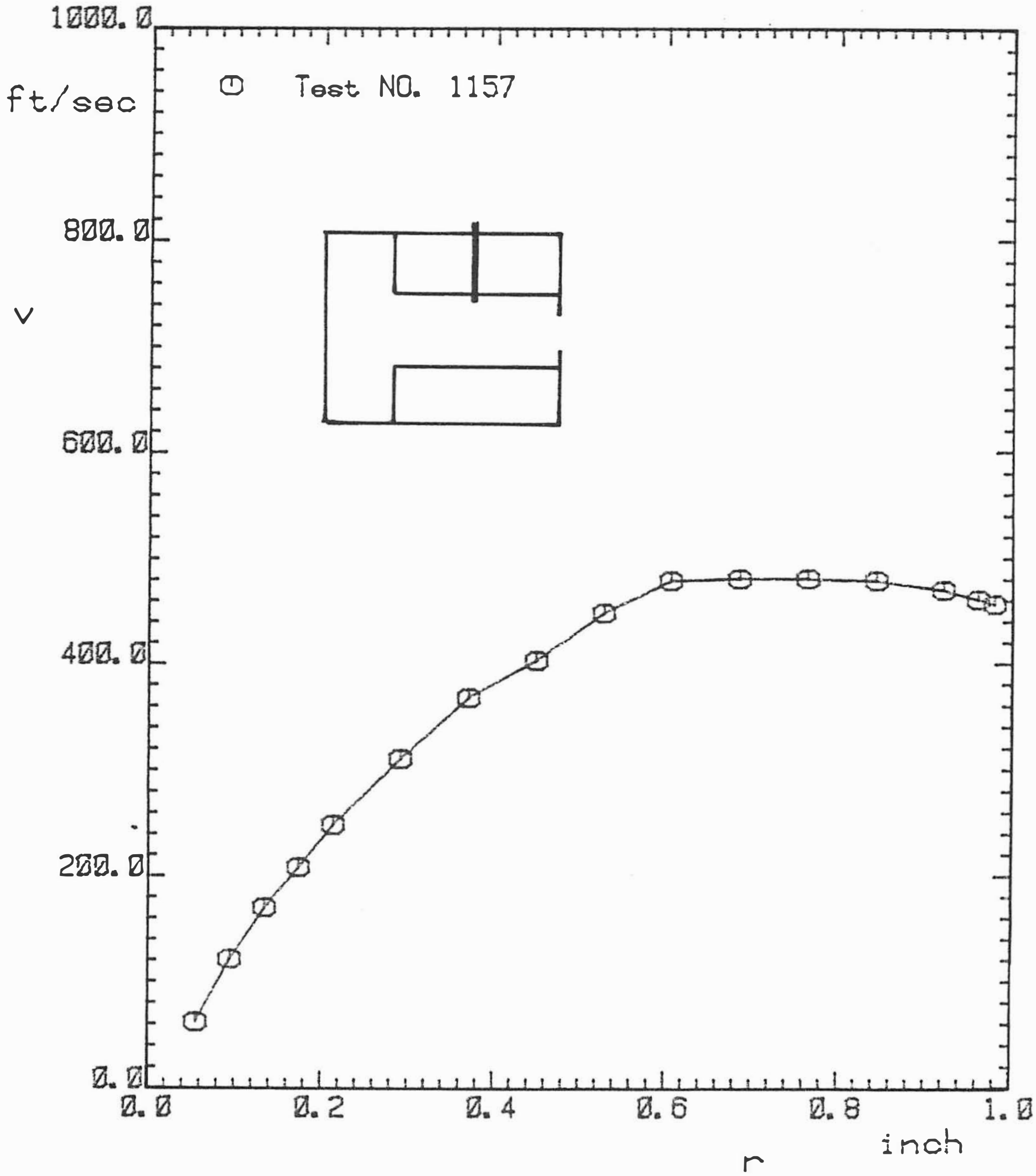

(a) tangential velocity

Figure 18. Data for 1.25 inches exit opening diameter.

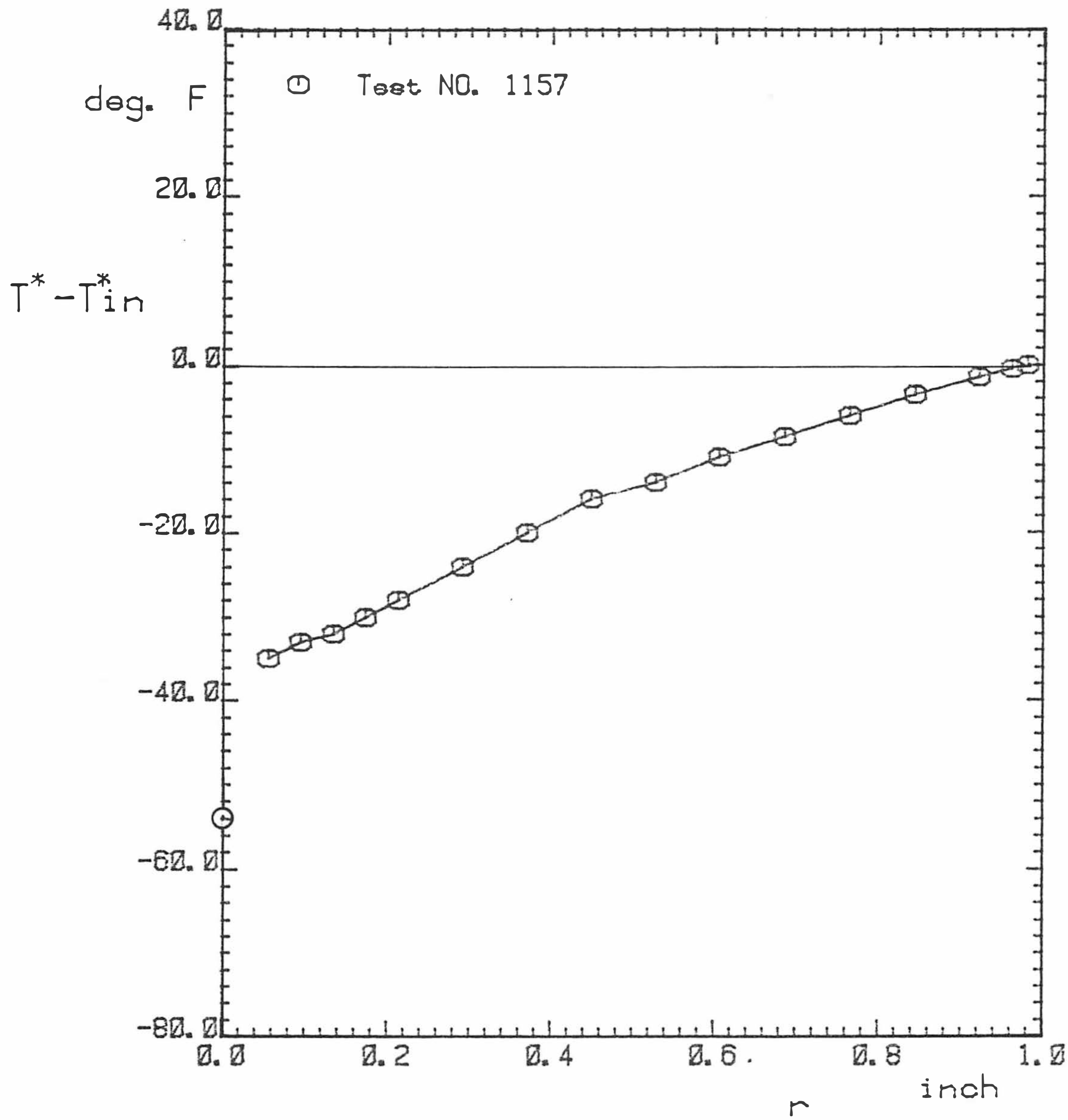

(b) total temperature

Figure 18. (Continued)

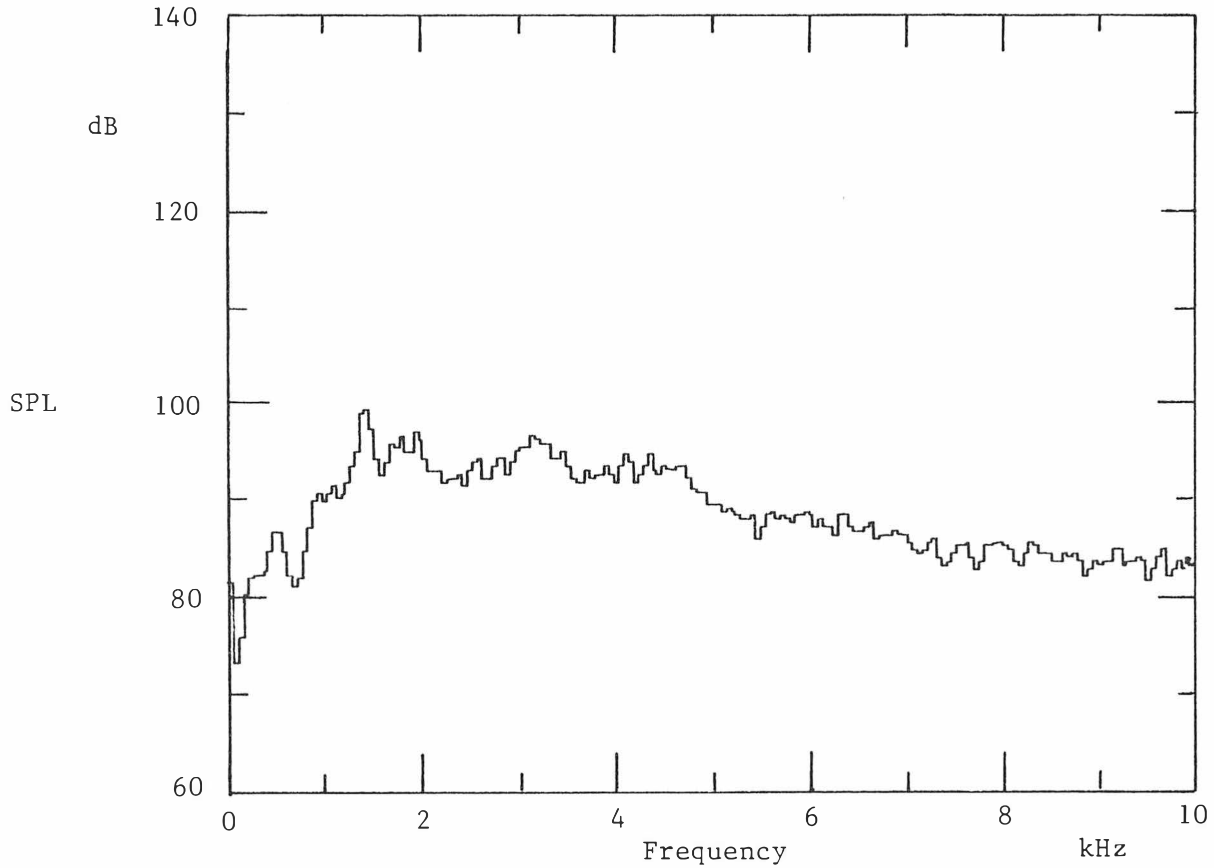

(c) frequency spectrum

Figure 18. (Continued)

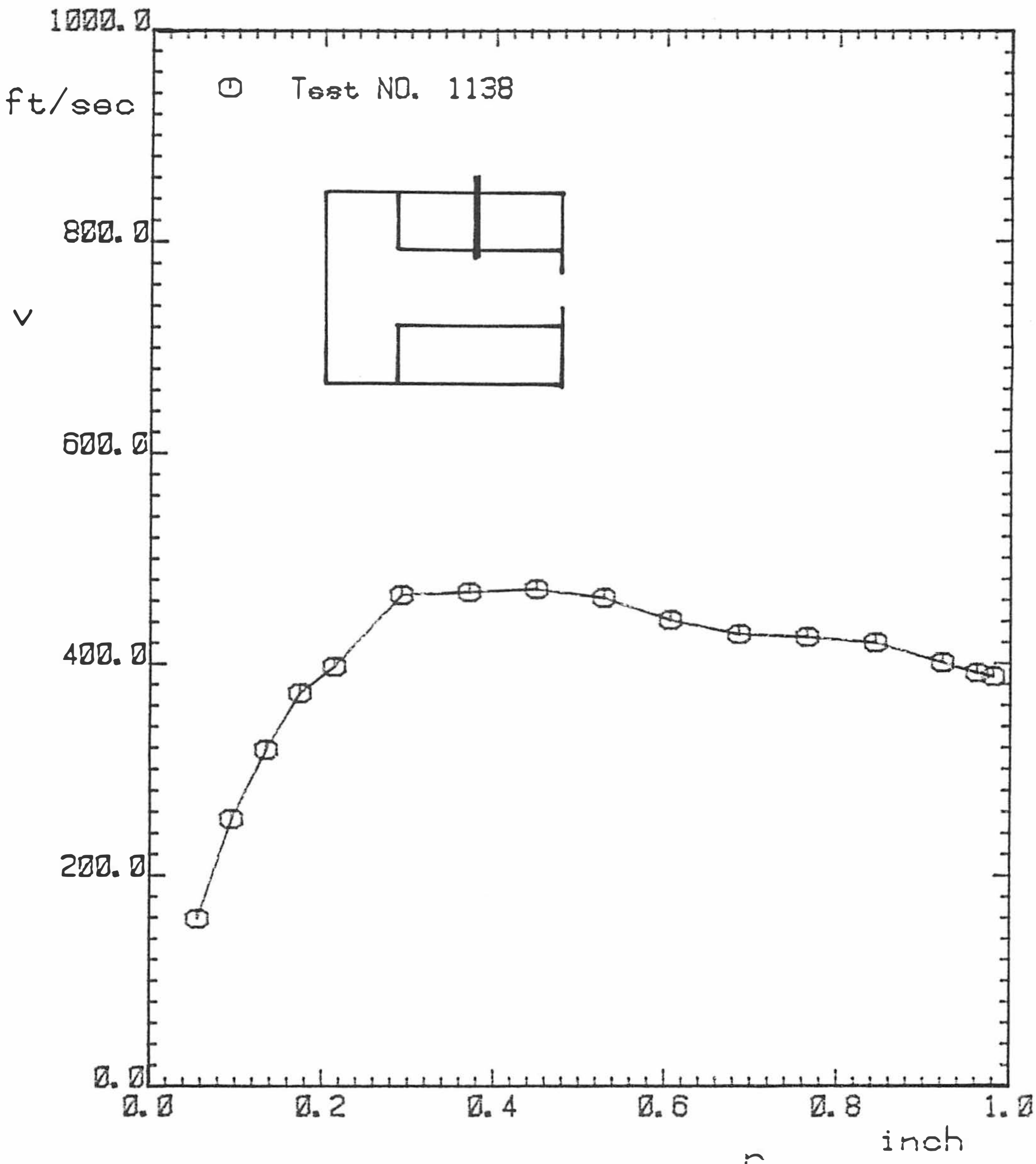

(a) tangential velocity

Figure 19. Data for 1.0 inch exit opening diameter.

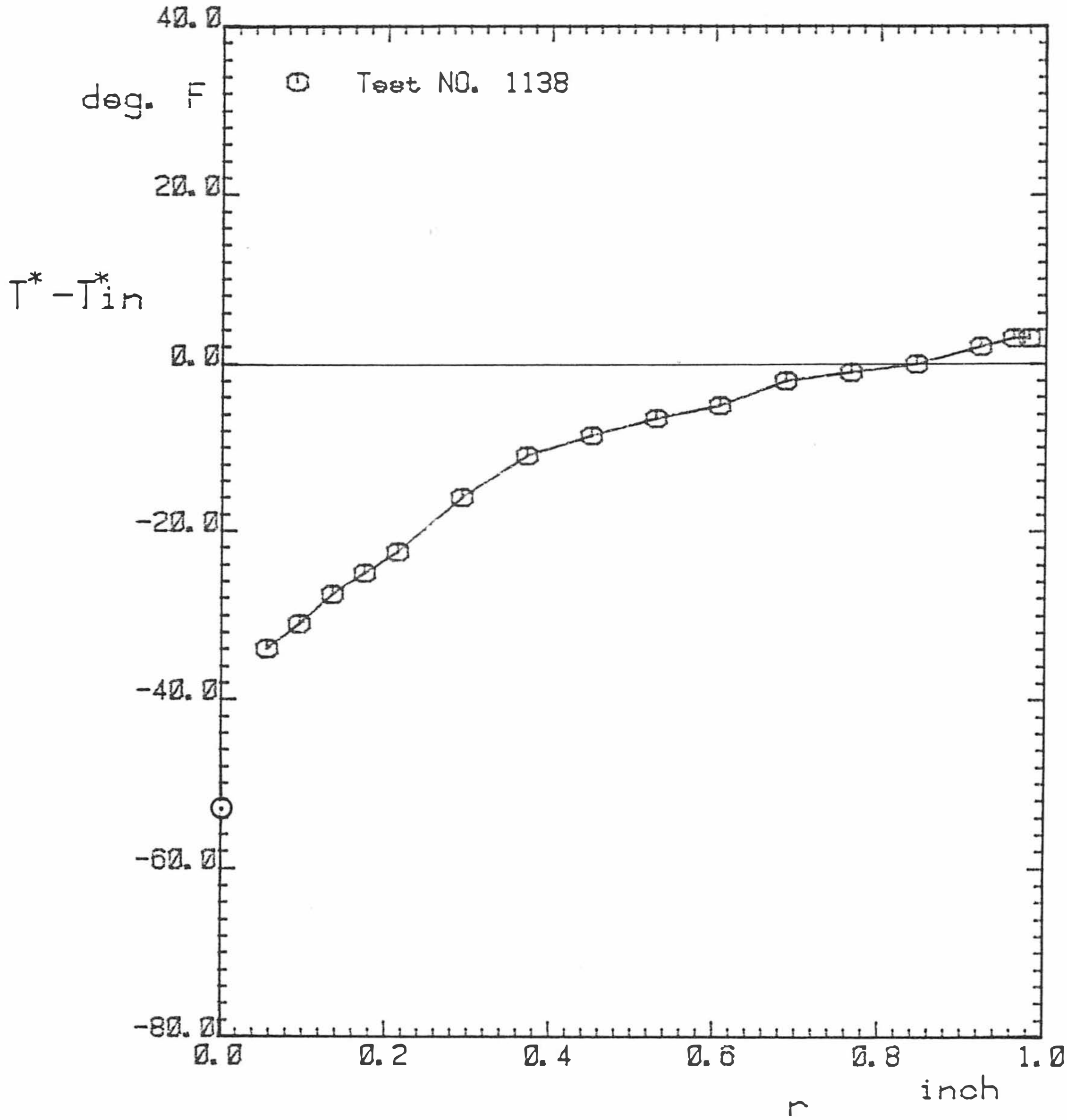

(b) total temperature

Figure 19. (Continued)

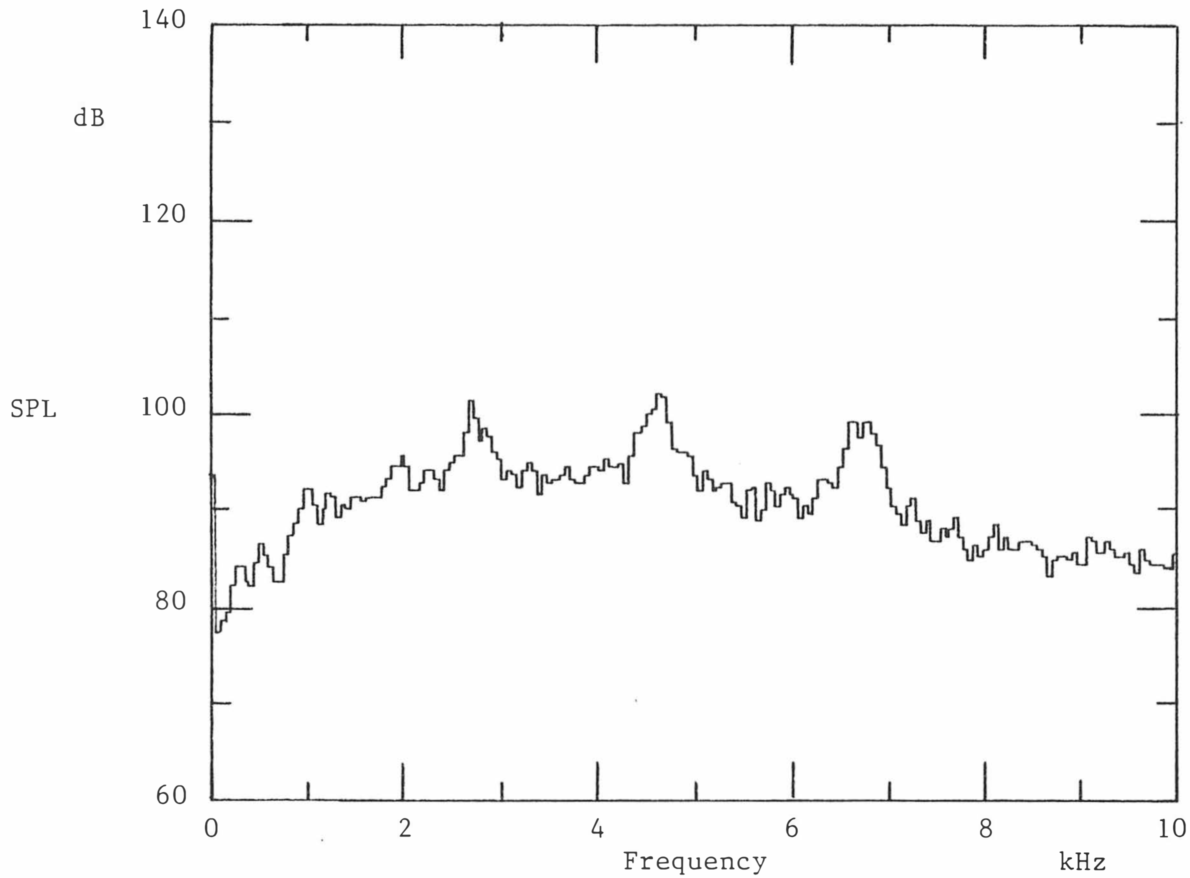

(c) frequency spectrum

Figure 19. (Continued)

with Figure 16(b) shows, this velocity profile is, however, not a Rankine vortex corresponding to a smaller exit opening diameter of 0.4 inch, discussed before. In addition, the total temperature distribution slightly changes from the one corresponding to a forced vortex, but it is different from the one corresponding to a Rankine vortex. The frequency spectrum shows that the pure tone is not as dominant as the one without restriction at the exit. However, the peaks of the vortex whistle still are visible in this case, as shown in Figure 17(c).

Figures 20 and 21 show the radial survey for the exit opening diameter of 0.8 and 0.6 inch, respectively, corresponding to a reduced exit area. From these, the gradual and continual process resulting from the decrease of intensity in the vortex whistle is clearly seen.

The conditions corresponding to this experiment are summarized in Table 1; here Q_{in} and Q are calculated from the following equations:

$$Q_{in} = c_p \, T^*_{in} \, G_{in}$$

$$Q = 2\pi \, c_p \int_o^{r_o} r \, T^* \, w \, dr \tag{24}$$

C. Effect of Sound Suppression

One observed in the previous section that the tangential velocity distribution was a forced vortex when the vortex whistle was present, and a Rankine vortex when the audible vortex whistle was absent. This section describes the effect of suppression of the vortex whistle.

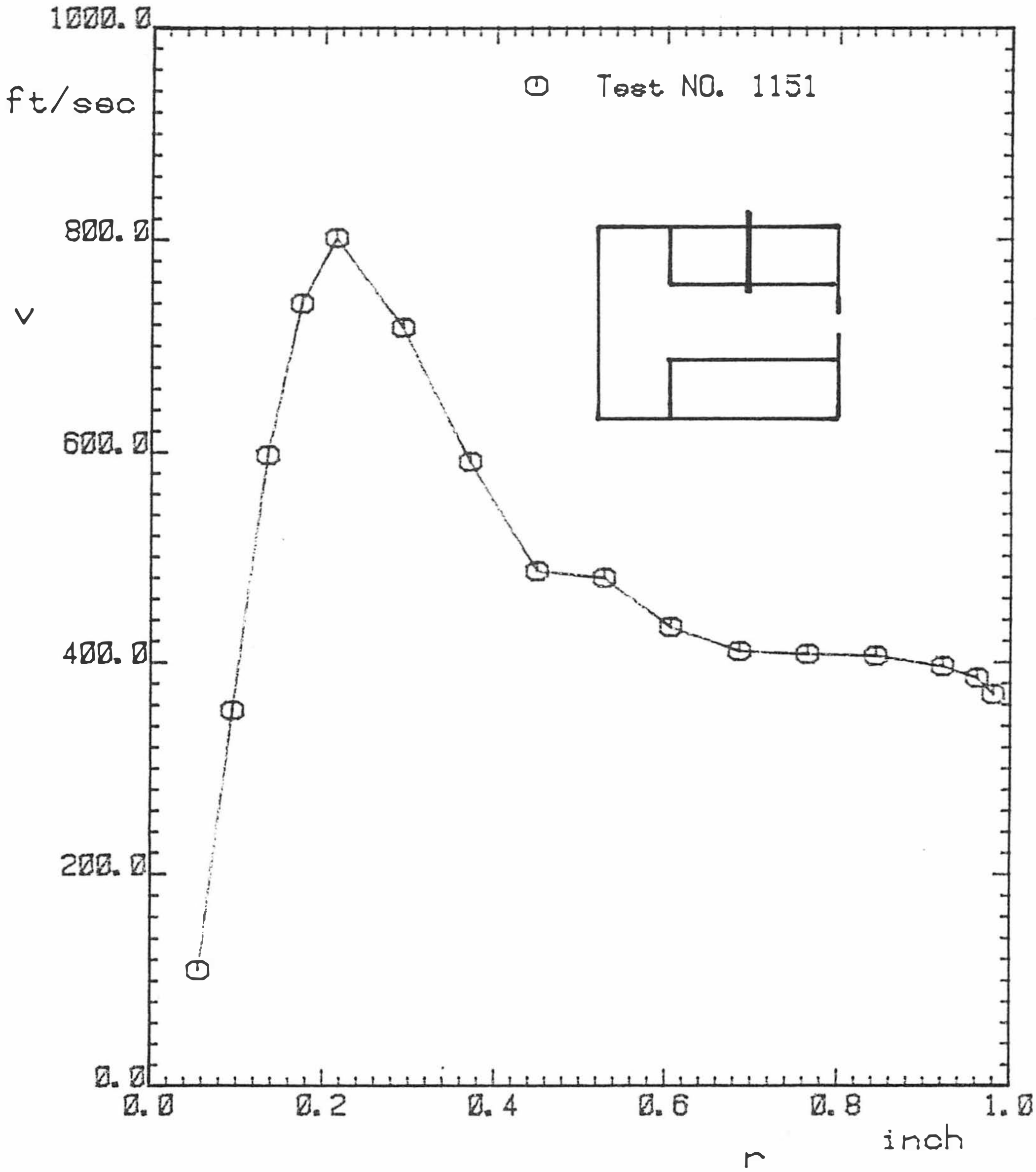

(a) tangential velocity

Figure 20. Data for 0.8 inch exit opening diameter.

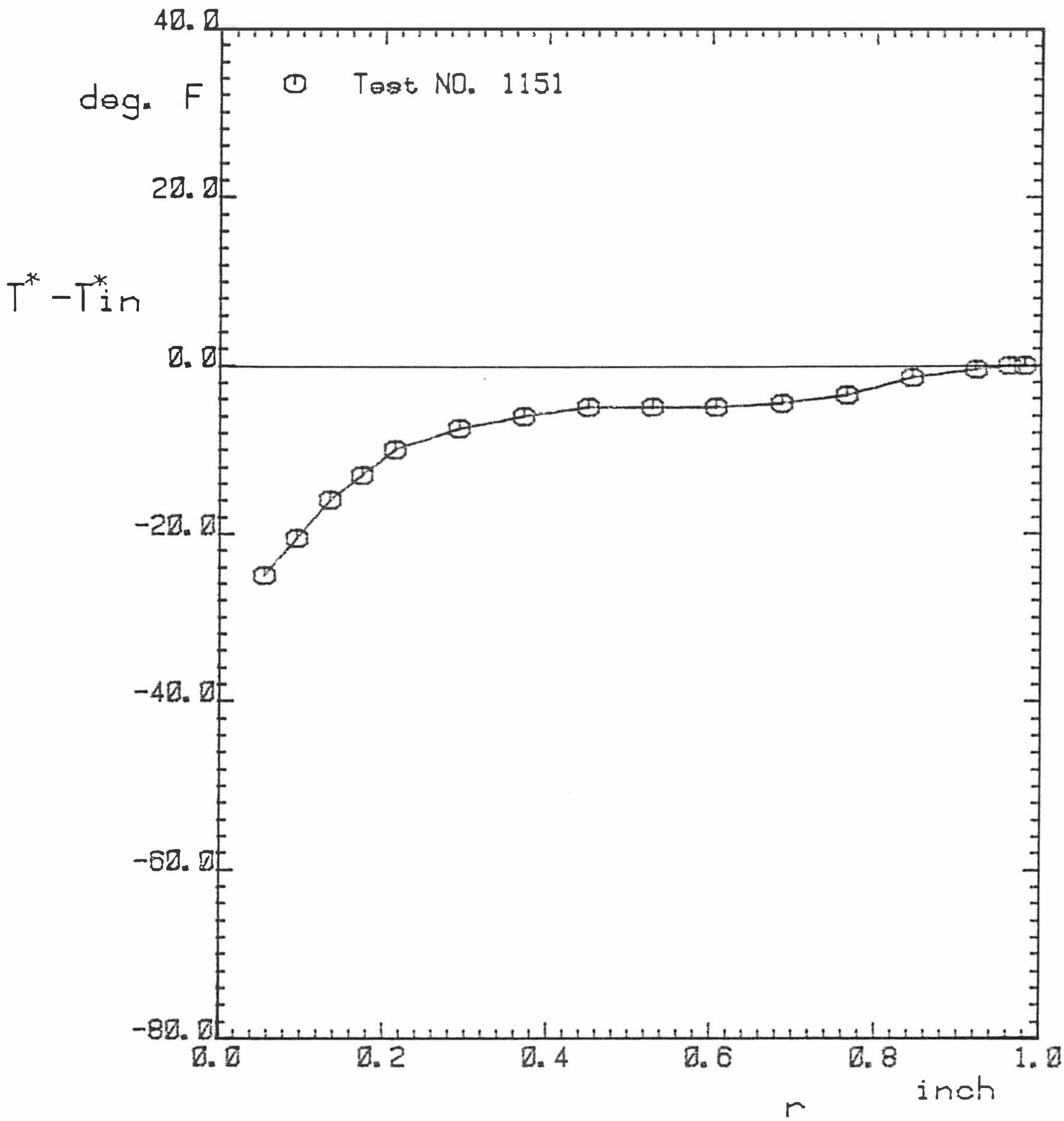

(b) total temperature

Figure 20. (Continued)

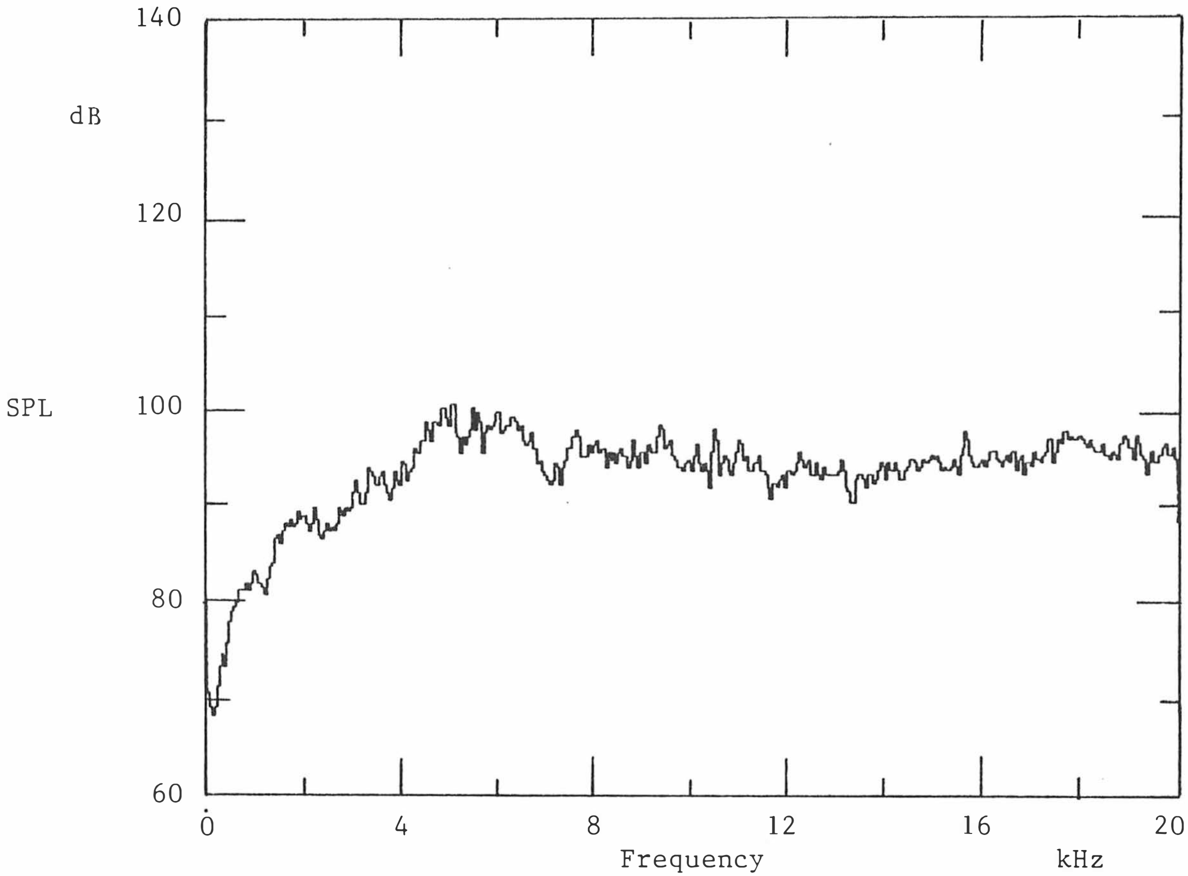

(c) frequency spectrum

Figure 20. (Continued)

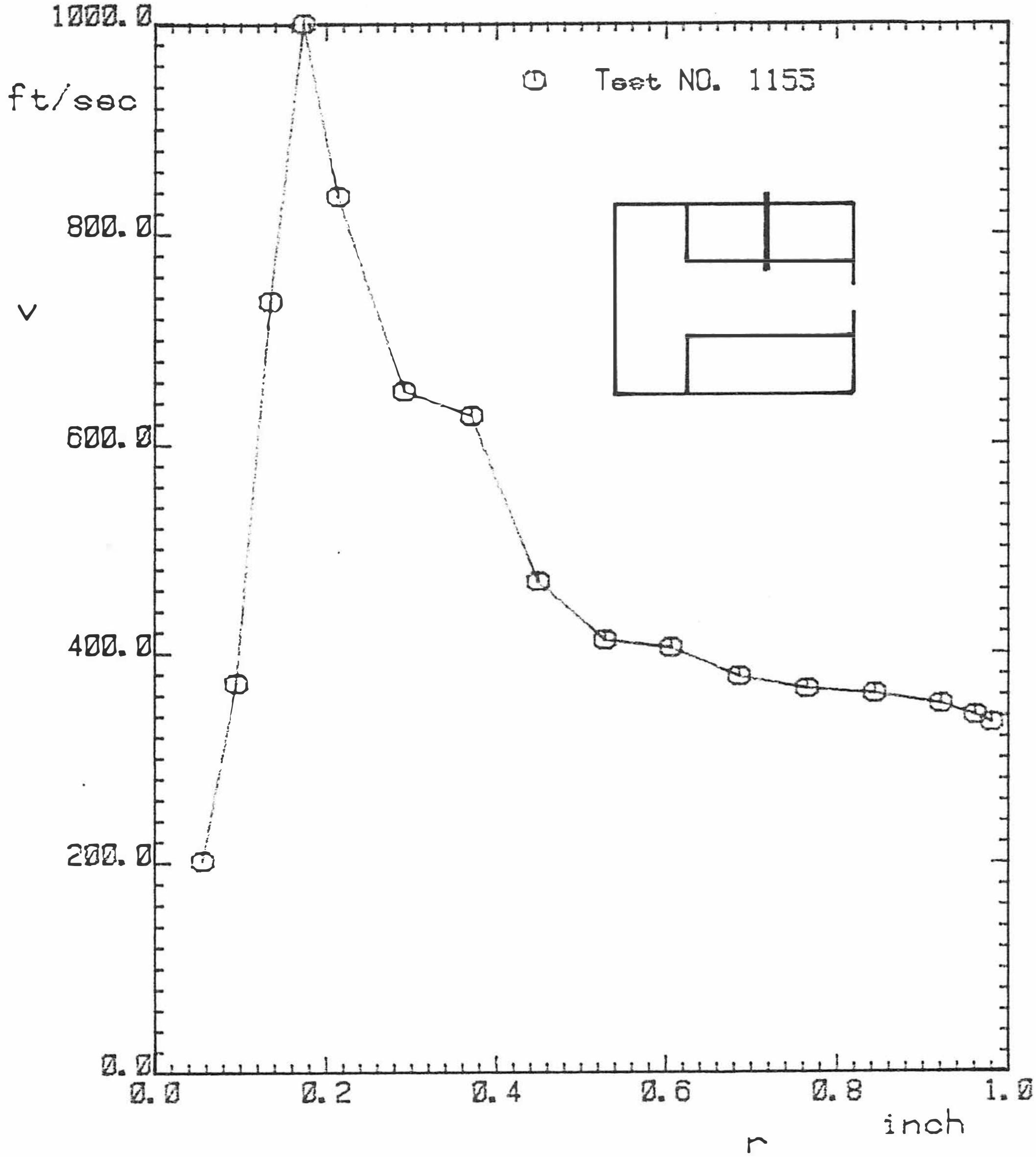

(a) tangential velocity

Figure 21. Data for 0.6 inch exit opening diameter.

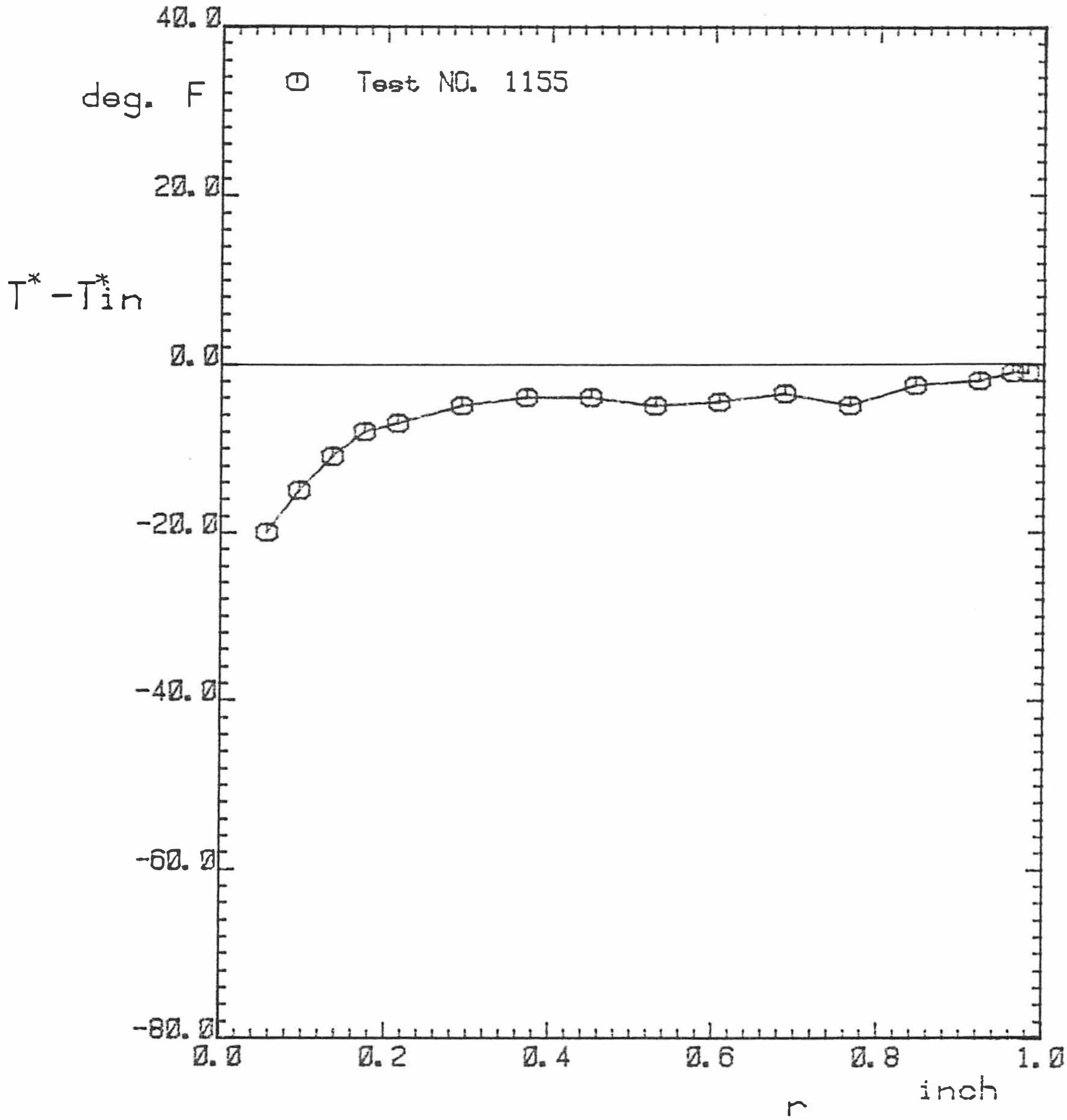

(b) total temperature

Figure 21. (Continued)

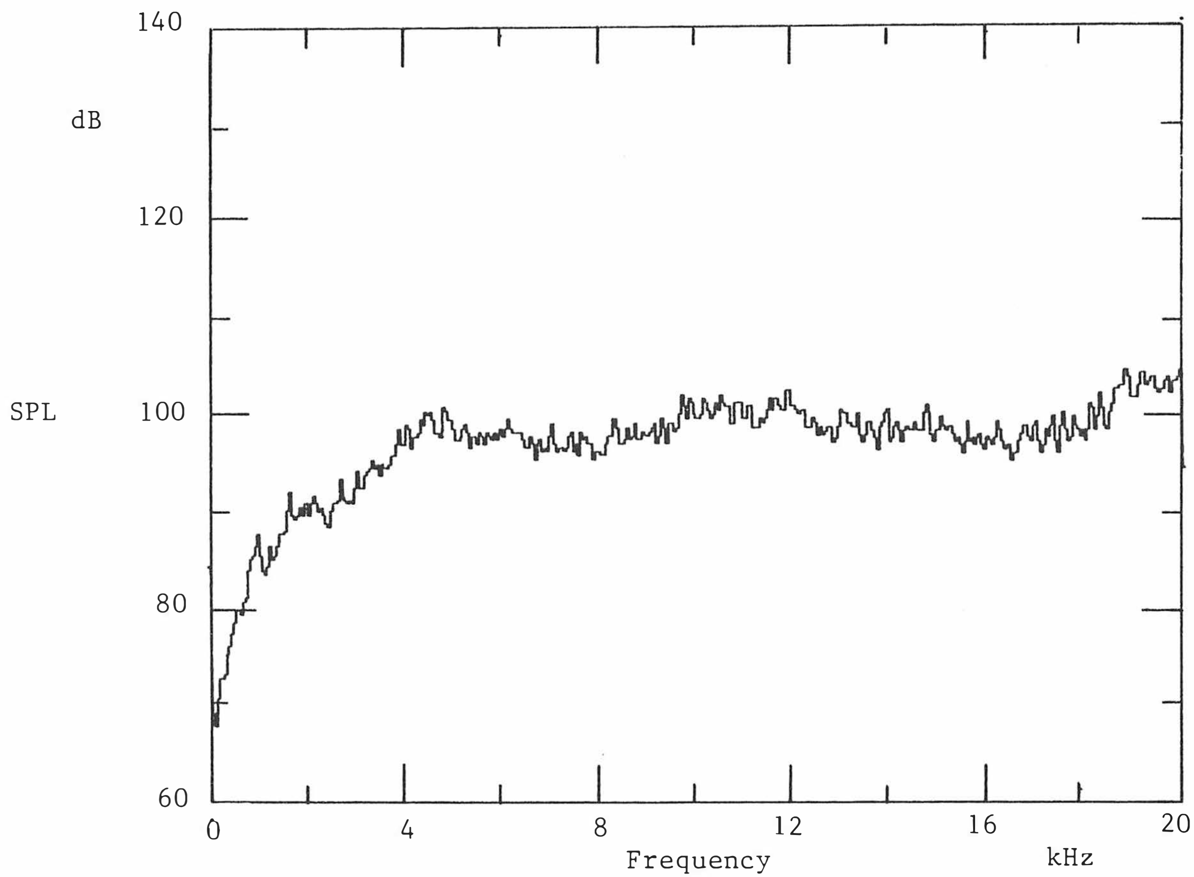

(c) frequency spectrum

Figure 21. (Continued)

Table 1

Mass Flow and Energy Flux

Test No.	d inch	P_{in} psi	G_{in} lbm/sec	$G^{\dagger}$ lbm/sec	$G^{\dagger\dagger}$ lbm/sec	Q_{in} Btu/sec	$Q^{\dagger}$ Btu/sec	$Q^{\dagger\dagger}$ Btu/sec
1220	2.0	29.90	.1035	.0996	.1051	13.0	12.6	13.2
1174	1.5	30.96	.1039	.1017	.1055	13.3	12.9	13.4
1157	1.25	31.80	.1041	.1019	.1053	13.2	12.8	13.2
1138	1.0	31.03	.0955	.0941	.0968	11.7	11.4	11.8
1151	0.8	35.98	.1036	.1041	.1050	13.0	13.0	13.1
1155	0.6	44.18	.1091	.1043	.1100	14.0	13.3	14.0
1172	0.4	60.52	.1024	.1129	.1038	13.0	14.3	13.0

†Calculated from P*, P, T* and α.

††Calculated from differential equation.

It was expected that the attenuation of the vortex whistle will reduce the total temperature separation and the swirl distribution will revert to a Rankine vortex.

To suppress the vortex whistle, the porous pipe, installed with an acoustic chamber with acoustic cavity length equal to 1 3/8 inches, was used as a main tube. Figures 22 to 24 show the radial distribution of flow field just before and just after the sound suppression, taken at three different axial positions: Z = 2 inches, Z = 3.5 inches and Z = 5.4 inches.

At Z = 2 inches, which corresponds to the position of the fourth cavity from the manifold--an axial position closest to the swirl generator--the tangential velocity profile just before the sound suppression (Figure 22(c) corresponding to circles) is found to be a forced vortex, as expected; this separates the total temperature in the radial direction (Figure 22(e)). The total temperature at the centerline, which is measured by the thermocouple inserted through the cold-end plug, indicates extremely low value (the difference between the centerline and inlet total temperature is as low as -81°F). Obviously, the vortex whistle dominates the frequency spectrum, as shown in Figure 22(g); the fundamental frequency, f_{11}, is 1.25 kHz, which, as mentioned, corresponds to the lowest frequency of the first tangential wave mode, $|m| = 1$. The presence of its higher harmonics, corresponding to nf_{11}, where n = 1, 2, . . . , is also evident.

Once the vortex whistle is suppressed, the precipitous fall of the sound level can be observed in the frequency spectrum (compare Figure 22(g) and (h)); the sound changes from a shrill whistle to a

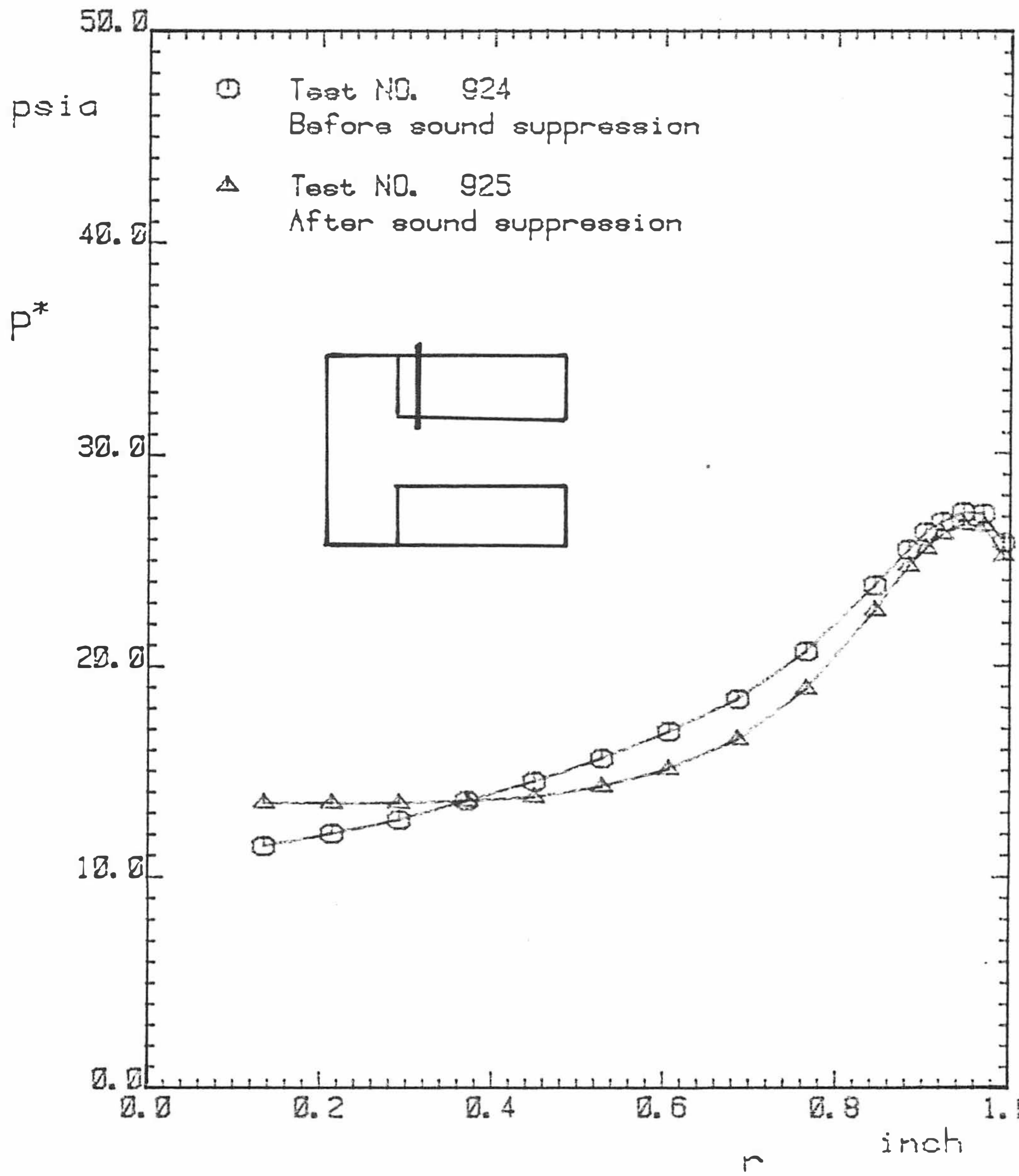

(a) total pressure

Figure 22. Data for 1.375 inches acoustic cavity length; taken at 4th acoustic cavity position.

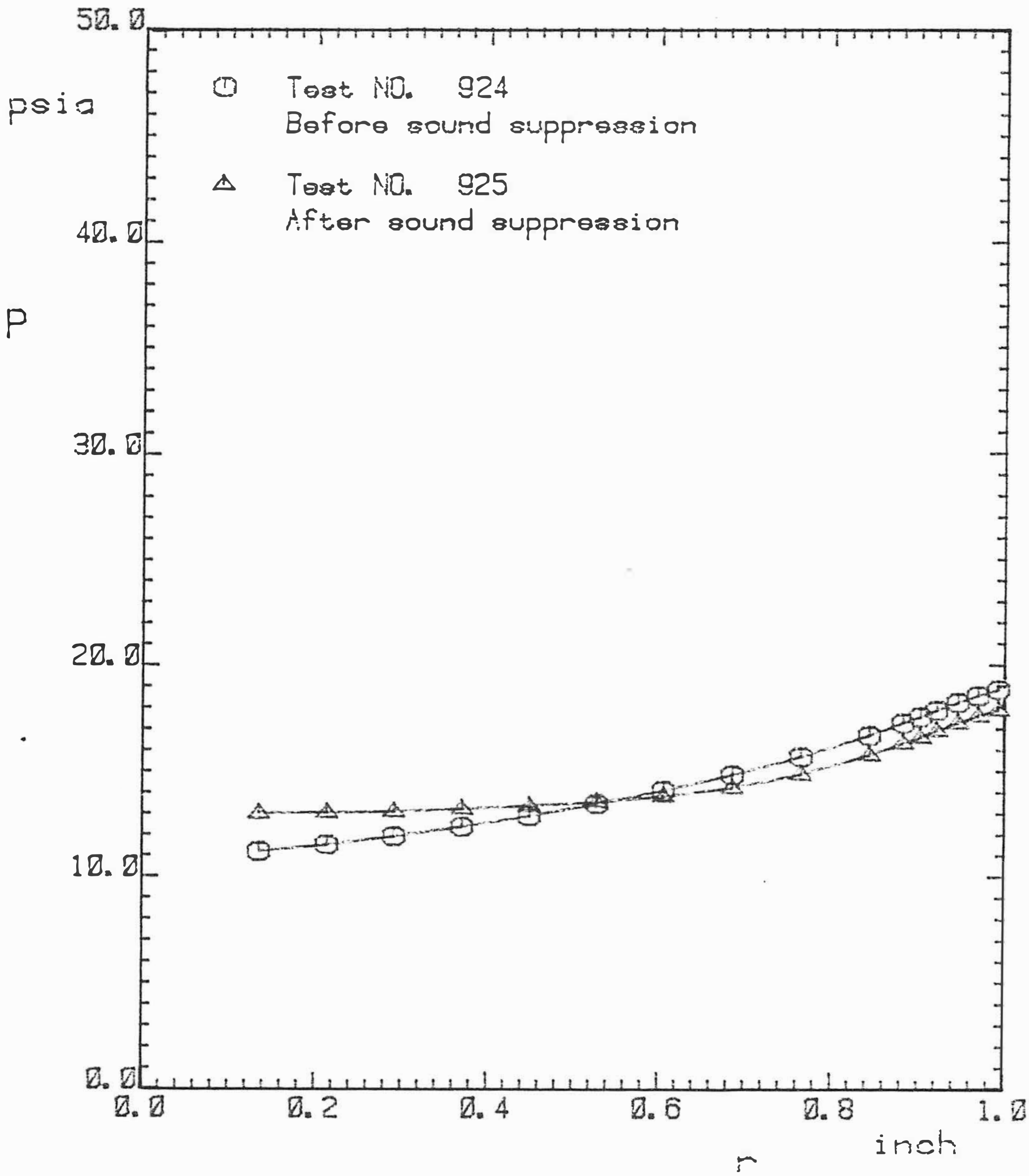

(b) static pressure

Figure 22. (Continued)

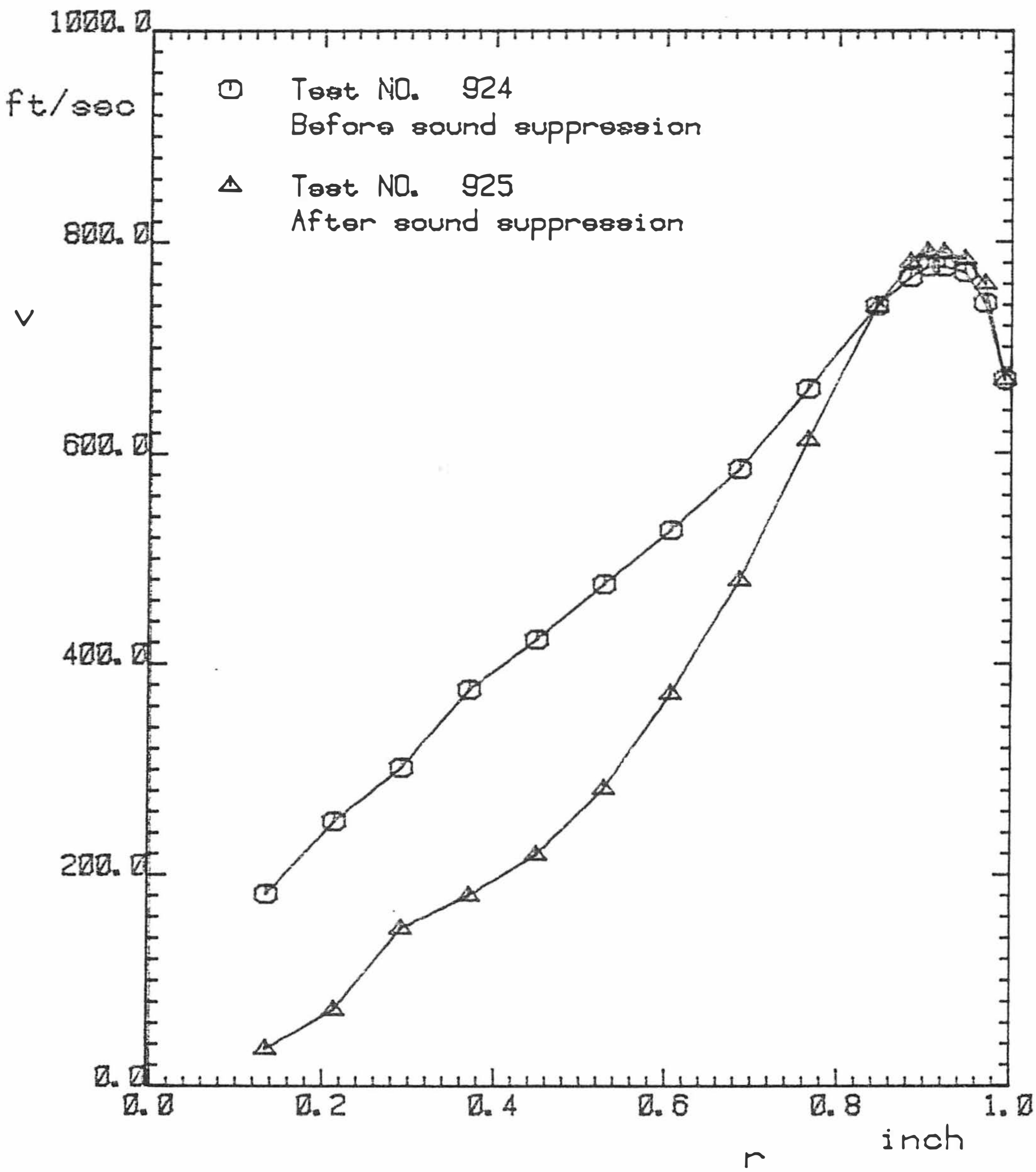

(c) tangential velocity

Figure 22. (Continued)

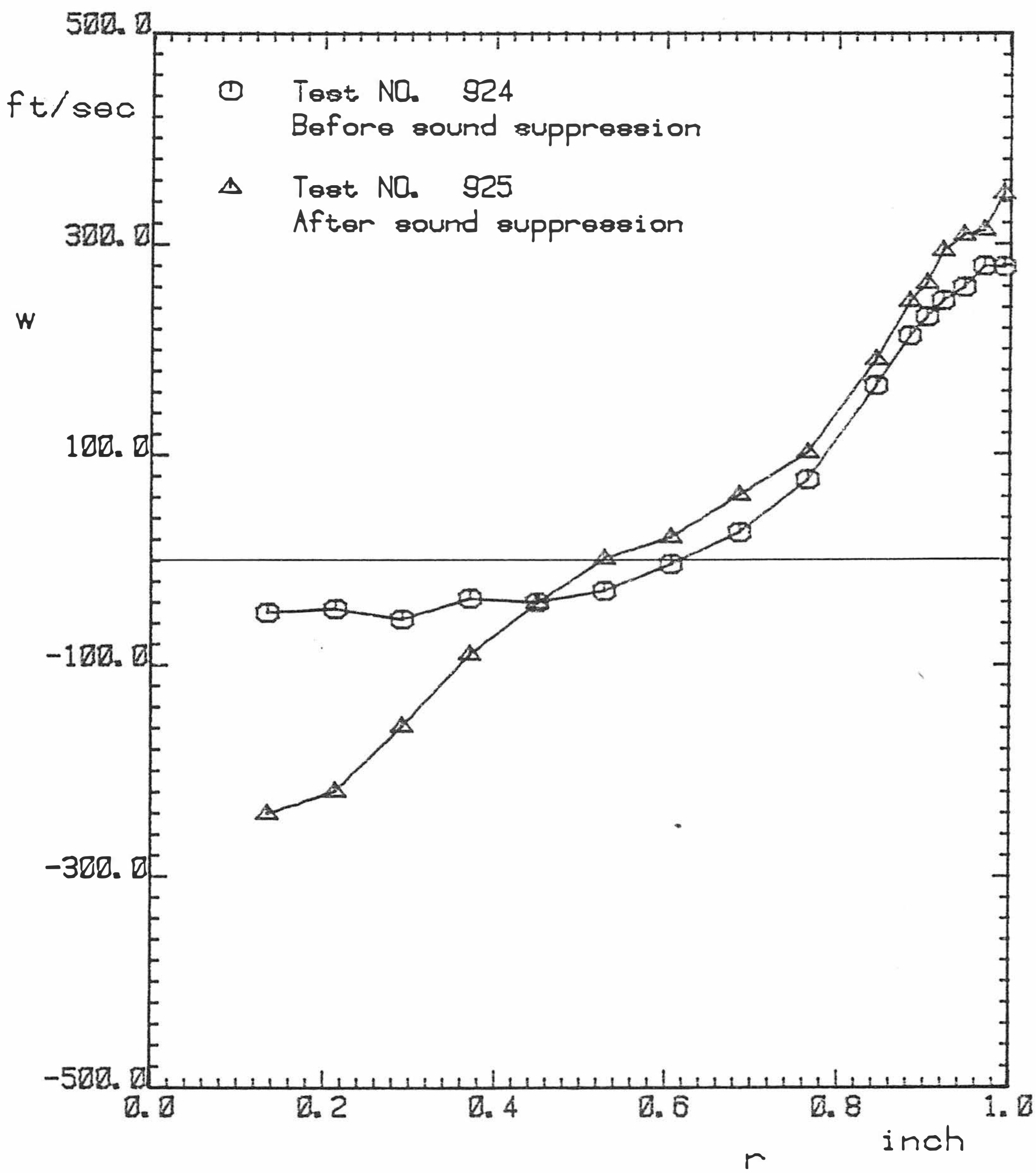

(d) axial velocity

Figure 22. (Continued)

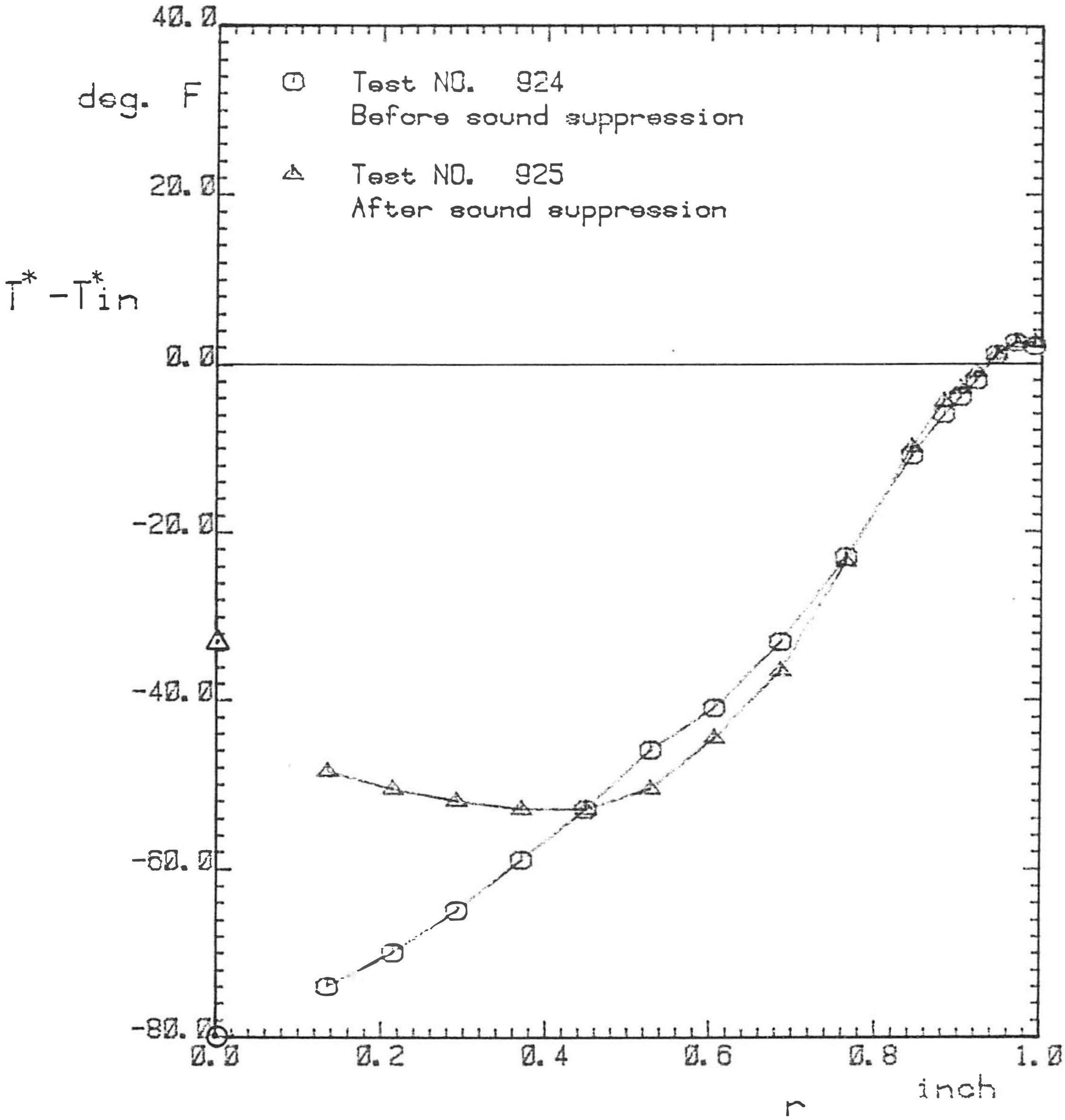

(e) total temperature

Figure 22. (Continued)

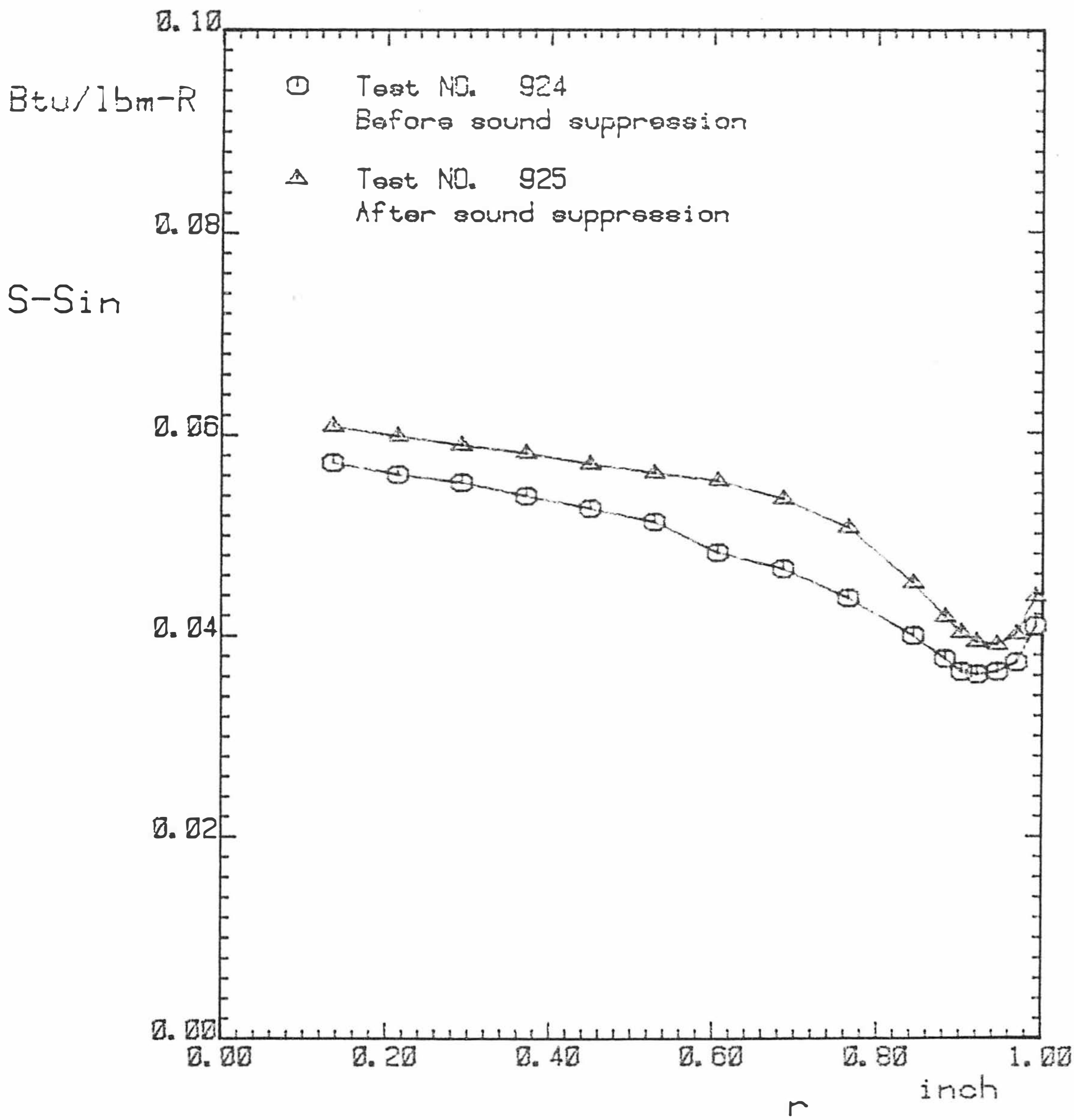

(f) entropy

Figure 22. (Continued)

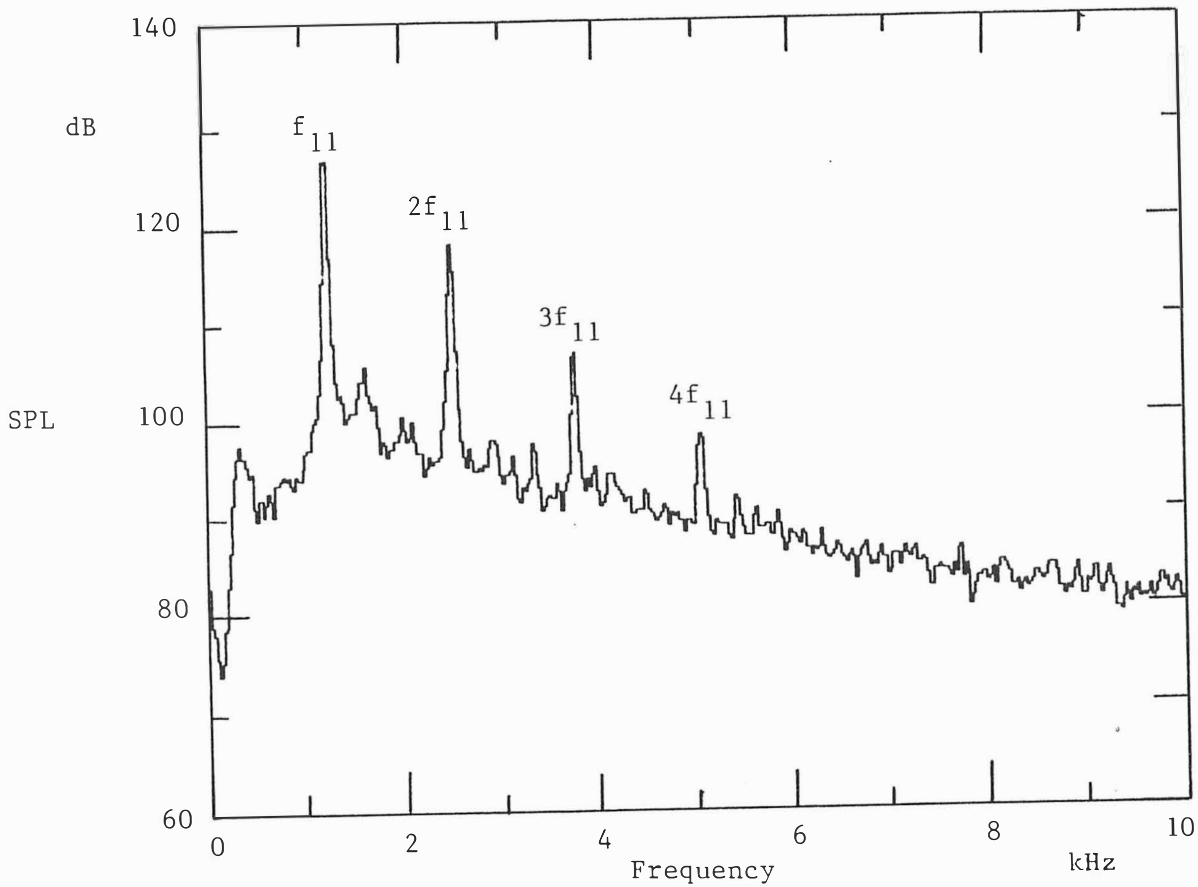

(g) frequency spectrum before sound suppression

Figure 22. (Continued)

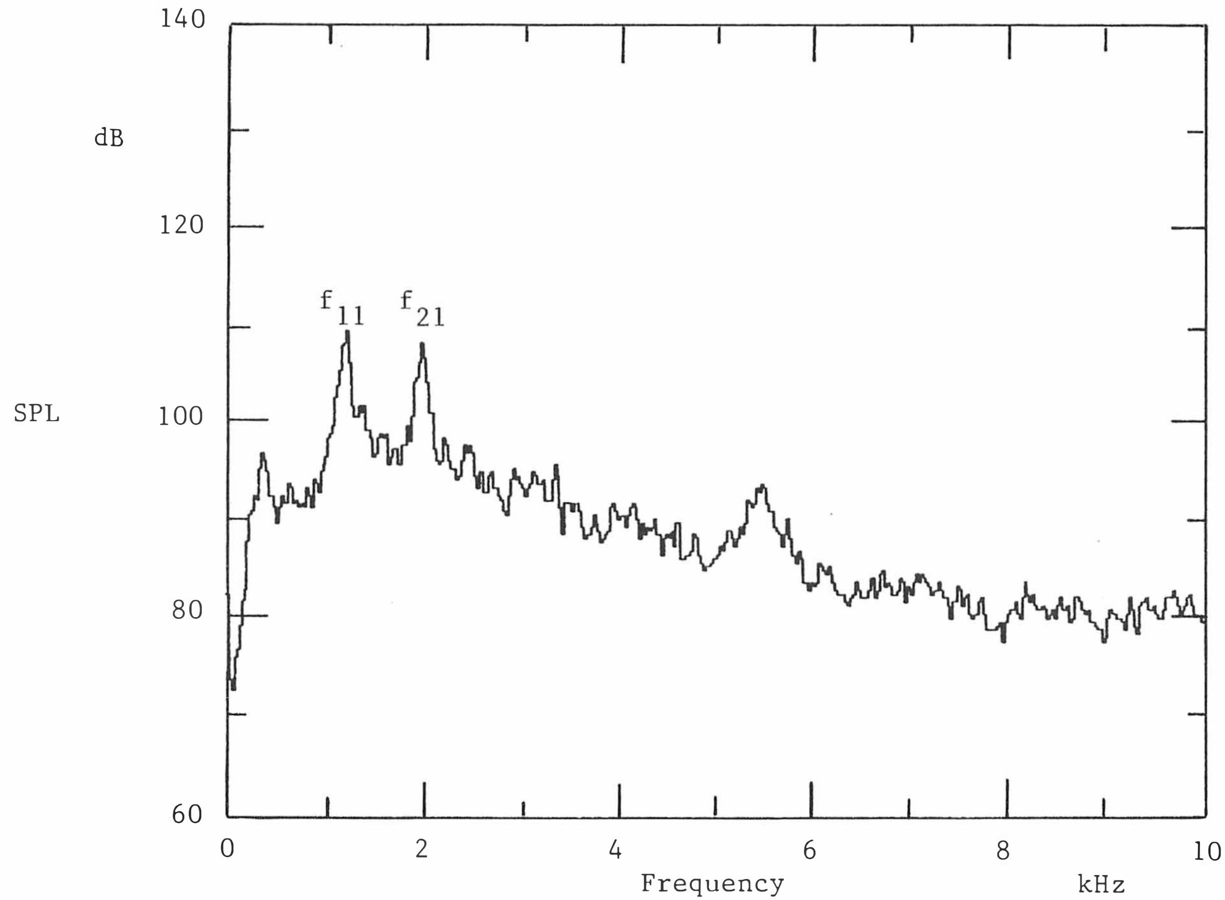

(h) frequency spectrum after sound suppression

Figure 22. (Continued)

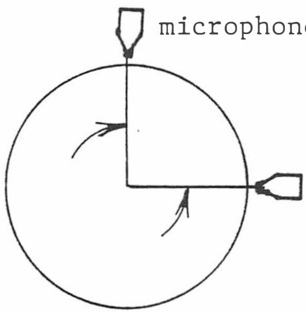

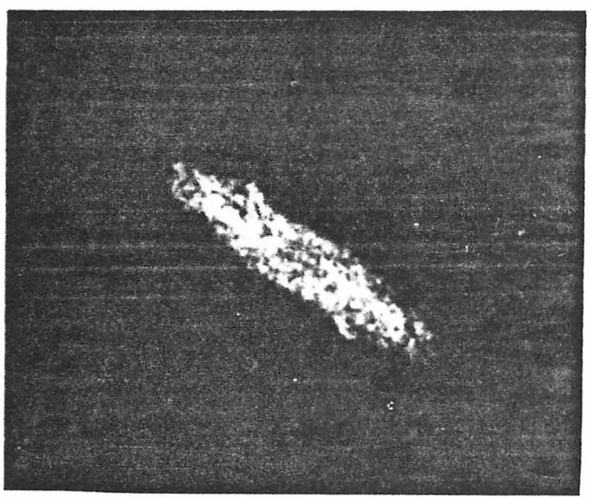

(X), (Y) filter only the second peak after sound suppression, f_{21}, of Figure 22(h)

(i) Lissajous figure

Figure 22. (Continued)

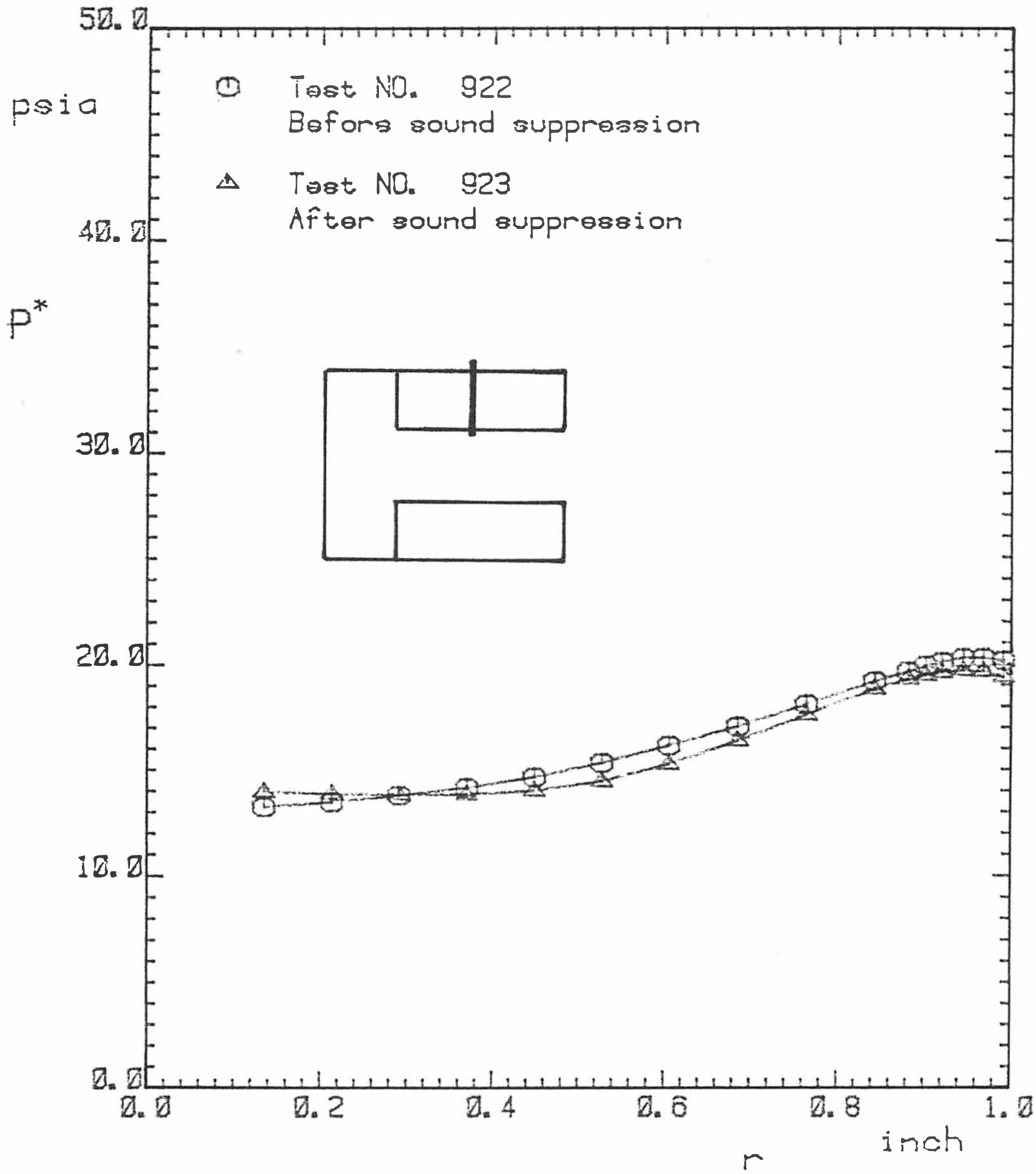

(a) total pressure

Figure 23. Data for 1.375 inches acoustic cavity length; taken at 12th acoustic cavity position.

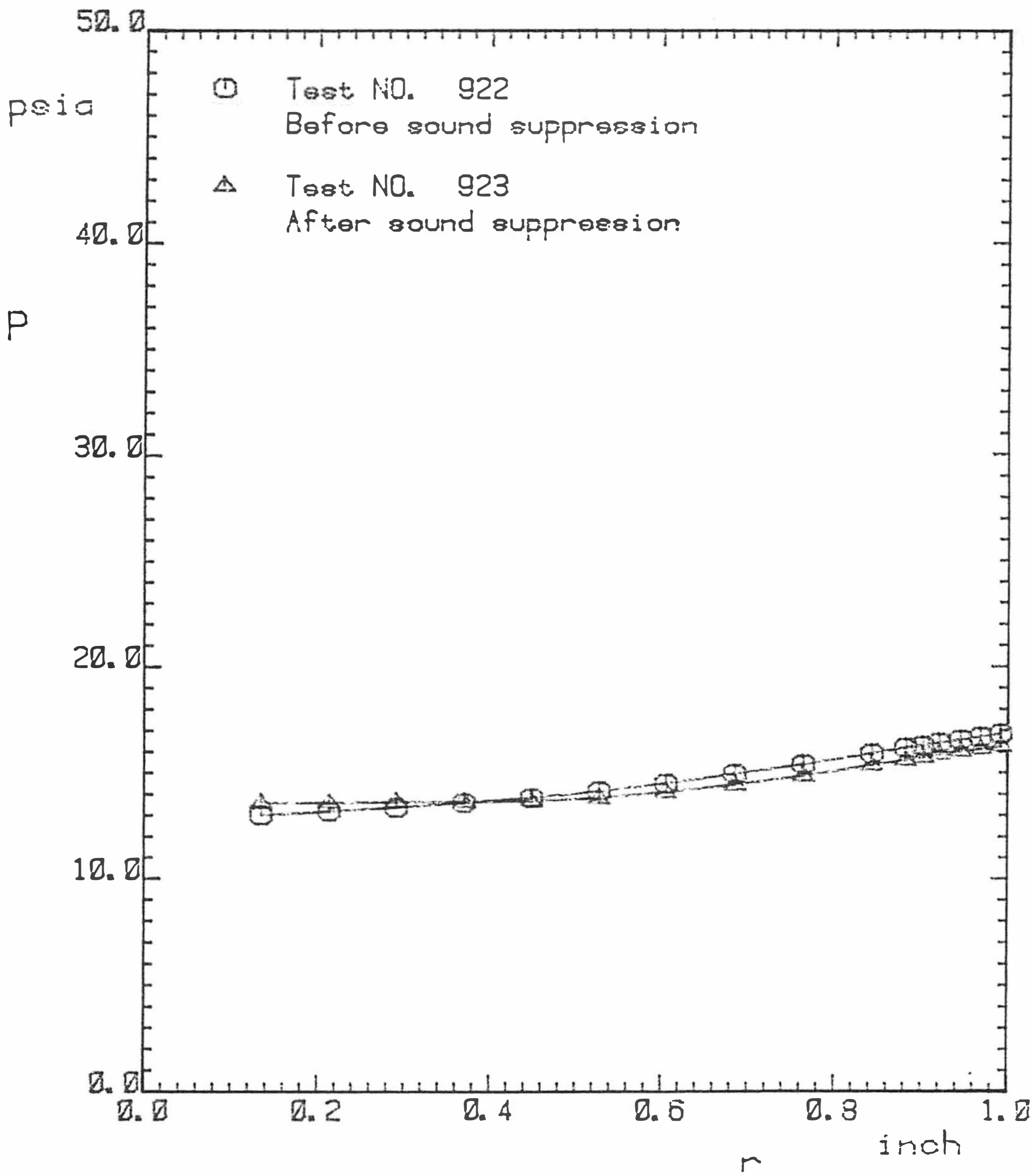

(b) static pressure

Figure 23. (Continued)

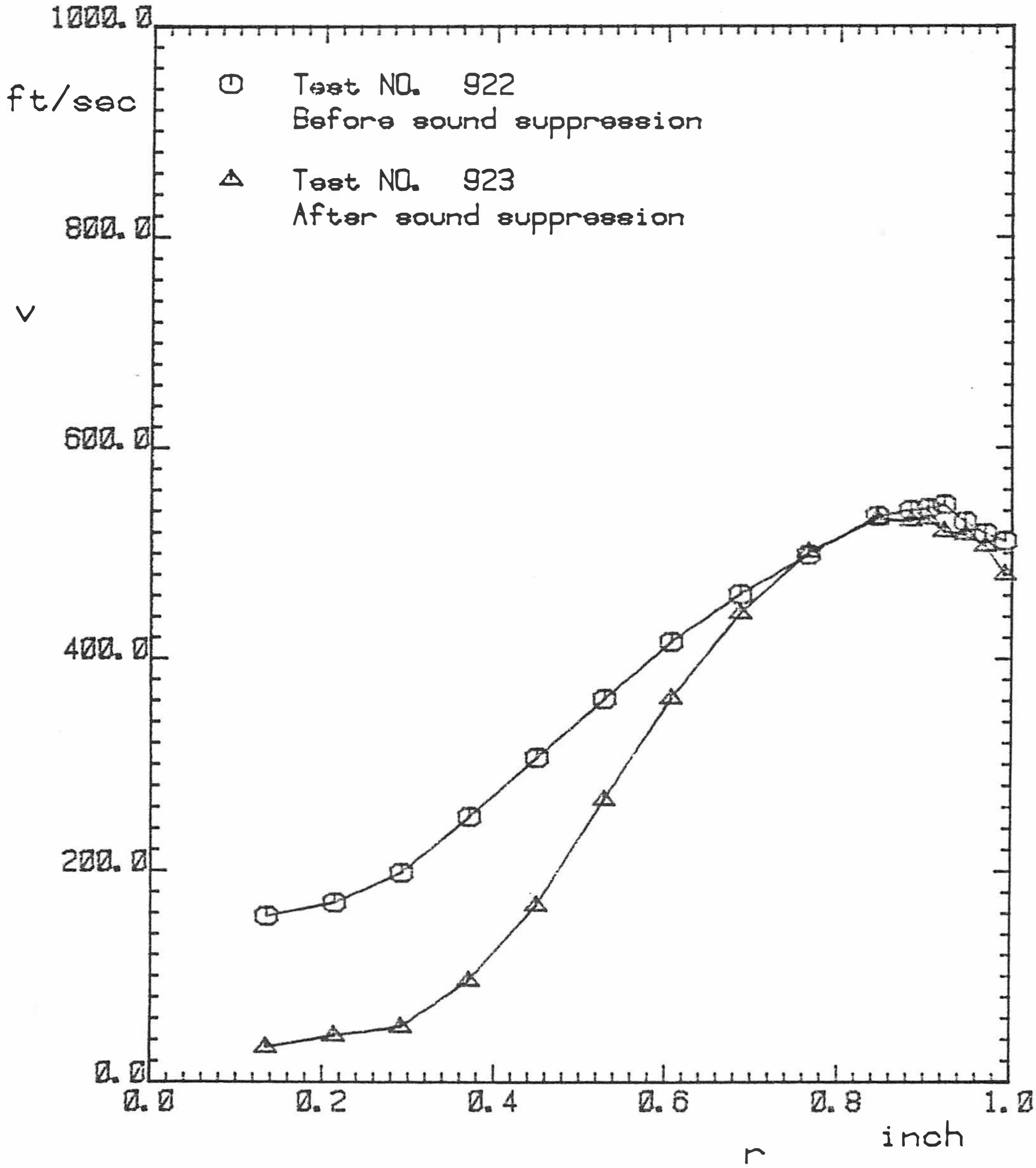

(c) tangential velocity

Figure 23. (Continued)

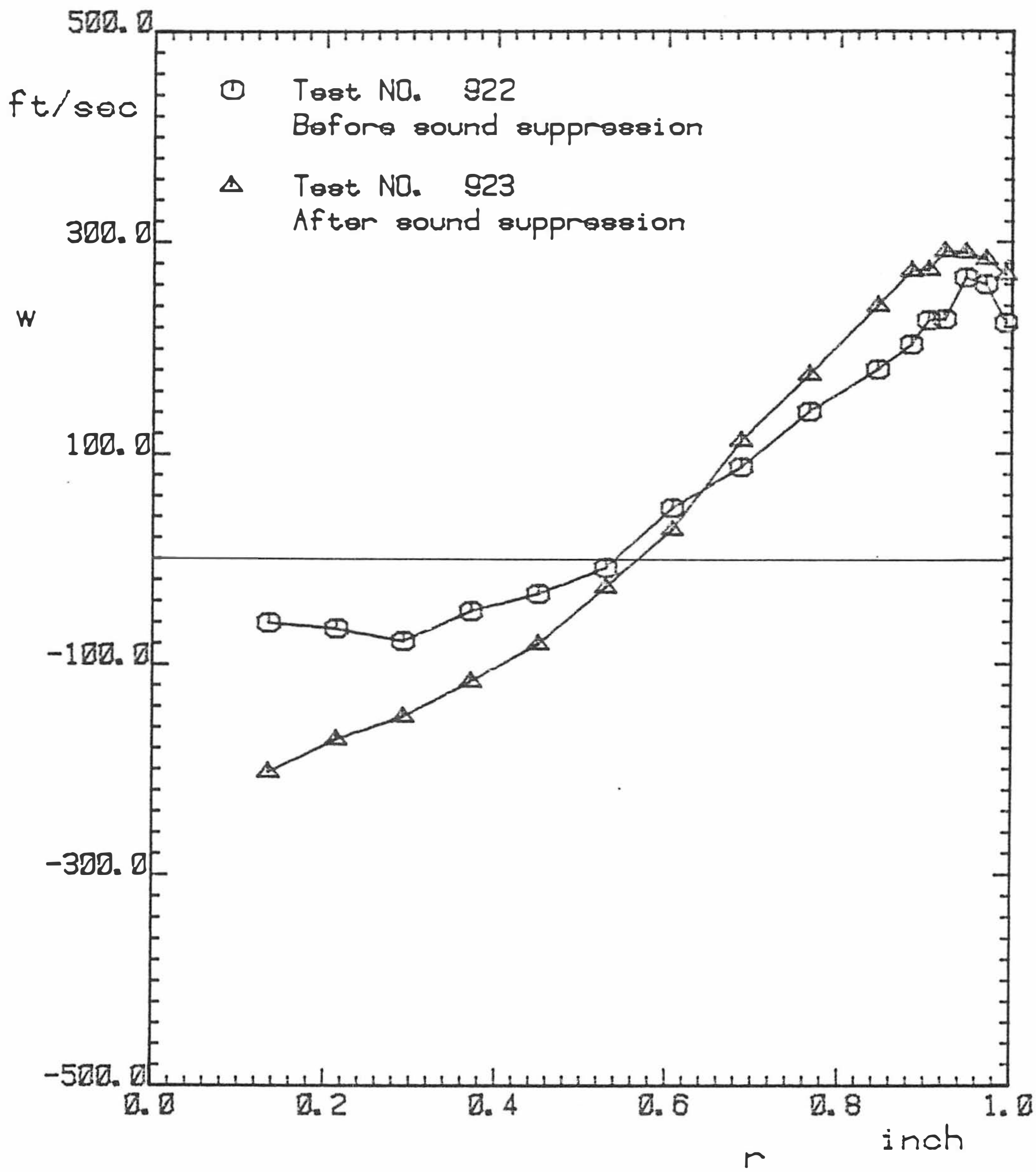

(d) axial velocity

Figure 23. (Continued)

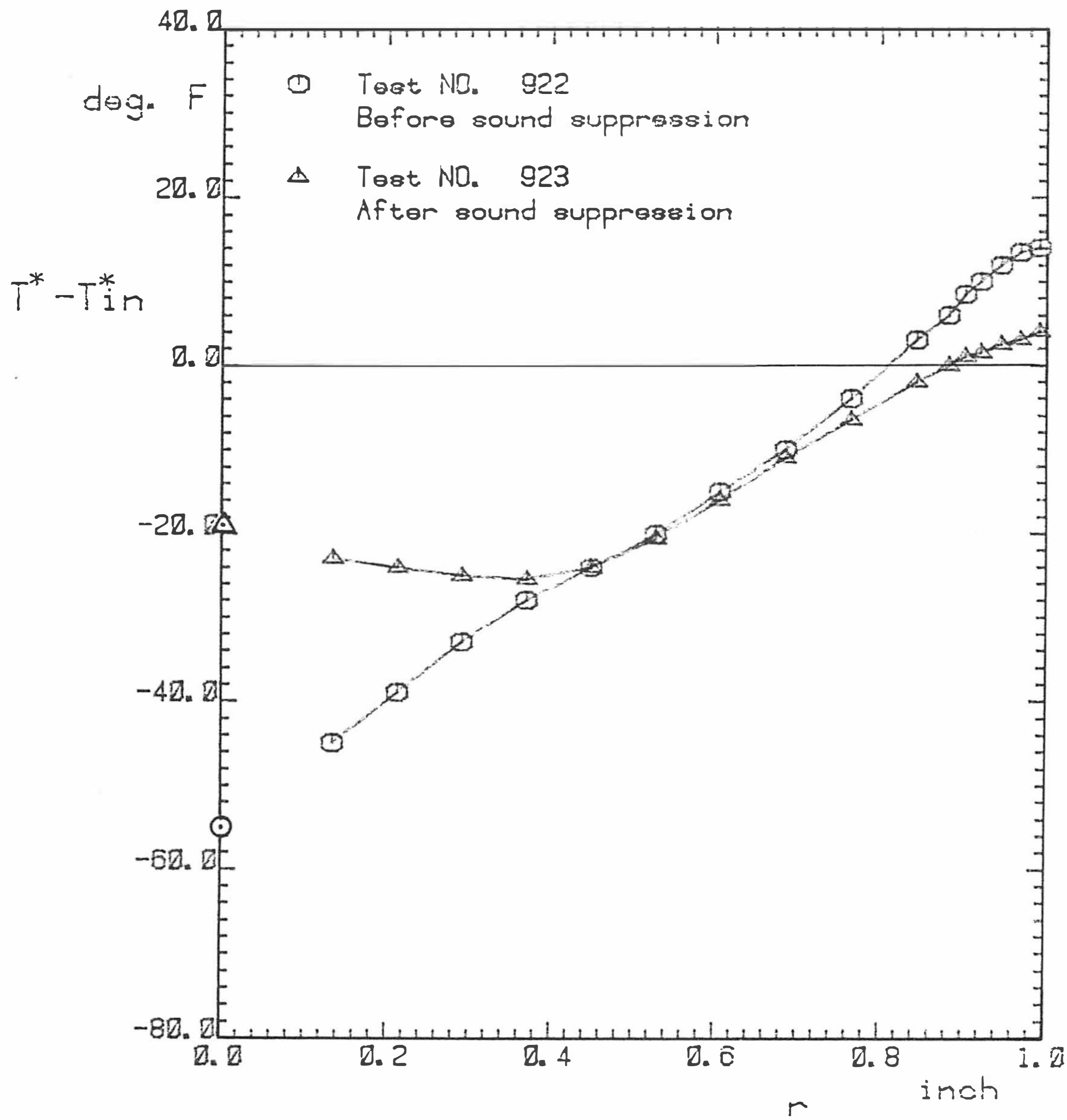

(e) total temperature

Figure 23. (Continued)

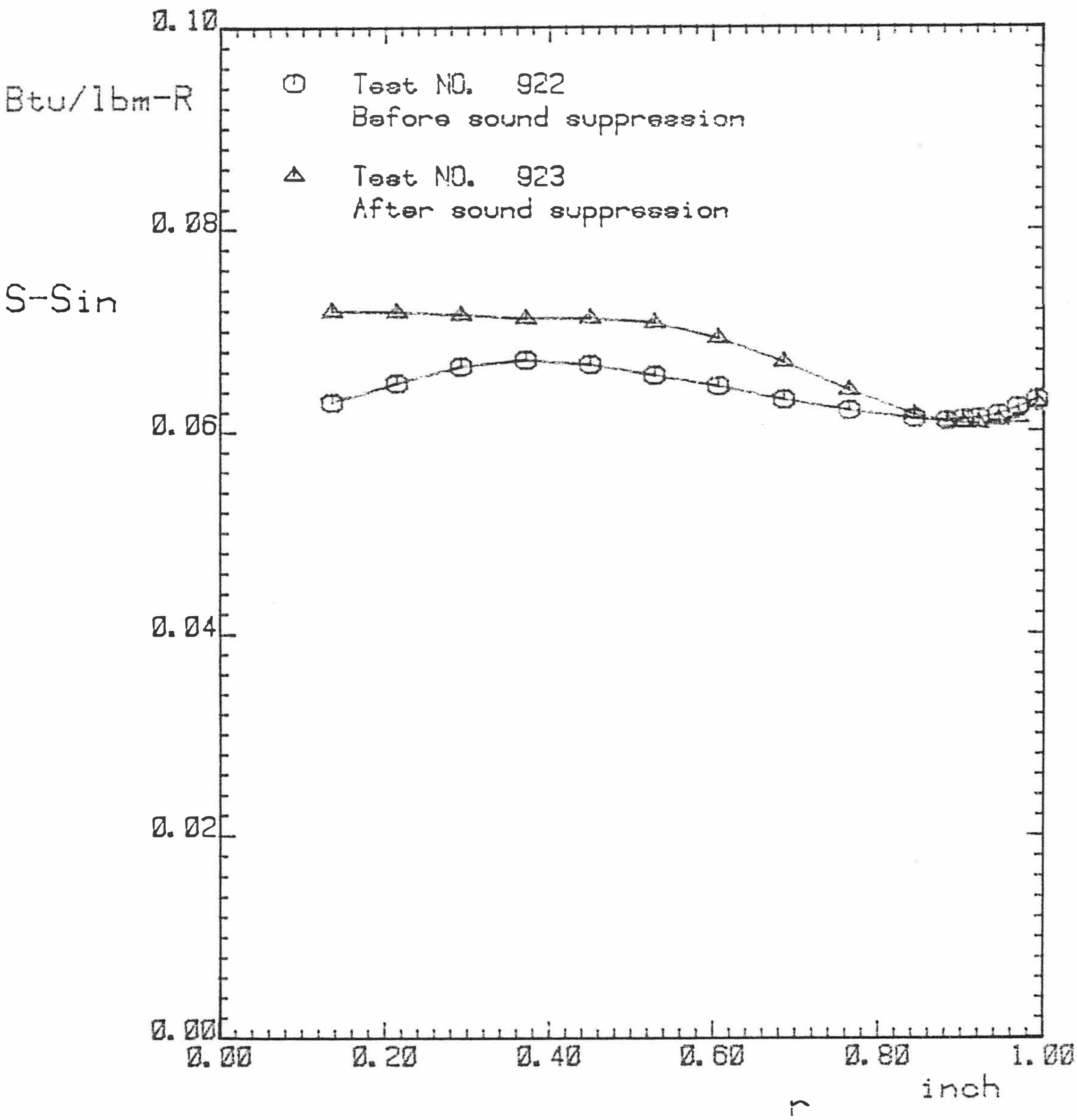

(f) entropy

Figure 23. (Continued)

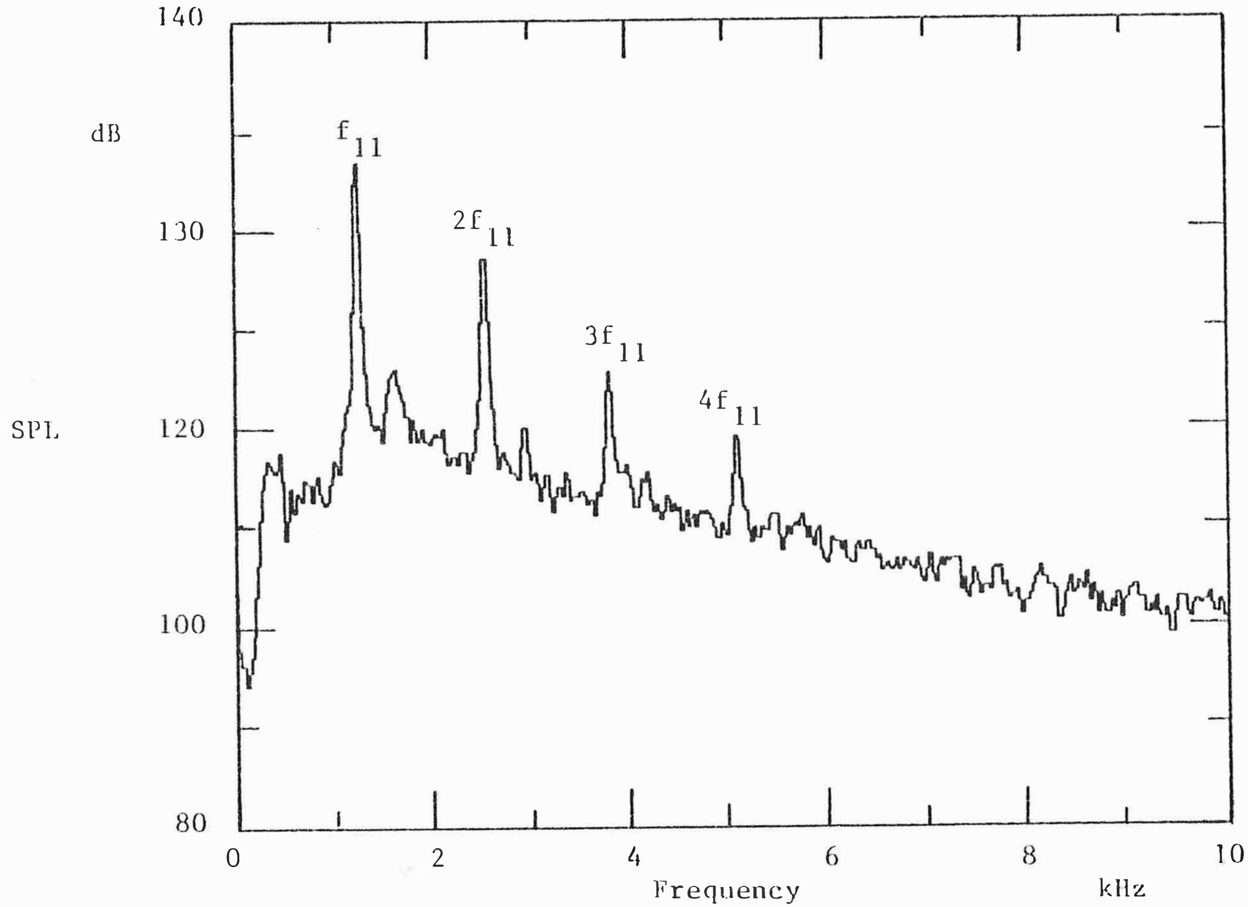

(g) frequency spectrum before sound suppression

Figure 23. (Continued)

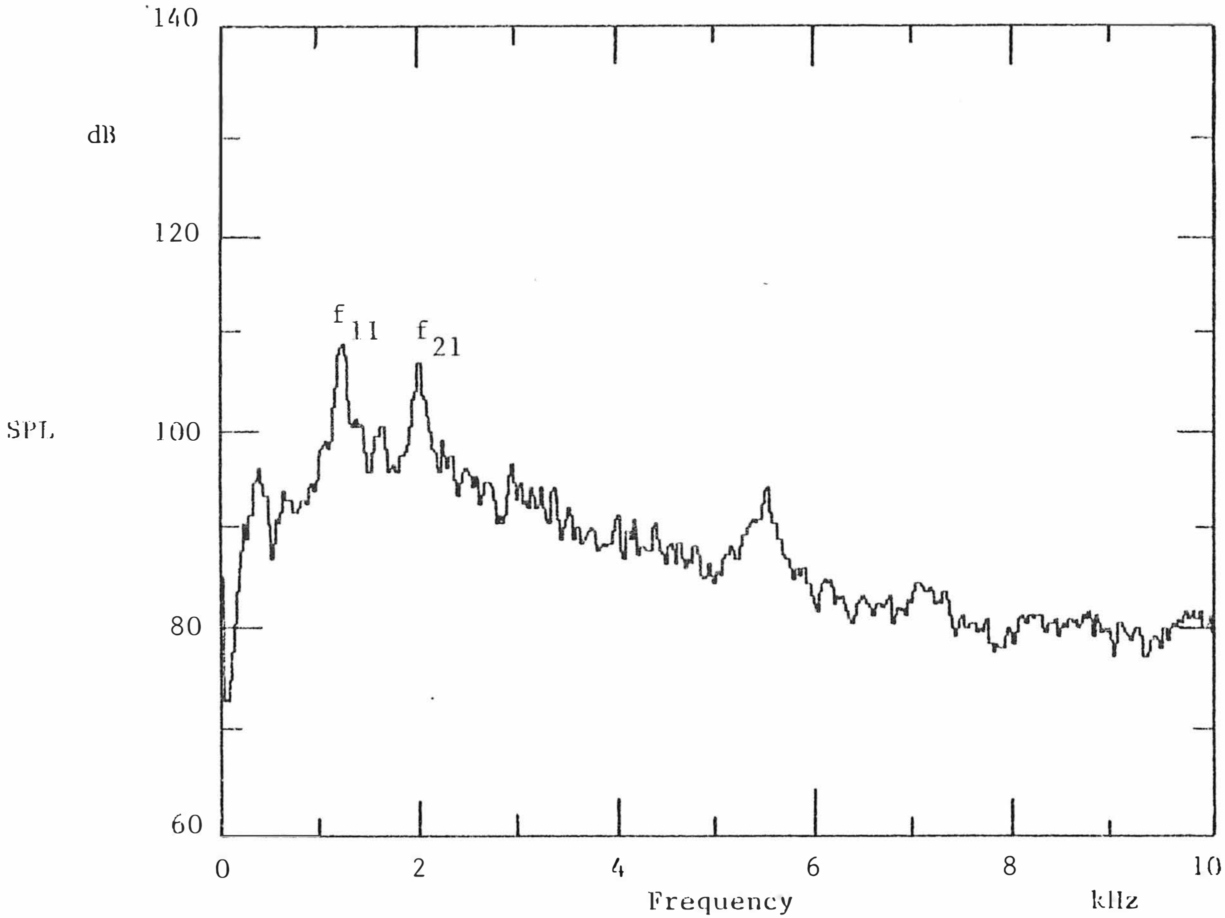

(h) frequency spectrum after sound suppression

Figure 23. (Continued)

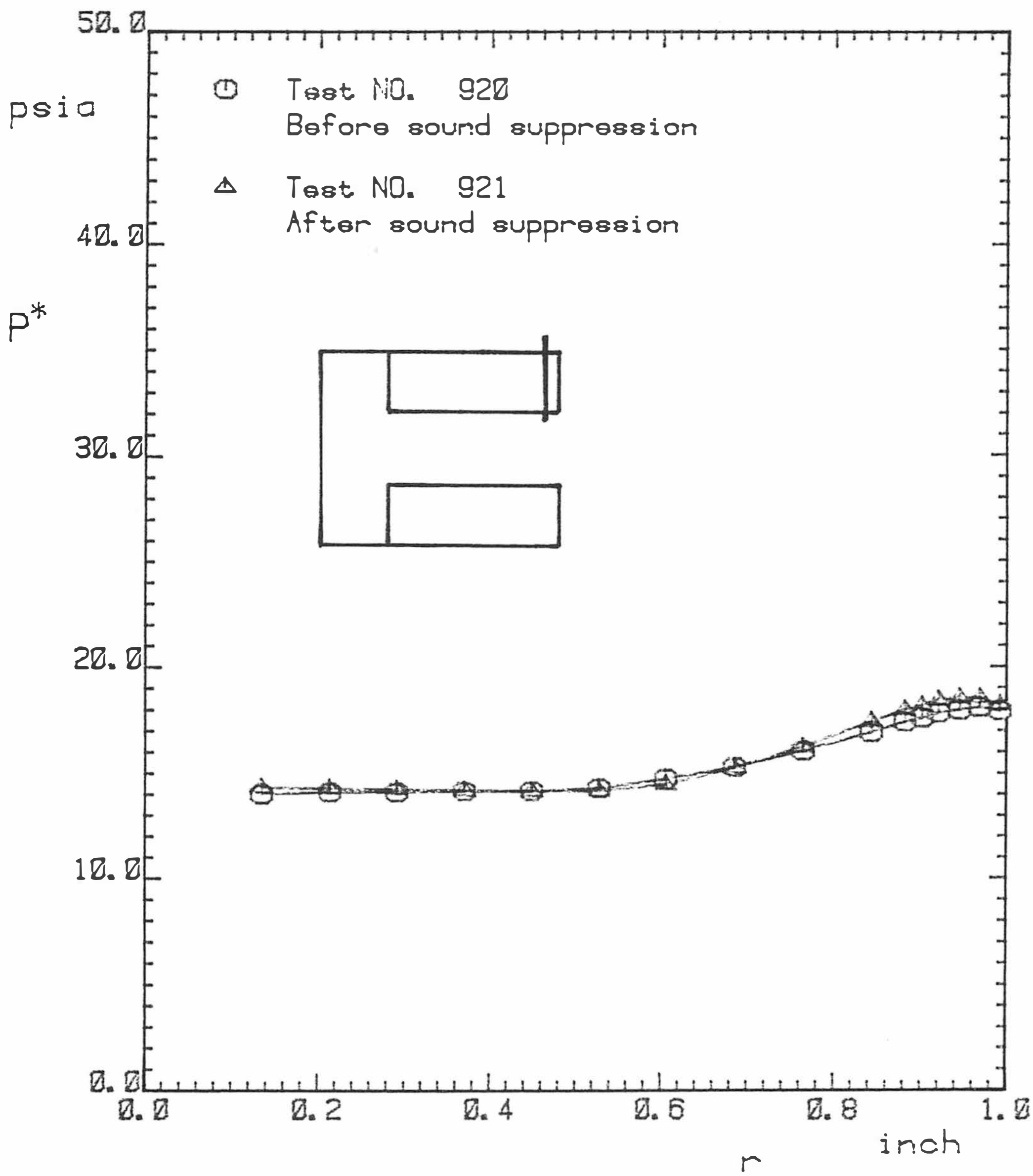

(a) total pressure

Figure 24. Data for 1.375 inches acoustic cavity length; taken at 22nd acoustic cavity position.

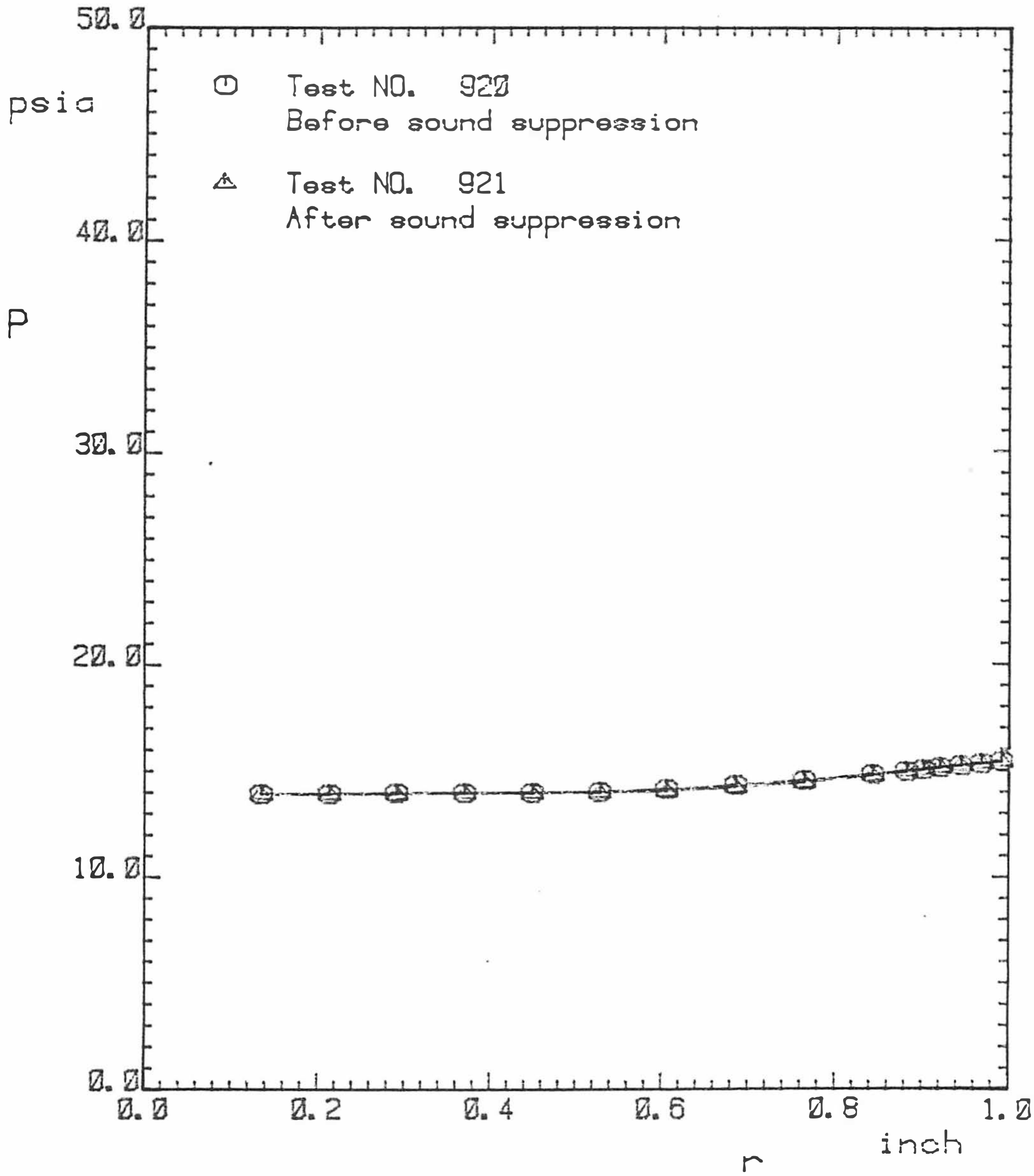

(b) static pressure

Figure 24. (Continued)

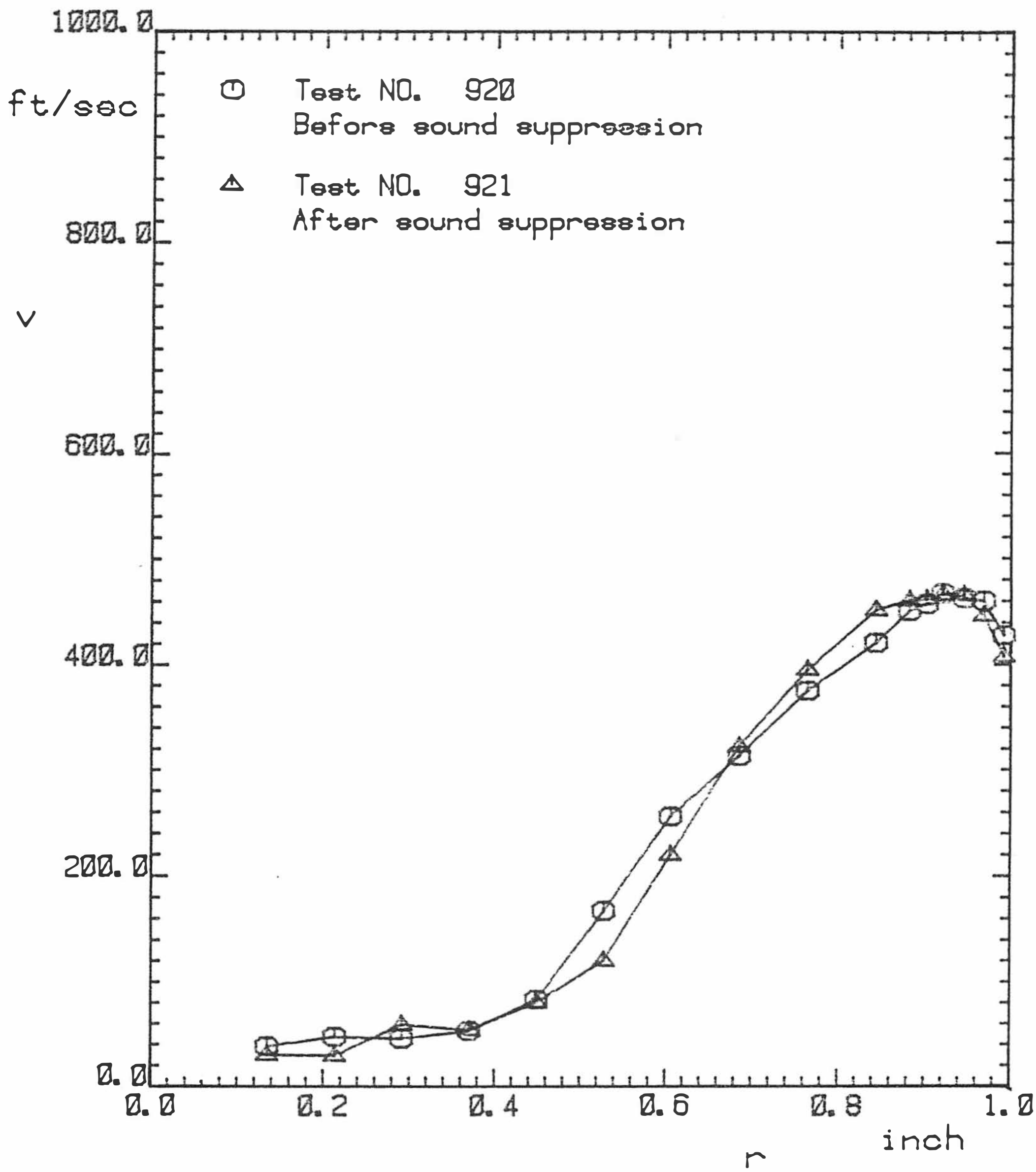

(c) tangential velocity

Figure 24. (Continued)

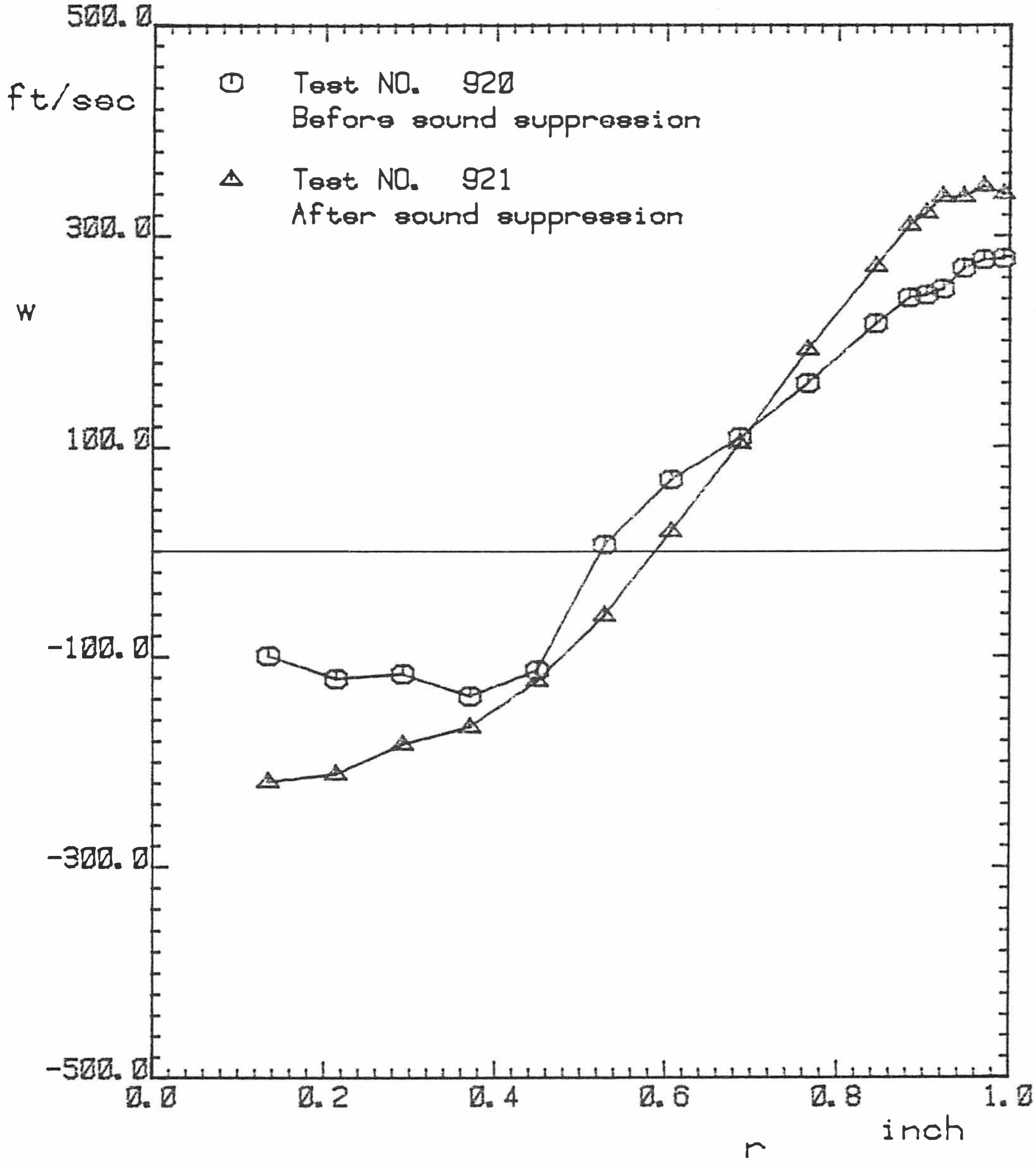

(d) axial velocity

Figure 24. (Continued)

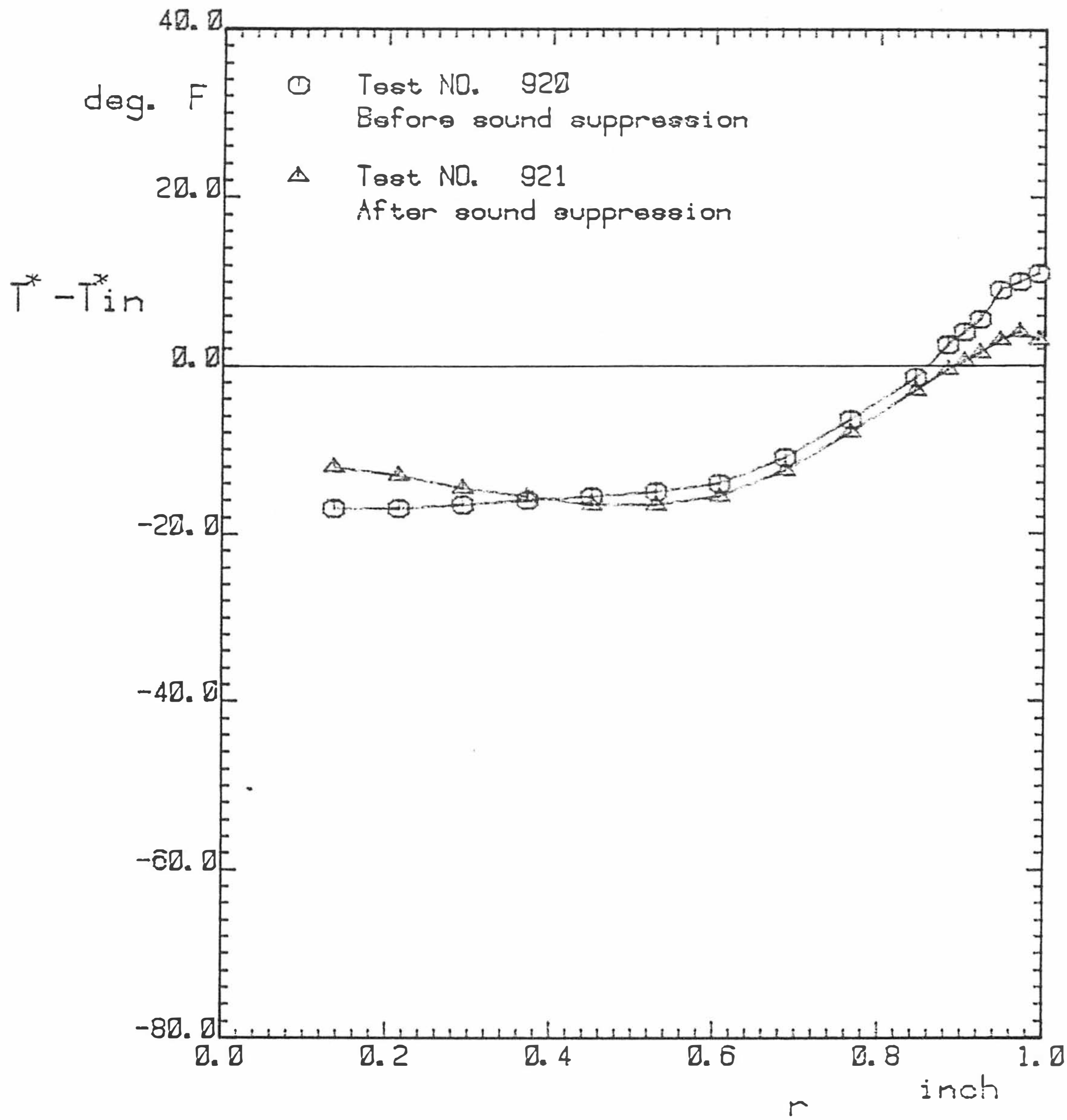

(e) total temperature

Figure 24. (Continued)

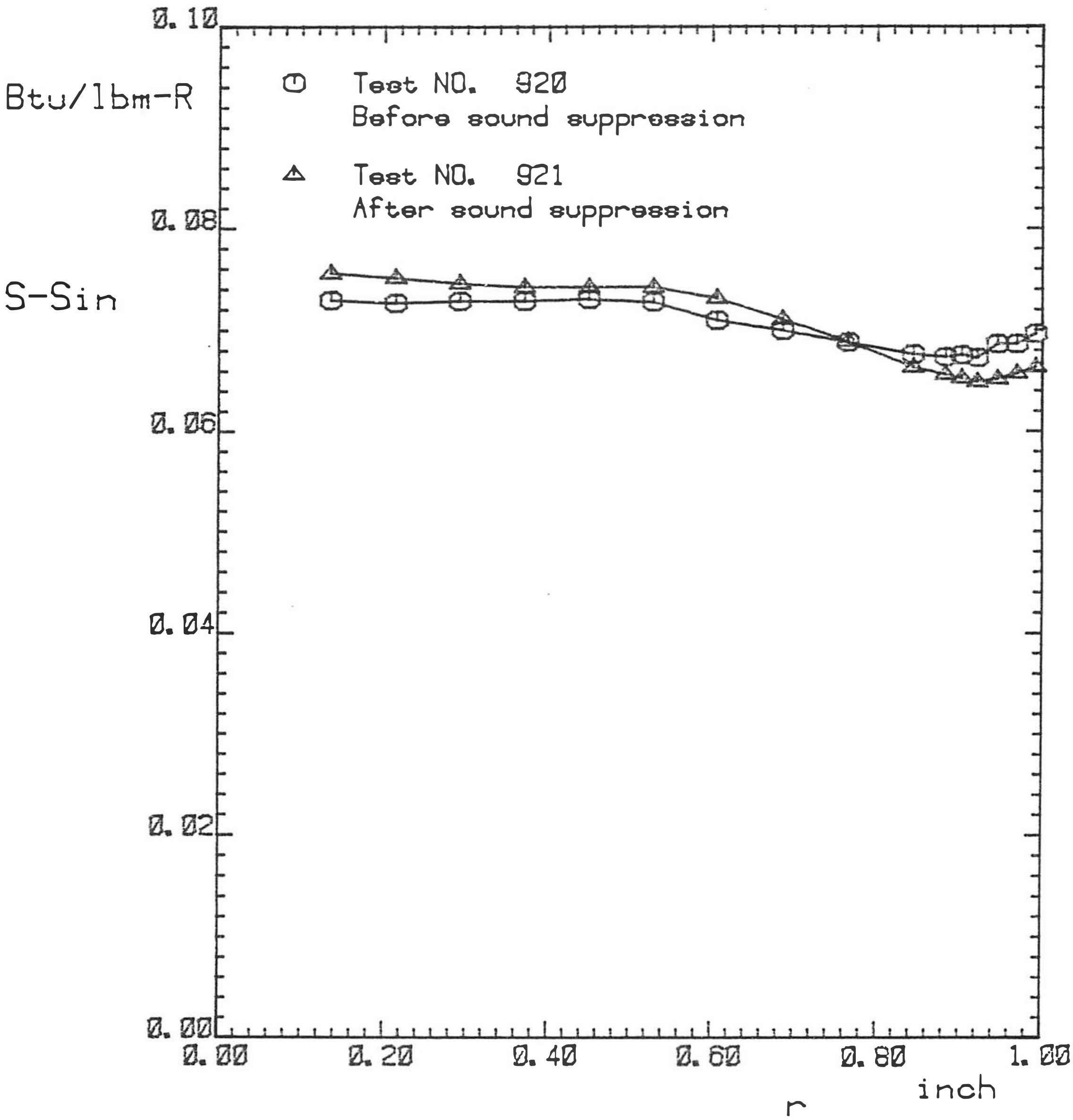

(f) entropy

Figure 24. (Continued)

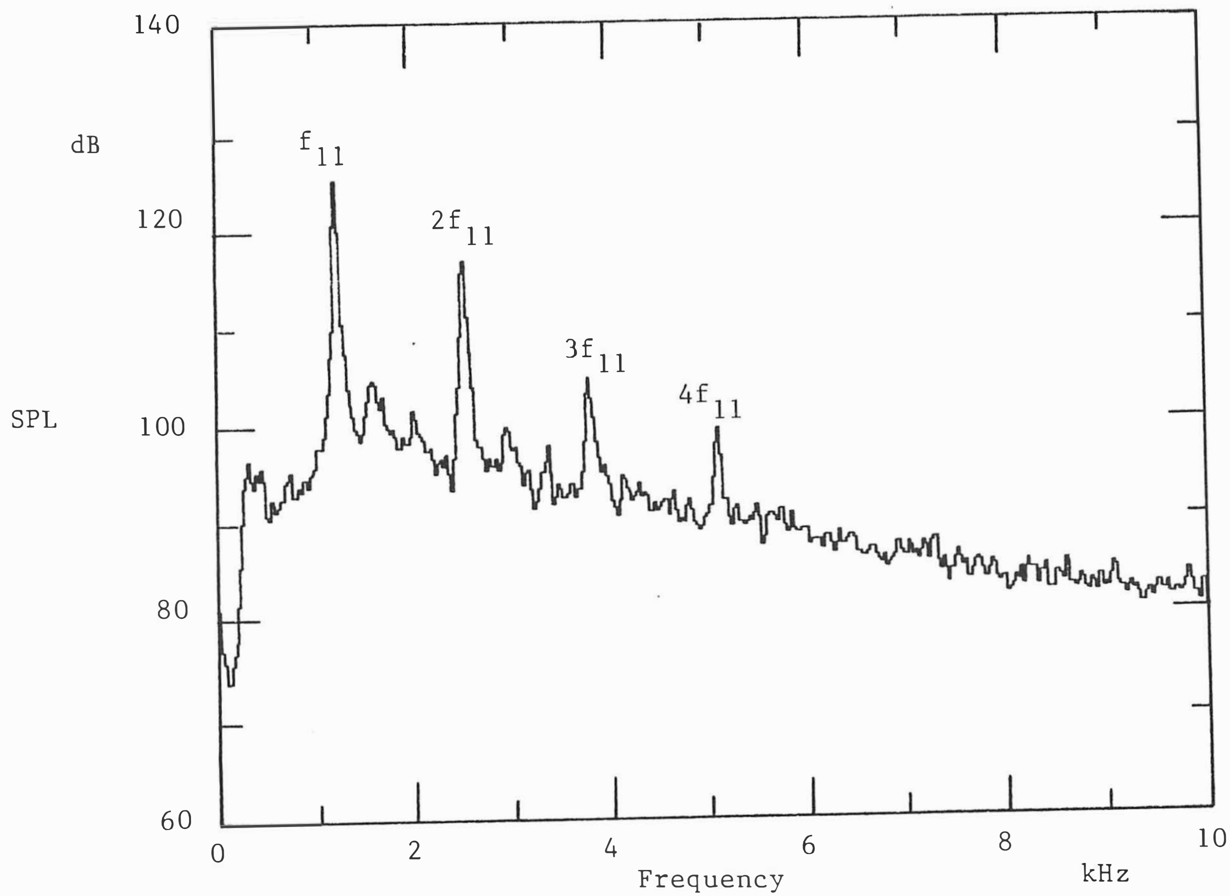

(g) frequency spectrum before sound suppression

Figure 24. (Continued)

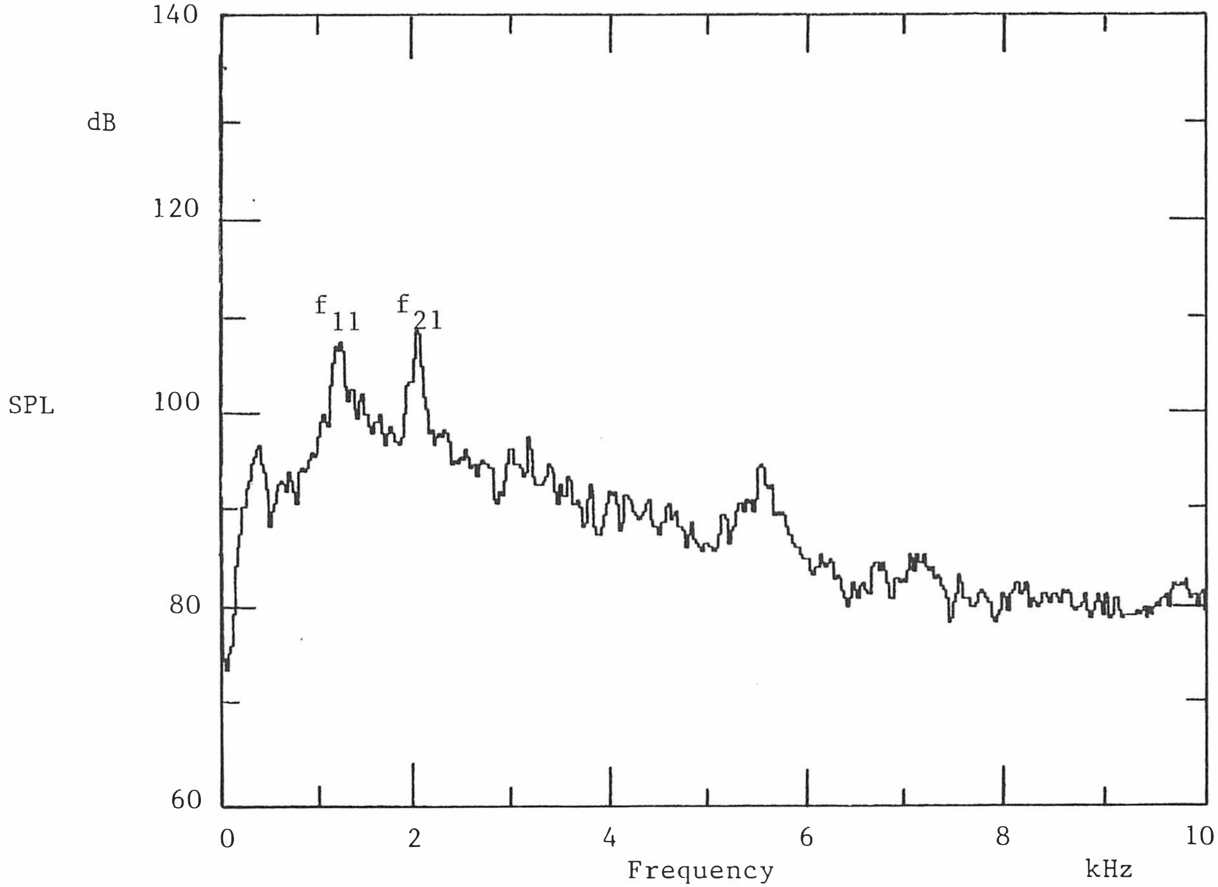

(h) frequency spectrum after sound suppression

Figure 24. (Continued)

muffled hiss. At the same time, the centerline total temperature, measured by the thermocouple inserted through the cold-end plug, suddenly jumps up. This amount of jump, ΔT^*, is 46.5°F; the difference between the centerline and inlet total temperature is now reduced to -34.5°F.

The radial profile of the total temperature (triangles of Figure 22(e)), measured by the radially inserted probe, shows that there is a compensating decrease of total temperature between around r = 0.5 inch and r = 0.8 inch and the pipe periphery temperature remains the same.

In spite of the observed change in the temperature separation, which is to be expected, the tangential velocity profile does not, however, revert to a Rankine vortex, as triangle points of Figure 22(b) show. This is contrary to all the expectations, and the question is "what has happened?"

A clue to this can be obtained from the inspection of the axial velocity (Figure 22(d)). Even before the sound suppression, the negative axial flow or reverse flow exists near the pipe centerline.

When the vortex whistle is suppressed, this reverse flow, however, increases about four times, as shown in Figure 22(d). This reverse flow or the entrainment of ambient air without any swirl may annihilate the potential regeneration of the higher tangential velocity near the centerline; it may thus prevent the reversion to a Rankine vortex. As Figure 22(e) shows, the temperature distribution in radial direction after the sound suppression is also different from that of a Rankine vortex; it is not like the radial distribution characterized by the almost uniform radial direction of a Rankine vortex observed in the previous IV-B. However, when the vortex whistle is suppressed, the total temperature at the centerline does jump up. Then, a question might be raised whether the observed temperature jump, ΔT*, may be due to the entrainment of the warm ambient air carried into the main pipe by the reverse flow. This was verified not to be so; by directly heating the ambient air near the main pipe exit to the temperature of 300°F, and observing the centerline temperature and change of ΔT* at the sound suppression; the centerline temperature is found to be affected by only 3°F.

Thus the presence of the reverse flow does not affect our key point that the temperature separation is caused by the vortex whistle. However, it is certainly nice if the increase of the reverse flow after the sound suppression could somehow be prevented. In spite of many attempts, none has been found to be successful in achieving this.

Another point worthy of attention is that in the frequency spectrum of Figure 22(h) after the sound suppression, the emergence of what is identified to be f_{21} frequency from the Lissajous figure of Figure 22(i); this and other points will be discussed in more detail later in Section D.

At the axial position of Z = 3.5 inches, which corresponds to the 12th acoustic cavity, the velocity profiles, as shown in Figure 23, are almost the same as that of the 4th cavity position, except that the tangential velocity devreases slightly due to the viscous effects. The total temperature near the centerline again jumps at the sound suppression, while here near the pipe periphery now clearly shows the temperature drops.

At the axial position of Z = 5.4 inches, which corresponds to the 22nd acoustic cavity (Figure 24), the tangential velocity before the sound suppression resembles the flow distribution after the sound suppression, rather than that of a forced vortex. The reason is that, since this position is only 0.1 inch upstream of the main pipe exit, the reverse flow or the entrainment of the ambient air which does not possess swirl, cannot attain sufficient amount of swirl flow and this effect will be felt most directly near the exit. The total temperature distributions also suffer from the effect of backflow, although near the centerline the temperature still increases after the sound suppression, while near the pipe periphery it decreases. The major data are tabulated in Table 2.

At the tuned condition, a striking transformation in flow takes place at the exhaust. This change in flow can be observed by placing a small rod with a tuft attached to its tip. Before the sound suppression, the air from the main pipe turns around the corner of the end plate surface, and flows along it. On the other hand, the region over the center is calm, but ambient flow is found to penetrate into the main pipe center; this is the aforementioned reverse flow region in the main pipe near the centerline, as shown in Figure 25(a).

After the tuned condition, however, the region outside of the pipe wall becomes, all of a sudden, quiescent, and the air from the main pipe now gushes out along the centerline with small amount of swirl, as shown in Figure 25(b), (these observations are consistent

Table 2

Mass Flow and Energy Flux

Test No.	Probe Position	P_{in} psia	G_{in} lbm/sec	$G^{\dagger}$ lbm/sec	$G^{\dagger\dagger}$ lbm/sec	Q_{in} Btu/sec	$Q^{\dagger}$ Btu/sec	$Q^{\dagger\dagger}$ Btu/sec
924*	4	46.13	.1817	.1814	.1841	22.1	22.1	22.4
922*	12	46.09	.1825	.1523	.1850	22.2	18.9	22.9
920*	22	46.09	.1824	.1410	.1750	22.2	17.3	21.5
925**	4	46.92	.1888	.1882	.1922	22.9	23.1	23.5
923**	12	46.92	.1888	.1701	.1912	22.9	20.9	23.4
921**	22	46.91	.1890	.1713	.1896	23.0	21.0	23.2

†Calculated from P*, P, T* and α.

††Calculated from differential equation.

*Before sound suppression.

**After sound suppression.

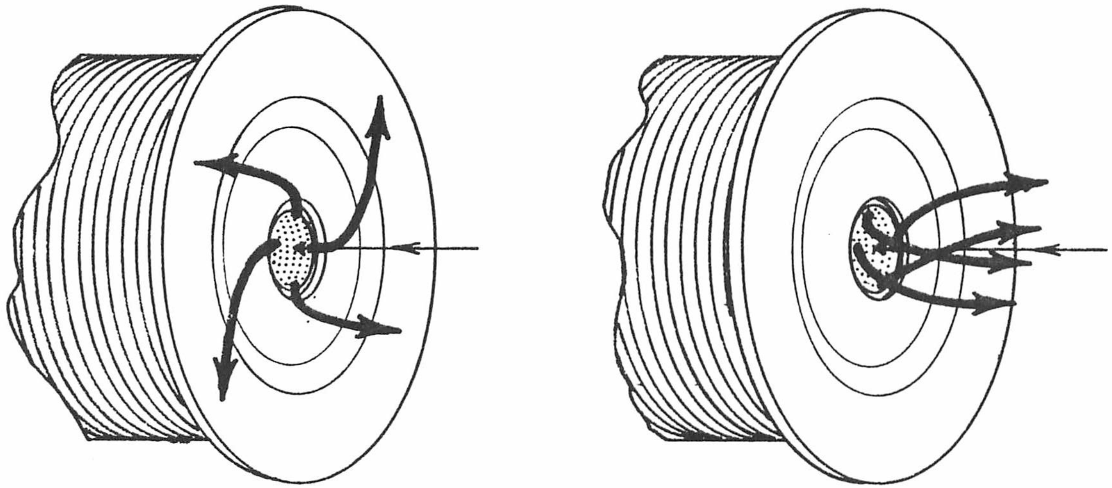

(a) before sound suppression (mainly radial flow)

(b) after sound suppression (mainly axial flow)

Figure 25. Schematic flow pattern near exhaust.

with the one observed in the small-scaled test rig by Chu [24]. Near the pipe periphery, the ambient air cannot penetrate into the main pipe. However, although the air from the main pipe gushes out, the reverse flow still exists near the centerline. This flow is very vigorous; for example, when the disk with the same size as that of the main pipe diameter is positioned at about one foot downstream from main pipe exit, the disk is pulled toward upstream with strong suction.

It was found that the flow pattern outside the main pipe and the manner and amount of sound suppression is extremely sensitive to the configuration of the end plate. Several kinds of the end plates were examined. Figure 26 shows the plates and their flow patterns before and after sound suppression (in Figure (a) to (g), the flow pattern shown above the pipe centerline corresponds to the flow before the sound suppression; the flow pattern shown below the centerline corresponds to the flow after the sound suppression).

The plate (a) is the original end plate, and almost all of the experiments used this; the flow patterns associated with this have been mentioned before, in connection with Figure 25. The plate (f) has almost the same characteristics of change in flow as plate (a). When the plates (b), (c), (d) or (g) are installed as the end plate, the temperature separation after the sound suppression is completely different from the one corresponding to the original plate, because the sound cannot be suppressed as sufficiently as by the original plate. (Before the sound suppression for any end plate, the sound level of the vortex whistle is virtually the same and the total temperature separation is also almost the same.)

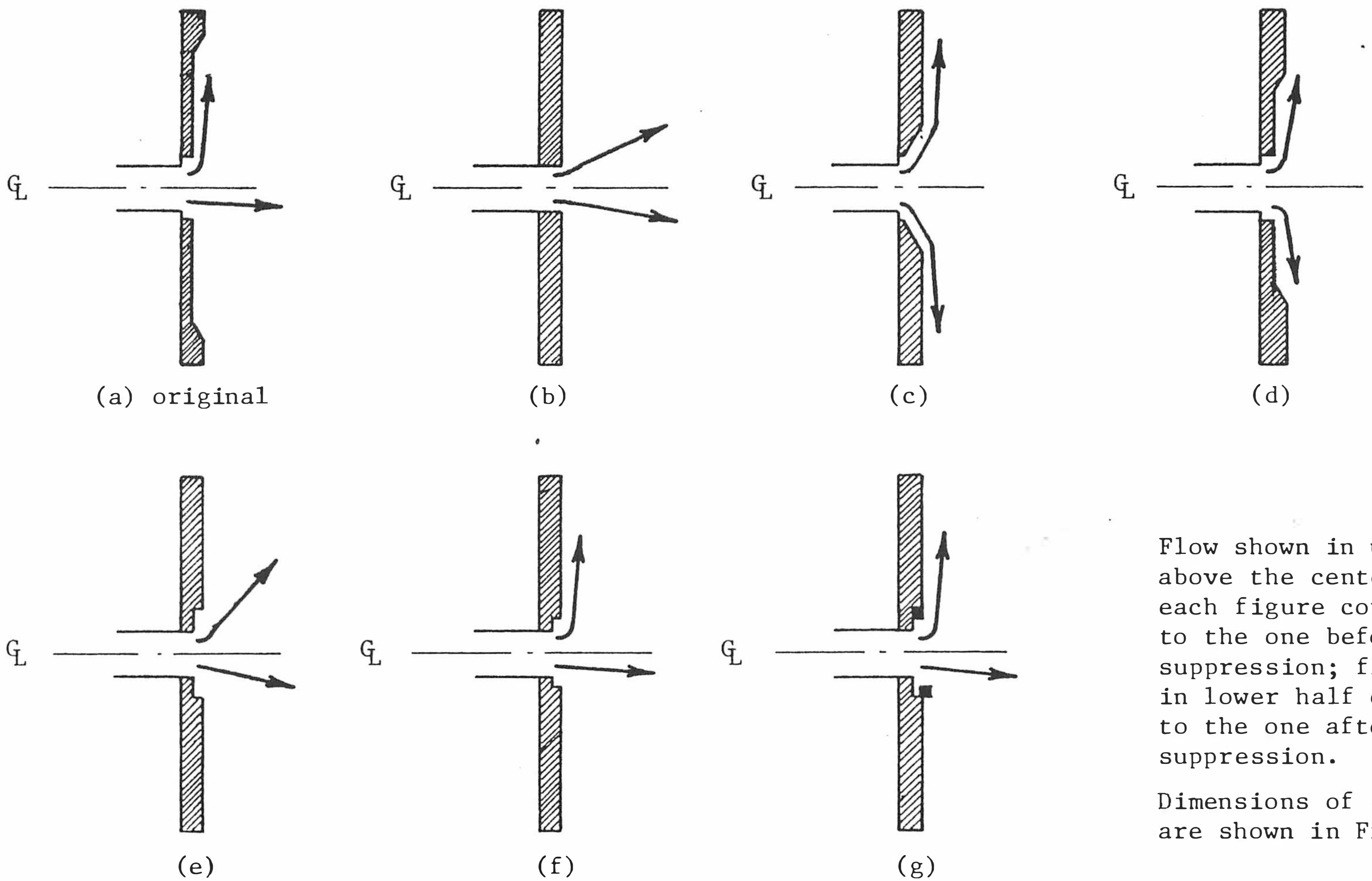

Flow shown in upper half above the centerline of each figure corresponds to the one before sound suppression; flow shown in lower half corresponds to the one after sound suppression.

Dimensions of end plates are shown in Figure 6.

Figure 26. Effect of end plates upon flow pattern.

The role of the end plate in the sound suppression and the subsequent change in the flow pattern has not been investigated in detail, although one can speculate that it may be related to the Coanda effect.

All of the above data corresponds to the sound suppression for a porous pipe without any restriction placed near its exit. When the exit plate with its opening diameter smaller than that of the main pipe is placed at the end of the porous pipe, the sound suppression does not suddenly take place at a fixed inlet pressure anymore. Instead, the sound level gradually decreases over a range of inlet pressure. However, the data taken for a small exit area does show the virtual absence of the reverse flow and reversion to what resembles a Rankine vortex.

Figure 27 shows the radial survey at 12th cavity position with smaller exit area, the opening diameter on the end plate equal to one inch. Since the tuned condition is over a range of pressure, the inlet pressure before the sound suppression is taken to be at 31.03 psia, and the inlet pressure after the sound suppression at 36.62 psia. Before the sound suppression, the vortex whistle is very small, as shown in frequency spectrum (Figure 27(d)). The tangential velocity distribution, indicated by circles in Figure 27(a), therefore, is not a forced vortex. After the sound suppression, the vortex whistle disappears, Figure 27(e) (but other peaks appear as in Figure 27). What is most interesting here is that, after the sound suppression, the tangential velocity, shown by triangles in Figure 27(a), is observed to become something like a Rankine vortex. Before and after the sound suppression, the axial velocities (Figure 27(b)) do not show any signs of

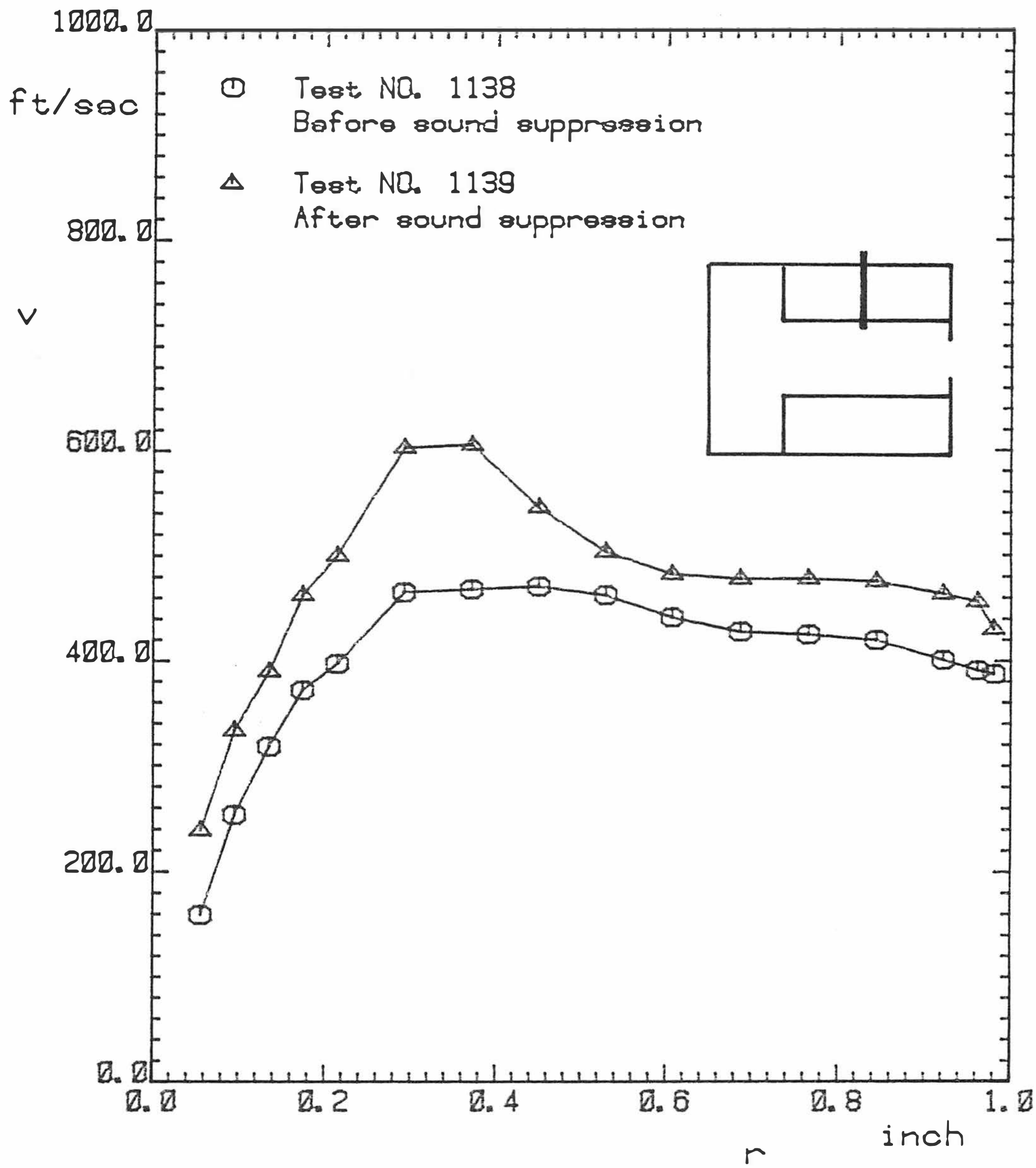

(a) tangential velocity

Figure 27. Data for 1.0 inch exit opening diameter and 1.375 inches acoustic cavity length.

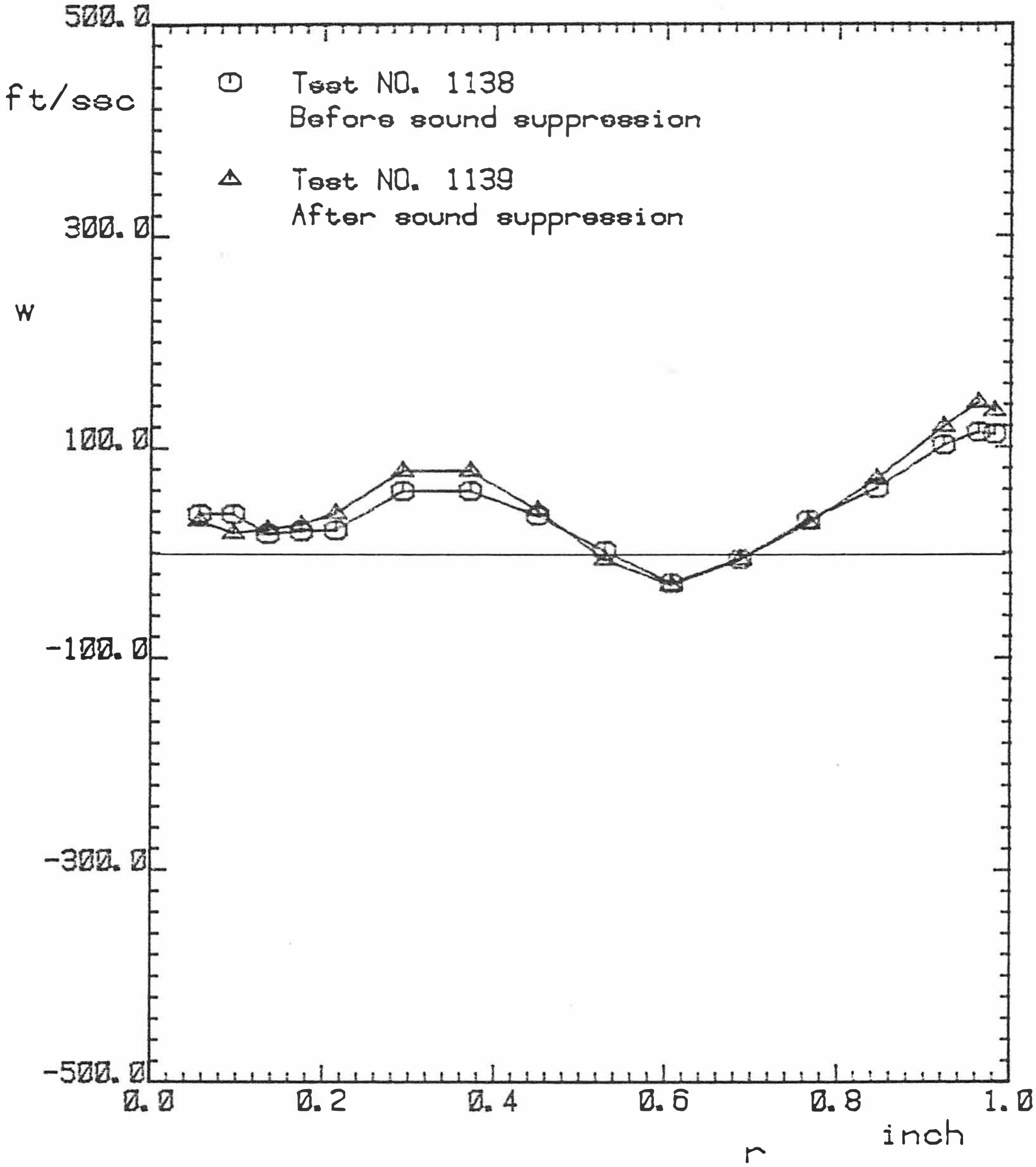

(b) axial velocity

Figure 27. (Continued)

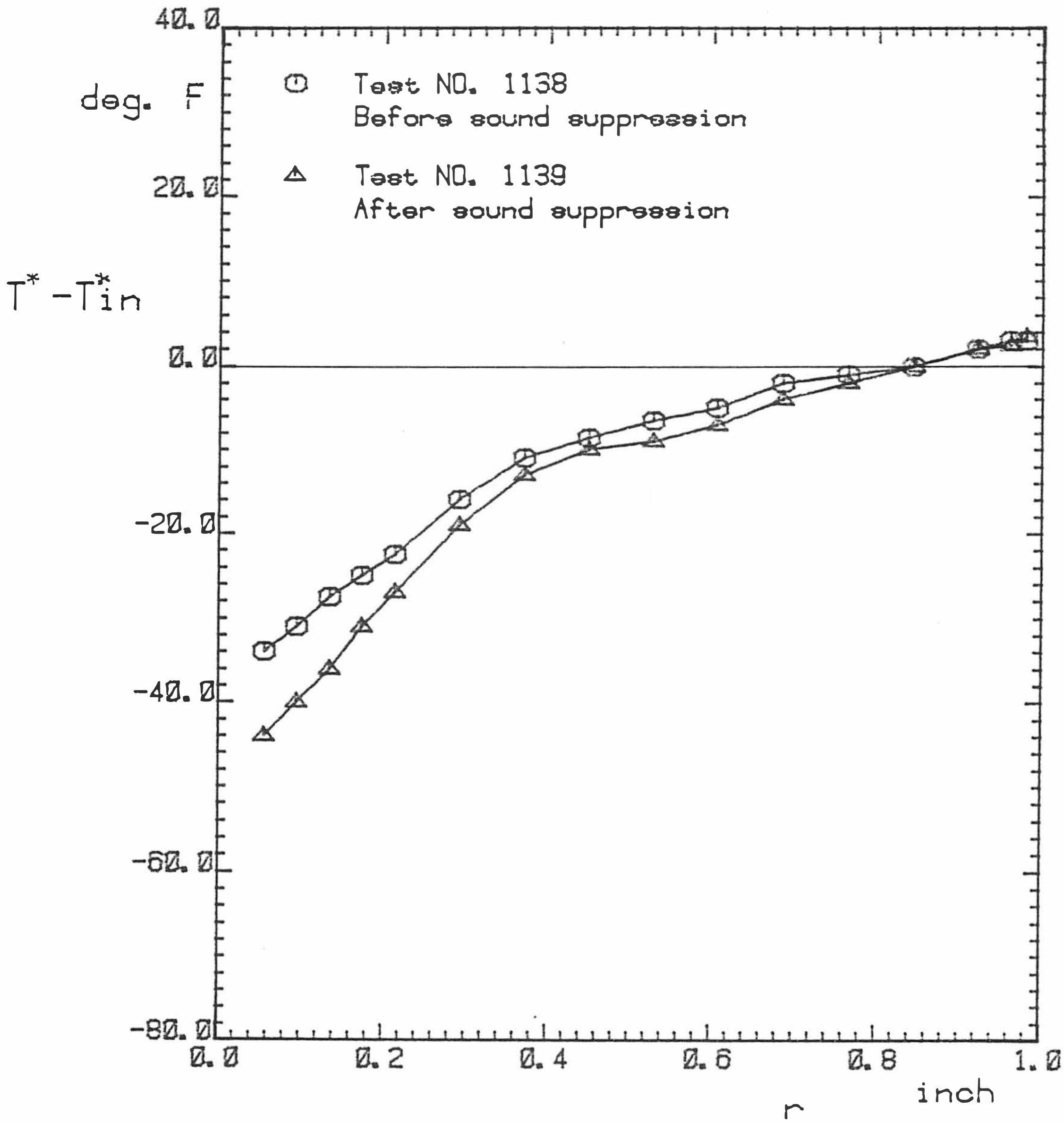

(c) total temperature

Figure 27. (Continued)

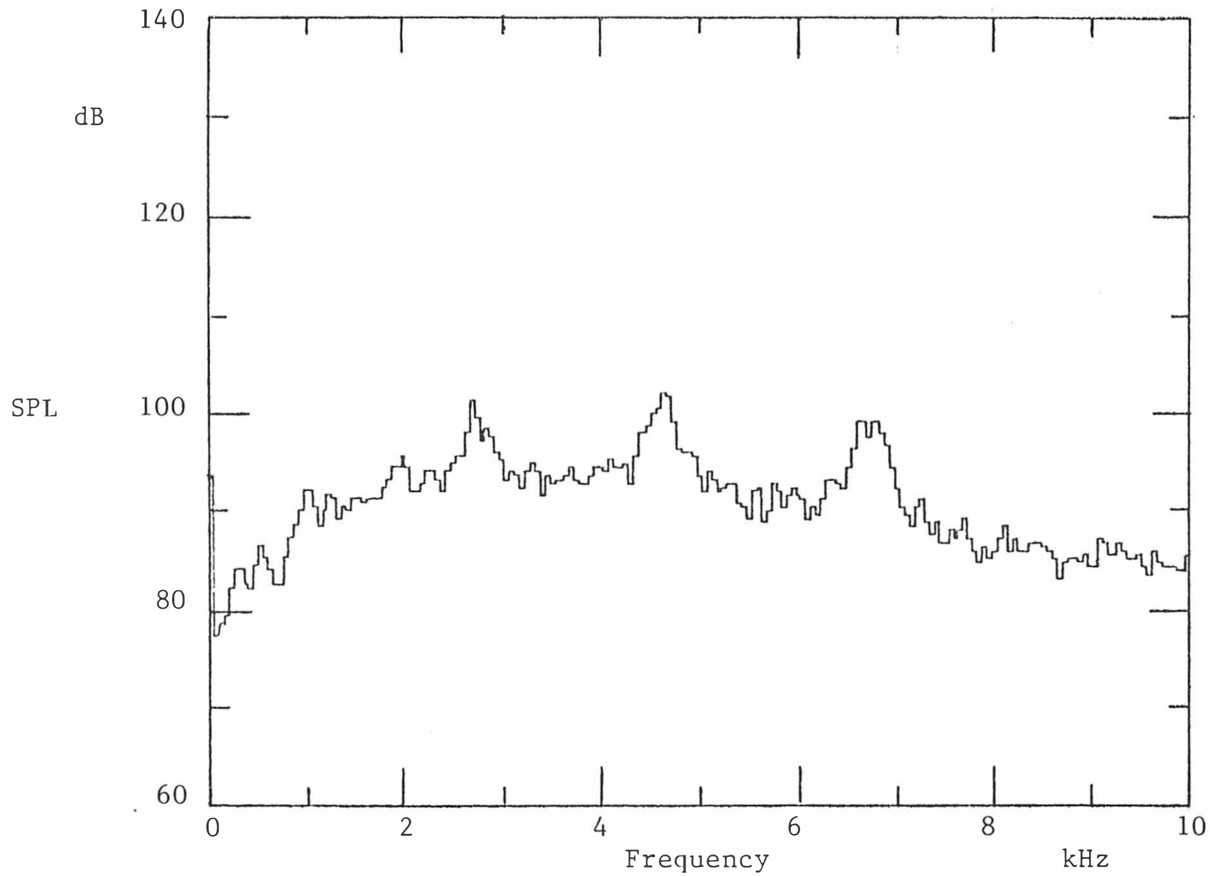

(d) frequency spectrum before sound suppression

Figure 27. (Continued)

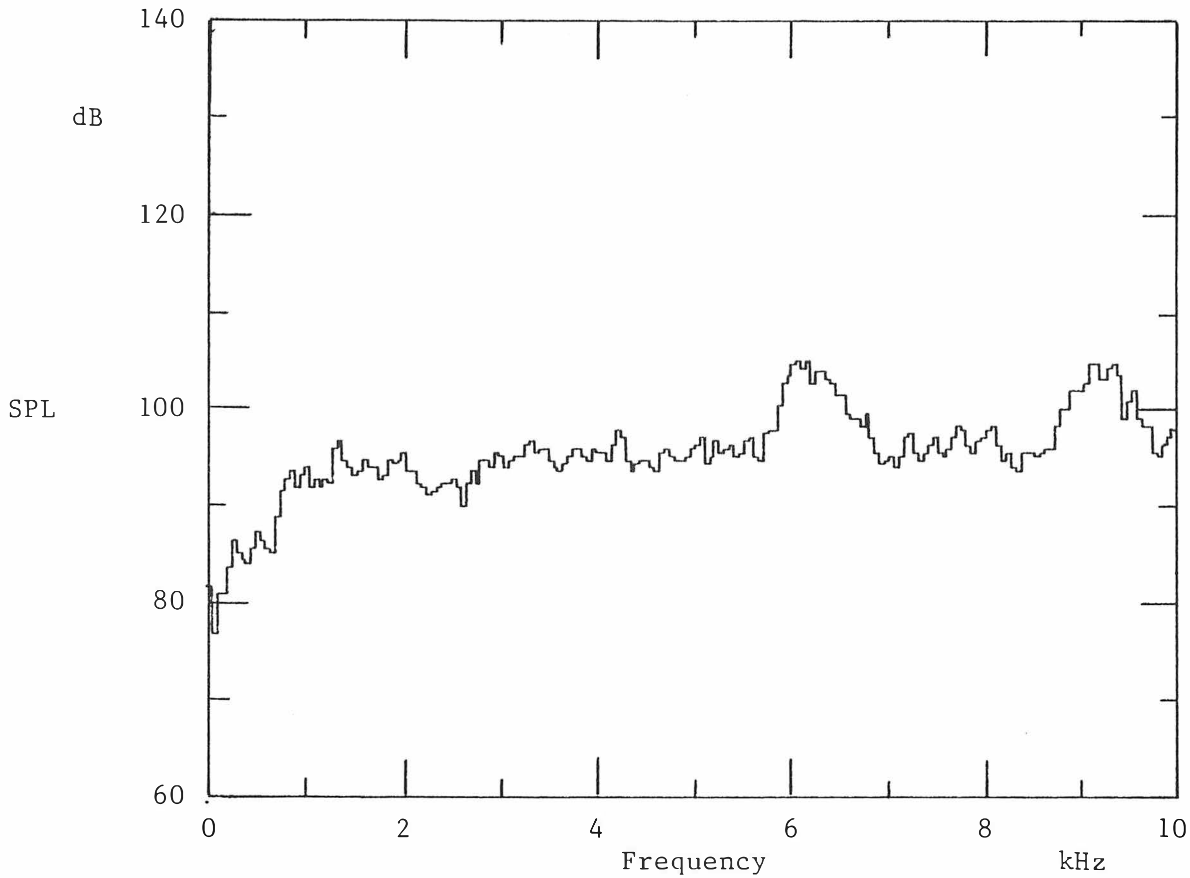

(e) frequency spectrum after sound suppression

Figure 27. (Continued)

reverse flow region near the centerline; slight amount of the reverse flow exists, however, in a small area corresponding to the radial position of $r = 0.6$ inch.

The total temperature near the centerline, before the sound suppression, is equal to 15°F ($T_t - T_{in} = -36°F$), and the one after the sound suppression is 6°F ($T_t - T_{in} = -47°F$). The total temperature jump, ΔT^*, drops 9°F, instead of the usual increase; this drop due to the sound suppression is, however, reasonable, when one takes into account the fact that the inlet pressure rises by 5 psi during the sound suppression. This data, which has no reverse flow near the centerline, indeed points out the possibility that once the increase of the reverse flow is somehow prevented for a pipe without an end restriction, the sound suppression appears to make the tangential velocity distribution revert to a Rankine vortex.

D. Effect of Backflow

In the previous section, it has been discussed that the effect of reverse flow near the centerline might be preventing the reversion to a Rankine vortex at the time of sound suppression.

To confirm the influence of the reverse flow near the centerline, a secondary air was injected into a pipe with an end plate having smaller opening; its direction was toward the upstream and the injection pipe of 3/8 inch was placed near the exit of the main pipe and along its centerline. The idea is to investigate whether this artificially created backflow can alter the profile of a Rankine vortex, which, as mentioned, can be realized by placing an exit plate with smaller opening at the exit.

Figure 28 shows the radial survey corresponding to 0.8 inch exit opening diameter, and the data were taken at the 12th acoustic cavity position. As seen before, without blowing (circles in Figure 28(a)) the tangential velocity profile is a Rankine vortex, and it has no reverse flow region near the centerline. The total temperature profile (circles in Figure 28(c)) is almost constant, except the core region near centerline; the peaks of vortex whistle are not recognizable in the frequency spectrum of Figure 28(e).

With the blowing, from Figure 28(a), the tangential velocity profile is seen to change from a Rankine vortex to something similar to a forced vortex. At the same time, the axial velocity near the centerline decreases due to the injection of a reverse flow (Figure 28(b)), as expected. Furthermore, the total temperature starts to show linear distribution in the radial direction (Figure 28(c)), because the vortex whistle, small though it is, now emerges (Figure 28(f)).

Thus it seems almost certain that for the main pipe without an exit plate, the reversion to a Rankine vortex after the sound suppression is prevented by the reverse flow near the center. To minimize the reverse flow, the test rig has to undergo major improvement.

Figure 29, (a) and (b), shows two suggested modifications of the test rig; as shown in (a) the shape of the cold-end plug may have to be changed in such a way as to accelerate the flow near the centerline [35], like a centerbody of the radial turbine. The other (b) is that the shape near the exit region may have to be changed considerably

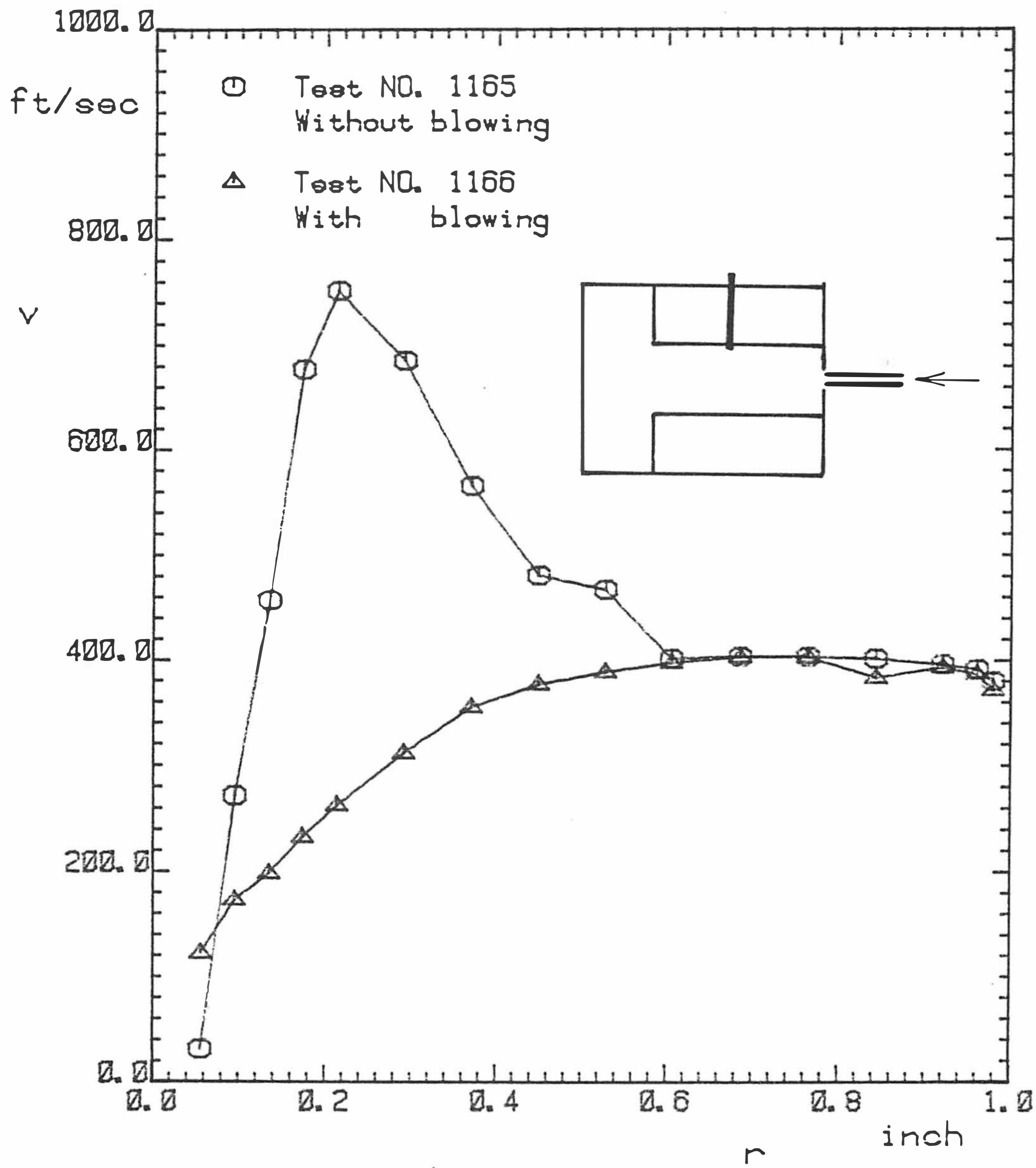

(a) tangential velocity

Figure 28. Artificial injection of backflow from exit with 0.8 inch opening diameter.

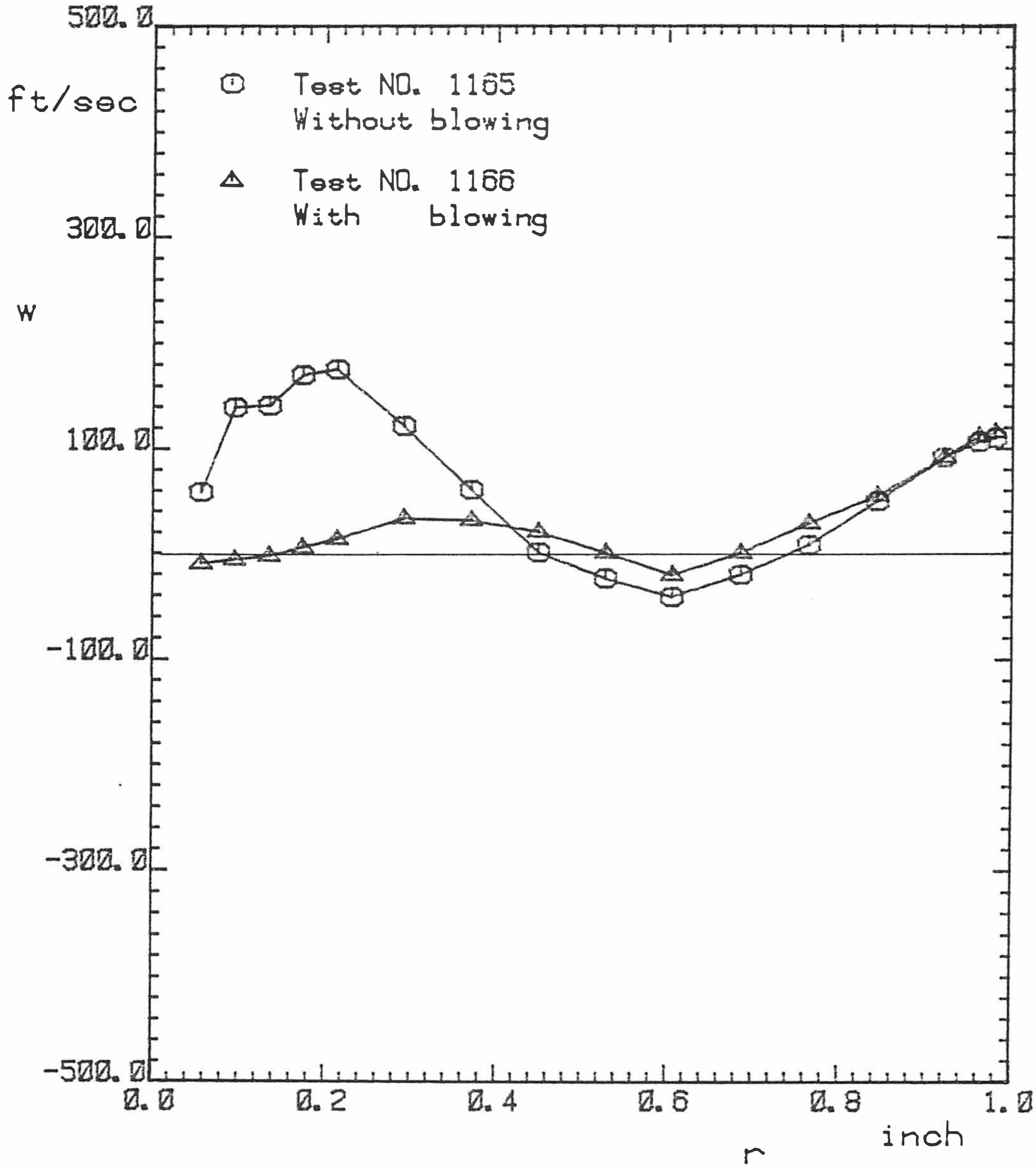

(b) axial velocity

Figure 28. (Continued)

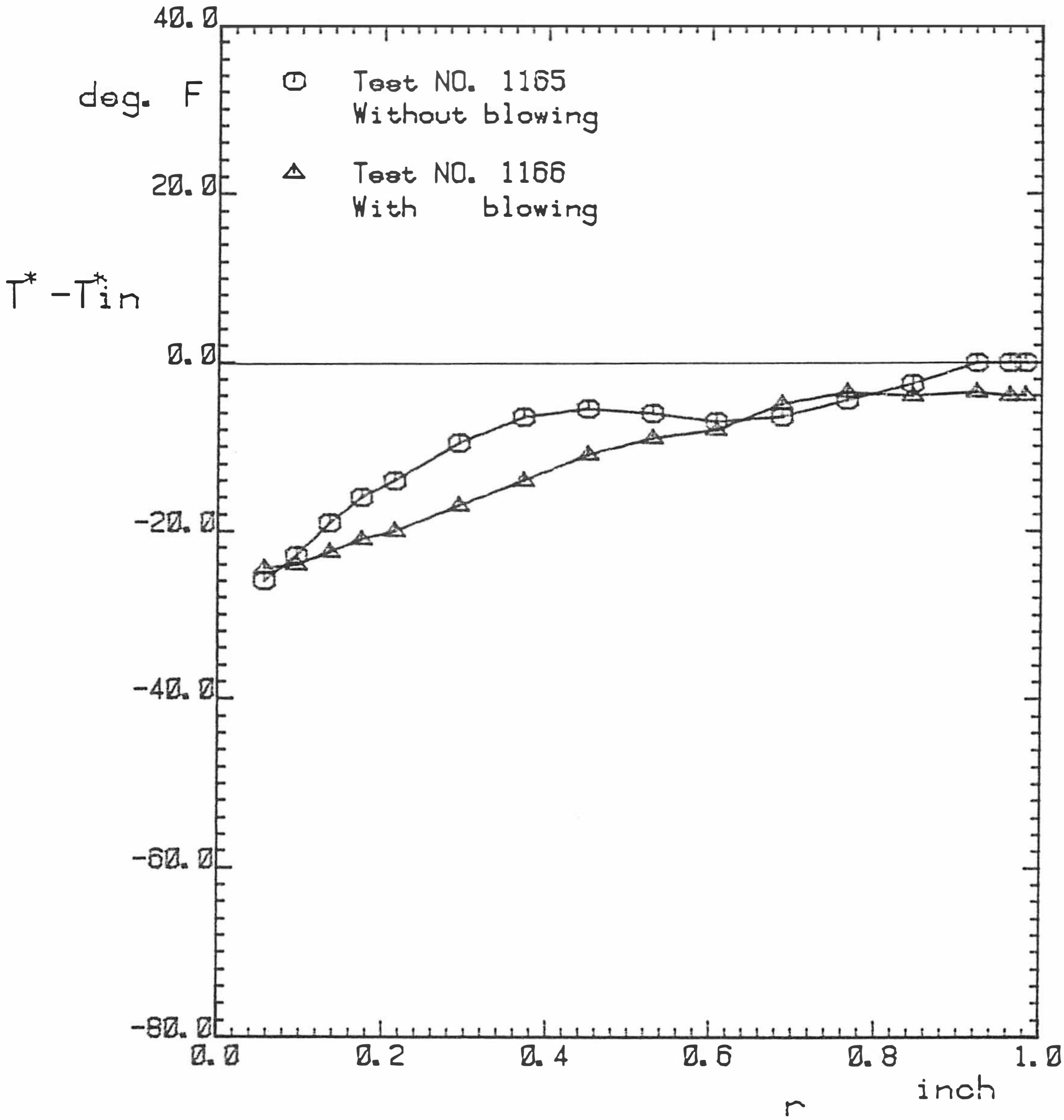

(c) total temperature

Figure 28. (Continued)

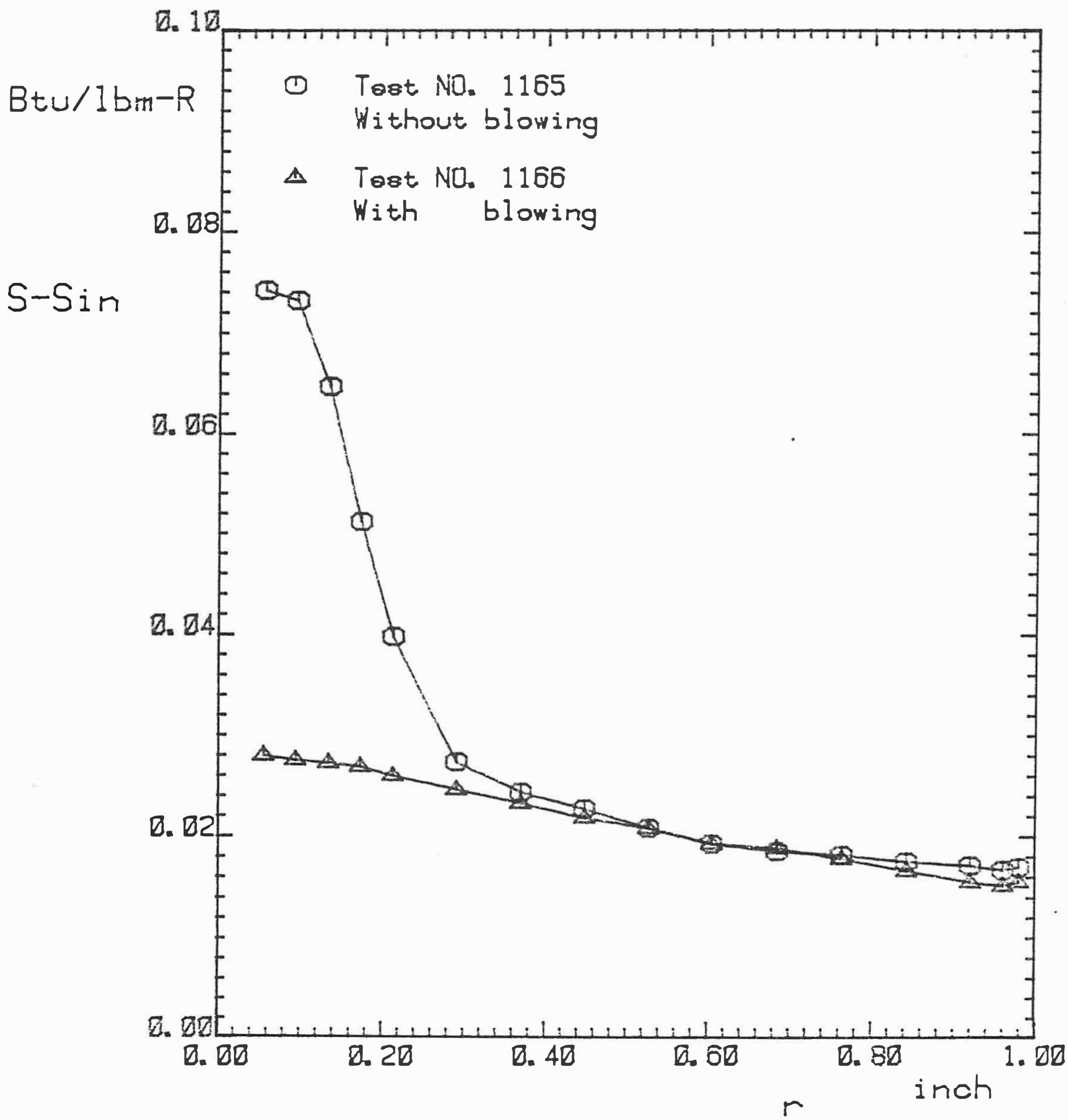

(d) entropy

Figure 28. (Continued)

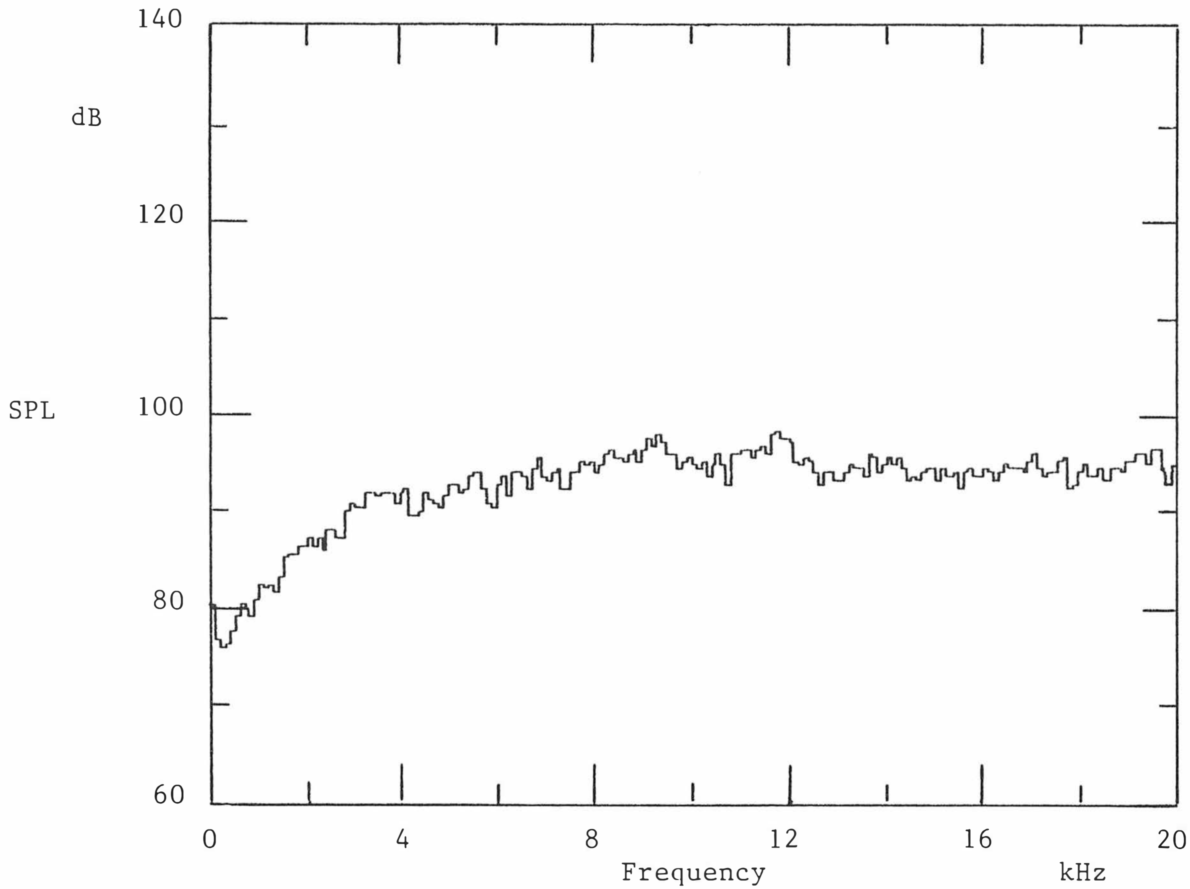

(e) frequency spectrum without blowing

Figure 28. (Continued)

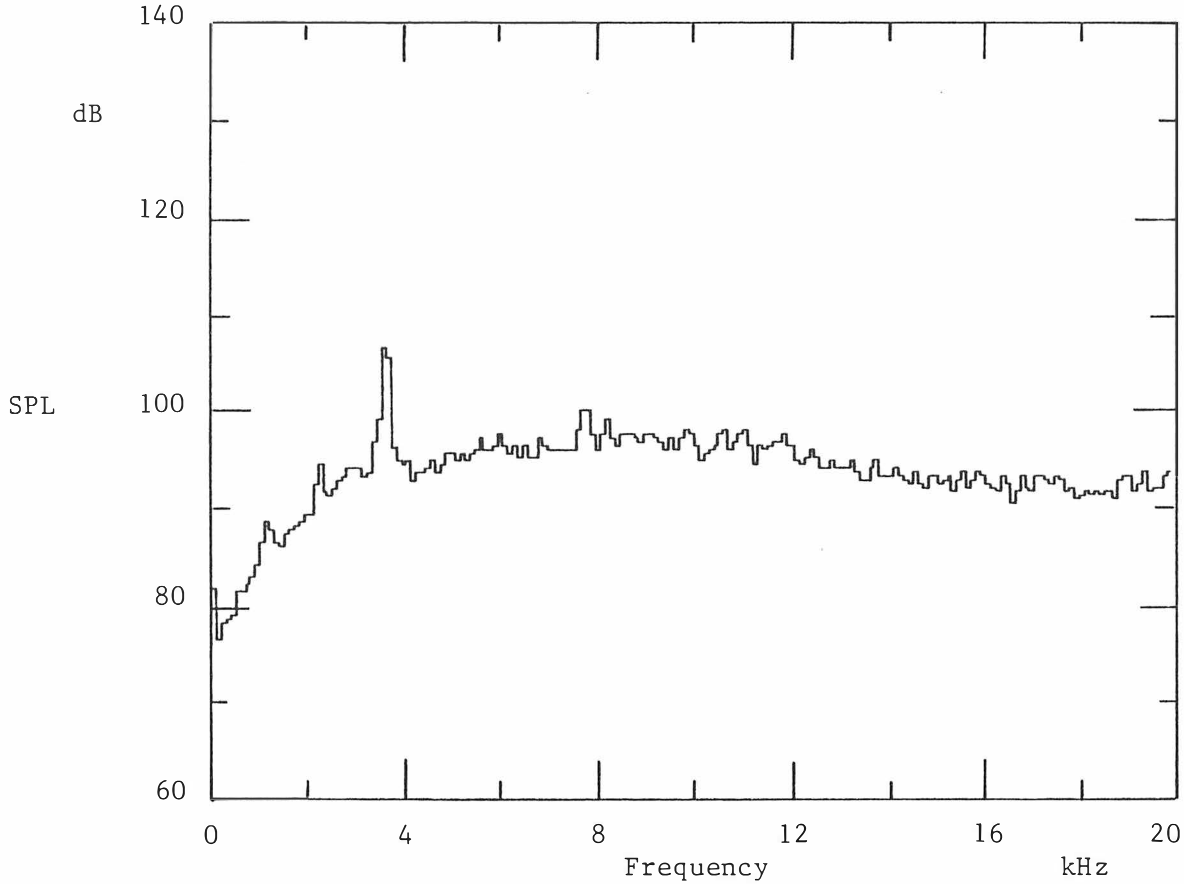

(f) frequency spectrum with blowing

Figure 28. (Continued)

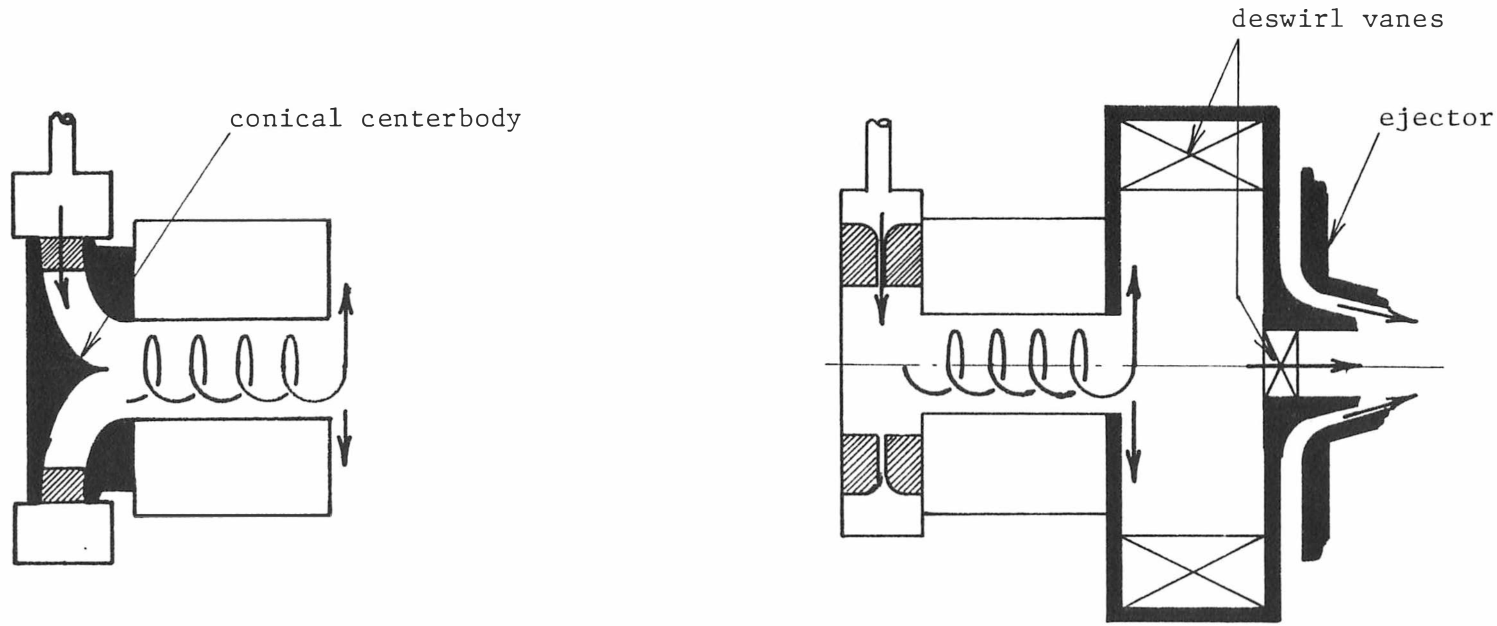

(a) upstream modification

(b) downstream modification

Figure 29. Suggested future modifications.

with the provision of a partially evacuated chamber installed at the exit of the main pipe; the evacuation will be achieved by connecting it to an ejector. These revisions are, however, beyond the scope and hardware capabilities of the present investigations.

E. Investigation on Tuning Frequency

In the preceding work [3, 24], it has been tacitly assumed that the tuned frequency for a given acoustic cavity length corresponds to the fundamental frequency of the vortex whistle. This was done in spite of the fact that, according to quarter wavelength resonator theory, considerable discrepancy was found to exist.

In the present thesis, this point was examined more carefully by creating a white noise and identifying the resonant tuned frequency. It was found that the supply of a white noise can be facilitated by installing a ring with an opening of 0.3 inch diameter between the swirl generator and the main pipe.

Figure 30 shows the frequency spectra for 1 3/8 inches acoustic cavity length corresponding to different mass flow.

Now if one assumes that the acoustic cavity acts as a quarter wavelength resonator, the tuned frequency, f_t, in the absence of the grazing flow, is given by

$$f_{t1} = a/4\ell, \quad f_{tn} = (2n - 1)\, f_{t1} \tag{25}$$

where a is the speed of sound, ℓ, the cavity length, and n = 1, 2, 3, ...

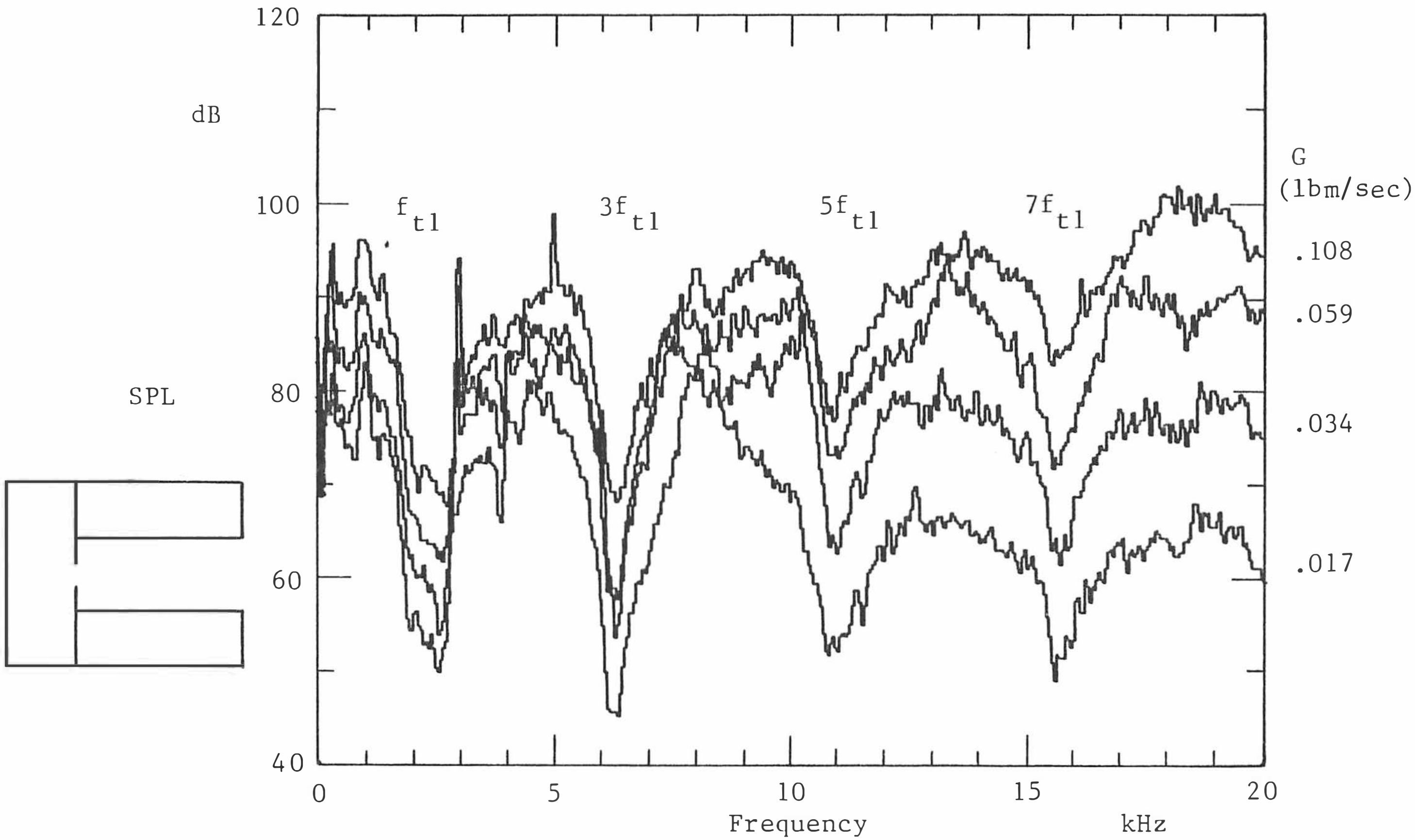

Figure 30. Tuned frequency corresponding to 1.375 inches acoustic cavity length and at various mass flow G.

The first dip of Figure 30 indeed corresponds to tuned frequency f_{t1}, the second to f_{t2} with $n = 2$, the third to f_{t3} with $n = 3$, and so forth. The tuned frequency f_{t1} is seen to remain almost the same regardless of the increase of the mass flow. Increasing the velocity of the grazing flow, in general, is known to increase the acoustic resistance of the cavity orifice [36, 37, 38], and decrease the resonant frequency [39]. When one observes carefully the shift in the position of the dip, the easily identifiable one being $f_{t4} = 7f_{t1}$, it can be recognized that the tuned frequency decreases as the mass flow is increased, but the amount of such a decrease is extremely small. Thus one can regard the resonant frequency as almost independent of the flow velocity. Even after the ring is removed, the tuned frequency of the vortex whistle is equal to these f_{tn} and they appear to be in good agreement with a quarter wavelength model.

Figure 31 shows the measured tuned frequency of the vortex whistle corresponding to the different acoustic cavity length. The results show fundamental, f_{11}, and second harmonics, $2f_{11}$, of the one obtained from the previous small test rig [3, 24], with its main pipe diameter equal to 11/16 inch as well as from the present one with 2 inches diameter. The solid line corresponds to the values calculated according to the quarter wavelength theory. From this it appears that, contrary to the previously held assumption, the second harmonic rather than the fundamental is suppressed for a given acoustic cavity length. Once the second harmonic is suppressed, the third harmonic also disappears because the latter is for the most part generated by the interference between the second and fundamental frequency. The sound

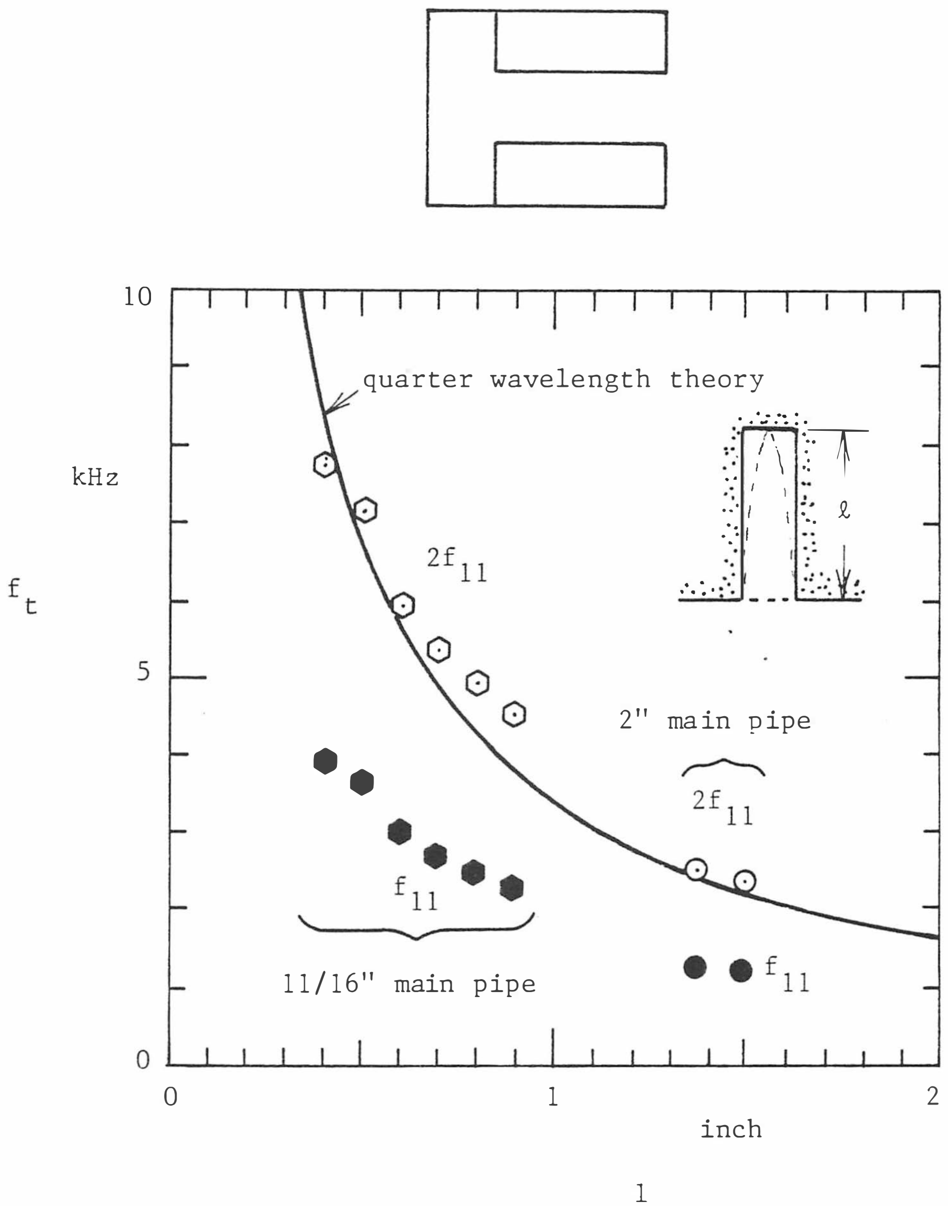

Figure 31. Tuned frequencies vs. acoustic cavity length.

level of the fundamental frequency decreases also, as the result of its generation due to the subtracting interference between the third and second harmonics, $f_{11} = 3f_{11} - 2f_{11}$.

It is easy to understand why the second harmonic rather than fundamental frequency corresponds to the tuned frequency of given acoustic cavity length, because the second harmonic approaches f_{t1} of Figure 30 before the arrival of the fundamental frequency. However, it is not clear why the other higher harmonics, for instance, the third harmonics, when it hits f_{t2}--and this happens before the arrival of the second harmonics--does not become suppressed.

As just described, after the sound suppression, the second harmonics almost completely disappears, while the sound level of the fundamental frequency f_{11} becomes reduced. What is interesting is that at this moment a new peak pops up, with its frequency located somewhere between the fundamental and second harmonics, as pointed out in connection with Figure 22(h). This frequency, f_{21}, is found to be $|m| = 2$, by examining a Lissajous figure, shown as Figure 22(i), as mentioned in Section IV-A. At present, except for its tangential wave number, the precise nature of f_{21}, which is incommensurate with f_{11}, is unclear. It appears to be related to the similar incommensurate frequency observed in the unsteady regime of Taylor vortex flow [40], a wave phenomenon still not well understood.

F. A Newly-Found Phenomenon

While we were conducting these experiments, we accidentally stumbled on a new phenomenon. When the solid main pipe with an exit plate of 0.3 inch diameter was used as the test section, then above a certain pressure, the spiky pure tones different from the vortex whistle emerged. As Figure 32(a) shows, the frequency of these pure tones were almost independent of the inlet pressure. So this cannot be the vortex whistle, whose frequency increases as the inlet pressure is raised.

At the low inlet pressure, the pure tone is not present, and the temperature of the main pipe is almost the same as that of the inlet. As the inlet pressure is raised and at the moment when the pure tones suddenly emerged, the temperature of the main pipe near the exit became warm; it became hotter as the inlet pressure was increased. The one near the inlet (Z = 2 inches, corresponding to 1.2 inches downstream from main pipe inlet) remained almost the same.

Figure 32(b) shows these temperature data: one measured near the exit (Z = 4.1 inches, corresponding to 0.9 inch upstream of the main pipe exit), and the other near the inlet (Z = 2 inches).

Figure 33 shows another frequency spectra and temperature data corresponding to 0.8 inch exit opening diameter. The frequency spectra are slightly different from the one with 0.3 inch exit diameter.

It is possible to relate these frequencies to that of the cylindrical modes. Since the frequency is not significantly affected by the pressure of swirl, one may take a simplified situation where the flow is absent. The wave equation for the perturbed velocity potential, ϕ, takes the following form in cylindrical coordinate,

$$\frac{\partial^2 \phi}{\partial r^2} + \frac{1}{r}\frac{\partial \phi}{\partial r} + \frac{1}{r^2}\frac{\partial^2 \phi}{\partial \theta^2} = \frac{1}{a^2}\frac{\partial^2 \phi}{\partial t^2} \tag{26}$$

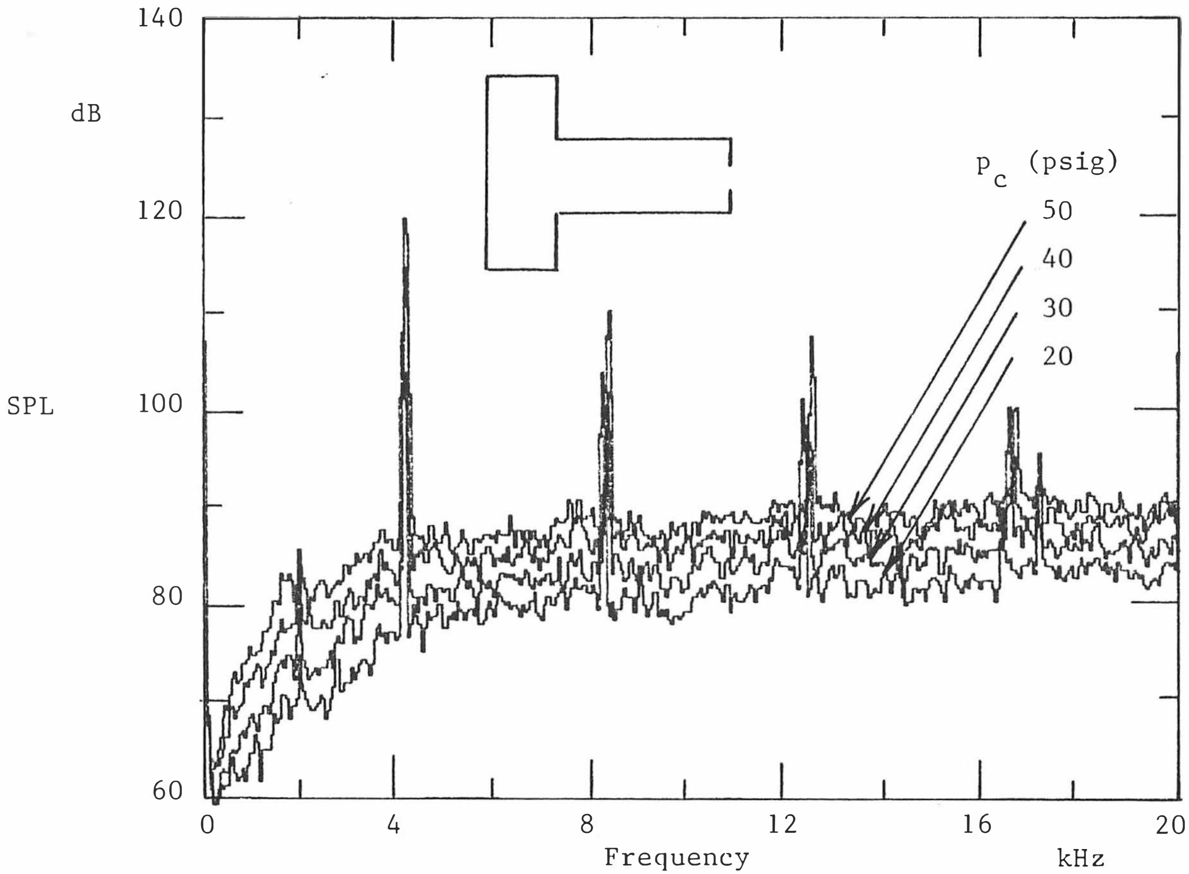

(a) frequency spectra

Figure 32. Data for solid main pipe with 0.3 inch exit opening diameter and at various inlet pressure p_c.

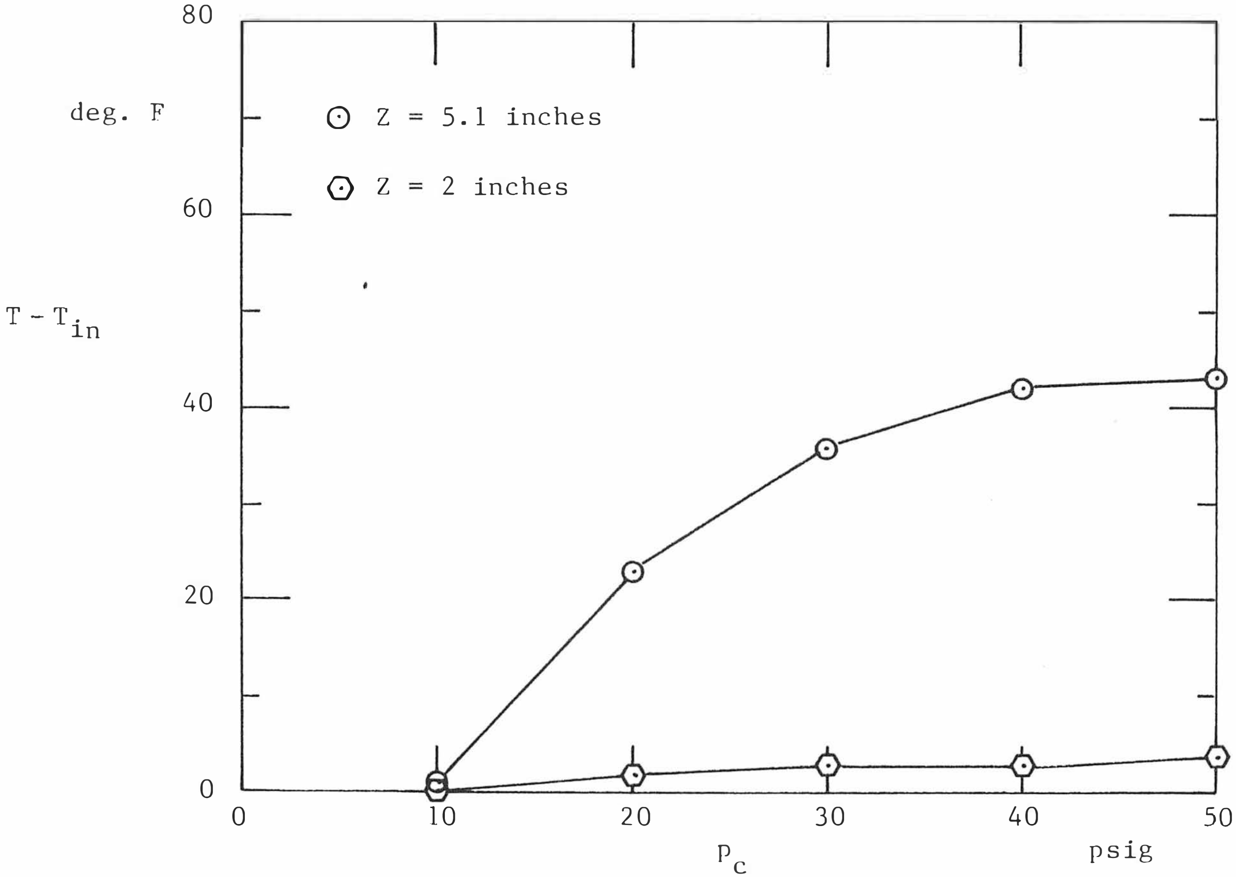

(b) temperature

Figure 32. (Continued)

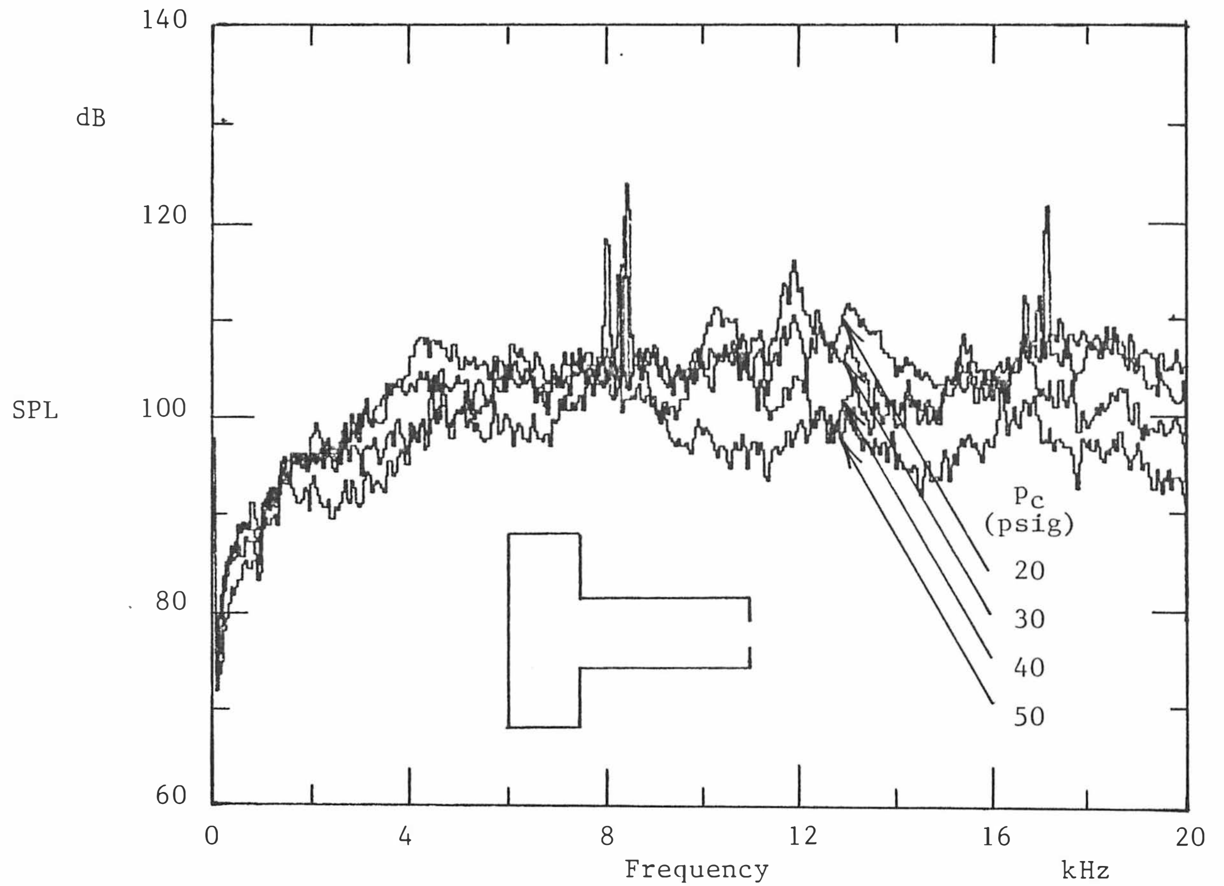

(a) frequency spectra

Figure 33. Data for solid main pipe with 0.8 inch exit opening diameter and at various inlet pressure p_c.

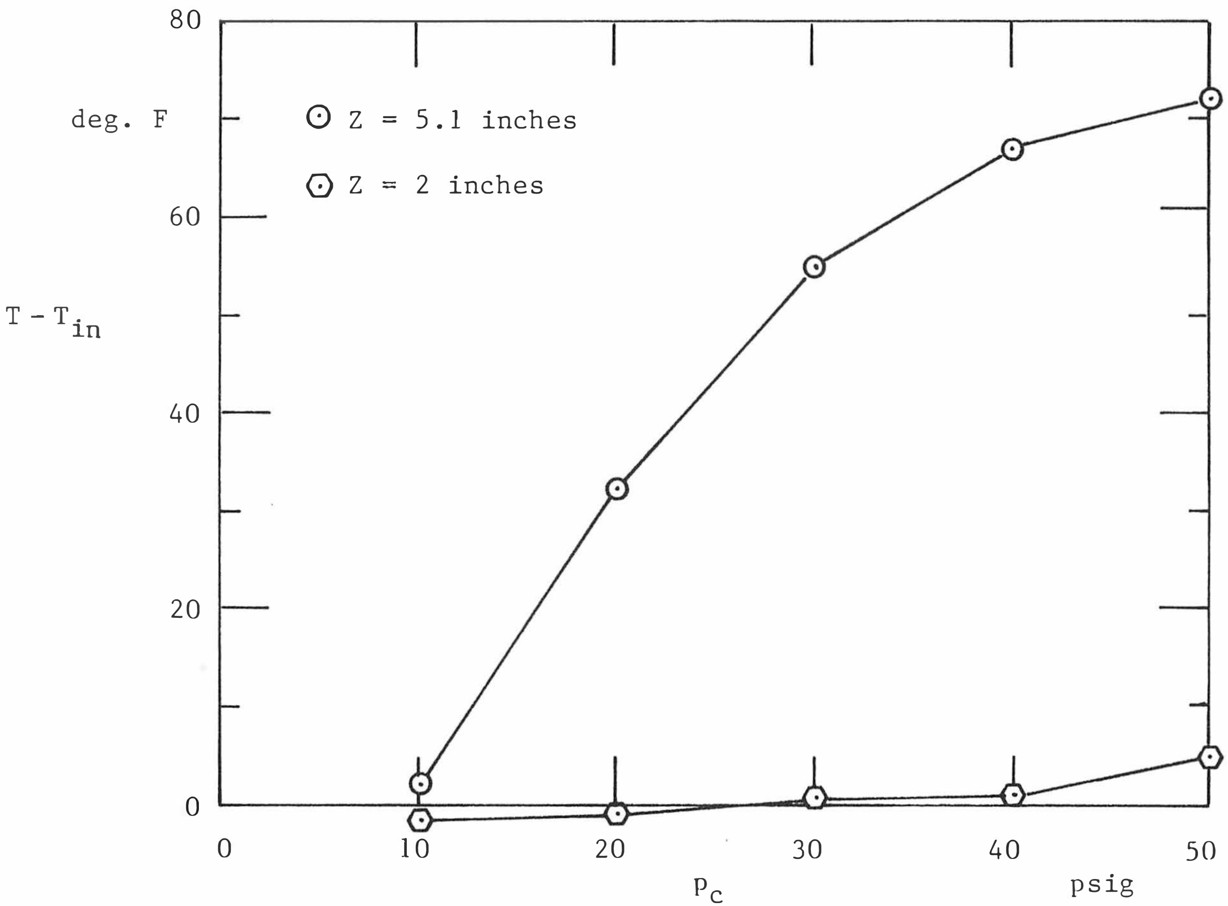

(b) temperature

Figure 33. (Continued)

with the boundary condition,

$$\frac{\partial \phi}{\partial r} = 0 \qquad \text{at } r = r_o. \tag{27}$$

The solution can be expressed in terms of the Bessel function

$$\phi = c\, e^{i\omega t} \sin (m\theta)\, J_m \left(\frac{\omega}{a} r\right). \tag{28}$$

The boundary condition on the wall yields

$$J_{m+1} \left(\frac{\omega}{a} r_o\right) - J_{m-1} \left(\frac{\omega}{a} r_o\right) = 0. \tag{29}$$

Figure 34 shows the various modes of cylindrical waves. By making comparison with the frequency spectra, the frequency corresponding to 0.3 inch exit opening diameter can be identified as that of f^*_{11}, and the one with 0.8 inch exit opening diameter as f^*_{02}.

This phenomenon occurring in the present test rig appears to be very interesting. This does not happen when the porous main pipe is used, even when the length of the acoustic cavities are reduced to zero.

This phenomenon is evidently indicative of a new type of acoustic streaming and may be related to a Hartmann-Sprenger tube [14, 15, 41]. But the detailed investigation of this is the outside scope of the present study and will be left to a future investigation.

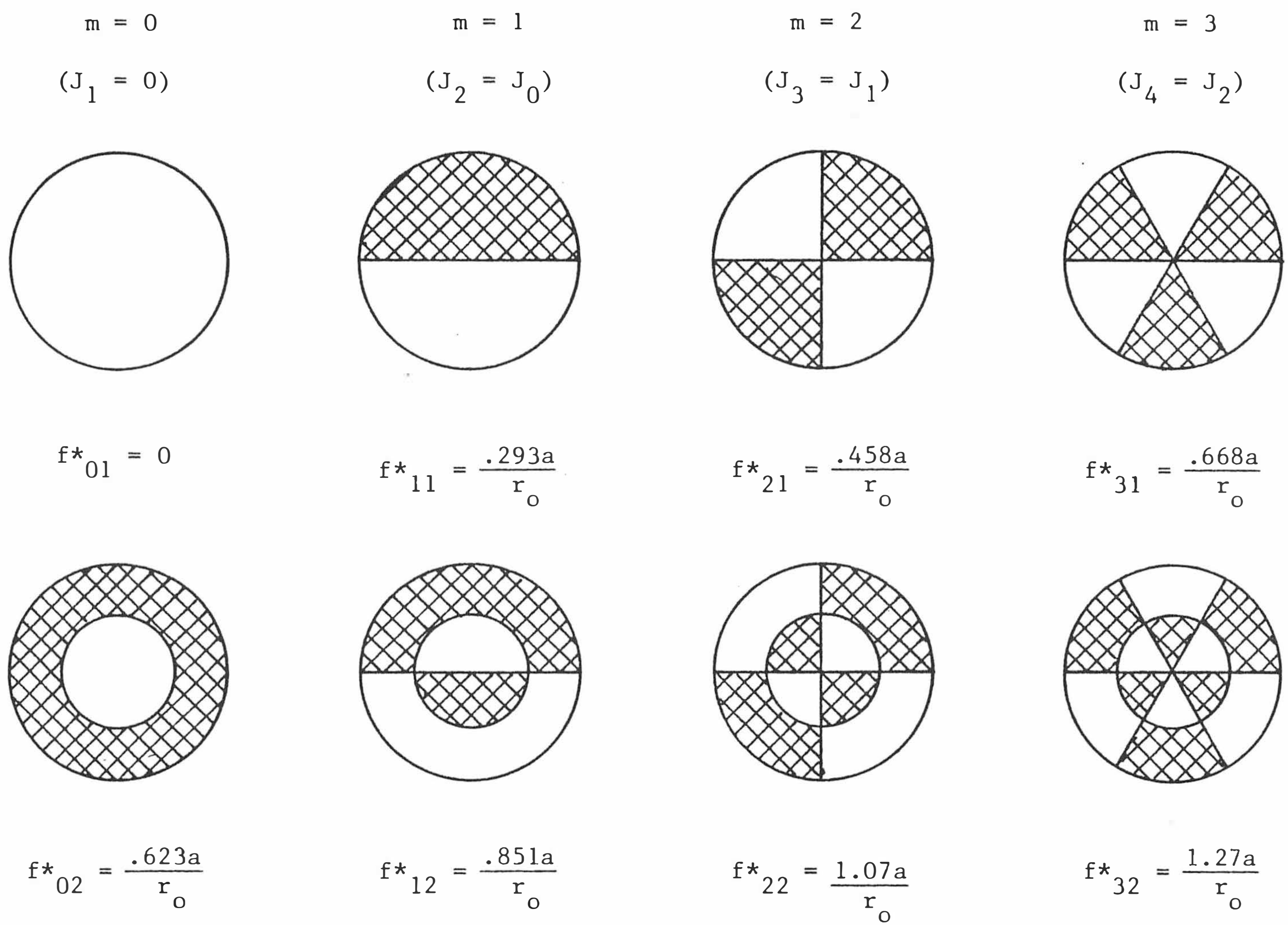

Figure 34. Pressure distribution corresponding to various cylindrical wave mode.

CHAPTER V

CONCLUSIONS

The experiment was conducted with the upscale version of the vortex test rig. By measuring the radial profile of flow field and the sound signal, the following results are obtained:

1. The Rankine vortex is found to exist in the vortex tube with the porous main pipe when its exit area is partially closed. The total temperature in the radial direction is almost the same except in the core region near the centerline, and in this case the vortex whistle is not observed.
2. By gradually increasing the exit area, the Rankine vortex changes to one resembling a forced vortex. The vortex whistle, though its sound pressure level is low, begins to emerge, and the total temperature separates in the radial direction. The transitional exit area corresponding to a change from a Rankine vortex to one reminiscent of a forced vortex is between 0.8 inch and 1.0 inch.
3. The forced vortex is clearly observed in the fully open exit area, where the shrill vortex whistle exists; the forced vortex occupies the entire tube, except for the boundary layer near the periphery wall. Corresponding to the presence of the vortex whistle, the total temperature separates in the radial direction.

4. When the sound is suppressed in the main pipe with the fully open exit area, the shrill vortex whistle suddenly changes to a muffled hiss. At that moment, the total temperature separation becomes reduced substantially. The forced vortex, however, does not revert to a Rankine vortex. This appears to be due to the effect of the entrainment of ambient air without swirl into a core region. This adverse effect of the entrainment was confirmed by injecting an artificial backflow into the Rankine vortex flow field and observing its change into a forced vortex type.
5. The second harmonic of the vortex whistle, rather than the fundamental, appears to be suppressed with an acoustic cavity.
6. When the solid main pipe with partially closed open area is used as the test section, a new type of heating effect associated with generically different pure tone was found. But details of this new phenomenon are not clear as yet.
7. It can be concluded that acoustic streaming is a major mechanism of the temperature separation in a vortex tube.

The experimental data and the error estimation of these measurements are shown in Appendices C and D, respectively.

BIBLIOGRAPHY

BIBLIOGRAPHY

1. Kurosaka, M., "Acoustic Streaming in Swirling Flow and the Ranque-Hilsch (vortex-tube) Effect," Journal of Fluid Mechanics, 124:139-172, 1982.

2. Kurosaka, M., "'Vortex Whistle': An Unsteady Phenomenon in Swirling Flow and its Effects on Steady Flow Field," AIAA Paper 81-0121, St. Louis, January, 1981.

3. Kurosaka, M., J. Q. Chu and J. R. Goodman, "Ranque-Hilsch Effect Revisited: Temperature Separation Traced to Orderly Spinning Waves or 'Vortex Whistle'", AIAA Paper 81-0952, St. Louis, June, 1982.

4. Lighthill, J. "Acoustic Streaming," Journal of Sound and Vibration, 61 (No. 3):391-418, December, 1978.

5. Lord Rayleigh (Rayleigh, J. W. S.), "On the Circulation of Air Observed in Kundt's Tubes and on Some Allied Acoustic Problems," Philosophical Transactions, 175:1-21, 1884 (Vol. II of "Scientific Papers," Dover, 239-257).

6. Eckart, C., "Vortices and Streams Caused by Sound Waves," Physical Review, 73 (No. 1):68-76, 1948.

7. Liebermann, L. N., "The Second Viscosity of Liquids," Physical Review, 75 (No. 9):1415-1422, 1949.

8. Markham, J. J., "Second-Order Acoustic Fields; Streaming with Viscosity and Relaxation," Physical Review, Series II, 86 (No. 4):497-502, 1952.

9. Nyborg, W. L., "Acoustic Streaming due to Attenuated Plane Waves," The Journal of the Acoustic Society of America, 25 (No. 1): 68-75, 1953.

10. Westervelt, P. J., "The Theory of Steady Rotational Flow Generated by a Sound Field," The Journal of the Acoustic Society of America, 25 (No. 1):60-67, 1953.

11. Nyborg, W. J., "Acoustic Streaming Equations: Laws of Rotational Motion for Fluid Elements," The Journal of the Acoustic Society of America, 25 (No. 5):938-944, 1953.

12. Andres, J. M. and V. Ingard, "Acoustic Streaming at High Reynolds Numbers," The Journal of the Acoustic Society of America, 25 (No. 5):928-932, 1953.

13. Andres, J. M. and V. Ingard, "Acoustic Streaming at Low Reynolds Numbers," The Journal of the Acoustic Society of America, 25 (No. 5):932-938, 1953.

14. Hartmann, J., "On the Production of Acoustic Waves by Means of an Air-Jet of a Velocity Exceeding that of Sound," Philosophical Magazine, Series 7, 11:926-948, 1931.

15. Sprenger, H., "Über Thermische Effekte in Resonanzrohren," Mitteilungen aus dem Institute für Aerodynamik ad der E. T. H., 21: Zürich, 1954.

16. Merkli, P. and H. Thomann, "Thermoacoustic Effects in a Resonance Tube," Journal of Fluid Mechanics, 70 (Part 1):161-177, 1975.

17. Eckert, E. R. G. and R. M. Drake, Jr., Analysis of Heat and Mass Transfer, New York: McGraw-Hill Book Company, 1972, p. 427.

18. Ryan, L. F., "Experiments in Aerodynamic Cooling," Ph.D. Thesis, Zürich: E. T. H., 1951.

19. Ackeret, J., "Über die Temperatureverteilung hinter angeströmten Zylindern," Mitteilungen aus dem Institute für Aerodynamik an der E. T. H., 21: Zürich, 1954.

20. Igarashi, T., "Unsteadyness of the Flow and Heat Transfer in Separated Region of a Circular Cylinder," 17th National Heat Transfer Symposium, 17:10-12, 1980 (Japanese).

21. Igarashi, T., "A New Dominating Factor of Heat Transfer in Separation Flow Region," 19th National Heat Transfer Symposium, 19:73-75, 1982 (Japanese).

22. Ranque, G. J., "Vortex Expansion with Experiments Concerning Simultaneous Production of Hot and Cold Air," (Bulletin) Bi-Mensuel de La Societe Francaise de Physique, 4 (Series 7): 112-115, 1933, (Translation in Schenectady Works Library of the General Electric Company, Data Folder No. 3294, 1947).

23. Hilsch, R., "The Use of Expansion of Gases in a Centrifugal Field as Cooling Process," The Review of Scientific Instruments, 18 (No. 2):108-113, 1947.

24. Chu, J. Q., "Acoustic Streaming as a Mechanism of the Ranque-Hilsch Effect," Ph.D. Thesis, Knoxville: The University of Tennessee, 1982.

25. Kurosaka, M., J. R. Goodman, J. Q. Chu, and H. Kuroda, "An Interplay between Acoustic Wave and Steady Vortical Flow," AIAA Paper 83-0740, Atlanta, April, 1983.

26. Eckert, E. R. G. and J. P. Hartnett, "Measurements of the Energy Separation in a High Velocity Vortex Type Flow," Proceedings of the Fourth Midwestern Conference on Fluid Mechanics, Purdue University, Lafayette, 69-92, 1955.

27. Lay, J. E., "An Experimental and Analytical Study of Vortex-Flow Temperature Separation by Superposition of Spiral and Axial Flows, Part 1," Transaction of the ASME, Journal of Heat Transfer, 81 (Series C):202, 1959.

28. Keyes, J. J., Jr., "An Experimental Study of Gas Dynamics in High Velocity Vortex Flow," Proceedings of the 1960 Heat Transfer and Fluid Mechanics Institute, Stanford: Stanford University Press, 31-46, 1960.

29. Silbukin, M., "Unsteady, Viscous, Circular Flow, Part 3: Applications to the Ranque-Hilsch Vortex Tube," Journal of Fluid Mechanics, 12 (Part 2):269-293, 1962.

30. Takahama, H., "Studies on Vortex Tubes," Bulletin of Japan Society of Mechanical Engineers, 8 (No. 31):431-440, 1965.

31. Bruun, H. H., "Experimental Investigation of the Energy Separation in Vortex Tubes," Journal of Mechanical Engineering Science, 11 (No. 6):567-582, 1969.

32. Bryer, D. W. and R. C. Pankhurst, Pressure-probe methods for determining wind speed and flow direction, London: National Physical Laboratory, 1971, pp. 41-74.

33. Bean, H. S., Editor, Fluid Meters: Their Theory and Application, 6th Edition, New York: The American Society of Mechanical Engineers, 1971, pp. 60-65.

34. Moore, F. K., Editor, High Speed Aerodynamics and Jet Propulsion: Volume IV, Theory of Laminar Flow, Princeton: Princeton University Press, 1964, p. 44.

35. Garg, A. K. and S. Leibovich, "Spectral characteristics of vortex brakedown flow fields," Physics of Fluids, 22 (No. 11): 2053-2064, 1979.

36. Kompenhans, J. and D. Ronneberger, "The Acoustic Impedance of Orifices in the Wall of a Flow Duct with a Laminar or Turbulent Flow Boundary Layer," AIAA Paper 80-0990, 1980.

37. Groeneweg, J. F., "Current Understanding of Helmholtz Resonator Arrays as Duct Boundary Conditions," Basic Aerodynamic Research Conference, Washington, D. C.: NASA, SP-207, 357-368, 1969.

38. Rogers, T. and A. S. Hersh, "Effect of Grazing Flow on the Steady-State Resistance of Square-Edge Orifice," AIAA Paper 75-493, 1975.

39. Mungur, P. and J. L. Whitesides, "Influence of Grazing Flow on Duct Wall Normal Impedances," AIAA Paper 75-494, 1975.

40. Fenstermacher, P. R., H. L. Swinney and J. P. Gollub, "Dynamical Instabilities and the Transition to Chaotic Taylor Vortex Flow," Journal of Fluid Mechanics, 94 (Part 1):103-128, 1979.

41. Scarton, H. A. and W. T. Rouleau, "Axisymmetric Waves in Compressible Newtonian Liquids Contained in Rigid Tubes: Steady-Periodic Mode Shapes and Dispersion by the Method of Eigenvalues," Journal of Fluid Mechanics, 58 (Part 3): 595-621, 1973.

APPENDICES

APPENDIX A

LISSAJOUS FIGURE

Consider a situation where two microphones, (X) and (Y), are placed at the same axial and radial position near the exhaust of the main pipe, but its relative position in the circumferential θ direction is different. When (X) is placed at $\theta = 0$ and filters only a signal with a frequency equal to ω, its output may be represented, without loss of generality, as

$$x = \cos(\omega t). \tag{A-1}$$

If (Y) is placed at θ and filters a signal with a frequency equal to $n\omega$, its output becomes

$$y = \cos(n\omega t - |m|\theta - \psi) \tag{A-2}$$

where m is wave number of fundamental frequency, n is an integer denoting higher harmonics ($n = 1$ corresponds to the fundamental frequency, $n = 2$ to the second harmonics, and so forth) and ψ is the phase lag between (X) and (Y) signals.

If (Y) microphone filters also the fundamental frequency, then $n = 1$ and $\psi = 0$. Eliminating time, t, from equations (A-1) and (A-2), one obtains

$$x^2 - 2xy\cos(|m|\theta) + y^2 = \sin^2(|m|\theta) \tag{A-3}$$

This equation, in general, represents an ellipse in x-y plane.

In the special case, if $\theta = 180°$ for $|m| = 1$ or $\theta = 90°$ for $|m| = 2$, then $|m|\theta = 180°$ and (A-3) becomes

$$x + y = 0. \tag{A-4}$$

This represents a straight line, inclined 45° and lying in the second and fourth quadrant of x-y plane.

As another special case, take $\theta = 90°$ for $|m| = 1$ or $\theta = 45°$ for $|m| = 2$. Then $|m|\theta = 90°$, and (A-3) becomes

$$x^2 + y^2 = 1. \tag{A-5}$$

This represents a circle in x-y plane.

If (Y) microphone filters the second harmonics, then $n = 2$. Eliminating time, t, from equations (A-1) and (A-2),

$$(2x^2 - 1)^2 - 2(2x^2 - 1)\, y \cos\,(|m|\theta + \psi) + y^2$$

$$= 1 + \cos^2\,(|m|\theta + \psi) \tag{A-6}$$

When $m = 2$, $\theta = 90°$, $\psi = 90°$, then $|m|\theta + \psi = 90°$, which means two frequencies are at right angle to each other, equation (A-6) becomes

$$(2x^2 - 1)^2 + y^2 = 1. \tag{A-7}$$

This represents a trajectory shaped like ∞.

APPENDIX B

EFFECT OF REVERSE FLOW

One can show quite generally that if there is a reverse flow, then even after the sound suppression, the tangential velocity distribution does not return to a Rankine vortex.

Take an axisymmetric inviscid flow, for an ideal case where the vortex whistle is completely suppressed, the flow can be considered to be steady. Assume also that the flow does not change in the axial direction. Then the following inviscid energy equation

$$c_p \frac{DT}{Dt} = \frac{1}{\rho} \frac{Dp}{Dt} \tag{B-1}$$

is reduced to

$$c_p \frac{dT}{dr} = \frac{1}{\rho} \frac{dp}{dr} . \tag{B-2}$$

Furthermore, from the radial equilibrium of motion,

$$\frac{v^2}{r} = \frac{1}{\rho} \frac{dp}{dr} . \tag{B-3}$$

From equations (B-2) and (B-3)

$$c_p \frac{dT}{dr} = \frac{v^2}{r} . \tag{B-4}$$

The total temperature, T*, is related to T by

$$c_p T^* = c_p T + \frac{1}{2} (u^2 + v^2 + w^2). \tag{B-5}$$

When one neglects u, which is small compared with v and w, then differentiation with respect to r yields

$$c_p \frac{dT^*}{dr} = c_p \frac{dT}{dr} + \frac{1}{2} \left(\frac{dv^2}{dr} + \frac{dw^2}{dr}\right). \tag{B-6}$$

Substituting equation (B-4) into equation (B-6)

$$c_p \frac{dT^*}{dr} = \frac{1}{r^2} \frac{d}{dr} \left(\frac{r^2 v^2}{2}\right) + \frac{dw^2}{dr} . \tag{B-7}$$

The total temperature in the absence of the vortex whistle should be constant, so that equation (B-7) becomes

$$\frac{d}{dr} \left(\frac{r^2 v^2}{2}\right) = -r^2 \frac{dw^2}{dr} . \tag{B-8}$$

Since $w \neq$ constant in the radial direction, then

$$\frac{d}{dr} \left(\frac{r^2 v^2}{2}\right) \neq 0. \tag{B-9}$$

Thus, the flow cannot form a free vortex even in the inviscid region outside of the core.

Thus, when there is a reverse flow region, the flow cannot revert to a Rankine vortex even after the sound suppression.

APPENDIX C

EXPERIMENTAL DATA

A complete listing of the experimental results of this investigation is attached in this appendix.

Note

Patm: Atmospheric pressure

Pinlet: Inlet pressure (p^*_{in})

Tinlet: Inlet total temperature (T^*_{in})

Gin: Mass flow through orifice

Ein: Energy flux through orifice

R/Rw: (= r)

THETA = $\alpha + 180°$

DELTA THETA: Absolute angle to compensate the relative angle THETA

Table 3

Data for this Experiment

Test NO. 920 N=2 NN=17 Patm=14.53 psia Pinlet=46.09 psia Tinlet=47.0 deg. F

Gin=0.1824 lbm/sec Gout=0.1410 lbm/sec GPout=0.1236 lbm/sec GDout=0.1750 lbm/sec
Ein= 0.222E+02 Btu/sec Eout= 0.173E+02 Btu/sec DPout= 0.152E+02 Btu/sec EDout= 0.215E+02 Btu/sec
DS= 0.102E-01 Btu/R.sec DSP= 0.113E-01 Btu/R.sec DSD= 0.133E-01 Btu/R.sec

DELTA THETA= 8.9 DEG

BASED ON PT PS AND THETA

R/Rw	Pt psia	Ps psia	Vt ft/sec	Va ft/sec	DTt deg	DTs deg	Tt F deg	Ts F deg	THETA deg	DS Btu/lbmR	G(psqin) lbm/sec
0.992	17.89	15.89	381.	249.	11.0	-6.2	57.0	39.8	236.9	0.0696	0.14816
0.969	18.09	16.05	391.	236.	10.0	-7.3	56.5	39.2	238.9	0.0686	0.14220
0.945	17.97	15.96	393.	228.	9.0	-8.2	55.5	38.3	239.9	0.0686	0.13693
0.921	17.81	15.88	393.	210.	5.5	-11.0	51.5	35.0	241.9	0.0673	0.12612
0.902	17.59	15.93	365.	195.	4.0	-10.2	50.0	35.8	241.9	0.0675	0.11742
0.882	17.43	15.90	351.	187.	2.5	-10.7	48.5	35.3	241.9	0.0674	0.11278
0.843	16.89	15.58	332.	170.	-1.5	-13.0	44.5	33.0	242.9	0.0676	0.10053
0.764	16.03	15.10	294.	125.	-6.5	-15.0	39.5	31.0	246.9	0.0688	0.07222
0.685	15.27	14.65	250.	87.	-11.0	-16.8	35.0	29.2	250.9	0.0700	0.04863
0.606	14.73	14.35	203.	55.	-14.0	-17.7	32.0	28.3	254.9	0.0710	0.03021
0.528	14.25	14.10	134.	5.	-15.0	-16.5	31.0	29.5	267.9	0.0728	0.00266
0.449	14.13	14.01	70.	-96.	-15.5	-16.7	30.5	29.3	323.9	0.0731	-0.05180
0.370	14.13	13.98	49.	-127.	-16.0	-17.5	30.0	28.5	338.9	0.0729	-0.06824
0.291	14.07	13.94	46.	-118.	-16.5	-17.8	29.5	28.2	338.9	0.0729	-0.06341
0.213	14.07	13.93	47.	-122.	-17.0	-18.4	29.0	27.6	338.9	0.0727	-0.06528
0.134	14.01	13.88	45.	-117.	-17.0	-18.3	29.0	27.7	338.9	0.0730	-0.06266
0.055	14.01	13.89	43.	-111.	-17.0	-18.2	29.0	27.8	338.9	0.0730	-0.05952

BASED ON DP/DR PS AND THETA

R/Rw	Pt psia	Ps psia	Vt ft/sec	Va ft/sec	DTt deg	DTs deg	Tt F deg	Ts F deg	THETA deg	DS Btu/lbmR	G(psqin) lbm/sec
0.969	16.05	16.05	0.	0.	10.0	10.0	56.5	56.5	238.9	0.0768	0.00000
0.945	18.36	15.96	427.	247.	9.0	-11.2	55.5	35.3	239.9	0.0671	0.14944
0.921	16.26	15.88	178.	95.	5.5	2.1	51.5	48.1	241.9	0.0736	0.05559
0.902	15.93	15.93	0.	0.	4.0	4.0	50.0	50.0	241.9	0.0743	0.00000
0.882	19.57	15.90	523.	279.	2.5	-26.8	48.5	19.2	241.9	0.0595	0.17372
0.843	19.50	15.58	546.	280.	-1.5	-32.9	44.5	13.1	242.9	0.0578	0.17263
0.764	17.92	15.10	492.	210.	-6.5	-30.4	39.5	15.6	246.9	0.0612	0.12505
0.685	16.56	14.65	427.	148.	-11.0	-28.0	35.0	18.0	250.9	0.0644	0.08505
0.606	15.52	14.35	350.	94.	-14.0	-24.9	32.0	21.1	254.9	0.0674	0.05276
0.528	14.67	14.10	258.	9.	-15.0	-20.6	31.0	25.4	267.9	0.0700	0.00516
0.449	14.53	14.01	145.	-198.	-15.5	-20.5	30.5	25.5	323.9	0.0712	-0.10734
0.370	14.67	13.98	102.	-265.	-16.0	-22.7	30.0	23.3	338.9	0.0703	-0.14392
0.291	14.28	13.94	72.	-187.	-16.5	-19.8	29.5	26.2	338.9	0.0719	-0.10044
0.213	14.23	13.93	68.	-176.	-17.0	-20.0	29.0	26.0	338.9	0.0719	-0.09470
0.134	14.00	13.88	43.	-112.	-17.0	-18.2	29.0	27.8	338.9	0.0730	-0.05959

BASED ON DIFERNTIAL EQUATION

R/Rw	Pt psia	Ps psia	Vt ft/sec	Va ft/sec	DTt deg	DTs deg	Tt F deg	Ts F deg	THETA deg	DS Btu/lbmR	G(psqin) lbm/sec
0.992	17.89	15.41	427.	278.	11.0	-10.6	57.0	35.4	236.9	0.0695	0.16236
0.969	18.09	15.32	460.	277.	10.0	-14.0	56.5	32.5	238.9	0.0686	0.16167
0.945	17.97	15.23	463.	269.	9.0	-14.9	55.5	31.6	239.9	0.0686	0.15593
0.921	17.81	15.13	467.	249.	5.5	-17.8	51.5	28.2	241.9	0.0673	0.14492
0.902	17.59	15.04	457.	244.	4.0	-18.3	50.0	27.7	241.9	0.0675	0.14104
0.882	17.43	14.96	451.	241.	2.5	-19.2	48.5	26.8	241.9	0.0674	0.13870
0.843	16.89	14.81	421.	216.	-1.5	-20.2	44.5	25.8	242.9	0.0676	0.12321
0.764	16.03	14.53	375.	160.	-6.5	-20.4	39.5	25.6	246.9	0.0688	0.08979
0.685	15.27	14.30	314.	109.	-11.0	-20.2	35.0	25.6	250.9	0.0700	0.06004
0.606	14.73	14.13	256.	69.	-14.0	-19.8	32.0	26.2	254.9	0.0710	0.03758
0.528	14.25	14.02	167.	6.	-15.0	-17.3	31.0	28.7	267.9	0.0728	0.00329
0.449	14.13	13.97	83.	-113.	-15.5	-17.1	30.5	28.9	323.9	0.0731	-0.06078
0.370	14.13	13.95	53.	-137.	-16.0	-17.8	30.0	28.2	338.9	0.0729	-0.07333
0.291	14.07	13.94	45.	-116.	-16.5	-17.8	29.5	28.2	338.9	0.0729	-0.06222
0.213	14.07	13.93	47.	-121.	-17.0	-18.4	29.0	27.6	338.9	0.0727	-0.06481
0.134	14.01	13.92	38.	-99.	-17.0	-17.9	29.0	28.1	338.9	0.0730	-0.05308
0.055	14.01	13.89	43.	-111.	-17.0	-18.2	29.0	27.8	338.9	0.0730	-0.05952

Table 3 (Continued)

Test NO. 921 N=2 NN=17 Patm=14.53 psia Pinlet=46.91 psia Tinlet=46.0 deg. F

Gin=0.1890 lbm/sec Gout=0.1713 lbm/sec GPout=0.1863 lbm/sec GDout=0.1896 lbm/sec
Ein= 0.230E+02 Btu/sec Eout= 0.210E+02 Btu/sec DPout= 0.226E+02 Btu/sec EDout= 0.232E+02 Btu/sec
DS= 0.116E-01 Btu/R.sec DSP= 0.161E-01 Btu/R.sec DSD= 0.136E-01 Btu/R.sec

DELTA THETA= 2.1 DEG

BASED ON PT PS AND THETA

R/Rw	Pt psia	Ps psia	Vt ft/sec	Va ft/sec	DTt deg	DTs deg	Tt F deg	Ts F deg	THETA deg	DS Btu/lbmR	G(psqin) lbm/sec
0.992	18.17	15.77	378.	316.	3.0	-17.2	49.0	28.8	230.1	0.0664	0.19105
0.969	18.49	15.45	437.	340.	4.0	-21.5	50.0	24.5	232.1	0.0657	0.20340
0.945	18.49	15.45	448.	325.	3.0	-22.5	49.0	23.5	234.1	0.0652	0.19440
0.921	18.39	15.37	447.	324.	1.5	-23.9	47.5	22.1	234.1	0.0649	0.19354
0.902	18.15	15.37	436.	304.	0.5	-23.1	46.5	22.9	235.1	0.0653	0.18150
0.882	17.95	15.46	418.	281.	-0.5	-21.6	45.5	24.4	236.1	0.0656	0.16818
0.843	17.43	15.34	400.	239.	-3.0	-21.1	43.0	24.9	239.1	0.0664	0.14197
0.764	16.23	14.85	349.	169.	-8.0	-20.5	38.0	25.5	244.1	0.0689	0.09703
0.685	15.23	14.35	301.	97.	-12.5	-20.8	33.5	25.2	252.1	0.0711	0.05390
0.606	14.47	14.06	220.	19.	-15.5	-19.6	30.5	26.4	265.1	0.0732	0.01019
0.528	14.13	13.93	139.	-71.	-16.5	-18.5	29.5	27.5	297.1	0.0743	-0.03822
0.449	14.13	13.90	91.	-141.	-16.5	-18.9	29.5	27.1	327.1	0.0743	-0.07546
0.370	14.19	13.92	55.	-172.	-15.5	-18.2	30.0	27.3	342.1	0.0743	-0.09205
0.291	14.23	13.96	56.	-173.	-14.5	-17.3	31.0	28.2	342.1	0.0746	-0.09293
0.213	14.29	13.95	28.	-201.	-13.0	-16.4	33.0	29.6	352.1	0.0752	-0.10760
0.134	14.31	13.95	29.	-208.	-12.0	-15.7	34.0	30.3	352.1	0.0756	-0.11068
0.055	14.29	13.90	-8.	-216.	-11.0	-14.9	34.0	30.1	362.1	0.0757	-0.11474

BASED ON DP/DR PS AND THETA

R/Rw	Pt psia	Ps psia	Vt ft/sec	Va ft/sec	DTt deg	DTs deg	Tt F deg	Ts F deg	THETA deg	DS Btu/lbmR	G(psqin) lbm/sec
0.969	21.51	15.45	587.	457.	4.0	-42.0	50.0	4.0	232.1	0.0553	0.29513
0.945	16.74	15.45	301.	218.	3.0	-8.5	49.0	37.5	234.1	0.0721	0.12693
0.921	16.72	15.37	308.	223.	1.5	-10.6	47.5	35.4	234.1	0.0715	0.12993
0.902	15.37	15.37	0.	0.	0.5	0.5	46.5	46.5	235.1	0.0768	0.00000
0.882	15.78	15.46	157.	105.	-0.5	-3.5	45.5	42.5	236.1	0.0745	0.06073
0.843	18.49	15.34	481.	288.	-3.0	-29.1	43.0	16.9	239.1	0.0624	0.17347
0.764	18.02	14.85	510.	248.	-8.0	-34.8	38.0	11.2	244.1	0.0618	0.14627
0.685	16.35	14.35	443.	143.	-12.5	-30.5	33.5	15.5	252.1	0.0663	0.08038
0.606	14.90	14.06	310.	27.	-15.5	-23.6	30.5	22.4	265.1	0.0712	0.01450
0.528	14.27	13.93	180.	-92.	-16.5	-19.9	29.5	26.1	297.1	0.0736	-0.04958
0.449	13.94	13.90	38.	-58.	-16.5	-16.9	29.5	29.1	327.1	0.0753	-0.03107
0.370	13.92	13.92	0.	0.	-15.5	-15.5	30.0	30.0	342.1	0.0756	0.00000
0.291	13.96	13.96	0.	0.	-14.5	-14.5	31.0	31.0	342.1	0.0759	0.00000
0.213	14.26	13.95	27.	-193.	-13.0	-16.1	33.0	29.9	352.1	0.0754	-0.10278
0.134	14.93	13.95	46.	-335.	-12.0	-21.5	34.0	24.5	352.1	0.0727	-0.18086

BASED ON DIFERNTIAL EQUATION

R/Rw	Pt psia	Ps psia	Vt ft/sec	Va ft/sec	DTt deg	DTs deg	Tt F deg	Ts F deg	THETA deg	DS Btu/lbmR	G(psqin) lbm/sec
0.992	18.17	15.41	407.	340.	3.0	-20.5	49.0	25.5	230.1	0.0664	0.20251
0.969	18.49	15.33	446.	347.	4.0	-22.7	50.0	23.3	232.1	0.0657	0.20657
0.945	18.49	15.23	465.	337.	3.0	-24.5	49.0	21.5	234.1	0.0652	0.19963
0.921	18.39	15.13	466.	337.	1.5	-26.0	47.5	20.0	234.1	0.0649	0.19928
0.902	18.15	15.05	462.	322.	0.5	-26.0	46.5	20.0	235.1	0.0653	0.18949
0.882	17.95	14.96	461.	310.	-0.5	-26.2	45.5	19.8	236.1	0.0656	0.18100
0.843	17.43	14.79	452.	271.	-3.0	-26.1	43.0	19.9	239.1	0.0664	0.15627
0.764	16.23	14.47	395.	192.	-8.0	-24.1	38.0	21.9	244.1	0.0689	0.10808
0.685	15.23	14.22	323.	104.	-12.5	-22.1	33.5	23.9	252.1	0.0711	0.05750
0.606	14.47	14.06	220.	19.	-15.5	-19.6	30.5	26.4	265.1	0.0732	0.01022
0.528	14.13	13.98	120.	-61.	-16.5	-18.0	29.5	28.0	297.1	0.0743	-0.03296
0.449	14.13	13.95	80.	-123.	-16.5	-18.3	29.5	27.7	327.1	0.0743	-0.06621
0.370	14.19	13.94	54.	-166.	-15.5	-18.0	30.0	27.5	342.1	0.0743	-0.08914
0.291	14.23	13.92	59.	-183.	-14.5	-17.6	31.0	27.9	342.1	0.0746	-0.09773
0.213	14.29	13.91	29.	-211.	-13.0	-16.8	33.0	29.2	352.1	0.0752	-0.11246
0.134	14.31	13.91	30.	-218.	-12.0	-16.0	34.0	30.0	352.1	0.0756	-0.11621
0.055	14.29	13.90	-8.	-216.	-11.0	-14.9	34.0	30.1	362.1	0.0757	-0.11474

Table 3 (Continued)

Test NO. 922 N=2 NN=17 Patm=14.53 psia Pinlet=46.Ø9 psia Tinlet=46.5 deg. F

Gin=Ø.1825 lbm/sec Gout=Ø.1523 lbm/sec GPout=Ø.17Ø3 lbm/sec GDout=Ø.185Ø lbm/sec
Ein= Ø.222E+Ø2 Btu/sec Eout= Ø.189E+Ø2 Btu/sec DPout= Ø.21ØE+Ø2 Btu/sec EDout= Ø.229E+Ø2 Btu/sec
DS= Ø.997E-Ø2 Btu/R.sec DSP= Ø.132E-Ø1 Btu/R.sec DSD= Ø.128E-Ø1 Btu/R.sec
DELTA THETA= 1.4 DEG

BASED ON PT PS AND THETA

R/Rw	Pt psia	Ps psia	Vt ft/sec	Va ft/sec	DTt deg	DTs deg	Tt F deg	Ts F deg	THETA deg	DS Btu/lbmR	G(psqin) lbm/sec
Ø.992	2Ø.13	17.73	432.	189.	14.Ø	-4.5	6Ø.Ø	41.5	246.4	Ø.Ø631	Ø.12536
Ø.969	2Ø.27	17.75	431.	216.	13.5	-5.8	59.5	4Ø.2	243.4	Ø.Ø624	Ø.14372
Ø.945	2Ø.29	17.7Ø	437.	219.	12.Ø	-7.9	58.Ø	38.1	243.4	Ø.Ø616	Ø.14578
Ø.921	2Ø.11	17.6Ø	444.	185.	1Ø.Ø	-9.3	56.Ø	36.7	247.4	Ø.Ø613	Ø.123Ø5
Ø.9Ø2	19.93	17.52	437.	182.	8.5	-1Ø.1	54.5	35.9	247.4	Ø.Ø612	Ø.12Ø51
Ø.882	19.65	17.32	437.	164.	6.Ø	-12.1	52.Ø	33.9	249.4	Ø.Ø61Ø	Ø.1Ø812
Ø.843	19.19	17.ØØ	432.	146.	3.Ø	-14.3	49.Ø	31.7	251.4	Ø.Ø613	Ø.Ø9443
Ø.764	18.Ø7	16.35	398.	111.	-4.Ø	-18.2	42.Ø	27.8	254.4	Ø.Ø621	Ø.Ø6991
Ø.685	17.Ø5	15.66	372.	7Ø.	-1Ø.Ø	-21.9	36.Ø	24.1	259.4	Ø.Ø632	Ø.Ø4231
Ø.6Ø6	16.13	15.Ø2	343.	4Ø.	-15.Ø	-24.9	31.Ø	21.1	263.4	Ø.Ø645	Ø.Ø2332
Ø.528	15.31	14.44	312.	-7.	-2Ø.Ø	-28.1	26.Ø	17.9	271.4	Ø.Ø656	-Ø.ØØ424
Ø.449	14.65	13.95	282.	-31.	-24.Ø	-3Ø.7	22.Ø	15.3	276.4	Ø.Ø667	-Ø.Ø1732
Ø.37Ø	14.13	13.57	252.	-51.	-28.Ø	-33.5	18.Ø	12.5	281.4	Ø.Ø672	-Ø.Ø2734
Ø.291	13.75	13.27	224.	-88.	-33.Ø	-37.8	13.Ø	8.2	291.4	Ø.Ø665	-Ø.Ø4662
Ø.213	13.47	13.Ø6	2Ø8.	-82.	-39.Ø	-43.2	7.Ø	2.8	291.4	Ø.Ø649	-Ø.Ø4313
Ø.134	13.23	12.88	192.	-75.	-45.Ø	-48.5	1.Ø	-2.5	291.4	Ø.Ø63Ø	-Ø.Ø3965
Ø.Ø55	12.95	12.69	155.	-94.	-48.Ø	-5Ø.7	-2.Ø	-4.7	3Ø1.4	Ø.Ø629	-Ø.Ø4925

BASED ON DP/DR PS AND THETA

R/Rw	Pt psia	Ps psia	Vt ft/sec	Va ft/sec	DTt deg	DTs deg	Tt F deg	Ts F deg	THETA deg	DS Btu/lbmR	G(psqin) lbm/sec
Ø.969	18.17	17.75	181.	91.	13.5	1Ø.1	59.5	56.1	243.4	Ø.Ø699	Ø.Ø5847
Ø.945	19.67	17.7Ø	384.	193.	12.Ø	-3.4	58.Ø	42.6	243.4	Ø.Ø638	Ø.12726
Ø.921	19.93	17.6Ø	429.	179.	1Ø.Ø	-8.Ø	56.Ø	38.Ø	247.4	Ø.Ø619	Ø.11855
Ø.9Ø2	21.56	17.52	55Ø.	229.	8.5	-21.1	54.5	24.9	247.4	Ø.Ø559	Ø.1554Ø
Ø.882	22.15	17.32	6Ø4.	227.	6.Ø	-28.7	52.Ø	17.3	249.4	Ø.Ø529	Ø.15474
Ø.843	21.21	17.ØØ	58Ø.	195.	3.Ø	-28.2	49.Ø	17.8	251.4	Ø.Ø544	Ø.13Ø38
Ø.764	2Ø.13	16.35	568.	159.	-4.Ø	-33.Ø	42.Ø	13.Ø	254.4	Ø.Ø547	Ø.1Ø299
Ø.685	18.85	15.66	545.	1Ø2.	-1Ø.Ø	-35.6	36.Ø	1Ø.4	259.4	Ø.Ø563	Ø.Ø6383
Ø.6Ø6	17.55	15.Ø2	5Ø3.	58.	-15.Ø	-36.3	31.Ø	9.7	263.4	Ø.Ø588	Ø.Ø35Ø2
Ø.528	16.31	14.44	446.	-11.	-2Ø.Ø	-36.6	26.Ø	9.4	271.4	Ø.Ø613	-Ø.ØØ618
Ø.449	15.25	13.95	378.	-42.	-24.Ø	-36.Ø	22.Ø	1Ø.Ø	276.4	Ø.Ø64Ø	-Ø.Ø2351
Ø.37Ø	14.43	13.57	3Ø9.	-62.	-28.Ø	-36.3	18.Ø	9.7	281.4	Ø.Ø657	-Ø.Ø337Ø
Ø.291	13.82	13.27	24Ø.	-94.	-33.Ø	-38.5	13.Ø	7.5	291.4	Ø.Ø662	-Ø.Ø4991
Ø.213	13.36	13.Ø6	178.	-7Ø.	-39.Ø	-42.1	7.Ø	3.9	291.4	Ø.Ø654	-Ø.Ø3686
Ø.134	13.Ø7	12.88	139.	-54.	-45.Ø	-46.9	1.Ø	-Ø.9	291.4	Ø.Ø639	-Ø.Ø2863

BASED ON DIFERNTIAL EQUATION

R/Rw	Pt psia	Ps psia	Vt ft/sec	Va ft/sec	DTt deg	DTs deg	Tt F deg	Ts F deg	THETA deg	DS Btu/lbmR	G(psqin) lbm/sec
Ø.992	2Ø.13	16.82	512.	224.	14.Ø	-12.Ø	6Ø.Ø	34.Ø	246.4	Ø.Ø631	Ø.143Ø4
Ø.969	2Ø.27	16.7Ø	519.	26Ø.	13.5	-14.5	59.5	31.5	243.4	Ø.Ø624	Ø.16563
Ø.945	2Ø.29	16.56	53Ø.	266.	12.Ø	-17.2	58.Ø	28.8	243.4	Ø.Ø616	Ø.16866
Ø.921	2Ø.11	16.42	546.	227.	1Ø.Ø	-19.1	56.Ø	26.9	247.4	Ø.Ø613	Ø.14374
Ø.9Ø2	19.93	16.29	543.	226.	8.5	-2Ø.3	54.5	25.7	247.4	Ø.Ø612	Ø.14234
Ø.882	19.65	16.16	541.	2Ø4.	6.Ø	-21.8	52.Ø	24.2	249.4	Ø.Ø61Ø	Ø.12741
Ø.843	19.19	15.91	535.	18Ø.	3.Ø	-23.6	49.Ø	22.4	251.4	Ø.Ø613	Ø.11156
Ø.764	18.Ø7	15.41	499.	14Ø.	-4.Ø	-26.4	42.Ø	19.6	254.4	Ø.Ø621	Ø.Ø84Ø7
Ø.685	17.Ø5	14.94	462.	87.	-1Ø.Ø	-28.4	36.Ø	17.6	259.4	Ø.Ø632	Ø.Ø5Ø81
Ø.6Ø6	16.13	14.52	416.	48.	-15.Ø	-29.6	31.Ø	16.4	263.4	Ø.Ø645	Ø.Ø2759
Ø.528	15.31	14.14	362.	-9.	-2Ø.Ø	-3Ø.9	26.Ø	15.1	271.4	Ø.Ø656	-Ø.ØØ485
Ø.449	14.65	13.83	3Ø6.	-34.	-24.Ø	-31.9	22.Ø	14.1	276.4	Ø.Ø667	-Ø.Ø1868
Ø.37Ø	14.13	13.58	251.	-5Ø.	-28.Ø	-33.5	18.Ø	12.5	281.4	Ø.Ø672	-Ø.Ø2719
Ø.291	13.75	13.37	198.	-78.	-33.Ø	-36.8	13.Ø	9.2	291.4	Ø.Ø665	-Ø.Ø4146
Ø.213	13.47	13.2Ø	17Ø.	-66.	-39.Ø	-41.8	7.Ø	4.2	291.4	Ø.Ø649	-Ø.Ø3536
Ø.134	13.23	13.ØØ	157.	-61.	-45.Ø	-47.4	1.Ø	-1.4	291.4	Ø.Ø63Ø	-Ø.Ø3256
Ø.Ø55	12.95	12.69	155.	-94.	-48.Ø	-5Ø.7	-2.Ø	-4.7	3Ø1.4	Ø.Ø629	-Ø.Ø4925

Table 3 (Continued)

Test NO. 923 N=2 NN=17 Patm=14.53 psia Pinlet=46.92 psia Tinlet=45.5 deg. F

Gin=0.1888 lbm/sec Gout=0.1701 lbm/sec GPout=0.1599 lbm/sec GDout=0.1912 lbm/sec
Ein= 0.229E+02 Btu/sec Eout= 0.209E+02 Btu/sec DPout= 0.195E+02 Btu/sec EDout= 0.234E+02 Btu/sec
DS= 0.108E-01 Btu/R.sec DSP= 0.138E-01 Btu/R.sec DSD= 0.129E-01 Btu/R.sec
DELTA THETA= 0.8 DEG

BASED ON PT PS AND THETA

R/Rw	Pt psia	Ps psia	Vt ft/sec	Va ft/sec	DTt deg	DTs deg	Tt F deg	Ts F deg	THETA deg	DS Btu/lbmR	G(psqin) lbm/sec
0.992	19.37	16.43	463.	259.	4.0	-19.4	50.0	26.6	240.8	0.0628	0.16402
0.969	19.65	16.40	485.	271.	3.0	-22.7	49.0	23.3	240.8	0.0613	0.17243
0.945	19.67	16.38	487.	273.	2.5	-23.4	48.5	22.6	240.8	0.0610	0.17341
0.921	19.57	16.32	485.	271.	1.5	-24.2	47.0	21.3	240.8	0.0607	0.17233
0.902	19.47	16.24	493.	254.	1.0	-24.6	46.5	20.9	242.8	0.0608	0.16869
0.882	19.29	16.11	491.	253.	0.0	-25.4	45.5	20.1	242.8	0.0609	0.15897
0.843	18.83	15.74	501.	225.	-2.0	-27.1	43.5	18.4	245.8	0.0616	0.13911
0.764	17.61	15.52	435.	152.	-6.5	-24.2	39.0	21.3	250.8	0.0641	0.09173
0.685	16.37	14.97	376.	95.	-11.0	-23.5	34.5	22.0	255.8	0.0669	0.05544
0.606	15.25	14.34	319.	24.	-16.0	-24.5	29.5	21.0	265.8	0.0693	0.01316
0.528	14.45	13.93	245.	-25.	-20.5	-25.5	25.0	20.0	275.8	0.0708	-0.01349
0.449	13.99	13.68	173.	-84.	-24.0	-27.1	21.5	18.4	295.8	0.0713	-0.04480
0.370	13.83	13.56	115.	-141.	-25.5	-28.3	20.0	17.2	320.8	0.0713	-0.07515
0.291	13.83	13.54	62.	-178.	-25.0	-28.0	20.5	17.5	340.8	0.0716	-0.09451
0.213	13.87	13.55	49.	-192.	-24.0	-27.3	21.5	18.2	345.8	0.0719	-0.10212
0.134	13.95	13.59	33.	-206.	-23.0	-26.6	22.5	18.9	350.8	0.0720	-0.10935
0.055	13.99	13.60	-3.	-218.	-21.0	-25.0	24.5	20.5	360.8	0.0728	-0.11590

BASED ON DP/DR PS AND THETA

R/Rw	Pt psia	Ps psia	Vt ft/sec	Va ft/sec	DTt deg	DTs deg	Tt F deg	Ts F deg	THETA deg	DS Btu/lbmR	G(psqin) lbm/sec
0.969	17.12	16.40	238.	133.	3.0	-3.2	49.0	42.8	240.8	0.0708	0.08154
0.945	17.45	16.38	288.	161.	2.5	-6.6	48.5	39.4	240.8	0.0693	0.09917
0.921	18.40	16.32	395.	221.	1.5	-15.6	47.0	29.9	240.8	0.0649	0.13804
0.902	19.50	16.24	496.	255.	1.0	-24.9	46.5	20.6	242.8	0.0607	0.16144
0.862	21.29	16.11	606.	312.	0.0	-38.7	45.5	6,8	242.8	0.0542	0.20171
0.843	18.38	15.74	467.	210.	-2.0	-23.8	43.5	21.7	245.8	0.0633	0.12864
0.764	17.73	15.52	446.	155.	-6.5	-25.1	39.0	20.4	250.8	0.0636	0.09420
0.685	17.88	14.97	526.	133.	-11.0.	-35.5	34.5	10.0	255.8	0.0609	0.07957
0.606	16.45	14.34	474.	35.	-16.0	-34.8	29.5	10.7	265.8	0.0642	0.01997
0.528	15.09	13.93	360.	-36.	-20.5	-31.4	25.0	14.1	275.8	0.0679	-0.02006
0.449	14.36	13.68	253.	-122.	-24.0	-30.6	21.5	14.9	295.8	0.0695	-0.06606
0.370	13.99	13.56	143.	-176.	-25.5	-29.8	20.0	15.7	320.8	0.0706	-0.09382
0.291	13.63	13.54	35.	-101.	-25.0	-25.9	20.5	19.6	340.8	0.0726	-0.05333
0.213	13.55	13.55	0.	0.	-24.0	-24.0	21.5	21.5	345.8	0.0735	0.00000
0.134	13.59	13.59	0.	0.	-23.0	-23.0	22.5	22.5	350.8	0.0738	0.00000

BASED ON DIFERNTIAL EQUATION

R/Rw	Pt psia	Ps psia	Vt ft/sec	Va ft/sec	DTt deg	DTs deg	Tt F deg	Ts F deg	THETA deg	DS Btu/lbmR	G(psqin) lbm/sec
0.992	19.37	16.22	480.	269.	4.0	-21.2	50.0	24.8	240.8	0.0628	0.16858
0.969	19.65	16.11	507.	284.	3.0	-25.1	49.0	20.9	240.8	0.0613	0.17820
0.945	19.67	15.98	518.	290.	2.5	-26.8	48.5	19.2	240.8	0.0610	0.18115
0.921	19.57	15.85	521.	291.	1.5	-28.2	47.0	17.3	240.8	0.0607	0.18143
0.902	19.47	15.73	533.	274.	1.0	-29.0	46.5	16.5	242.8	0.0608	0.16980
0.882	19.29	15.61	531.	273.	0.0	-29.7	45.5	15.8	242.8	0.0609	0.16797
0.843	18.83	15.37	533.	240.	-2.0	-30.4	43.5	15.1	245.8	0.0616	0.14538
0.764	17.61	14.88	502.	175.	-6.5	-30.0	39.0	15.5	250.8	0.0641	0.10259
0.685	16.37	14.44	444.	113.	-11.0	-28.5	34.5	17.0	255.8	0.0669	0.06385
0.606	15.25	14.08	363.	27.	-16.0	-27.1	29.5	18.4	265.8	0.0693	0.01480
0.528	14.45	13.84	267.	-27.	-20.5	-26.5	25.0	19.0	275.8	0.0708	-0.01463
0.449	13.99	13.70	167.	-81.	-24.0	-26.9	21.5	18.6	295.8	0.0713	-0.04339
0.370	13.83	13.65	95.	-116.	-25.5	-27.4	20.0	18.1	320.8	0.0713	-0.06213
0.291	13.83	13.62	52.	-150.	-25.0	-27.1	20.5	18.4	340.8	0.2716	-0.08002
0.213	13.87	13.61	44.	-172.	-24.0	-26.6	21.5	18.9	345.8	0.0719	-0.09161
0.134	13.95	13.60	33.	-203.	-23.0	-26.5	22.5	19.0	350.8	0.0720	-0.10913
0.055	13.99	13.60	-3.	-218.	-21.0	-25.0	24.5	20.5	360.8	0.0728	-0.11590

Table 3 (Continued)

Test NO. 924 N=2 NN=17 Patm=14.53 psia Pinlet=46.13 psia Tinlet=46.Ø deg. F

GIn=Ø.1817 lbm/sec Gout=Ø.18Ø3 lbm/sec GPout=Ø.1939 lbm/sec GDout=Ø.1841 lbm/sec
EIn= Ø.221E+Ø2 Btu/sec Eout= Ø.219E+Ø2 Btu/sec DPout= Ø.236E+Ø2 Btu/sec EDout= Ø.224E+Ø2 Btu/sec
DS= Ø.717E-Ø2 Btu/R.sec DSP= Ø.85ØE-Ø2 Btu/R.sec DSD= Ø.76ØE-Ø2 Btu/R.sec

DELTA THETA= -2.6 DEG

BASED ON PT PS AND THETA

R/Rw	Pt psia	Ps psia	Vt ft/sec	Va ft/sec	DTt deg	DTs deg	Tt F deg	Ts F deg	THETA deg	DS Btu/lbmR	G(psqin) lbm/sec
Ø.992	25.79	19.89	61Ø.	254.	2.Ø	-34.4	48.Ø	11.6	247.4	Ø.Ø4Ø8	Ø.2ØØ48
Ø.969	27.13	18.94	723.	271.	2.5	-47.1	48.Ø	-1.6	249.4	Ø.Ø373	Ø.21ØØ1
Ø.945	27.23	18.57	753.	253.	1.Ø	-51.5	46.5	-6.Ø	251.4	Ø.Ø364	Ø.19384
Ø.921	26.79	18.29	753.	238.	-2.Ø	-54.Ø	43.5	-8.5	252.4	Ø.Ø361	Ø.18117
Ø.9Ø2	26.27	17.94	756.	225.	-4.Ø	-55.8	41.5	-1Ø.3	253.4	Ø.Ø364	Ø.16817
Ø.882	25.47	17.56	749.	2Ø9.	-6.Ø	-56.3	39.5	-1Ø.8	254.4	Ø.Ø376	Ø.15295
Ø.843	23.79	16.63	742.	165.	-11.Ø	-59.1	34.5	-13.6	257.4	Ø.Ø399	Ø.11548
Ø.764	2Ø.67	15.66	66Ø.	76.	-23.Ø	-59.8	22.5	-14.3	263.4	Ø.Ø436	Ø.Ø5ØØ6
Ø.685	18.41	15.17	552.	25.	-33.Ø	-58.4	12.5	-12.9	267.4	Ø.Ø465	Ø.Ø1573
Ø.6Ø6	16.85	14.Ø8	528.	-4.	-41.Ø	-64.2	4.Ø	-19.2	27Ø.4	Ø.Ø482	-Ø.ØØ241
Ø.528	15.57	13.69	446.	-27.	-46.Ø	-62.7	-Ø.5	-17.2	273.4	Ø.Ø513	-Ø.Ø1554
Ø.449	14.49	12.87	424.	-4Ø.	-53.Ø	-68.1	-7.5	-22.6	275.4	Ø.Ø526	-Ø.Ø2225
Ø.37Ø	13.57	12.43	364.	-35.	-59.Ø	-7Ø.1	-13.5	-24.6	275.4	Ø.Ø539	-Ø.Ø1852
Ø.291	12.67	11.75	331.	-61.	-65.Ø	-74.4	-19.5	-28.9	28Ø.4	Ø.Ø553	-Ø.Ø3114
Ø.213	12.Ø3	11.28	3Ø5.	-56.	-7Ø.Ø	-78.Ø	-24.5	-32.5	28Ø.4	Ø.Ø561	-Ø.Ø2778
Ø.134	11.45	1Ø.89	262.	-72.	-74.Ø	-8Ø.2	-28.5	-34.7	285.4	Ø.Ø573	-Ø.Ø3479
Ø.Ø55	11.15	1Ø.71	235.	-65.	-76.Ø	-81.Ø	-3Ø.5	-35.5	285.4	Ø.Ø58Ø	-Ø.Ø3Ø73

BASED ON DP/DR PS AND THETA

R/Rw	Pt psia	Ps psia	Vt ft/sec	Va ft/sec	DTt deg	DTs deg	Tt F deg	Ts F deg	THETA deg	DS Btu/lbmR	G(psqin) lbm/sec
Ø.969	39.43	18.94	1ØØ6.	377.	2.5	-93.5	48.Ø	-48.Ø	249.4	Ø.Ø117	Ø.325Ø7
Ø.945	26.73	18.57	735.	247.	1.Ø	-49.1	46.5	-3.6	251.4	Ø.Ø377	Ø.18828
Ø.921	26.76	18.29	752.	238.	-2.Ø	-53.8	43.5	-8.3	252.4	Ø.Ø361	Ø.18Ø84
Ø.9Ø2	28.84	17.94	839.	249.	-4.Ø	-67.6	41.5	-22.1	253.4	Ø.Ø3Ø1	Ø.19142
Ø.882	3Ø.56	17.56	9Ø3.	251.	-6.Ø	-79.1	39.5	-33.6	254.4	Ø.Ø251	Ø.19414
Ø.843	24.9Ø	16.63	785.	175.	-11.Ø	-64.9	34.5	-19.4	257.4	Ø.Ø368	Ø.12379
Ø.764	19.55	15.66	593.	68.	-23.Ø	-52.6	22.5	-7.1	263.4	Ø.Ø474	Ø.Ø4422
Ø.685	18.9Ø	15.17	587.	26.	-33.Ø	-61.8	12.5	-16.3	267.4	Ø.Ø447	Ø.Ø1685
Ø.6Ø6	17.15	14.Ø8	553.	-4.	-41.Ø	-66.4	4.Ø	-21.4	27Ø.4	Ø.Ø47Ø	-Ø.ØØ254
Ø.528	15.83	13.69	474.	-28.	-46.Ø	-64.7	-Ø.5	-19.2	273.4	Ø.Ø5Ø2	-Ø.Ø1656
Ø.449	14.77	12.87	456.	-43.	-53.Ø	-7Ø.5	-7.5	-25.Ø	275.4	Ø.Ø513	-Ø.Ø24Ø8
Ø.37Ø	13.81	12.43	397.	-38.	-59.Ø	-72.3	-13.5	-26.8	275.4	Ø.Ø527	-Ø.Ø2Ø33
Ø.291	12.89	11.75	365.	-67.	-65.Ø	-76.5	-19.5	-31.Ø	28Ø.4	Ø.Ø542	-Ø.Ø3454
Ø.213	11.89	11.28	275.	-51.	-7Ø.Ø	-76.5	-24.5	-31.Ø	28Ø.4	Ø.Ø57Ø	-Ø.Ø2498
Ø.134	11.15	1Ø.89	181.	-5Ø.	-74.Ø	-76.9	-28.5	-31.4	285.4	Ø.Ø591	-Ø.Ø2376

BASED ON DIFERNTIAL EQUATION

R/Rw	Pt psia	Ps psia	Vt ft/sec	Va ft/sec	DTt deg	DTs deg	Tt F deg	Ts F deg	THETA deg	DS Btu/lbmR	G(psqin) lbm/sec
Ø.992	25.79	18.83	669.	278.	2.Ø	-41.7	48.Ø	4.3	247.4	Ø.Ø4Ø8	Ø.21132
Ø.969	27.13	18.54	742.	279.	2.5	-49.9	48.Ø	-4.4	249.4	Ø.Ø373	Ø.2125Ø
Ø.945	27.23	18.21	771.	259.	1.Ø	-54.Ø	46.5	-8.5	251.4	Ø.Ø364	Ø.19569
Ø.921	26.79	17.86	776.	246.	-2.Ø	-57.1	43.5	-11.6	252.4	Ø.Ø361	Ø.18332
Ø.9Ø2	26.27	17.56	776.	231.	-4.Ø	-58.6	41.5	-13.1	253.4	Ø.Ø364	Ø.16995
Ø.882	25.47	17.26	766.	213.	-6.Ø	-58.6	39.5	-13.1	254.4	Ø.Ø376	Ø.15437
Ø.843	23.79	16.69	739.	165.	-11.Ø	-58.7	34.5	-13.2	257.4	Ø.Ø399	Ø.11524
Ø.764	2Ø.67	15.66	661.	76.	-23.Ø	-59.8	22.5	-14.3	263.4	Ø.Ø436	Ø.Ø52Ø6
Ø.685	18.41	14.81	585.	26.	-33.Ø	-61.5	12.5	-16.Ø	267.4	Ø.Ø465	Ø.Ø1636
Ø.6Ø6	16.85	14.Ø9	527.	-4.	-41.Ø	-64.2	4.Ø	-19.2	27Ø.4	Ø.Ø482	-Ø.ØØ241
Ø.528	15.57	13.45	475.	-29.	-46.Ø	-64.9	-Ø.5	-19.4	273.4	Ø.Ø513	-Ø.Ø1633
Ø.449	14.49	12.88	423.	-4Ø.	-53.Ø	-68.Ø	-7.5	-22.5	275.4	Ø.Ø526	-Ø.Ø2223
Ø.37Ø	13.57	12.35	375.	-36.	-59.Ø	-7Ø.8	-13.5	-25.3	275.4	Ø.Ø539	-Ø.Ø19Ø4
Ø.291	12.57	11.9Ø	3Ø2.	-56.	-65.Ø	-72.8	-19.5	-27.3	28Ø.4	Ø.Ø553	-Ø.Ø2868
Ø.213	12.Ø3	11.52	251.	-46.	-7Ø.Ø	-75.4	-24.5	-29.9	28Ø.4	Ø.Ø561	-Ø.Ø2318
Ø.134	11.45	11.18	182.	-5Ø.	-74.Ø	-77.Ø	-28.5	-31.5	285.4	Ø.Ø573	-Ø.Ø2462
Ø.Ø55	11.15	1Ø.71	235.	-65.	-76.Ø	-81.Ø	-3Ø.5	-35.5	285.4	Ø.Ø58Ø	-Ø.Ø3Ø73

Table 3 (Continued)

Test NO. 925 N=2 NN=17 Patm=14.53 psia Pinlet=46.92 psia Tinlet=45.5 deg. F

Gin=0.1888 lbm/sec Gout=0.1856 lbm/sec GPout=0.2104 lbm/sec GDout=0.1922 lbm/sec
Ein= 0.229E+02 Btu/sec Eout= 0.228E+02 Btu/sec DPout= 0.254E+02 Btu/sec EDout= 0.235E+02 Btu/sec
DS= 0.781E-02 Btu/R.sec DSP= 0.951E-02 Btu/R.sec DSD= 0.847E-02 Btu/R.sec
DELTA THETA= -3.4 DEG

BASED ON PT PS AND THETA

R/Rw	Pt psia	Ps psia	Vt ft/sec	Va ft/sec	DTt deg	DTs deg	Tt F deg	Ts F deg	THETA deg	DS Btu/lbmR	G(psqin) lbm/sec
0.992	25.15	18.94	612.	317.	2.5	-37.0	47.5	8.0	242.6	0.0437	0.24064
0.969	26.53	17.70	754.	311.	2.5	-52.9	47.5	-7.9	247.6	0.0400	0.22836
0.945	26.65	17.26	784.	308.	1.0	-58.1	46.0	-13.1	248.6	0.0390	0.22266
0.921	26.17	16.91	790.	294.	-1.0	-60.1	44.0	-15.1	249.6	0.0393	0.20945
0.902	25.49	16.89	776.	258.	-3.0	-58.7	42.0	-13.7	251.6	0.0402	0.18332
0.882	24.67	16.88	750.	235.	-4.5	-55.9	40.5	-10.9	252.6	0.0417	0.16576
0.843	22.59	16.18	713.	183.	-10.0	-55.1	35.0	-10.1	255.6	0.0451	0.12342
0.764	18.91	15.15	588.	98.	-23.5	-53.1	21.5	-8.1	260.6	0.0506	0.06128
0.685	16.49	14.16	486.	63.	-36.5	-56.5	8.5	-11.5	262.6	0.0535	0.03739
0.606	15.09	13.72	386.	23.	-44.5	-56.9	0.5	-11.9	266.6	0.0554	0.01319
0.528	14.25	13.38	313.	2.	-50.5	-58.6	-5.5	-13.6	269.6	0.0562	0.00126
0.449	13.79	13.19	258.	-48.	-53.0	-58.8	-8.0	-13.8	280.6	0.0571	-0.02677
0.370	13.57	13.08	213.	-107.	-53.0	-57.7	-8.0	-12.7	296.6	0.0582	-0.05850
0.291	13.51	13.03	162.	-172.	-52.0	-56.6	-7.0	-11.6	316.6	0.0590	-0.09353
0.213	13.49	13.01	75.	-226.	-50.5	-55.2	-5.5	-10.2	341.6	0.0599	-0.12273
0.134	13.51	13.02	35.	-239.	-48.5	-53.3	-3.5	-8.3	351.6	0.0609	-0.12890
0.055	13.49	13.00	14.	-240.	-46.5	-51.3	-1.5	-6.3	356.6	0.0620	-0.12893

BASED ON DP/DR PS AND THETA

R/Rw	Pt psia	Ps psia	Vt ft/sec	Va ft/sec	DTt deg	DTs deg	Tt F deg	Ts F deg	THETA deg	DS Btu/lbmR	G(psqin) lbm/sec
0.969	47.51	17.70	1132.	467.	2.5	-122.2	47.5	-77.2	247.6	0.0001	0.40461
0.945	28.15	17.26	829.	325.	1.0	-65.0	46.0	-20.0	248.6	0.0353	0.23906
0.921	21.85	16.91	613.	228.	-1.0	-36.6	44.0	8.4	249.6	0.0517	0.15430
0.902	17.32	16.89	199.	66.	-3.0	-6.7	42.0	38.3	251.6	0.0667	0.04207
0.882	23.46	16.88	701.	220.	-4.5	-49.4	40.5	-4.4	252.6	0.0452	0.15265
0.843	23.79	16.18	763.	196.	-10.0	-61.6	35.0	-16.6	255.6	0.0415	0.13407
0.764	20.79	15.15	698.	116.	-23.5	-65.2	21.5	-20.2	260.6	0.0441	0.07469
0.685	17.58	14.16	576.	75.	-36.5	-64.6	8.5	-19.6	262.6	0.0491	0.04517
0.606	15.29	13.72	410.	24.	-44.5	-58.5	0.5	-13.5	266.6	0.0545	0.01407
0.528	14.28	13.38	318.	2.	-50.5	-58.9	-5.5	-13.9	269.6	0.0560	0.00129
0.449	13.63	13.19	222.	-41.	-53.0	-57.2	-8.0	-12.2	280.6	0.0579	-0.02299
0.370	13.31	13.08	146.	-73.	-53.0	-55.2	-8.0	-10.2	296.6	0.0595	-0.03988
0.291	13.18	13.03	91.	-96.	-52.0	-53.5	-7.0	-8.5	316.6	0.0607	-0.05208
0.213	13.12	13.01	36.	-108.	-50.5	-51.6	-5.5	-6.6	341.6	0.0619	-0.05820
0.134	13.08	13.02	12.	-83.	-48.5	-49.1	-3.5	-4.1	351.6	0.0631	-0.04423

BASED ON DIFERNTIAL EQUATION

R/Rw	Pt psia	Ps psia	Vt ft/sec	Va ft/sec	DTt deg	DTs deg	Tt F deg	Ts F deg	THETA deg	DS Btu/lbmR	G(psqin) lbm/sec
0.992	25.15	17.87	669.	347.	2.5	-44.7	47.5	0.3	242.6	0.0437	0.25238
0.969	26.53	17.59	760.	313.	2.5	-53.7	47.5	-8.7	247.6	0.0400	0.22898
0.945	26.65	17.26	784.	308.	1.0	-58.1	46.0	-13.1	248.6	0.0390	0.22265
0.921	26.17	16.91	790.	294.	-1.0	-60.2	44.0	-15.2	249.6	0.0393	0.20947
0.902	25.49	16.61	791.	263.	-3.0	-60.8	42.0	-15.8	251.6	0.0402	0.18454
0.882	24.67	16.32	781.	245.	-4.5	-60.3	40.5	-15.3	252.6	0.0417	0.16846
0.843	22.59	15.76	738.	190.	-10.0	-58.4	35.0	-13.4	255.6	0.0451	0.12554
0.764	18.91	14.85	613.	102.	-23.5	-55.7	21.5	-10.7	260.6	0.0506	0.06296
0.685	16.49	14.22	479.	62.	-36.5	-55.9	8.5	-10.9	262.6	0.0535	0.03699
0.606	15.09	13.81	372.	22.	-44.5	-56.0	0.5	-11.0	266.6	0.0554	0.01278
0.528	14.25	13.54	282.	2.	-50.5	-57.1	-5.5	-12.1	269.6	0.0562	0.00115
0.449	13.79	13.36	219.	-41.	-53.0	-57.1	-8.0	-12.1	280.6	0.0571	-0.02292
0.370	13.57	13.22	180.	-90.	-53.0	-56.4	-8.0	-11.4	296.6	0.0582	-0.04986
0.291	13.51	13.11	149.	-158.	-52.0	-55.9	-7.0	-10.9	316.6	0.0590	-0.08644
0.213	13.49	13.04	73.	-219.	-50.5	-55.0	-5.5	-10.0	341.6	0.0599	-0.11917
0.134	13.51	13.01	35.	-240.	-48.5	-53.4	-3.5	-8.4	351.6	0.0609	-0.12956
0.055	13.49	13.00	14.	-240.	-46.5	-51.3	-1.5	-6.3	356.6	0.0620	-0.12893

Table 3 (Continued)

Test NO. 1138 N=2 NN=17 Patm=14.24 psia Pinlet=31.03 psia Tinlet=49.0 deg. F

Gin=0.0955 lbm/sec Gout=0.0941 lbm/sec GPout=0.0886 lbm/sec GDout=0.0968 lbm/sec
Ein= 0.117E+02 Btu/sec Eout= 0.114E+02 Btu/sec DPout= 0.108E+02 Btu/sec EDout= 0.118E+02 Btu/sec
DS= 0.224E-02 Btu/R.sec DSP= 0.249E-02 Btu/R.sec DSD= 0.343E-02 Btu/R.sec
DELTA THETA= 3.8 DEG

BASED ON PT PS AND THETA

R/Rw	Pt psia	Ps psia	Vt ft/sec	Va ft/sec	DTt deg	DTs deg	Tt F deg	Ts F deg	THETA deg	DS Btu/lbmR	G(psqin) lbm/sec
0.980	22.80	20.75	387.	112.	3.0	-10.5	49.5	36.0	253.8	0.0214	0.08823
0.961	22.92	20.82	391.	114.	3.0	-10.8	50.0	36.2	253.8	0.0212	0.08941
0.921	22.74	20.58	401.	102.	2.0	-12.3	49.0	34.7	255.8	0.0213	0.07932
0.843	22.46	20.22	420.	61.	0.0	-15.0	48.0	33.0	261.8	0.0217	0.04664
0.764	21.98	19.77	425.	31.	-1.0	-16.1	47.0	31.9	265.8	0.0227	0.02359
0.685	21.46	19.28	428.	-6.	-2.0	-17.2	46.0	30.8	270.8	0.0239	-0.00432
0.606	20.98	18.69	442.	-29.	-5.0	-21.3	43.5	27.2	273.8	0.0242	-0.02103
0.528	20.34	17.92	463.	2.	-6.5	-24.3	42.5	24.7	269.8	0.0259	0.00120
0.449	19.48	17.07	471.	35.	-8.5	-27.0	40.5	22.0	265.8	0.0279	0.02303
0.370	18.46	16.17	468.	59.	-11.0	-29.5	38.0	19.5	262.8	0.0304	0.03742
0.291	17.10	14.98	465.	59.	-16.0	-34.3	33.0	14.7	262.8	0.0332	0.03480
0.213	15.56	14.14	397.	22.	-22.5	-35.6	27.0	13.9	266.8	0.0367	0.01246
0.173	14.82	13.62	372.	21.	-25.0	-36.6	25.0	13.4	266.8	0.0391	0.01127
0.134	14.10	13.25	318.	18.	-27.5	-35.9	22.5	14.1	266.8	0.0413	0.00936
0.094	13.50	12.97	254.	37.	-31.0	-36.5	19.0	13.5	261.8	0.0425	0.01860
0.055	12.92	12.71	159.	37.	-34.0	-36.2	17.0	14.8	256.8	0.0445	0.01879
0.016	12.50	12.48	40.	24.	-36.0	-36.2	15.0	14.8	238.8	0.0458	0.01181

BASED ON DP/DR PS AND THETA

R/Rw	Pt psia	Ps psia	Vt ft/sec	Va ft/sec	DTt deg	DTs deg	Tt F deg	Ts F deg	THETA deg	DS Btu/lbmR	G(psqin) lbm/sec
0.961	22.35	20.82	336.	98.	3.0	-7.2	50.0	39.8	253.8	0.0230	0.07640
0.921	23.18	20.58	438.	111.	2.0	-15.0	49.0	32.0	255.8	0.0200	0.08700
0.843	22.53	20.22	426.	62.	0.0	-15.4	48.0	32.6	261.8	0.0215	0.04736
0.764	22.17	19.77	441.	33.	-1.0	-17.3	47.0	30.7	265.8	0.0221	0.02456
0.685	21.73	19.28	452.	-6.	-2.0	-19.0	46.0	29.0	270.8	0.0230	-0.00458
0.606	21.45	18.69	481.	-32.	-5.0	-24.4	43.5	24.1	273.8	0.0227	-0.02307
0.528	20.80	17.92	501.	2.	-6.5	-27.4	42.5	21.6	269.8	0.0243	0.00131
0.449	19.72	17.07	492.	36.	-8.5	-28.7	40.5	20.3	265.8	0.0270	0.02414
0.370	18.80	16.17	498.	63.	-11.0	-32.0	38.0	17.0	262.8	0.0291	0.04006
0.291	16.98	14.98	452.	57.	-16.0	-33.3	33.0	15.7	262.8	0.0337	0.03380
0.213	15.41	14.14	376.	21.	-22.5	-34.3	27.0	15.2	266.8	0.0374	0.01179
0.173	14.62	13.62	341.	19.	-25.0	-34.7	25.0	15.3	266.8	0.0400	0.01030
0.134	13.82	13.25	261.	15.	-27.5	-33.2	22.5	16.8	266.8	0.0426	0.00765
0.094	13.30	12.97	203.	29.	-31.0	-34.5	19.0	15.5	261.8	0.0435	0.01498
0.055	12.89	12.71	148.	35.	-34.0	-35.9	17.0	15.1	256.8	0.0447	0.01737

BASED ON DIFERNTIAL EQUATION

R/Rw	Pt psia	Ps psia	Vt ft/sec	Va ft/sec	DTt deg	DTs deg	Tt F deg	Ts F deg	THETA deg	DS Btu/lbmR	G(psqin) lbm/sec
0.980	22.80	20.65	397.	115.	3.0	-11.2	49.5	35.3	253.8	0.0214	0.09021
0.961	22.92	20.57	415.	121.	3.0	-12.5	50.0	34.5	253.8	0.0212	0.09407
0.921	22.74	20.39	420.	106.	2.0	-13.6	49.0	33.4	255.8	0.0213	0.08238
0.843	22.46	19.99	442.	64.	0.0	-16.6	48.0	31.4	261.8	0.0217	0.04866
0.764	21.98	19.54	448.	33.	-1.0	-17.8	47.0	30.2	265.8	0.0227	0.02464
0.685	21.46	19.03	452.	-6.	-2.0	-19.0	46.0	29.0	270.8	0.0239	-0.00453
0.606	20.98	18.46	465.	-31.	-5.0	-23.1	43.5	25.4	273.8	0.0242	-0.02194
0.528	20.34	17.79	476.	2.	-6.5	-25.4	42.5	23.6	269.8	0.0259	0.00123
0.449	19.48	17.02	475.	35.	-8.5	-27.4	40.5	21.6	265.8	0.0279	0.02321
0.370	18.46	16.16	469.	59.	-11.0	-29.6	38.0	19.4	262.8	0.0304	0.03748
0.291	17.10	15.23	436.	55.	-16.0	-32.1	33.0	16.9	262.8	0.0332	0.03302
0.213	15.56	14.29	375.	21.	-22.5	-34.2	27.0	15.3	266.8	0.0367	0.01186
0.173	14.82	13.84	335.	19.	-25.0	-34.4	25.0	15.6	266.8	0.0391	0.01026
0.134	14.10	13.43	283.	16.	-27.5	-34.2	22.5	15.8	266.8	0.0413	0.00840
0.094	13.50	13.05	232.	34.	-31.0	-35.6	19.0	14.4	261.8	0.0425	0.01730
0.055	12.92	12.72	154.	36.	-34.0	-36.1	17.0	14.9	256.8	0.0445	0.01816
0.016	12.50	12.48	40.	24.	-36.0	-36.2	15.0	14.8	238.8	0.0458	0.01181

Table 3 (Continued)

Test NO. 1139 N=2 NN=17 Patm=14.24 psia Pinlet=36.62 psia Tinlet=53.0 deg. F

Gin=0.1172 lbm/sec Gout=0.1190 lbm/sec GPout=0.1061 lbm/sec GDout=0.1185 lbm/sec
Ein= 0.144E+02 Btu/sec Eout= 0.146E+02 Btu/sec DPout= 0.130E+02 Btu/sec EDout= 0.145E+02 Btu/sec
DS= 0.326E-02 Btu/R.sec DSP= 0.349E-02 Btu/R.sec DSD= 0.452E-02 Btu/R.sec

DELTA THETA= 4.7 DEG

BASED ON PT PS AND THETA

R/Rw	Pt psia	Ps psia	Vt ft/sec	Va ft/sec	DTt deg	DTs deg	Tt F deg	Ts F deg	THETA deg	DS Btu/lbmR	G(psqin) lbm/sec
0.980	25.88	23.03	430.	134.	3.5	-13.4	55.5	38.6	252.7	0.0250	0.11623
0.961	25.92	22.73	456.	142.	2.5	-16.5	54.5	35.5	252.7	0.0244	0.12221
0.921	25.88	22.67	464.	119.	2.0	-17.1	54.0	34.9	255.7	0.0243	0.10176
0.843	25.38	22.21	475.	70.	0.0	-19.2	52.5	33.3	261.7	0.0249	0.05867
0.764	24.76	21.67	478.	28.	-2.0	-21.1	50.5	31.4	266.7	0.0257	0.02297
0.685	24.22	21.19	478.	-6.	-4.0	-23.1	48.5	29.4	270.7	0.0262	-0.00455
0.606	23.56	20.53	483.	-31.	-7.0	-26.5	46.0	26.5	273.7	0.0270	-0.02453
0.528	22.78	19.60	504.	-6.	-9.0	-30.2	44.0	22.8	270.7	0.0283	-0.00450
0.449	21.66	18.14	545.	41.	-10.0	-34.8	43.0	18.2	265.7	0.0313	0.02932
0.370	20.32	16.25	605.	78.	-13.0	-44.0	40.0	9.0	262.7	0.0342	0.05052
0.291	18.20	14.53	603.	78.	-19.0	-49.8	34.0	3.2	262.7	0.0389	0.04560
0.213	15.48	13.27	500.	38.	-27.0	-47.9	26.0	5.1	265.7	0.0461	0.02023
0.173	14.24	12.47	463.	27.	-31.0	-48.9	22.0	4.1	266.7	0.0498	0.01357
0.134	13.20	12.01	390.	23.	-36.0	-48.7	17.0	4.3	266.7	0.0525	0.01100
0.094	12.36	11.53	334.	19.	-40.0	-49.3	13.0	3.7	266.7	0.0550	0.00906
0.055	11.68	11.26	239.	31.	-44.0	-48.8	9.0	4.2	262.7	0.0568	0.01397
0.016	11.16	11.06	111.	41.	-47.0	-48.2	6.0	4.8	249.7	0.0584	0.01842

BASED ON DP/DR PS AND THETA

R/Rw	Pt psia	Ps psia	Vt ft/sec	Va ft/sec	DTt deg	DTs deg	Tt F deg	Ts F deg	THETA deg	DS Btu/lbmR	G(psqin) lbm/sec
0.961	26.10	22.73	467.	146.	2.5	-17.4	54.5	34.6	252.7	0.0239	0.12558
0.921	24.90	22.67	391.	100.	2.0	-11.6	54.0	40.4	255.7	0.0269	0.08491
0.843	25.06	22.21	452.	66.	0.0	-17.4	52.5	35.1	261.7	0.0258	0.05564
0.764	24.26	21.67	440.	26.	-2.0	-18.2	50.5	34.3	266.7	0.0271	0.02105
0.685	23.78	21.19	445.	-5.	-4.0	-20.5	48.5	32.0	270.7	0.0275	-0.00421
0.606	23.76	20.53	498.	-32.	-7.0	-27.7	46.0	25.3	273.7	0.0264	-0.02534
0.528	23.89	19.60	577.	-7.	-9.0	-36.7	44.0	16.3	270.7	0.0250	-0.00522
0.449	23.42	18.14	650.	49.	-10.0	-45.4	43.0	7.6	265.7	0.0259	0.03581
0.370	20.98	16.25	645.	83.	-13.0	-48.2	40.0	4.8	262.7	0.0320	0.05440
0.291	17.53	14.53	552.	71.	-19.0	-44.7	34.0	8.3	262.7	0.0415	0.04127
0.213	15.23	13.27	473.	36.	-27.0	-45.7	26.0	7.3	265.7	0.0472	0.01907
0.173	13.92	12.47	423.	25.	-31.0	-45.9	22.0	7.1	266.7	0.0513	0.01231
0.134	12.84	12.01	328.	19.	-36.0	-45.0	17.0	8.0	266.7	0.0544	0.00918
0.094	11.98	11.53	249.	15.	-40.0	-45.2	13.0	7.8	266.7	0.0571	0.00670
0.055	11.43	11.26	152.	20.	-44.0	-46.0	9.0	7.0	262.7	0.0583	0.00885

BASED ON DIFERNTIAL EQUATION

R/Rw	Pt psia	Ps psia	Vt ft/sec	Va ft/sec	DTt deg	DTs deg	Tt F deg	Ts F deg	THETA deg	DS Btu/lbmR	G(psqin) lbm/sec
0.980	25.88	22.95	436.	136.	3.5	-13.9	55.5	38.1	252.7	0.0250	0.11760
0.961	25.92	22.84	447.	139.	2.5	-15.7	54.5	36.3	252.7	0.0244	0.12030
0.921	25.88	22.61	468.	120.	2.0	-17.5	54.0	34.5	255.7	0.0243	0.10255
0.843	25.38	22.07	485.	71.	0.0	-20.0	52.5	32.5	261.7	0.0249	0.05971
0.764	24.76	21.47	494.	29.	-2.0	-22.4	50.5	30.1	266.7	0.0257	0.02360
0.685	24.22	20.77	512.	-6.	-4.0	-25.8	48.5	26.7	270.7	0.0262	-0.00450
0.606	23.56	19.96	529.	-34.	-7.0	-30.4	46.0	22.6	273.7	0.0270	-0.02531
0.528	22.78	19.01	552.	-6.	-9.0	-34.4	44.0	18.6	270.7	0.0283	-0.00482
0.449	21.66	17.87	567.	43.	-10.0	-36.9	43.0	16.1	265.7	0.0313	0.03018
0.370	20.32	16.53	581.	75.	-13.0	-41.6	40.0	11.4	262.7	0.0342	0.04516
0.291	18.20	15.02	558.	72.	-19.0	-45.4	34.0	7.6	262.7	0.0389	0.04324
0.213	15.48	13.52	469.	36.	-27.0	-45.4	26.0	7.6	265.7	0.0461	0.01926
0.173	14.24	12.87	405.	24.	-31.0	-44.7	22.0	8.3	266.7	0.0498	0.01215
0.134	13.20	12.31	336.	20.	-36.0	-45.4	17.0	7.6	266.7	0.0525	0.00964
0.094	12.36	11.83	265.	15.	-40.0	-45.9	13.0	7.1	266.7	0.0550	0.00733
0.055	11.68	11.42	188.	24.	-44.0	-47.0	9.0	5.0	262.7	0.0568	0.01112
0.016	11.16	11.06	111.	41.	-47.0	-48.2	6.0	4.8	249.7	0.0584	0.01842

Table 3 (Continued)

Test NO. 1151 N=1 NN=17 Patm=14.32 psia Pinlet=35.98 psia Tinlet=64.0 deg. F

Gin=0.1036 lbm/sec Gout=0.1041 lbm/sec GPout=0.0921 lbm/sec GDout=0.1050 lbm/sec
Ein= 0.130E+02 Btu/sec Eout= 0.130E+02 Btu/sec DPout= 0.115E+02 Btu/sec EDout= 0.131E+02 Btu/sec
DS= 0.232E-02 Btu/R.sec DSP= 0.273E-02 Btu/R.sec DSD= 0.312E-02 Btu/R.sec
DELTA THETA= 3.4 DEG

BASED ON PT PS AND THETA

R/Rw	Pt psia	Ps psia	Vt ft/sec	Va ft/sec	DTt deg	DTs deg	Tt F deg	Ts F deg	THETA deg	DS Btu/lbmR	G(psqin) lbm/sec
0.980	28.32	26.03	370.	114.	0.0	-12.5	64.0	51.5	252.9	0.0164	0.10900
0.961	28.38	25.92	385.	112.	0.0	-13.4	64.0	50.6	253.9	0.0163	0.10618
0.921	28.26	25.74	396.	96.	-0.5	-14.3	63.5	49.7	256.4	0.0163	0.09099
0.843	27.96	25.43	406.	54.	-1.5	-15.5	62.5	48.5	262.4	0.0166	0.05109
0.764	27.52	25.04	408.	22.	-3.5	-17.4	60.5	46.6	266.9	0.0168	0.02078
0.685	27.00	24.53	411.	-6.	-4.5	-18.6	59.5	45.4	270.9	0.0176	-0.00557
0.606	26.50	23.80	434.	-25.	-5.0	-20.7	59.0	43.3	273.4	0.0187	-0.02252
0.528	26.12	22.89	480.	-28.	-5.0	-24.2	59.0	39.8	273.4	0.0197	-0.02413
0.449	25.52	22.29	486.	-11.	-5.0	-24.7	59.0	39.3	271.4	0.0212	-0.00961
0.370	24.58	20.07	591.	38.	-6.0	-35.2	58.0	28.8	266.4	0.0234	0.02898
0.291	23.32	17.15	717.	90.	-7.5	-51.0	56.5	13.0	262.9	0.0263	0.06109
0.213	19.36	12.95	802.	165.	-10.0	-65.8	54.0	-1.8	258.4	0.0379	0.08759
0.173	16.32	11.56	740.	166.	-13.0	-60.9	50.0	2.1	257.4	0.0477	0.07786
0.134	13.18	10.53	597.	145.	-16.0	-47.5	47.0	15.5	256.4	0.0609	0.06024
0.094	10.72	9.79	355.	170.	-20.5	-33.4	42.5	29.6	244.4	0.0730	0.06391
0.055	9.98	9.74	110.	171.	-25.0	-28.4	38.0	34.6	212.9	0.0757	0.06298
0.016	9.74	9.73	25.	47.	-29.0	-29.2	34.0	33.8	208.4	0.0754	0.01735

BASED ON DP/DR PS AND THETA

R/Rw	Pt psia	Ps psia	Vt ft/sec	Va ft/sec	DTt deg	DTs deg	Tt F deg	Ts F deg	THETA deg	DS Btu/lbmR	G(psqin) lbm/sec
0.961	28.57	25.92	399.	115.	0.0	-14.3	64.0	49.7	253.9	0.0158	0.11010
0.921	27.81	25.74	361.	88.	-0.5	-12.0	63.5	52.0	256.4	0.0174	0.08256
0.843	27.39	25.43	360.	48.	-1.5	-12.5	62.5	51.5	262.4	0.0180	0.04503
0.764	27.32	25.04	392.	22.	-3.5	-16.3	60.5	47.7	266.9	0.0173	0.01990
0.685	27.32	24.53	435.	-6.	-4.5	-20.3	59.5	43.7	270.9	0.0168	-0.00591
0.606	27.12	23.80	477.	-28.	-5.0	-24.0	59.0	40.0	273.4	0.0171	-0.02492
0.528	25.53	22.89	437.	-26.	-5.0	-20.9	59.0	43.1	273.4	0.0212	-0.02183
0.449	26.57	22.29	552.	-13.	-5.0	-30.4	59.0	33.6	271.4	0.0185	-0.01104
0.370	26.82	20.07	702.	45.	-6.0	-47.2	58.0	16.8	266.4	0.0174	0.03531
0.291	24.82	17.15	783.	98.	-7.5	-59.3	56.5	4.7	262.9	0.0220	0.06790
0.213	18.99	12.95	783.	161.	-10.0	-63.3	54.0	0.7	258.4	0.0392	0.08509
0.173	14.60	11.56	613.	138.	-13.0	-45.9	50.0	17.1	257.4	0.0554	0.06251
0.134	12.22	10.53	488.	119.	-16.0	-37.0	47.0	26.0	256.4	0.0661	0.04819
0.094	10.38	9.79	287.	138.	-20.5	-28.9	42.5	34.1	244.4	0.0752	0.05113
0.055	9.82	9.74	62.	96.	-25.0	-26.1	38.0	36.9	212.9	0.0768	0.03516

BASED ON DIFERNTIAL EQUATION

R/Rw	Pt psia	Ps psia	Vt ft/sec	Va ft/sec	DTt deg	DTs deg	Tt F deg	Ts F deg	THETA deg	DS Btu/lbmR	G(psqin) lbm/sec
0.980	28.32	25.90	381.	117.	0.0	-13.2	64.0	50.8	252.9	0.0164	0.11164
0.961	28.38	25.81	394.	114.	0.0	-14.0	64.0	50.0	253.9	0.0163	0.10831
0.921	28.26	25.61	406.	98.	-0.5	-15.0	63.5	49.0	256.4	0.0163	0.09292
0.843	27.96	25.16	428.	57.	-1.5	-17.0	62.5	47.0	262.4	0.0166	0.05345
0.764	27.52	24.63	441.	24.	-3.5	-19.7	60.5	44.3	266.9	0.0168	0.02221
0.685	27.00	24.02	453.	-7.	-4.5	-21.6	59.5	42.4	270.9	0.0176	-0.00604
0.606	26.50	23.30	474.	-28.	-5.0	-23.7	59.0	40.3	273.4	0.0187	-0.02423
0.528	26.12	22.39	517.	-30.	-5.0	-27.4	59.0	36.6	273.4	0.0197	-0.02561
0.449	25.52	21.17	569.	-13.	-5.0	-32.0	59.0	32.0	271.4	0.0212	-0.01084
0.370	24.58	19.50	630.	40.	-6.0	-39.2	58.0	24.8	266.4	0.0234	0.03027
0.291	23.32	17.10	720.	90.	-7.5	-51.3	56.5	12.7	262.9	0.0263	0.06122
0.213	19.36	13.96	727.	150.	-10.0	-55.8	54.0	8.2	258.4	0.0379	0.08376
0.173	16.32	12.32	671.	150.	-13.0	-52.3	50.0	10.7	257.4	0.0477	0.07388
0.134	13.18	10.93	548.	133.	-16.0	-42.5	47.0	20.5	256.4	0.0609	0.05670
0.094	10.72	10.06	298.	143.	-20.5	-29.6	42.5	33.4	244.4	0.0730	0.05466
0.055	9.98	9.79	100.	154.	-25.0	-27.8	38.0	35.2	212.9	0.0757	0.05722
0.016	9.74	9.73	25.	47.	-29.0	-29.2	34.0	33.8	208.4	0.0754	0.01735

Table 3 (Continued)

Test NO. 1157 N=1 NN=17 Patm=14.29 psia Pinlet=31.80 psia Tinlet=67.0 deg. F

Gin=0.1041 lbm/sec Gout=0.1019 lbm/sec GPout=0.0812 lbm/sec GDout=0.1053 lbm/sec
Ein= 0.132E+02 Btu/sec Eout= 0.128E+02 Btu/sec DPout= 0.102E+02 Btu/sec EDout= 0.132E+02 Btu/sec
DS= 0.286E-02 Btu/R.sec DSP= 0.267E-02 Btu/R.sec DSD= 0.436E-02 Btu/R.sec

DELTA THETA= -2.9 DEG

BASED ON PT PS AND THETA

R/Rw	Pt psia	Ps psia	Vt ft/sec	Va ft/sec	DTt deg	DTs deg	Tt F deg	Ts F deg	THETA deg	DS Btu/lbmR	G(psqin) lbm/sec
0.980	21.49	18.85	456.	156.	0.0	-19.4	67.0	47.6	251.1	0.0269	0.10874
0.961	21.57	18.89	461.	149.	-0.5	-20.0	66.5	47.0	252.1	0.0264	0.10406
0.921	21.51	18.82	470.	125.	-1.5	-21.2	65.5	45.8	255.1	0.0261	0.08715
0.843	20.91	18.29	479.	84.	-3.5	-23.1	63.5	43.9	260.1	0.0272	0.05684
0.764	20.27	17.74	481.	41.	-6.0	-25.4	61.0	41.6	265.1	0.0281	0.02737
0.685	19.51	17.09	481.	8.	-8.5	-27.8	58.5	39.2	269.1	0.0296	0.00485
0.606	18.73	16.41	479.	-26.	-11.0	-30.1	56.0	36.9	273.1	0.0312	-0.01604
0.528	17.83	15.88	448.	-1.	-14.0	-30.7	53.0	36.3	270.1	0.0332	-0.00047
0.449	16.81	15.30	403.	20.	-16.0	-29.6	51.0	37.4	267.1	0.0363	0.01179
0.370	15.89	14.68	367.	31.	-20.0	-31.3	47.0	35.7	265.1	0.0383	0.01749
0.291	15.09	14.26	310.	32.	-24.0	-32.1	43.0	34.9	264.1	0.0399	0.01728
0.213	14.41	13.89	248.	21.	-28.0	-33.1	39.0	33.9	265.1	0.0412	0.01121
0.173	14.09	13.73	208.	14.	-30.0	-33.6	37.0	33.4	266.1	0.0418	0.00740
0.134	13.83	13.59	170.	6.	-32.0	-34.4	35.0	32.6	268.1	0.0421	0.00293
0.094	13.61	13.49	121.	2.	-33.0	-34.2	34.0	32.8	269.1	0.0427	0.00098
0.055	13.45	13.42	62.	0.	-35.0	-35.3	32.0	31.7	270.1	0.0425	-0.00006
0.016	13.35	13.34	34.	0.	-35.5	-35.6	31.5	31.4	270.1	0.0428	-0.00003

BASED ON DP/DR PS AND THETA

R/Rw	Pt psia	Ps psia	Vt ft/sec	Va ft/sec	DTt deg	DTs deg	Tt F deg	Ts F deg	THETA deg	DS Btu/lbmR	G(psqin) lbm/sec
0.961	19.15	18.89	147.	48.	-0.5	-2.5	66.5	64.5	252.1	0.0346	0.03210
0.921	21.47	18.82	467.	124.	-1.5	-20.9	65.5	46.1	255.1	0.0262	0.08657
0.843	21.43	18.29	520.	91.	-3.5	-26.7	63.5	40.3	260.1	0.0255	0.06222
0.764	20.86	17.74	530.	45.	-6.0	-29.5	61.0	37.5	265.1	0.0262	0.03037
0.685	20.17	17.09	537.	8.	-8.5	-32.5	58.5	34.5	269.1	0.0273	0.00547
0.606	18.86	16.41	491.	-27.	-11.0	-31.1	56.0	35.9	273.1	0.0308	-0.01650
0.528	17.83	15.88	448.	-1.	-14.0	-30.7	53.0	36.3	270.1	0.0332	-0.00046
0.449	17.07	15.30	435.	22.	-16.0	-31.8	51.0	35.2	267.1	0.0352	0.01277
0.370	15.95	14.68	376.	32.	-20.0	-31.8	47.0	35.2	265.1	0.0380	0.01790
0.291	15.01	14.26	295.	30.	-24.0	-31.3	43.0	35.7	264.1	0.0403	0.01643
0.213	14.38	13.89	240.	21.	-28.0	-32.8	39.0	34.2	265.1	0.0413	0.01086
0.173	14.07	13.73	202.	14.	-30.0	-33.4	37.0	33.6	266.1	0.0419	0.00720
0.134	13.80	13.59	160.	5.	-32.0	-34.1	35.0	32.9	268.1	0.0422	0.00274
0.094	13.60	13.49	115.	2.	-33.0	-34.1	34.0	32.9	269.1	0.0427	0.00093
0.055	13.47	13.42	80.	0.	-35.0	-35.5	32.0	31.5	270.1	0.0424	-0.00007

BASED ON DIFERNTIAL EQUATION

R/Rw	Pt psia	Ps psia	Vt ft/sec	Va ft/sec	DTt deg	DTs deg	Tt F deg	Ts F deg	THETA deg	DS Btu/lbmR	G(psqin) lbm/sec
0.980	21.49	18.80	460.	158.	0.0	-19.7	67.0	47.3	251.1	0.0269	0.10955
0.961	21.57	18.71	479.	154.	-0.5	-21.5	66.5	45.5	252.1	0.0264	0.10705
0.921	21.51	18.49	499.	133.	-1.5	-23.7	65.5	43.3	255.1	0.0261	0.09147
0.843	20.91	18.02	504.	88.	-3.5	-25.3	63.5	41.7	260.1	0.0272	0.05923
0.764	20.27	17.50	505.	43.	-6.0	-27.4	61.0	39.6	265.1	0.0281	0.02845
0.685	19.51	16.95	495.	8.	-8.5	-28.9	58.5	38.1	269.1	0.0296	0.00495
0.606	18.73	16.38	481.	-26.	-11.0	-30.3	56.0	36.7	273.1	0.0312	-0.01612
0.528	17.83	15.81	456.	-1.	-14.0	-31.3	53.0	35.7	270.1	0.0332	-0.00047
0.449	16.81	15.25	410.	21.	-16.0	-30.0	51.0	37.0	267.1	0.0363	0.01194
0.370	15.89	14.75	356.	31.	-20.0	-30.7	47.0	36.3	265.1	0.0383	0.01703
0.291	15.09	14.31	300.	31.	-24.0	-31.6	43.0	35.4	264.1	0.0399	0.01680
0.213	14.41	13.92	242.	21.	-28.0	-32.9	39.0	34.1	265.1	0.0412	0.01097
0.173	14.09	13.75	203.	14.	-30.0	-33.4	37.0	33.6	266.1	0.0418	0.00722
0.134	13.83	13.61	165.	5.	-32.0	-34.3	35.0	32.7	268.1	0.0421	0.00283
0.094	13.61	13.49	121.	2.	-33.0	-34.2	34.0	32.8	269.1	0.0427	0.00098
0.055	13.45	13.41	73.	0.	-35.0	-35.4	32.0	31.6	270.1	0.0425	-0.00006
0.016	13.35	13.34	34.	0.	-35.5	-35.6	31.5	31.4	270.1	0.0428	-0.00003

Table 3 (Continued)

Test NO. 1165 N=2 NN=17 Patm=14.12 psia Pinlet=35.97 psia Tinlet=60.5 deg. F

Gin=0.1015 lbm/sec Gout=0.0948 lbm/sec GPout=0.0934 lbm/sec GDout=0.0998 lbm/sec
Ein= 0.127E+02 Btu/sec Eout= 0.118E+02 Btu/sec DPout= 0.116E+02 Btu/sec EDout= 0.124E+02 Btu/sec
DS= 0.228E-02 Btu/R.sec DSP= 0.272E-02 Btu/R.sec DSD= 0.324E-02 Btu/R.sec
DELTA THETA= 8.9 DEG

BASED ON PT PS AND THETA

R/Rw	Pt psia	Ps psia	Vt ft/sec	Va ft/sec	DTt deg	DTs deg	Tt F deg	Ts F deg	THETA deg	DS Btu/lbmR	G(psqin) lbm/sec
0.980	28.06	25.68	380.	110.	0.0	-13.0	60.5	47.5	253.9	0.0170	0.10414
0.961	28.18	25.66	392.	106.	0.0	-13.7	60.5	46.8	254.9	0.0167	0.10048
0.921	27.98	25.47	396.	92.	0.0	-13.8	60.5	46.7	256.9	0.0172	0.08695
0.843	27.42	24.96	402.	50.	-2.5	-16.2	58.0	44.3	262.9	0.0175	0.04662
0.764	26.78	24.38	404.	8.	-4.5	-18.1	56.0	42.4	268.9	0.0182	0.00717
0.685	26.30	23.94	404.	-20.	-6.5	-20.1	54.0	40.4	272.9	0.0185	-0.01824
0.606	25.90	23.57	402.	-41.	-7.0	-20.6	53.5	39.9	275.9	0.0193	-0.03662
0.528	25.52	22.50	467.	-24.	-6.0	-24.2	54.5	36.3	272.9	0.0208	-0.01998
0.449	24.88	21.77	481.	1.	-5.5	-24.8	55.0	35.7	269.9	0.0227	0.00081
0.370	24.02	19.90	565.	61.	-6.5	-33.4	53.5	26.6	263.9	0.0244	0.04640
0.291	22.54	16.90	685.	122.	-9.5	-49.8	50.5	10.2	259.9	0.0274	0.08237
0.213	18.24	12.71	752.	175.	-14.0	-63.6	46.0	-3.6	256.9	0.0398	0.09145
0.173	15.24	11.35	677.	170.	-16.0	-56.6	44.0	3.4	255.9	0.0512	0.07626
0.134	12.26	10.70	457.	141.	-19.0	-38.0	41.0	22.0	252.9	0.0647	0.05858
0.094	10.52	9.95	272.	139.	-23.0	-30.8	37.0	29.2	242.9	0.0732	0.05306
0.055	10.15	10.13	31.	58.	-26.0	-26.4	34.0	33.6	207.9	0.0742	0.02238
0.016	10.06	9.79	99.	186.	-29.0	-32.7	31.0	27.3	207.9	0.0734	0.07026

BASED ON DP/DR PS AND THETA

R/Rw	Pt psia	Ps psia	Vt ft/sec	Va ft/sec	DTt deg	DTs deg	Tt F deg	Ts F deg	THETA deg	DS Btu/lbmR	G(psqin) lbm/sec
0.961	27.48	25.66	336.	91.	0.0	-10.1	60.5	50.4	254.9	0.0185	0.08557
0.921	28.46	25.47	430.	100.	0.0	-16.3	60.5	44.2	256.9	0.0162	0.09499
0.843	28.05	24.96	448.	56.	-2.5	-19.4	58.0	41.1	262.9	0.0159	0.05221
0.764	26.97	24.38	419.	8.	-4.5	-19.1	56.0	41.4	268.9	0.0177	0.00745
0.685	25.75	23.94	357.	-18.	-6.5	-17.1	54.0	43.4	272.9	0.0199	-0.01601
0.606	26.50	23.57	448.	-46.	-7.0	-23.9	53.5	36.6	275.9	0.0177	-0.04107
0.528	25.68	22.50	478.	-24.	-6.0	-25.1	54.5	35.4	272.9	0.0203	-0.02050
0.449	25.69	21.77	535.	1.	-5.5	-29.3	55.0	31.2	269.9	0.0205	0.00091
0.370	26.31	19.90	684.	73.	-6.5	-45.9	53.5	14.1	263.9	0.0182	0.05769
0.291	24.82	16.90	786.	140.	-9.5	-62.6	50.5	-2.6	259.9	0.0208	0.09716
0.213	18.79	12.71	781.	182.	-14.0	-67.5	46.0	-7.5	256.9	0.0377	0.09580
0.173	13.88	11.35	563.	142.	-16.0	-44.1	44.0	15.9	255.9	0.0576	0.06337
0.134	12.07	10.70	430.	132.	-19.0	-35.9	41.0	24.1	252.9	0.0657	0.05489
0.094	10.40	9.95	242.	124.	-23.0	-29.2	37.0	30.8	242.9	0.0740	0.04713
0.055	10.38	10.13	96.	182.	-26.0	-29.5	34.0	30.5	207.9	0.0727	0.07037

BASED ON DIFERNTIAL EQUATION

R/Rw	Pt psia	Ps psia	Vt ft/sec	Va ft/sec	DTt deg	DTs deg	Tt F deg	Ts F deg	THETA deg	DS Btu/lbmR	G(psqin) lbm/sec
0.980	28.06	25.29	411.	119.	0.0	-15.2	60.5	45.3	253.9	0.0170	0.11131
0.961	28.18	25.19	429.	116.	0.0	-16.4	60.5	44.1	254.9	0.0167	0.10847
0.921	27.98	24.96	436.	102.	0.0	-16.7	60.5	43.8	256.9	0.0172	0.09437
0.843	27.42	24.47	443.	55.	-2.5	-19.1	58.0	41.4	262.9	0.0175	0.05058
0.764	26.78	23.92	443.	9.	-4.5	-20.8	56.0	39.7	268.9	0.0182	0.00775
0.685	26.30	23.32	456.	-23.	-6.5	-23.9	54.0	36.6	272.9	0.0185	-0.02021
0.606	25.90	22.59	483.	-50.	-7.0	-26.6	53.5	33.9	275.9	0.0193	-0.04270
0.528	25.52	21.66	531.	-27.	-6.0	-29.6	54.5	30.9	272.9	0.0208	-0.02212
0.449	24.88	20.40	584.	1.	-5.5	-33.9	55.0	26.6	269.9	0.0227	0.00094
0.370	24.02	18.68	650.	70.	-6.5	-42.1	53.5	17.9	263.9	0.0244	0.05104
0.291	22.54	16.25	728.	130.	-9.5	-55.0	50.5	5.0	259.9	0.0274	0.08511
0.213	18.24	13.26	708.	165.	-14.0	-58.1	46.0	1.9	256.9	0.0398	0.08883
0.173	15.24	11.80	633.	159.	-16.0	-51.5	44.0	8.5	255.9	0.0512	0.07521
0.134	12.26	10.68	460.	142.	-19.0	-38.3	41.0	21.7	252.9	0.0647	0.05866
0.094	10.52	10.10	232.	119.	-23.0	-28.7	37.0	31.3	242.9	0.0732	0.04584
0.055	10.15	9.92	92.	173.	-26.0	-29.2	34.0	30.8	207.9	0.0742	0.06571
0.016	10.06	9.79	99.	186.	-29.0	-32.7	31.0	27.3	207.9	0.0734	0.07026

Table 3 (Continued)

Test NO. 1166 N=2 NN=17 Patm=14.12 psia Pinlet=36.02 psia Tinlet=60.5 deg. F

Gin=0.1020 lbm/sec Gout=0.1024 lbm/sec GPout=0.0797 lbm/sec GDout=0.1018 lbm/sec
Ein= 0.127E+02 Btu/sec Eout= 0.127E+02 Btu/sec DPout= 0.985E+01 Btu/sec EDout= 0.126E+02 Btu/sec
DS= 0.174E-02 Btu/R.sec DSP= 0.174E-02 Btu/R.sec DSD= 0.254E-02 Btu/R.sec
DELTA THETA= 7.9 DEG

BASED ON PT PS AND THETA

R/Rw	Pt psia	Ps psia	Vt ft/sec	Va ft/sec	DTt deg	DTs deg	Tt F deg	Ts F deg	THETA deg	DS Btu/lbmR	G(psqin) lbm/sec
0.980	27.98	25.66	372.	115.	-4.0	-16.6	56.5	43.9	252.9	0.0155	0.10955
0.961	28.10	25.61	387.	112.	-4.0	-17.5	56.5	43.0	253.9	0.0152	0.10691
0.921	28.06	25.55	394.	92.	-3.5	-17.1	57.0	43.4	256.9	0.0155	0.08754
0.843	27.52	25.25	384.	55.	-4.0	-16.5	56.5	44.0	261.9	0.0166	0.05156
0.764	27.12	24.69	404.	29.	-3.5	-17.2	57.0	43.3	265.9	0.0178	0.02693
0.685	26.46	24.09	404.	1.	-5.0	-18.6	55.5	41.9	269.9	0.0188	0.00090
0.606	25.74	23.49	398.	-20.	-8.0	-21.2	52.5	39.3	272.9	0.0193	-0.01752
0.528	25.02	22.92	389.	1.	-9.0	-21.6	51.5	38.9	269.9	0.0208	0.00083
0.449	24.32	22.39	377.	21.	-11.0	-22.9	49.5	37.6	266.9	0.0218	0.01746
0.370	23.32	21.66	355.	32.	-14.0	-24.6	46.5	35.9	264.9	0.0233	0.02614
0.291	22.42	21.17	312.	34.	-17.0	-25.2	43.5	35.3	263.9	0.0246	0.02686
0.213	21.50	20.64	263.	14.	-20.0	-25.8	40.5	34.7	266.9	0.0260	0.01128
0.173	21.08	20.42	233.	5.	-21.0	-25.5	39.5	35.0	268.9	0.0269	0.00359
0.134	20.74	20.27	198.	-3.	-22.5	-25.8	38.0	34.7	270.9	0.0273	-0.00227
0.094	20.46	20.10	173.	-6.	-24.0	-26.5	36.5	34.0	271.9	0.0275	-0.00427
0.055	20.22	20.04	122.	-10.	-24.5	-25.7	36.0	34.8	274.9	0.0280	-0.00785
0.016	20.04	19.90	104.	-27.	-25.5	-26.5	35.0	34.0	284.9	0.0282	-0.02075

BASED ON DP/DR PS AND THETA

R/Rw	Pt psia	Ps psia	Vt ft/sec	Va ft/sec	DTt deg	DTs deg	Tt F deg	Ts F deg	THETA deg	DS Btu/lbmR	G(psqin) lbm/sec
0.961	26.53	25.61	240.	69.	-4.0	-9.2	56.5	51.3	253.9	0.0191	0.06518
0.921	27.03	25.55	306.	71.	-3.5	-11.7	57.0	48.8	256.9	0.0181	0.06731
0.843	27.70	25.25	398.	57.	-4.0	-17.4	56.5	43.1	261.9	0.0162	0.05358
0.764	27.63	24.69	443.	32.	-3.5	-19.9	57.0	40.6	265.9	0.0166	0.02963
0.685	26.81	24.09	431.	1.	-5.0	-20.5	55.5	40.0	269.9	0.0179	0.00097
0.606	25.83	23.49	405.	-20.	-8.0	-21.7	52.5	38.8	272.9	0.0191	-0.01787
0.528	24.81	22.92	371.	1.	-9.0	-20.4	51.5	40.1	269.9	0.0214	0.00079
0.449	24.25	22.39	371.	20.	-11.0	-22.5	49.5	38.0	266.9	0.0220	0.01716
0.370	23.14	21.66	336.	30.	-14.0	-23.5	46.5	37.0	264.9	0.0238	0.02473
0.291	22.13	21.17	275.	30.	-17.0	-23.4	43.5	37.1	263.9	0.0254	0.02363
0.213	21.33	20.64	236.	13.	-20.0	-24.7	40.5	35.8	266.9	0.0265	0.01013
0.173	20.83	20.42	186.	4.	-21.0	-23.9	39.5	36.6	268.9	0.0277	0.00286
0.134	20.54	20.27	150.	-2.	-22.5	-24.4	38.0	36.1	270.9	0.0279	-0.00172
0.094	20.24	20.10	107.	-3.	-24.0	-25.0	36.5	35.5	271.9	0.0282	-0.00264
0.055	20.11	20.04	77.	-7.	-24.5	-25.0	36.0	35.5	274.9	0.0284	-0.00496

BASED ON DIFERNTIAL EQUATION

R/Rw	Pt psia	Ps psia	Vt ft/sec	Va ft/sec	DTt deg	DTs deg	Tt F deg	Ts F deg	THETA deg	DS Btu/lbmR	G(psqin) lbm/sec
0.980	27.98	25.79	360.	111.	-4.0	-15.8	56.5	44.7	252.9	0.0155	0.10654
0.961	28.10	25.71	378.	110.	-4.0	-16.9	56.5	43.6	253.9	0.0152	0.10486
0.921	28.06	25.53	396.	92.	-3.5	-17.3	57.0	43.2	256.9	0.0155	0.08796
0.843	27.52	25.11	396.	57.	-4.0	-17.3	56.5	43.2	261.9	0.0166	0.05298
0.764	27.12	24.66	407.	29.	-3.5	-17.3	57.0	43.2	265.9	0.0178	0.02706
0.685	26.46	24.16	398.	1.	-5.0	-18.2	55.5	42.3	269.9	0.0188	0.00089
0.606	25.74	23.64	383.	-19.	-8.0	-20.3	52.5	40.2	272.9	0.0193	-0.01696
0.528	25.02	23.10	371.	1.	-9.0	-20.5	51.5	40.0	269.9	0.0208	0.00080
0.449	24.32	22.52	363.	20.	-11.0	-22.0	49.5	38.5	266.9	0.0218	0.01690
0.370	23.32	21.93	324.	29.	-14.0	-22.8	46.5	37.7	264.9	0.0233	0.02405
0.291	22.42	21.37	285.	31.	-17.0	-23.8	43.5	36.7	263.9	0.0246	0.02474
0.213	21.50	20.85	229.	13.	-20.0	-24.4	40.5	36.1	266.9	0.0260	0.00989
0.173	21.08	20.62	193.	4.	-21.0	-24.1	39.5	36.4	268.9	0.0269	0.00299
0.134	20.74	20.43	159.	-2.	-22.5	-24.6	38.0	35.9	270.9	0.0273	-0.00184
0.094	20.46	20.26	129.	-4.	-24.0	-25.4	36.5	35.1	271.9	0.0275	-0.00322
0.055	20.22	20.08	106.	-9.	-24.5	-25.4	36.0	35.1	274.9	0.0280	-0.00685
0.016	20.04	19.90	104.	-27.	-25.5	-26.5	35.0	34.0	284.9	0.0282	-0.02075

Table 3 (Continued)

Test NO. 1172 N=1 NN=17 Patm=14.26 psia Pinlet=60.52 psia Tinlet=69.0 deg. F

Gin=0.1024 lbm/sec Gout=0.1129 lbm/sec GPout=0.0957 lbm/sec GDout=0.1038 lbm/sec
Ein= 0.130E+02 Btu/sec Eout= 0.143E+02 Btu/sec DPout= 0.121E+02 Btu/sec EDout= 0.131E+02 Btu/sec
DS= 0.892E-03 Btu/R.sec DSP= 0.992E-03 Btu/R.sec DSD= 0.965E-03 Btu/R.sec
DELTA THETA= 2.3 DEG

BASED ON PT PS AND THETA

R/Rw	Pt psia	Ps psia	Vt ft/sec	Va ft/sec	DTt deg	DTs deg	Tt F deg	Ts F deg	THETA deg	DS Btu/lbmR	G(psqin) lbm/sec
0.980	57.50	55.83	221.	66.	-0.5	-5.0	68.5	64.0	253.3	0.0033	0.13245
0.961	57.62	55.84	228.	68.	-1.5	-6.2	67.5	62.8	253.3	0.0027	0.13667
0.921	57.56	55.61	243.	59.	-0.5	-5.7	68.5	63.3	256.3	0.0032	0.11753
0.843	57.36	55.42	247.	38.	-1.5	-6.7	67.5	62.3	261.3	0.0030	0.07476
0.764	57.20	55.24	251.	12.	-1.5	-6.7	67.5	62.3	267.3	0.0032	0.02318
0.685	56.78	54.85	250.	-6.	-1.5	-6.7	67.5	62.3	271.3	0.0037	-0.01142
0.606	56.60	54.45	263.	-29.	-2.0	-7.8	67.0	61.2	276.3	0.0037	-0.05706
0.528	56.48	54.03	280.	-41.	-2.0	-8.6	67.0	60.4	278.3	0.0038	-0.07970
0.449	56.30	53.25	316.	-18.	-1.5	-9.8	67.5	59.2	273.3	0.0043	-0.03536
0.370	55.64	52.17	340.	-2.	-1.0	-10.6	68.0	58.4	270.3	0.0053	-0.00371
0.291	54.98	50.18	403.	33.	-1.0	-14.6	68.0	54.4	265.3	0.0061	0.06018
0.213	53.64	46.89	486.	48.	-3.5	-23.3	65.5	45.7	264.3	0.0067	0.08381
0.173	52.04	42.58	587.	79.	-4.5	-33.7	64.5	35.3	262.3	0.0083	0.12747
0.134	48.32	34.83	724.	189.	-6.5	-53.1	62.0	15.4	255.3	0.0122	0.26028
0.094	38.52	22.56	868.	362.	-9.5	-83.1	59.0	-14.6	247.3	0.0264	0.34405
0.055	28.70	24.83	322.	380.	-19.5	-40.1	49.0	28.4	220.3	0.0419	0.36190
0.016	24.30	23.95	44.	151.	-29.0	-31.0	39.5	37.5	196.3	0.0488	0.13584

BASED ON DP/DR PS AND THETA

R/Rw	Pt psia	Ps psia	Vt ft/sec	Va ft/sec	DTt deg	DTs deg	Tt F deg	Ts F deg	THETA deg	DS Btu/lbmR	G(psqin) lbm/sec
0.961	57.79	55.84	238.	71.	-1.5	-6.6	67.5	62.4	253.3	0.0025	0.14278
0.921	57.38	55.61	231.	56.	-0.5	-5.2	68.5	63.8	256.3	0.0234	0.11195
0.843	56.45	55.42	180.	27.	-1.5	-4.3	67.5	64.7	261.3	0.0041	0.05437
0.764	56.62	55.24	211.	10.	-1.5	-5.2	67.5	63.8	267.3	0.0039	0.01946
0.685	56.52	54.85	237.	-6.	-1.5	-6.2	67.5	62.8	271.3	0.0039	-0.01082
0.606	56.07	54.45	229.	-25.	-2.0	-6.4	67.0	62.6	276.3	0.0043	-0.04953
0.528	56.11	54.03	258.	-38.	-2.0	-7.7	67.0	61.3	278.3	0.0043	-0.07336
0.449	55.96	53.25	298.	-17.	-1.5	-8.9	67.5	60.1	273.3	0.0047	-0.03333
0.370	55.86	52.17	350.	-2.	-1.0	-11.2	68.0	57.8	270.3	0.0050	-0.00383
0.291	55.27	50.18	414.	34.	-1.0	-15.4	68.0	53.6	265.3	0.0058	0.06196
0.213	54.17	46.89	503.	50.	-3.5	-24.7	65.5	44.3	264.3	0.0060	0.08697
0.173	57.67	42.58	717.	97.	-4.5	-48.1	64.5	20.9	262.3	0.0013	0.16021
0.134	56.66	34.83	873.	228.	-6.5	-74.2	62.0	-5.7	255.3	0.0013	0.32841
0.094	30.43	22.56	660.	276.	-9.5	-52.0	59.0	16.5	247.3	0.0426	0.24453
0.055	24.83	24.83	0.	0.	-19.5	-19.5	49.0	49.0	220.3	0.0518	0.00000

BASED ON DIFERNTIAL EQUATION

R/Rw	Pt psia	Ps psia	Vt ft/sec	Va ft/sec	DTt deg	DTs deg	Tt F deg	Ts F deg	THETA deg	DS Btu/lbmR	G(psqin) lbm/sec
0.980	57.50	56.11	202.	60.	-0.5	-4.2	68.5	64.8	253.3	0.0033	0.12116
0.961	57.62	56.05	214.	64.	-1.5	-5.6	67.5	63.4	253.3	0.0027	0.12857
0.921	57.56	55.93	222.	54.	-0.5	-4.8	68.5	64.2	256.3	0.0032	0.10791
0.843	57.36	55.64	231.	35.	-1.5	-6.1	67.5	62.9	261.3	0.0030	0.07041
0.764	57.20	55.30	247.	12.	-1.5	-6.6	67.5	62.4	267.3	0.0032	0.02283
0.685	56.78	54.89	247.	-6.	-1.5	-6.6	67.5	62.4	271.3	0.0037	-0.01131
0.606	56.60	54.40	266.	-29.	-2.0	-7.9	67.0	61.1	276.3	0.0037	-0.05766
0.528	56.48	53.74	296.	-43.	-2.0	-9.4	67.0	59.6	278.3	0.0038	-0.08403
0.449	56.30	52.76	341.	-20.	-1.5	-11.2	67.5	57.8	273.3	0.0043	-0.03769
0.370	55.64	51.29	382.	-2.	-1.0	-13.1	68.0	55.9	270.3	0.0053	-0.00411
0.291	54.98	48.93	454.	37.	-1.0	-18.3	68.0	50.7	265.3	0.0061	0.06665
0.213	53.64	44.56	568.	56.	-3.5	-30.6	65.5	38.4	264.3	0.0067	0.09451
0.173	52.04	40.80	645.	87.	-4.5	-39.8	64.5	29.2	262.3	0.0083	0.13574
0.134	48.32	35.45	705.	185.	-6.5	-50.7	62.0	17.8	255.3	0.0122	0.25673
0.094	38.52	29.30	632.	264.	-9.5	-48.6	59.0	19.9	247.3	0.0264	0.30208
0.055	28.70	25.05	313.	368.	-19.5	-38.9	49.0	29.6	220.3	0.0419	0.35324
0.016	24.30	23.95	44.	151.	-29.0	-31.0	39.5	37.5	196.3	0.0488	0.13584

Table 3 (Continued)

Test NO. 1174 N=1 NN=17 Patm=14.26 psia Pinlet=30.96 psia Tinlet=74.5 deg. F

Gin=0.1039 lbm/sec Gout=0.1017 lbm/sec GPout=0.0767 lbm/sec GDout=0.1055 lbm/sec
Ein= 0.133E+02 Btu/sec Eout= 0.129E+02 Btu/sec DPout= 0.974E+01 Btu/sec EDout= 0.134E+02 Btu/sec
DS= 0.304E-02 Btu/R.sec DSP= 0.254E-02 Btu/R.sec DSD= 0.481E-02 Btu/R.sec
DELTA THETA= 0.6 DEG

BASED ON PT PS AND THETA

R/Rw	Pt psia	Ps psia	Vt ft/sec	Va ft/sec	DTt deg	DTs deg	Tt F deg	Ts F deg	THETA deg	DS Btu/lbmR	G(psqin) lbm/sec
0.980	19.62	17.20	460.	161.	-1.0	-20.8	73.5	53.7	250.6	0.0308	0.10132
0.961	19.86	17.37	465.	154.	-2.0	-22.0	72.5	52.5	251.6	0.0295	0.09806
0.921	19.90	17.28	480.	150.	-3.0	-24.1	71.5	50.4	252.6	0.0290	0.09522
0.843	19.40	16.78	498.	100.	-6.0	-27.5	68.5	47.0	258.6	0.0293	0.06209
0.764	18.66	16.25	492.	55.	-9.0	-29.4	65.5	45.1	263.6	0.0306	0.03304
0.685	17.68	15.49	482.	11.	-13.0	-32.4	61.5	42.1	268.6	0.0325	0.00659
0.606	16.68	15.08	421.	-5.	-16.0	-30.8	58.5	43.7	270.6	0.0351	-0.00256
0.528	15.80	14.52	384.	-11.	-21.0	-33.3	53.5	41.2	271.6	0.0365	-0.00599
0.449	15.10	14.26	316.	7.	-25.0	-33.3	49.5	41.2	268.6	0.0377	0.00399
0.370	14.56	14.11	234.	6.	-28.0	-32.6	46.5	41.9	268.6	0.0388	0.00292
0.291	14.24	14.03	160.	4.	-31.0	-33.1	43.5	41.4	268.6	0.0389	0.00199
0.213	14.12	14.02	112.	3.	-32.0	-33.0	42.5	41.5	268.6	0.0390	0.00139
0.173	14.04	13.98	91.	-3.	-33.0	-33.7	41.5	40.8	271.6	0.0389	-0.00137
0.134	14.00	13.95	83.	-7.	-33.0	-33.6	41.5	40.9	274.6	0.0391	-0.00352
0.094	13.98	13.95	63.	-14.	-32.0	-32.4	42.0	41.6	282.6	0.0395	-0.00740
0.055	14.02	13.96	80.	-33.	-32.0	-32.6	42.0	41.4	292.6	0.0393	-0.01741
0.016	14.00	13.96	64.	-37.	-32.0	-32.5	42.0	41.5	299.6	0.0394	-0.01912

BASED ON DP/DR PS AND THETA

R/Rw	Pt psia	Ps psia	Vt ft/sec	Va ft/sec	DTt deg	DTs deg	Tt F deg	Ts F deg	THETA deg	DS Btu/lbmR	G(psqin) lbm/sec
0.961	17.37	17.37	0.	0.	-2.0	-2.0	72.5	72.5	251.6	0.0387	0.00000
0.921	19.97	17.28	486.	152.	-3.0	-24.6	71.5	49.9	252.6	0.0287	0.09645
0.843	19.81	16.78	532.	107.	-6.0	-30.5	68.5	44.0	258.6	0.0279	0.06668
0.764	19.63	16.25	573.	64.	-9.0	-36.7	65.5	37.8	263.6	0.0272	0.03904
0.685	18.19	15.49	530.	13.	-13.0	-36.4	61.5	38.1	268.6	0.0306	0.00731
0.606	17.04	15.08	462.	-5.	-16.0	-33.8	58.5	40.7	270.6	0.0337	-0.00294
0.528	15.94	14.52	403.	-12.	-21.0	-34.6	53.5	39.9	271.6	0.0359	-0.00631
0.449	14.85	14.26	265.	6.	-25.0	-30.9	49.5	43.6	268.6	0.0389	0.00333
0.370	14.37	14.11	179.	4.	-28.0	-30.7	46.5	43.8	268.6	0.0397	0.00223
0.291	14.12	14.03	101.	2.	-31.0	-31.8	43.5	42.7	268.6	0.0395	0.00124
0.213	14.07	14.02	80.	2.	-32.0	-32.5	42.5	42.0	268.6	0.0393	0.00099
0.173	14.06	13.98	100.	-3.	-33.0	-33.8	41.5	40.7	271.6	0.0389	-0.00150
0.134	13.97	13.95	52.	-4.	-33.0	-33.2	41.5	41.3	274.6	0.0393	-0.00221
0.094	13.95	13.95	0.	0.	-32.0	-32.0	42.0	42.0	282.6	0.0396	0.00000
0.055	13.96	13.96	0.	0.	-32.0	-32.0	42.0	42.0	292.6	0.0396	0.00000

BASED ON DIFERNTIAL EQUATION

R/Rw	Pt psia	Ps psia	Vt ft/sec	Va ft/sec	DTt deg	DTs deg	Tt F deg	Ts F deg	THETA deg	DS Btu/lbmR	G(psqin) lbm/sec
0.980	19.62	17.26	453.	159.	-1.0	-20.2	73.5	54.3	250.6	0.0308	0.10021
0.961	19.86	17.17	485.	161.	-2.0	-23.7	72.5	50.8	251.6	0.0295	0.10135
0.921	19.90	16.97	509.	159.	-3.0	-26.7	71.5	47.8	252.6	0.0290	0.09967
0.843	19.40	16.51	525.	105.	-6.0	-29.9	68.5	44.6	258.6	0.0293	0.06462
0.764	18.66	16.01	517.	58.	-9.0	-31.6	65.5	42.9	263.6	0.0306	0.03438
0.685	17.68	15.51	480.	11.	-13.0	-32.2	61.5	42.3	268.6	0.0325	0.00657
0.606	16.68	15.07	423.	-5.	-16.0	-30.9	58.5	43.6	270.6	0.0351	-0.00267
0.528	15.80	14.70	355.	-10.	-21.0	-31.5	53.5	43.0	271.6	0.0365	-0.00559
0.449	15.10	14.42	284.	7.	-25.0	-31.7	49.5	42.8	268.6	0.0377	0.00361
0.370	14.56	14.22	204.	5.	-28.0	-31.5	46.5	43.0	268.6	0.0388	0.00255
0.291	14.24	14.10	131.	3.	-31.0	-32.4	43.5	42.1	268.6	0.0389	0.00163
0.213	14.12	14.03	107.	3.	-32.0	-32.9	42.5	41.6	268.6	0.0390	0.00132
0.173	14.04	14.00	70.	-2.	-33.0	-33.4	41.5	41.1	271.6	0.0389	-0.00106
0.134	14.00	13.99	42.	-3.	-33.0	-33.2	41.5	41.3	274.6	0.0391	-0.00181
0.094	13.98	13.98	2.	0.	-32.0	-32.0	42.0	42.0	282.6	0.0395	-0.00022
0.055	14.02	13.95	85.	-35.	-32.0	-32.7	42.0	41.3	292.6	0.0393	-0.01846
0.016	14.00	13.80	64.	-37.	-32.0	-32.5	42.0	41.5	299.6	0.0394	-0.01912

Table 3 (Continued)

Test NO. 1220 N=1 NN=17 Patm=14.21 psia Pinlet=29.90 psia Tinlet=65.0 deg. F

Gin=0.1035 lbm/sec Gout=0.0996 lbm/sec GPout=0.0962 lbm/sec GDout=0.1051 lbm/sec
Ein= 0.130E+02 Btu/sec Eout= 0.126E+02 Btu/sec DPout= 0.121E+02 Btu/sec EDout= 0.132E+02 Btu/sec
DS= 0.373E-02 Btu/R.sec DSP= 0.524E-02 Btu/R.sec DSD= 0.551E-02 Btu/R.sec

DELTA THETA= -1.5 DEG

BASED ON PT PS AND THETA

R/Rw	Pt psia	Ps psia	Vt ft/sec	Va ft/sec	DTt deg	DTs deg	Tt F deg	Ts F deg	THETA deg	DS Btu/lbmR	G(psqin) lbm/sec
0.980	17.93	16.04	415.	164.	0.5	-16.0	65.5	49.0	248.5	0.0353	0.09659
0.961	18.09	15.85	453.	170.	0.0	-19.5	65.0	45.5	249.5	0.0344	0.09970
0.941	18.13	15.87	460.	154.	-1.0	-20.6	64.0	44.4	251.5	0.0338	0.09085
0.921	18.11	15.84	463.	146.	-2.0	-21.6	63.0	43.4	252.5	0.0335	0.08631
0.902	18.01	15.76	465.	138.	-3.0	-22.6	62.0	42.4	253.5	0.0334	0.08115
0.882	17.95	15.68	469.	130.	-4.0	-23.7	61.0	41.3	254.5	0.0331	0.07647
0.843	17.65	15.44	471.	113.	-5.0	-24.6	60.0	40.4	256.5	0.0338	0.06559
0.764	16.87	14.79	471.	88.	-9.0	-28.1	56.5	37.4	259.5	0.0353	0.04882
0.685	16.07	14.53	416.	48.	-13.0	-27.6	52.5	37.9	263.5	0.0368	0.02604
0.606	15.35	14.00	398.	25.	-17.0	-30.2	48.5	35.3	266.5	0.0380	0.01300
0.528	14.75	13.70	356.	3.	-21.0	-31.6	44.5	33.9	269.5	0.0369	0.00170
0.449	14.21	13.43	311.	-24.	-25.5	-33.6	39.5	31.4	274.5	0.0390	-0.01245
0.370	13.77	13.23	256.	-47.	-30.0	-35.6	35.0	29.4	280.5	0.0390	-0.02396
0.291	13.45	13.08	209.	-62.	-34.0	-38.0	31.0	27.0	286.5	0.0387	-0.03114
0.213	13.21	12.95	169.	-70.	-37.0	-39.8	28.0	25.2	292.5	0.0385	-0.03500
0.134	13.01	12.85	130.	-65.	-42.0	-43.8	23.0	21.2	296.5	0.0370	-0.03251
0.055	12.91	12.82	98.	-53.	-43.0	-44.0	22.0	21.0	298.5	0.0371	-0.02669

BASED ON DP/DR PS AND THETA

R/Rw	Pt psia	Ps psia	Vt ft/sec	Va ft/sec	DTt deg	DTs deg	Tt F deg	Ts F deg	THETA deg	DS Btu/lbmR	G(psqin) lbm/sec
0.961	18.22	15.85	464.	174.	0.0	-20.5	65.0	44.5	249.5	0.0340	0.10238
0.941	15.99	15.87	100.	36.	-1.0	-2.1	64.0	62.9	251.5	0.0425	0.02060
0.921	17.41	15.84	390.	123.	-2.0	-15.9	63.0	49.1	252.5	0.0362	0.07188
0.902	17.84	15.76	448.	133.	-3.0	-21.2	62.0	43.8	253.5	0.0341	0.07794
0.882	18.42	15.68	511.	142.	-4.0	-27.4	61.0	37.6	254.5	0.0314	0.08381
0.843	19.10	15.44	590.	142.	-5.0	-35.7	60.0	39.3	256.5	0.0284	0.08401
0.764	17.19	14.79	503.	93.	-9.0	-30.8	56.5	34.7	259.5	0.0340	0.05234
0.685	16.33	14.53	447.	51.	-13.0	-29.9	52.5	35.6	263.5	0.0357	0.02811
0.606	15.67	14.00	439.	27.	-17:0	-33.1	48.5	32.4	266.5	0.0367	0.01441
0.528	14.69	13.70	345.	3.	-21.0	-30.9	44.5	34.6	269.5	0.0392	0.00165
0.449	14.11	13.43	289.	-23.	-25.5	-32.5	39.5	32.5	274.5	0.0396	-0.01156
0.370	13.66	13.23	228.	-42.	-30.0	-34.5	35.0	30.5	280.5	0.0396	-0.02131
0.291	13.36	13.08	183.	-54.	-34.0	-37.0	31.0	28.0	286.5	0.0392	-0.02714
0.213	13.13	12.95	141.	-58.	-37.0	-38.9	28.0	26.1	292.5	0.0389	-0.02920
0.134	12.92	12.85	86.	-43.	-42.0	-42.8	23.0	22.2	296.5	0.0375	-0.02143

BASED ON DIFERNTIAL EQUATION

R/Rw	Pt psia	Ps psia	Vt ft/sec	Va ft/sec	DTt deg	DTs deg	Tt F deg	Ts F deg	THETA deg	DS Btu/lbmR	G(psqin) lbm/sec
0.980	17.93	15.85	435.	172.	0.5	-17.7	65.5	47.3	248.5	0.0353	0.10052
0.961	18.09	15.78	461.	172.	0.0	-20.1	65.0	44.9	249.5	0.0344	0.10107
0.941	18.13	15.70	478.	160.	-1.0	-22.2	64.0	42.8	251.5	0.0338	0.09380
0.921	18.11	15.61	488.	154.	-2.0	-23.8	63.0	41.2	252.5	0.0335	0.08997
0.902	18.01	15.51	491.	146.	-3.0	-24.8	62.0	40.2	253.5	0.0334	0.08470
0.882	17.95	15.41	498.	138.	-4.0	-26.2	61.0	38.8	254.5	0.0331	0.08012
0.843	17.65	15.21	496.	119.	-5.0	-26.6	60.0	38.4	256.5	0.0338	0.06826
0.764	16.87	14.81	468.	87.	-9.0	-27.9	56.5	37.6	259.5	0.0353	0.04856
0.685	16.07	14.43	429.	49.	-13.0	-28.5	52.5	37.0	263.5	0.0368	0.02672
0.606	15.35	14.10	383.	24.	-17.0	-29.3	48.5	36.2	266.5	0.0380	0.01253
0.528	14.75	13.80	339.	3.	-21.0	-30.6	44.5	34.9	269.5	0.0389	0.00163
0.449	14.21	13.54	287.	-22.	-25.5	-32.4	39.5	32.6	274.5	0.0390	-0.01158
0.370	13.77	13.33	232.	-43.	-30.0	-34.6	35.0	30.4	280.5	0.0390	-0.02185
0.291	13.45	13.16	184.	-54.	-34.0	-37.1	31.0	27.9	286.5	0.0387	-0.02751
0.213	13.21	13.03	141.	-58.	-37.0	-38.9	28.0	26.1	292.5	0.0385	-0.02935
0.134	13.01	12.93	93.	-47.	-42.0	-42.9	23.0	22.1	296.5	0.0370	-0.02339
0.055	12.91	12.82	98.	-53.	-43.0	-44.0	22.0	21.0	298.5	0.0371	-0.02669

Table 3 (Continued)

Test NO. 1225 N=1 NN=17 Patm=14.24 psia Pinlet=24.46 psia Tinlet=8Ø.Ø deg. F

GIn=Ø.Ø79Ø lbm/sec Gout=Ø.Ø736 lbm/sec GPout=Ø.Ø94Ø lbm/sec GDout=Ø.Ø8Ø2 lbm/sec
EIn= Ø.1Ø2E+Ø2 Btu/sec Eout= Ø.943E+Ø1 Btu/sec DPout= Ø.121E+Ø2 Btu/sec EDout= Ø.1Ø3E+Ø2 Btu/sec
DS= Ø.18ØE-Ø2 Btu/R.sec DSP= Ø.284E-Ø2 Btu/R.sec DSD= Ø.276E-Ø2 Btu/R.sec
DELTA THETA= -Ø.3 DEG

BASED ON PT PS AND THETA

R/Rw	Pt psia	Ps psia	Vt ft/sec	Va ft/sec	DTt deg	DTs deg	Tt F deg	Ts F deg	THETA deg	DS Btu/lbmR	G(psqin) lbm/sec
Ø.98Ø	18.16	15.87	466.	163.	-Ø.5	-2Ø.8	78.5	58.2	25Ø.7	Ø.Ø198	Ø.Ø9364
Ø.961	18.12	15.79	474.	157.	-1.Ø	-21.8	79.Ø	58.2	251.7	Ø.Ø2Ø1	Ø.Ø8946
Ø.941	17.98	15.68	478.	14Ø.	-2.Ø	-22.6	78.Ø	57.4	253.7	Ø.Ø2Ø2	Ø.Ø7927
Ø.921	17.8Ø	15.57	474.	129.	-3.Ø	-23.1	77.Ø	56.9	254.7	Ø.Ø2Ø5	Ø.Ø7312
Ø.9Ø2	17.52	15.43	463.	118.	-5.Ø	-24.Ø	75.Ø	56.Ø	255.7	Ø.Ø2Ø7	Ø.Ø66Ø6
Ø.882	17.18	15.2Ø	459.	1ØØ.	-6.Ø	-24.4	74.Ø	55.6	257.7	Ø.Ø216	Ø.Ø5516
Ø.843	16.52	14.75	454.	82.	-9.Ø	-26.8	71.Ø	53.2	259.7	Ø.Ø225	Ø.Ø4437
Ø.764	15.52	14.Ø7	414.	53.	-14.Ø	-28.5	66.Ø	51.5	262.7	Ø.Ø249	Ø.Ø2725
Ø.685	14.76	13.86	333.	31.	-19.Ø	-28.3	61.Ø	51.7	264.7	Ø.Ø261	Ø.Ø1559
Ø.6Ø6	14.24	13.77	243.	1Ø.	-23.Ø	-27.9	57.Ø	52.1	267.7	Ø.Ø267	Ø.ØØ485
Ø.528	14.ØØ	13.74	182.	-6.	-25.Ø	-27.8	55.Ø	52.2	271.7	Ø.Ø269	-Ø.ØØ277
Ø.449	13.84	13.71	127.	-29.	-27.Ø	-28.4	53.Ø	51.6	282.7	Ø.Ø268	-Ø.Ø1439
Ø.37Ø	13.72	13.67	76.	-32.	-28.Ø	-28.6	52.Ø	51.4	292.7	Ø.Ø269	-Ø.Ø1586
Ø.291	13.7Ø	13.67	51.	-33.	-28.Ø	-28.3	52.Ø	51.7	3Ø2.7	Ø.Ø27Ø	-Ø.Ø1644
Ø.213	13.68	13.66	3Ø.	-33.	-28.Ø	-28.2	52.Ø	51.8	317.7	Ø.Ø271	-Ø.Ø1656
Ø.134	13.68	13.65	26.	-51.	-28.Ø	-28.3	52.Ø	51.7	332.7	Ø.Ø271	-Ø.Ø2531
Ø.Ø55	13.68	13.65	17.	-54.	-27.Ø	-27.3	53.Ø	52.7	342.7	Ø.Ø276	-Ø.Ø2717

BASED ON DP/DR PS AND THETA

R/Rw	Pt psia	Ps psia	Vt ft/sec	Va ft/sec	DTt deg	DTs deg	Tt F deg	Ts F deg	THETA deg	DS Btu/lbmR	G(psqin) lbm/sec
Ø.961	18.57	15.79	514.	17Ø.	-1.Ø	-25.4	79.Ø	54.6	251.7	Ø.Ø185	Ø.Ø9759
Ø.941	18.69	15.68	54Ø.	158.	-2.Ø	-28.3	78.Ø	51.7	253.7	Ø.Ø176	Ø.Ø9Ø49
Ø.921	18.84	15.57	564.	154.	-3.Ø	-31.4	77.Ø	48.6	254.7	Ø.Ø166	Ø.Ø8837
Ø.9Ø2	2Ø.5Ø	15.43	686.	174.	-5.Ø	-46.7	75.Ø	33.3	255.7	Ø.ØØ99	Ø.1Ø226
Ø.882	21.22	15.2Ø	746.	162.	-6.Ø	-54.6	74.Ø	25.4	257.7	Ø.ØØ71	Ø.Ø9527
Ø.843	19.34	14.75	678.	123.	-9.Ø	-48.5	71.Ø	31.5	259.7	Ø.Ø121	Ø.Ø6914
Ø.764	16.41	14.Ø7	517.	66.	-14.Ø	-36.6	66.Ø	43.4	262.7	Ø.Ø211	Ø.Ø3457
Ø.685	14.52	13.86	288.	27.	-19.Ø	-26.Ø	61.Ø	54.Ø	264.7	Ø.Ø272	Ø.Ø1341
Ø.6Ø6	14.ØØ	13.77	171.	7.	-23.Ø	-25.4	57.Ø	54.6	267.7	Ø.Ø278	Ø.ØØ34Ø
Ø.528	13.85	13.74	118.	-4.	-25.Ø	-26.2	55.Ø	53.8	271.7	Ø.Ø276	-Ø.ØØ179
Ø.449	13.81	13.71	114.	-26.	-27.Ø	-28.1	53.Ø	51.9	282.7	Ø.Ø269	-Ø.Ø1291
Ø.37Ø	13.72	13.67	74.	-31.	-28.Ø	-28.5	52.Ø	51.5	292.7	Ø.Ø269	-Ø.Ø1553
Ø.291	13.67	13.67	19.	-13.	-28.Ø	-28.Ø	52.Ø	52.Ø	3Ø2.7	Ø.Ø271	-Ø.ØØ627
Ø.213	13.69	13.66	38.	-42.	-28.Ø	-28.3	52.Ø	51.7	317.7	Ø.Ø27Ø	-Ø.Ø2Ø84
Ø.134	13.67	13.65	23.	-45.	-28.Ø	-28.2	52.Ø	51.8	332.7	Ø.Ø271	-Ø.Ø223Ø

BASED ON DIFERNTIAL EQUATION

R/Rw	Pt psia	Ps psia	Vt ft/sec	Va ft/sec	DTt deg	DTs deg	Tt F deg	Ts F deg	THETA deg	DS Btu/lbmR	G(psqin) lbm/sec
Ø.98Ø	18.16	15.23	531.	186.	-Ø.5	-26.9	78.5	52.1	25Ø.7	Ø.Ø198	Ø.1Ø354
Ø.961	18.12	15.13	541.	179.	-1.Ø	-28.Ø	79.Ø	52.Ø	251.7	Ø.Ø2Ø1	Ø.Ø9898
Ø.941	17.98	15.Ø3	545.	159.	-2.Ø	-28.9	78.Ø	51.1	253.7	Ø.Ø2Ø2	Ø.Ø8772
Ø.921	17.8Ø	14.92	543.	148.	-3.Ø	-29.4	77.Ø	5Ø.6	254.7	Ø.Ø2Ø5	Ø.Ø8123
Ø.9Ø2	17.52	14.82	531.	135.	-5.Ø	-3Ø.Ø	75.Ø	5Ø.Ø	255.7	Ø.Ø2Ø7	Ø.Ø7359
Ø.882	17.18	14.71	515.	112.	-6.Ø	-29.1	74.Ø	5Ø.9	257.7	Ø.Ø216	Ø.Ø6Ø47
Ø.843	16.62	14.52	483.	88.	-9.Ø	-29.1	71.Ø	5Ø.9	259.7	Ø.Ø225	Ø.Ø4663
Ø.764	15.52	14.21	393.	5Ø.	-14.Ø	-27.1	66.Ø	52.9	262.7	Ø.Ø249	Ø.Ø26Ø5
Ø.685	14.76	13.99	3Ø6.	28.	-19.Ø	-26.9	61.Ø	53.1	264.7	Ø.Ø261	Ø.Ø1444
Ø.6Ø6	14.24	13.85	22Ø.	9.	-23.Ø	-27.Ø	57.Ø	53.Ø	267.7	Ø.Ø267	Ø.ØØ441
Ø.528	14.ØØ	13.77	171.	-5.	-25.Ø	-27.4	55.Ø	52.6	271.7	Ø.Ø269	-Ø.ØØ26Ø
Ø.449	13.84	13.71	124.	-28.	-27.Ø	-28.3	53.Ø	51.7	282.7	Ø.Ø268	-Ø.Ø14Ø7
Ø.37Ø	13.72	13.68	62.	-26.	-28.Ø	-28.4	52.Ø	51.6	292.7	Ø.Ø269	-Ø.Ø13Ø4
Ø.291	13.7Ø	13.67	49.	-32.	-28.Ø	-28.3	52.Ø	51.7	3Ø2.7	Ø.Ø27Ø	-Ø.Ø1594
Ø.213	13.68	13.66	29.	-32.	-28.Ø	-28.2	52.Ø	51.8	317.7	Ø.Ø271	-Ø.Ø1612
Ø.134	13.68	13.66	23.	-45.	-28.Ø	-28.2	52.Ø	51.8	332.7	Ø.Ø271	-Ø.Ø2243
Ø.Ø55	13.68	13.65	17.	-54.	-27.Ø	-27.3	53.Ø	52.7	342.7	Ø.Ø276	-Ø.Ø2717

Table 3 (Continued)

Test NO. 1226 N=1 NN=17 Patm=14.24 psia Pinlet=34.55 psia Tinlet=80.0 deg. F

Gin=0.1243 lbm/sec Gout=0.1175 lbm/sec GPout=0.1156 lbm/sec GDout=0.1261 lbm/sec
Ein= 0.161E+02 Btu/sec Eout= 0.153E+02 Btu/sec DPout= 0.150E+02 Btu/sec EDout= 0.163E+02 Btu/sec
DS= 0.373E-02 Btu/R.sec DSP= 0.555E-02 Btu/R.sec DSD= 0.519E-02 Btu/R.sec
DELTA THETA= 2.9 DEG

BASED ON PT PS AND THETA

R/Rw	Pt psia	Ps psia	Vt ft/sec	Va ft/sec	DTt deg	DTs deg	Tt F deg	Ts F deg	THETA deg	DS Btu/lbmR	G(psqin) lbm/sec
0.980	23.14	17.69	668.	192.	4.0	-36.2	84.0	43.8	253.9	0.0293	0.12649
0.961	23.12	17.45	682.	196.	3.0	-38.9	83.0	41.1	253.9	0.0289	0.12816
0.941	22.90	17.23	688.	185.	1.5	-40.8	81.5	39.2	254.9	0.0289	0.11980
0.921	22.56	17.04	685.	172.	-1.0	-42.5	79.0	37.5	255.9	0.0288	0.11016
0.902	22.12	16.91	669.	168.	-3.5	-43.1	76.5	36.9	255.9	0.0290	0.10634
0.882	21.64	16.80	652.	151.	-6.0	-43.3	74.0	36.7	256.9	0.0294	0.09583
0.843	20.64	16.44	620.	121.	-10.5	-43.8	68.5	35.2	258.9	0.0302	0.07545
0.764	18.84	15.37	587.	83.	-20.0	-49.3	59.0	29.7	261.9	0.0321	0.04894
0.685	17.34	14.68	510.	45.	-29.0	-50.8	50.0	28.2	264.9	0.0336	0.02579
0.606	16.06	14.17	460.	17.	-36.0	-53.6	43.0	25.4	267.9	0.0355	0.00905
0.528	14.88	13.21	446.	-15.	-43.0	-59.6	36.0	19.4	271.9	0.0374	-0.00781
0.449	13.88	12.55	406.	-35.	-50.0	-63.8	28.5	14.7	274.9	0.0385	-0.01741
0.370	13.08	11.98	375.	-52.	-56.0	-67.9	22.5	10.6	277.9	0.0396	-0.02494
0.291	12.36	11.52	331.	-64.	-62.0	-71.5	16.5	7.0	280.9	0.0405	-0.02961
0.213	11.84	11.26	275.	-73.	-67.0	-73.8	11.0	4.2	284.9	0.0406	-0.03338
0.134	11.42	11.14	188.	-61.	-71.0	-74.3	7.0	3.7	287.9	0.0411	-0.02749
0.055	11.42	11.14	188.	-61.	-71.0	-74.3	7.0	3.7	287.9	0.0411	-0.02749

BASED ON DP/DR PS AND THETA

R/Rw	Pt psia	Ps psia	Vt ft/sec	Va ft/sec	DTt deg	DTs deg	Tt F deg	Ts F deg	THETA deg	DS Btu/lbmR	G(psqin) lbm/sec
0.961	24.36	17.45	740.	213.	3.0	-46.3	83.0	33.7	253.9	0.0253	0.14116
0.941	23.13	17.23	700.	188.	1.5	-42.2	81.5	37.8	254.9	0.0282	0.12216
0.921	21.36	17.04	617.	155.	-1.0	-34.7	79.0	45.3	255.9	0.0325	0.09772
0.902	20.01	16.91	534.	134.	-3.5	-28.7	76.5	51.3	255.9	0.0359	0.08287
0.882	20.77	16.80	598.	139.	-6.0	-37.4	74.0	42.6	256.9	0.0322	0.08700
0.843	22.36	16.44	717.	140.	-10.5	-55.0	68.5	24.0	258.9	0.0247	0.08929
0.764	19.59	15.37	640.	91.	-20.0	-54.8	59.0	24.2	261.9	0.0294	0.05390
0.685	17.68	14.88	541.	48.	-29.0	-53.5	50.0	25.5	264.9	0.0322	0.02749
0.606	17.66	14.17	606.	22.	-36.0	-66.6	43.0	12.4	267.9	0.0290	0.01225
0.528	16.14	13.21	575.	-19.	-43.0	-70.5	36.0	8.5	271.9	0.0318	-0.01030
0.449	14.40	12.55	474.	-41.	-50.0	-68.8	28.5	9.7	274.9	0.0359	-0.02053
0.370	13.27	11.98	403.	-56.	-56.0	-69.8	22.5	8.7	277.9	0.0386	-0.02697
0.291	12.23	11.52	307.	-59.	-62.0	-70.1	16.5	8.4	280.9	0.0412	-0.02734
0.213	11.53	11.26	191.	-51.	-67.0	-70.2	11.0	7.8	284.9	0.0424	-0.02297
0.134	11.20	11.14	83.	-27.	-71.0	-71.6	7.0	6.4	287.9	0.0424	-0.01207

BASED ON DIFERNTIAL EQUATION

R/Rw	Pt psia	Ps psia	Vt ft/sec	Va ft/sec	DTt deg	DTs deg	Tt F deg	Ts F deg	THETA deg	DS Btu/lbmR	G(psqin) lbm/sec
0.980	23.14	17.17	702.	202.	4.0	-40.5	84.0	39.5	253.9	0.0293	0.13027
0.961	23.12	16.96	714.	206.	3.0	-43.0	83.0	37.0	253.9	0.0289	0.13152
0.941	22.90	16.75	720.	194.	1.5	-44.8	81.5	35.2	254.9	0.0289	0.12282
0.921	22.56	16.54	719.	180.	-1.0	-46.8	79.0	33.2	255.9	0.0288	0.11320
0.902	22.12	16.32	710.	178.	-3.5	-48.1	76.5	31.9	255.9	0.0290	0.11063
0.882	21.64	16.11	701.	163.	-6.0	-49.2	74.0	30.8	256.9	0.0294	0.10011
0.843	20.64	15.70	678.	133.	-10.5	-50.2	68.5	29.8	258.9	0.0302	0.07979
0.764	18.84	14.93	627.	89.	-20.0	-53.4	59.0	25.6	261.9	0.0321	0.05114
0.685	17.34	14.24	577.	51.	-29.0	-56.9	50.0	22.1	264.9	0.0336	0.02828
0.606	16.06	13.60	529.	19.	-36.0	-59.3	43.0	19.7	267.9	0.0355	0.01010
0.528	14.88	13.04	469.	-16.	-43.0	-61.4	36.0	17.6	271.9	0.0374	-0.00814
0.449	13.88	12.55	406.	-35.	-50.0	-63.9	28.5	14.6	274.9	0.0385	-0.01742
0.370	13.08	12.13	348.	-49.	-56.0	-66.3	22.5	12.2	277.9	0.0396	-0.02338
0.291	12.36	11.78	274.	-53.	-62.0	-68.5	16.5	10.0	280.9	0.0405	-0.02486
0.213	11.84	11.52	204.	-54.	-67.0	-70.7	11.0	7.3	284.9	0.0406	-0.02511
0.134	11.42	11.35	95.	-31.	-71.0	-71.8	7.0	6.2	287.9	0.0411	-0.01405
0.055	11.42	11.14	188.	-61.	-71.0	-74.3	7.0	3.7	287.9	0.0411	-0.02749

APPENDIX D

ERROR ESTIMATION OF MEASUREMENT

The measured values were sound pressure level (SPL), total temperature (T*), total pressure (p*), static pressure (p), and flow angle (α), obtained at various radial positions (r).

The error of sound pressure level was ± 0.2 dB, using the frequency analyzer (Bluel and Kjaer, Model 2033).

The error of total pressure was smaller than the error of pressure transducer; the pressure transducer used for the total pressure was Kulite, Model ETM-375, the accuracy of which was within ± 1% at full scale (100 psig).

The error of static pressure was ± 0.5% including the error of pressure transducer (Honeywell, Model 415, accuracy: ± 0.35%).

The total temperature was measured by using Chromel-Alumel thermocouple made by Omega; its error was ± 0.5°F.

To measure the flow direction and the positioning of the probe, the traversing unit was used. The accuracy of positioning was within ± 0.1 mm (0.004 inch), and flow angle ± 0.5 degree.

VITA

Hiromoto Kuroda was born in Shobara-City, Hiroshima, Japan on February 11, 1942.

He received his Bachelor of Science degree in Physics at the Science University of Tokyo in March 1965. He has been employed by The National Defense Academy of Japan in the Department of Aeronautical Engineering since April 1965. Meanwhile, he took the postgraduate course on Aerospace Vehicle Engineering at The National Defense Academy during April 1967 and March 1969.

He began to take the graduate education in September 1979 at The University of Tennessee Space Institute. He subsequently received a Master of Science and a Doctor of Philosophy degree with a major in Engineering Science in June 1981 and December 1983, respectively.

Mr. Kuroda is a member of the Japan Society of Mechanical Engineers (JSME), Japan Society for Aeronautical and Space Sciences, the Gas Turbine Society of Japan, and Heat Transfer Society of Japan. He is an associate member of the American Society of Mechanical Engineers (ASME), Sigma Xi Society, and a student member of the American Institute of Aeronautics and Astronautics (AIAA).

He is married to the former Yasuko Horie and has two sons, Akihiro and Nobuhiro.